UILU-ENG-82-2001

CIVIL ENGINEERING STUDIES
STRUCTURAL RESEARCH SERIES NO. 496
Illinois Cooperative Highway and Transportation
Series No. 193



# EFFECT OF WELD PROCEDURES ON WELD QUALITY



By
R. G. BEHRENS
R. MARSHALLA
W. HANDEL
W. H. MUNSE

A Report of the Investigation on
Steel Bridge Design Criteria to Help
Minimize the Probability of Fracture
Project IHR-304
Illinois Cooperative Highway and
Transportation Research Program

A COOPERATIVE INVESTIGATION
Conducted by
THE STRUCTURAL RESEARCH LABORATORY
DEPARTMENT OF CIVIL ENGINEERING
ENGINEERING EXPERIMENT STATION
UNIVERSITY OF ILLINOIS
AT URBANA-CHAMPAIGN

in cooperation with the
STATE OF ILLINOIS
DEPARTMENT OF TRANSPORTATION
and the
U.S. DEPARTMENT OF TRANSPORTATION
FEDERAL HIGHWAY ADMINISTRATION

UNIVERSITY OF ILLINOIS
AT URBANA-CHAMPAIGN
URBANA, ILLINOIS
JULY 1982

TECHNICAL REPORT STANDARD TITLE PAGE

| 1. Report No. | 2. Government Accession No. | 3. Recipient's Catalog No. |
|---|---|---|
| FHWA/IL/UI-193 | | |

| 4. Title and Subtitle | 5. Report Date |
|---|---|
| Effect of Welding Procedures on Weld Quality | July 1982 |
| | 6. Performing Organization Code |

| 7. Author(s) | 8. Performing Organization Report No. |
|---|---|
| R. G. Behrens, R. Marshalla, W. Handel and W. H. Munse | UILU-ENG-82-2001 |

| 9. Performing Organization Name and Address | 10. Work Unit No. |
|---|---|
| Department of Civil Engineering<br>Engineering Experiment Station<br>University of Illinois at Urbana-Champaign<br>Urbana, Illinois 61820 | 11. Contract or Grant No.<br>IHR-304 |
| | 13. Type of Report and Period Covered |
| 12. Sponsoring Agency Name and Address<br>Illinois Department of Transportation<br>126 E. Ash Street<br>Springfield, Illinois 62706 | Interim Report |
| | 14. Sponsoring Agency Code |

15. Supplementary Notes

Study was conducted in cooperation with the U.S. Department of Transportation, Federal Highway Administration.

16. Abstract

The objective of this study was planned to develop welding procedures that would help to minimize the occurrence of cold cracking, hot cracking, porosity, slag inclusions, and lack of fusion in shielded metal arc welding (SMAW).

A literature survey was conducted to identify the welding variables related to each of the discontinuities, and relationships between the welding variables and the occurrence of discontinuities were examined in detail. These relationships were then used to establish preliminary welding requirements.

A test program was conducted to verify the validity of the preliminary proposed requirements. Recommended welding requirements were then developed on the basis of the preliminary proposed requirements and the test results.



| 17. Key Words | 18. Distribution Statement |
|---|---|
| welds, cold cracking, hot crakcing, porosity, slag inclusions, lack of fusion, welding procedures, steel, preheat heat input, electrodes | No restrictions. This document is available to the public through the National Technical Information Service, Springfield, Virginia, 22161. |

| 19. Security Classif. (of this report) | 20. Security Classif. (of this page) | 21. No. of Pages | 22. Price |
|---|---|---|---|
| Unclassified | Unclassified | 191 | |

Form DOT F 1700.7 (8-69)

# Table of Contents

## List of Tables

## List of Figures

# 1.0 INTRODUCTION

## 1.1 Discussion of Problem

During the welding of a steel changes occur in the physical and chemical properties of the steel due to rapid heating and cooling. In addition, shrinkage stresses are imposed on the weld and contaminants may be introduced. These factors contribute to the potential for discontinuities to form in either the weld deposit or the immediately adjacent base metal which has been affected by the welding.

Various aspects of the procedures used in welding have a significant effect on the quality of a weld or weldment and on the physical and chemical changes that take place during welding. These include such factors as the preheat and interpass temperature, the heat input employed, the restraint to which the weld is subjected, the types of electrodes used, the geometry of the welds, etc. Although some of these factors are considered in current design specifications, it would appear that better control of these variables and control over some that are not now included would make possible an improvement in the quality of welds being produced for steel structures. This may be of considerable importance, particularly in bridges, where fatigue is of importance and defects and discontinuities are of great concern.[19]

The concern of the study presented herein is to better define procedures that will help to minimize such weld discontinuities as cold cracking, hot cracking, porosity, slag inclusions, and lack of fusion.

## 1.2 Object and Scope of Investigation

The object of the investigation was to develop welding requirements to minimize the occurrence of weld discontinuities in shielded metal arc welding (SMAW). Compliance with these welding requirements should also result in welds with adequate strength and ductility.

Present codes do not consider some of the welding variables related to the occurrence of discontinuities. The AWS Structural Welding Code (AWS D1.1-81)[1] for example, has recognized this fact in its commentary.

The study presented herein has tried to include the effect of these welding variables to develop more effective welding requirements. These requirements can then be used to supplement or modify current codes such as the AWS Structural Welding Code and the AASHTO Bridge Specifications.

To fully understand the various causes for each type of weld discontinuity, a literature survey was conducted first. The welding variables related to each discontinuity were identified, and relationships between these variables and the occurrence of discontinuities were examined in detail. These relationships were then used to develop preliminary SMAW welding requirements to minimize the occurrence of such discontinuities.[2,3]

Based on the preliminary proposed welding requirements a test program was developed to evaluate the validity of the proposed requirements. Fifty welded specimens were fabricated and tested; welds were made using the shielded metal arc (SMAW) process by a qualified welder.* Recommended welding requirements were then developed.

In Section 2 of this report a discussion of the various types of discontinuities is presented along with a discussion of the principal causes for such discontinuities and the methods by which they might be controlled. The test program is defined in Section 3, a description of the tests is presented in Section 4, and the test results are given in Section 5. A discussion and analysis of the test results is given in Section 6, welding procedure recommendations for the minimization of weld discontinuities are presented in Section 7, and a brief summary of the investigation is provided in Section 8.

*The welder has 30 years of experience in industrial and research applications. This experience has included extensive work with the types of joints and electrodes used in the tests.

## 1.3 Acknowledgements

This study was conducted as a part of the Illinois Cooperative Highway and Transportation Research Program, Project IHR-304, "Steel Bridge Design Criteria to Help Minimize the Probability of Fracture," by the Department of Civil Engineering, Engineering Experiment Station, University of Illinois at Urbana-Champaign, in cooperation with the Illinois Department of Transportation, Federal Highway Administration.

The research reported herein was conducted by R. G. Behrens, R. Marshalla, and W. Handel, Research Assistants in Civil Engineering, working under the direction of W. H. Munse, Professor of Civil Engineering at the Univeristy of Illinois. Appreciation is extended to Mr. John R. Williams, who prepared the weldments and to the laboratory mechanics, technicians, draftsmen, and secretaries who assisted in the preparation of the test specimens, the conduct of the tests and the preparation of this report.

The authors also wish to acknowledge the assistance of the IHR-304 Project Advisory Committee in the development and evaluation of the programs and the resulting report, and of D. R. Schwartz and R. Taylor of the Bureau of Materials and Physical Research of the Illinois Department of Transportation. This committee consisted of R. M. Kiel, J. C. Stuemke and J. J. Wavering of the Illinois Department of Transportation, of R. A. Scarr and F. Grabski of the Federal Highway Administration, and Professors F. V. Lawrence and J. E. Stallmeyer of the University of Illinois.

# 2.0 WELD DISCONTINUITIES

## 2.1 Introduction

During SMAW welding, the filler metal and a portion of the base metal are melted and blended to form the weld deposit. Portions of base metal and weld metal (multi-pass welds) adjacent to the weld deposit are subjected to a thermal cycle which does not melt the metal, but causes complex microstructural changes therein. These regions are referred to as the base metal "heat-affected zone" (HAZ) and "retempered zone" respectively. At some distance from a weld pass, the base metal and previously deposited weld metal are not raised to high enough temperatures during the thermal cycle to cause microstructural changes, although other factors (diffusion of hydrogen for example) may cause changes in the weld and base metal properties.

As stated in Section 1.1, the quality of a weld depends on several factors. The properties of the base metal and filler metal are affected by the welding thermal cycle, shrinkage stresses, and contaminants introduced into the weld from rust, mill scale, moisture, or other foreign materials. Sources of these contaminants can be the surface being welded, the atmosphere, or filler metal.

The presence of contaminants or the existence of conditions which cause discontinuities generally depends on the welding procedure. Welding variables such as the welding process, welder, welding equipment, base metal, filler metal, joint geometry, thickness of members, restraint heat input, travel speed and preheat define a particular procedure. Through proper control of the welding procedure, discontinuities can be minimized. The effect of these variables on each of the different types of weld discontinuities, and methods to properly control these variables will now be discussed.

## 2.2 Cold Cracking

### 2.2.1 Introduction

Cold cracking is the term used for cracks which occur after the weld has solidified and cooled. They can occur in either the HAZ or weld metal.

There are several other names for cold cracking that are derived from the characteristics of the cracking. For instance, these cracks occur only in the presence of hydrogen, thus the name "hydrogen cracking" has often been used. Since these cracks occur under conditions of restraint, they are often referred to as "restraint cracks". The cracks can form several hours or days after the weld has cooled so the term "delayed cracking" has sometimes been used. The cracks often occur in the HAZ, hence the name "HAZ cracking" has been used. These HAZ cracks might occur either directly beneath the weld bead, at the root of the weld or at the toe of the weld (see Figure 2.1). Depending on the location, these types of cracks are referred to as "underbead cracking", "toe cracking" or "root cracking". The cracks can also occur in the weld metal. These cracks are referred to as "weld metal cracking". The smaller microscopic weld metal cracks are often referred to as "microfissures" or "microcracks".

For cold cracks to occur, three principal factors must be present. The first factor is the presence of atomic hydrogen. As will be discussed in more detail later, atomic hydrogen can be introduced to the weld during welding and must be present in order for cold cracking to occur. The second factor is a HAZ (HAZ cracking) or weld metal (weld metal cracking) which is susceptible to hydrogen embrittlement. Hydrogen embrittlement is primarily related to chemical composition and microstructure. The third factor necessary for cold cracking to occur is stress resulting from restraint. Restraint is dependent upon the geometry of the joint or structure. Stresses due to restraint develop as the weldment cools and contracts while the rest of the joint or structure tends to restrain the contraction. It is safe to assume that every weldment is subject to some restraint; however, the degree of restraint that causes these stresses may vary greatly from one member or joint to another.

The case in which cracking occurs in the HAZ has been studied in great detail[4] and much information concerning the mechanism of this cracking has been obtained. However, relatively little information has been gathered for the case of weld metal cracking. In fact, traditional methods for predicting preheat levels to avoid cold cracking have been based on only HAZ cracking considerations. These methods may or may not prevent weld metal cracking, depending on which of the two types of cracking is more critical.

### 2.2.2 Principal Factors Affecting Cold Cracking

#### 2.2.2.1 Hydrogen

As noted earlier, atomic hydrogen must be present for cold cracking to occur. It is introduced to the weldment during welding, primarily from the electrode coating. Some electrode coatings have various hydrogen compounds which break down during welding and are subsequently introduced into the weldment. These coatings generally contain cellulose sodium, cellulose potassium, titania sodium, titania potassium, iron oxide, and iron powder. Besides the above ingredients, moisture in the coatings can also introduce hydrogen into the weld. Proper baking and electrode care can reduce or eliminate this factor; however, moisture in the arc atmosphere or on the surface being welded can also introduce unwanted hydrogen. Other possible sources of hydrogen are rust, oil, dirt, grease, or any other contaminants on the electrodes or welding surface which contain hydrogen compounds.

#### 2.2.2.2 Susceptibility of the Head-Affected Zone to Hydrogen Embrittlement (HAZ Cracking)

In order for cold cracking to occur in the HAZ, the microstructure must be susceptible to hydrogen embrittlement. It has been shown that hardness of the HAZ is a useful indication of this susceptibility.[4] The harder the HAZ microstructure, the more susceptible it is to hydrogen embrittlement.

A principal source or cause of hardening in the HAZ's is the presence of alloying elements in the steels. In general, the greater the alloy content, the harder the HAZ will be after welding. The carbon content is the main factor responsible for hardening. Other alloys such as manganese, silicon, nickel, chromium, molybdenum, vanadium, copper, phosphorus, sulfur, boron, and titanium also have an affect on the final HAZ hardness. The effect of the various alloying elements on hardness can be conveniently combined with that of carbon by formulas known as carbon equivalent formulas. These formulas give weighted values to each of the alloys in order to show how much they affect hardness as compared to carbon. For example, most carbon equivalent formulas give manganese a weight factor of (1/6). By adding together all of the alloy contents multiplied by their respective weight factors, a single numerical indication (carbon equivalent) can be derived which gives the tentative hardenability index for the steel. There are a number of formulas which are used to calculate the carbon equivalent of steel; formulas which are by no means in total agreement with each other. Two commonly accepted formulas are listed below.

One formula, used by F. R. Coe[5], N. Bailey[6], and the British Standards Association[5] is as follows.

$$CE = \text{Carbon equivalent} = C + \frac{Mn + Si}{6} + \frac{Cr + Mo + V}{5} + \frac{Ni + Cu}{15} \quad (1)$$

Where: C and the other symbols represent the weighted percentage of the elements in the steel.

Another formula, derived by K. Winterton[7] is as follows:

$$CE = C + \frac{Mn}{6} + \frac{Ni}{20} + \frac{Cr}{10} - \frac{Mo}{50} - \frac{V}{10} + \frac{Cu}{40} \quad (2)$$

Note that Winterton's formula assigns minus signs to Mo and V, both tending to reduce the hardness of the steel.

Another primary factor or source of HAZ hardening in some steels is the cooling rate after welding. Rapid cooling through the martensitic transformation temperature of a steel with an appropriate chemistry will cause that steel to form martensite. Cooling rates measured at 300°C

(572°F) give a good indication of how hard the final microstructure will be. Several typical cooling rate formulas are listed below.

From reference (8), based on empirical data:

$$\frac{1}{\sqrt{R_{300}}} = \frac{E + 1000N}{54To\ (1 + To/1000)\ (N + 0.5)} \tag{3}$$

Where: $R_{300}$ = Cooling rate at 300°C in °C/sec

$E$ = Arc energy in Joules/inch

$N$ = Thermal Severity Number

$T_o$ = (300°C - Preheat or initial plate temperature)

Another formula is as follows:

$$R_{572} = K_1 \left(\frac{T}{E}\right)^2 (T_i)^3, \text{.....Thin plates} \quad (9,10) \tag{4}$$

$$R_{572} = \frac{K_2}{E}(T_i)^2, \text{.....Thick plates} \quad (9,10) \tag{5}$$

Where $R_{572}$ = Cooling rate at 572°F in °F/sec

$$R_{300}\ ^{\circ}C/sec = (R_{572}\ ^{\circ}F/sec)\ 5/9 \tag{6}$$

$T$ = Thickness of the plate

$E$ = Arc energy in Joules/inch

$T_i$ = (572°F - Preheat or initial plate temperature)

$K_1, K_2$ Represent the combined effects of thermal conductivity, density, and the specific heat of the steel

$K_1$ = 161.48 for mild steel,....Thin plates

$K_2$ = 5.961 mild steel,....Thick plates

It is apparent from the cooling rate formulas that the cooling rate is dependent upon plate thickness or the thermal severity number, arc energy, and the preheat or initial plate temperature.

The thicker a member being welded, the greater its ability to serve as a heat sink; thus taking heat away from the joint. The thermal severity number serves as a useful means of expressing this capability. Basically, the thermal severity number or TSN is four times the total plate thickness capable of removing heat from the joint. For examples of TSN determinations see Figure 2.2. In this figure it can be seen that a greater plate thickness will result in a larger TSN and thus a higher cooling rate since more steel is available to remove heat from the joint.

The cooling rate is also dependent upon the arc energy E; the greater the arc energy introduced into a weld, the higher the heat input. By increasing the heat input, the cooling rate at 300°C is decreased as is illustrated in Figure 2.3. The arc energy can be calculated by either of the following formulas:

$$E, \frac{\text{Joules}}{\text{inch}} = \frac{\text{Volts x Amps x 60}}{\text{travel speed, } (\frac{\text{inches}}{\text{minute}})} \tag{7}$$

$$E, \frac{\text{Joules}}{\text{mm}} = \frac{\text{Volts x Amps x 60}}{\text{travel speed, } (\frac{\text{mm}}{\text{minute}})} \tag{8}$$

A third factor in cooling rate determination is preheat or initial plate temperature. By preheating the steel, some of the steels capability of removing heat from the joint is diminished; the temperature gradient through the steel is reduced by the preheat. The effect of preheat on cooling rate is illustrated in Figure 2.3. By maintaining the preheat after welding is completed, a further reduction in the cooling rate can be achieved.

To summarize, the hardness of the HAZ of many steels is dependent upon two principal factors, steel chemistry or the CE, and the cooling rate $R_{572F}$ (or $R_{300C}$). Steels with a higher CE value will generally form harder HAZ's. Also, higher cooling rates in many steels will result in a harder HAZ. As the hardness of the HAZ increases, the susceptibility to hydrogen embrittlement, and thus cold cracking, increases.

2.2.2.3 Susceptibility of the Weld Metal to Hydrogen Embrittlement (Weld Metal Cracking)

In order for cold cracking to occur in the weld metal, the microstructure must be susceptible to hydrogen embrittlement. As noted previously, little information is available to explain weld metal embrittlement. The authors are not aware of any quantitative studies which relate a property of the weld metal (i.e. hardness) to hydrogen embrittlement susceptibility, such as that developed for HAZ cracking. However, it does seem reasonable that chemical composition and cooling rate would be important factors in much the same way as in HAZ cracking.

2.2.2.4 Stresses

Residual stresses in a weldment are caused by thermal contraction of the cooling weld metal under conditions of restraint. Restraint is a measure of the degree to which the structure or the material adjacent to the weld prevents this thermal contraction. This restraint is a function of the stiffness and the geometry of the joint, the members, and the structure containing the joint. The degree of restraint is a very difficult factor to evaluate quantitatively and is probably best judged by experience. Figure 2.4 shows examples of what may be classified as high, medium, or low restraint.

Poor joint fitup can also cause an increase in stresses. When the parts to be welded are not positioned properly, more weld metal is required to make the connection. The stress from thermal contraction of the weld metal is increased due to the larger amount of metal in the joint.

It should be emphasized that all joints have some residual stresses in them after welding. These stresses come from restraint, excessive weld metal and internal weld shrinkage as the joint cools. The important question is not whether or not there are stresses, but rather the magnitude of these stresses.

### 2.2.3 Phenomenon of Cold Cracking

The principal factors involved in cold cracking have been discussed. Following is a short summary of how these factors working together cause cold cracking in weldments.

#### 2.2.3.1 Phenomenon of Heat-Affected Zone Cracking

The process of HAZ cracking has been described by Stout and Doty[11] as follows:

1) Hydrogen is introduced to the hot weld metal and dissolves into the weld pool as atomic or ionized hydrogen.
2) As the weld metal cools, it becomes supersaturated in hydrogen and some diffuses into the HAZ.
3) Under rapid cooling, the hydrogen does not have enough time to diffuse out of the HAZ. Also, the rapid cooling increases the chance for the HAZ to transform from austenite to hardened martensite.
4) Atomic hydrogen is insoluble in martensite and seeks rifts and discontinuities in the lattice where it collects at a high energy state.
5) External stress caused by thermal contraction combined with the effects of the trapped, high energy hydrogen causes the discontinuities to enlarge to crack size.
6) It takes time for the hydrogen to diffuse to the new crack root and cause the crack to enlarge by the same mechanism as step 5. (Delayed Cracking)
7) This process repeats itself until the stress in the weld is relieved.

#### 2.2.3.2 Phenomenon of Weld Metal Cracking

Again, relatively little information is available to explain the mechanism of weld metal cracking. Hydrogen and stress play an important role in much the same way as in HAZ cracking. However the process of crack formation is not clearly understood. It has been observed that

microcracks in the weld metal are often associated with small non-metallic inclusions which provide sites for initiation. Results reported later for this study confirm that observation.

### 2.2.4 Methods of Controlling Cold Cracking

Since cold cracking is caused by the combined actions of hydrogen, a susceptible microstructure, and stress, it can be expected that by controlling or minimizing one or more of these three factors, the occurrence of cold cracking can be reduced. However, control of these factors must be such that considerations for both HAZ cracks and weld metal cracks are satisfied.

The basic relationships among the variables responsible for cold cracking and the methods of controlling these variables are summarized in the flow diagrams in Figures 2.5 and 2.6. These methods will now be discussed.

#### 2.2.4.1 Control of Hydrogen

There are several ways of minimizing the hydrogen content of a weldment. The first is the use of low hydrogen electrodes such as AWS classes EXX15, EXX16, EXX18, and EXX28. Also, different welding processes such as submerged arc welding, gas metal arc welding with Ar or $CO_2$ gas, and flux-cored welding with $CO_2$ give lower hydrogen contents than the shielded metal-arc welding process. Another measure to control hydrogen is to insure that no moisture is introduced into the weld. All welding surfaces should be dry and electrodes should be properly baked to remove moisture. Cleanliness is another important consideration in controlling hydrogen. Removal of paint, grease, rust, crayon marks, oil, soil, or any other contaminants will reduce the hydrogen level of the final weld. If hydrogen is introduced into the weld, maintaining joint heat after welding for a sufficient time to allow the hydrogen to diffuse out of the weldment can help to minimize the hydrogen before it has a chance to do any damage. Post heating tends to increase the diffusion rate as well as reduce the cooling rate and thus serves a double purpose.

2.2.4.2 Control of Hydrogen Embrittlement in the Heat-Affected Zone

In order to control hardening of the HAZ microstructure of many steels, it is necessary to provide a cooling rate that is compatible with the steel chemistry. In other words, the higher the CE value for a given steel, the slower the cooling rate through 572°F (300°C) ($R_{572}$ or $R_{300}$) must be to avoid hardening. A slower cooling rate can be achieved in several ways. One way is to preheat the steel to a predetermined temperature and to maintain the same temperature as interpass temperature throughout the welding process. The effects of preheat on reducing the cooling rate have already been discussed. Another method is to increase the arc energy which will also reduce the cooling rate. By carefully selecting the arc energy and the preheat, a cooling rate which is low enough to restrict HAZ hardening to the desired level can be achieved. The voltage or amperage can be increased or the weld speed can be decreased to modify the arc energy. However, caution must be taken in adjusting these variables since they are also important factors in controlling other types of discontinuities. Post-heat by retention of the interpass temperature for a period after the completion of welding can also be used to reduce the cooling rate. The three methods for controlling cooling rate, namely preheat, higher arc energy, and post-heat, should be coordinated to produce the most efficient means of reducing the cooling rate to the desired level.

Bailey[6] has developed relationships between steel chemistry and the cooling rate necessary to give a specified critical hardness; he used 350HV as the critical hardness for other than low hydrogen conditions and 400HV as the critical hardness for low hydrogen conditions* to protect against HAZ cracking. In his tests, he found approximately straight line relationships between CE and $(R_{300})_{cr}$, where $(R_{300})_{cr}$ is the critical 300°C cooling rate to produce a maximum HAZ hardness of 350HV or 400HV. The relationships are as follows:

*The microstructure can tolerate an increased hardness without cracking due to the lower level of hydrogen present.

$$\frac{1}{(R_{300})_{cr}} (350\ HV) = [2.1(CE) - 0.63] \quad (9)$$

$$\frac{1}{(R_{300})_{cr}} (400\ HV) = [1.9(CE) - 0.63] \quad (10)$$

Where: $R(_{300})_{cr}$ is in $^{o}C$/sec.

$$CE = C + \frac{Mn+Si}{6} + \frac{Cr+Mo+V}{5} + \frac{Ni+Cu}{15} \quad (1)$$

By using these relationships, the hardness of the HAZ can be controlled in an attempt to avoid cold cracking.

Bailey[12], Coe[5], and Bradstreet[13] have presented welding requirements to avoid cold cracking based on relationships similar to those described above and in Section 2.2.2.2. By relating the critical cooling rates to preheat temperature, arc energy, and thermal severity, the investigators developed suggested welding procedures to avoid HAZ cold cracking.

#### 2.2.4.3 Control of Hydrogen Embrittlement in the Weld Metal

Since the mechanism of hydrogen embrittlement in the weld metal is not clearly understood, it is not possible at this time to clearly define how to control embrittlement. Control of hardness could be a key, as is the case for HAZ embrittlement, but more analysis and testing will be required to confirm this.

#### 2.2.4.4 Control of Stresses

The third factor that might be controlled to minimize the possibility of cold cracking is stress, but stress is the most difficult of the three factors to control. To minimize stress on a welded joint, the joint should have as little restraint as possible and all members properly fit-up for welding. Since it is often difficult to assess restraint or fit-up, these variables are obviously difficult to control. Experience and

judgement should be used wherever possible to reduce joint stress, insure proper fit-up and avoid the use of excessive weld.

## 2.3 Hot Cracking

### 2.3.1 Introduction

Hot cracking is the term used for cracks which form while the weld metal is solidifying. Shrinkage stresses in the weld tend to tear the weld while it is in a hot plastic condition and at high temperatures. The cracks are usually intercrystalline in nature so the conditions between the crystals are of importance. Hot cracks can occur in either the weld metal or the base metal HAZ, but the phenomenon of formation and the methods for avoiding the flaws are basically the same for either type of hot crack.

### 2.3.2 Principal Factors Affecting Hot Cracking

There are two categories of factors affecting the formation of hot cracks: metallurgical and mechanical factors.

#### 2.3.2.1 Metallurgical Factors

During the solidification of weld metal there are many compounds formed that are present in their liquid phase at the grain boundaries which can produce hot cracks. Various elements in the base metal and filler metal have an affect on the formation or presence of these compounds. Sulfur is probably the most harmful element since it can react to form many low freezing temperature compounds, such as iron sulfide (FeS). Carbon is another harmful element because it has an influence on the liquid phase of the weld metal. Carbon tends to decrease the high temperature ductility of the weld metal.

The silicon, phosphorous, and nickel contents also have an effect on the hot cracking tendencies of a weld. Silicon and phosphorous do not affect the liquid phase of the weld metal directly, but they promote segregation of the sulfur and therefore aid the sulfur reactions. Nickel has a more

direct influence on the liquid phase but its effects on cracking are not clearly understood.

#### 2.3.2.2 Mechanical Factors

No matter how pronounced the liquid phase is in the weld metal, hot cracks will not form unless tensile stresses are imposed on the weld. Unfortunately stresses are impossible to avoid, and the greater the stresses imposed during solidification, the more severe the cracking will be. Size and thickness of the base metal, joint design, and size and shape of the weld bead all have an influence on the mechanical stresses present in a weld.

### 2.3.3 Phenomenon of Hot Cracking

Basically, hot cracks are intercrystalline tears occurring at or just below the range of solidification of the weld metal (generally greater than 1000$^{o}$c). Usually the cracks are located in the metal last to freeze.

Borland[14], in considering the mechanism of cracking, suggests that during solidification of a weld, the metal goes through many phases and the various compounds produced during these phases affect the hot cracking tendencies of the weld. Two factors are considered necessary for a compound to cause hot cracking: it must exist over a wide freezing range; and while in a liquid state, it must be present in a distribution which will allow high stresses to be built up between the grains.

Considering these two factors, a relative potency factor is established for each element found in the weld metal. The higher this factor is, the higher the potential for compounds formed from the element to produce hot cracking. Potency factors for various elements will not be quoted here, but the five most important elements causing hot cracking (sulfur, phosphorous, carbon, silicon and nickel) were all found to have relatively high potency factors.

### 2.3.4 Methods of Controlling Hot Cracking

Since certain compounds produced in the weld metal during solidification are the major source of hot cracks, controlling the presence of these compounds, or the elements which produce them, should minimize hot cracking.

Sulfur compounds have the greatest influence on hot cracking; therefore, the sulfur content in the base metal and filler metal should be kept low to keep the sulfur content in the weld metal low.*

Carbon is another element that has been shown to have a major influence on hot cracking. The level of carbon present in a base metal can't be altered to any great extent but the effects of carbon can be offset by high Mn/S ratios. It has been shown[15] that with a carbon content of the weld metal between 0.06% and 0.11%, hot cracks can be completely eliminated when Mn/S >22, while for carbon contents between 0.11% and 0.13%, a ratio over 30 is required to eliminate hot cracking. With carbon contents greater than 0.13%, the Mn/S ratio does not seem to have much effect because the carbon content becomes so critical. These values were determined from tests made on welds under high restraint in a Murex hot cracking test.

Very little data is available concerning control over the other elements reported to affect hot cracking. The best approach is to keep the phosphorous, silicon, and nickel content reasonably low in the base metal to keep their effects minimal.

Considering all the factors discussed above, Borland[14] has suggested the following weld metal composition to minimize hot cracking.

C = 0.12 max
Mn = 0.50 min
S = 0.035 max
P = 0.040 max
Mn/S = 14.3 min

---

*Limitating or minimizing the sulfur content will also help to reduce somewhat the tendency for lamellar tearing to develop in certain types of joints.

In general, this composition should produce crack free welds in semi-killed or killed steel under low restraint conditions. If the restraint is high, the manganese content should be increased.

Another factor which must be considered to minimize hot cracking is stress but, as noted in Section 2.2.2.4, stress is a very difficult factor to assess and control. The joint design should provide good joint fit-up, avoid excessive amounts of weld, and specify procedures and details that minimize the restraint to which the weld is subjected. Minimal restraint is important to insure crack free welds and must be considered in the original design as well as in fabrication.

The basic relationships among variables causing hot cracking and methods of controlling hot cracking are summarized by the flow diagrams in Figure 2.8 and 2.9.

Based on the limited information available, preliminary welding requirements to minimize hot cracking were developed during the early phases of this study. These requirements were directed towards controlling the weld metal composition as suggested by Borland[14]. Considering the chemical content of most common bridge steels and electrodes[16], it was assumed that if the weld metal composition was controlled to yield a maximum carbon content of 0.12%, then the other chemical content limitations suggested by Borland will generally be achieved.

To find the content of a certain element in the weld metal, a nomogram such as that shown in Fig. 2.13 can be used. To use this nomogram, the content of the element in the base metal and the filler metal must be known as well as the dilution percentage caused by the particular welding conditions. The compositions of the base metal and filler metal can be found or assumed from chemical analysis or from specification, but the dilution percentage is a variable that must be considered further.

The dilution percentage can be found for a given weld by cutting through the weld to reveal the cross-sectional area of the weld nugget. Dilution is then calculated as the area of the weld within the initial outline of the base metal (penetration), divided by the total nugget area. Using the diagrams shown in Fig. 2.14 of some typical weld configurations, dilution is calculated as $\frac{B}{A}$, where A is the total nugget area (B+C) and

B is the penetration area. To calculate the dilution percentage expected for given welding procedures, graphs presented by Jackson and Goodwin[17] were used. Jackson and Goodwin conducted studies on the weld configuration and penetration for weld - 1, shown in Fig. 2.14. They developed graphs which relate width of the weld, w, to the weld speed, the penetration of the weld, p, to the arc energy and the total nugget area, A, to the arc energy. From these graphs, a theoretical penetration area, B', for a weld can be calculated as B' = (wxp). For weld -1 shown in Fig. 2.14, if the weld shape is assumed to be parabolic, the actual penetration area, B, is B = 0.75B'. The dilution percentage can then be calculated as $\frac{B}{A}$.

The weld configuration also has an affect on the actual penetration area, B. Figure 2.14 shows the various welding configurations considered herein. Weld 1 is the base weld used by Jackson and Goodwin[17], which is not a common type of weld. To use the data from Jackson's graphs[17] on more common types of welds, assumptions were made also of the correlation between degrees of penetration (low, medium or high) and the actual penetration areas. These assumptions are as follows:

| | |
|---|---|
| Low Penetration | $B = \frac{1}{4} B'$ |
| Medium Penetration | $B = \frac{1}{2} B'$ |
| High Penetration | $B = \frac{2}{3} B'$ |

The degree of penetration of a weld can be assumed from experience with a particular weld configuration, or the penetration levels shown in Fig. 2.14 for various welds (weld 2, 3, or 4) can be used.

The data in Jackson's and Goodwin's graphs[17] show that dilution increases with increasing arc energy, increasing weld speed, and increasing degree of penetration. Using the values for B given in the previous paragraph and the actual nugget areas, A, given in Jackson's graphs, the expected dilution percentages, shown in Table 2.1, were calculated for various combinations of arc energy, weld speed, and penetration level.

With dilution percentages established for given welding conditions, the next step was to find the allowable dilution percentage that will yield the desired chemical composition in the weld metal. Using Table 2.1, Figure 2.13, and the desired weld metal carbon content of 0.12%, the maximum weld speed to minimize hot cracking can be determined at a given arc energy level for a particular combination of base metal and electrode carbon content.

Figure 2.15 is a typical plot[3] which was developed using the procedure described in the preceding paragraph. The plots give the maximum allowable weld speed, for three degrees of penetration, to control hot cracking as a function of arc energy (arc energies ranging from 20 - 65 KJ/in.). A separate plot was developed for each of several combinations of base metal and filler metal carbon contents. The electrodes have been placed into three groups, determined by the expected carbon content of the deposited weld metal for each electrode, with group 1 having the lowest carbon levels. Table 2.2 is a list of the electrodes and their corresponding groupings.

## 2.4 Porosity

### 2.4.1 Introduction

Porosity consists of gas pockets formed in the weld metal as a result of entrapment of gases evolved during the welding process. These pockets are usually rounded or globular voids that have smooth bright interiors. The voids are found in many shapes and sizes, from pinholes to large voids. They can be elongated or pear shaped with constrictions and expansions, depending on how the gases evolve. Two particular types of porosity are often identified by specific names, wormholes and blowholes. Wormholes are so called because they are elongated voids with a definite worm-type shape and texture. Blowholes are voids which appear on the surface of the weld and form as the weld metal is solidifying.

### 2.4.2 Principal Factors Affecting Porosity

Several factors have an influence on the presence of porosity in welds. The gases produced during welding are the principal source of porosity; elements that produce these gases must be considered. Elements such as sulfur, carbon, and oxygen in the base metal, and hydrogen and oxygen from the filler metal or welding atmosphere produce gaseous compounds which promote porosity. Excessive moisture in the electrode coating will provide hydrogen and foreign contaminants such as oil, paint, or rust in the welding area can introduce oxygen and hydrogen to the welds.

Another important factor in porosity formation is the speed with which a weld deposit solidifies, and thus prevents the escape of gas bubbles from the weld metal. Low welding current, unacceptable arc length, or high travel speed produce rapid freezing rates that shorten the escape time. Too high a welding current or heat input may produce a weld which penetrates so deeply that gas bubbles have difficulty diffusing through the weld.

### 2.4.3 Phenomenon of Porosity Formation

During welding chemical reactions occur which produce gaseous compounds that dissolve in the hot metal and form porosity at the solid-liquid interface during solidification. Since these gases are less soluble in the coolest liquid steel than in the hotest liquid steel, and the rate of diffusion of the gases to the surface is lower than the rate of advancement of the liquid-solid interface, the gases are entrapped. Thus, two factors can obstruct the assent of gas bubbles to the surface: if the weld pool cools too fast the bubbles won't have time to reach the surface, and if the weld penetrates too deep the bubbles may have too long a distance to travel to the surface.

The three reactions listed below are the most common causes of porosity producing gases:

$$C + O \rightarrow CO$$

$$S + H_2 \rightarrow H_2S$$

$$S + O_2 \rightarrow SO_2$$

Two other reactions can produce harmful gases but they are much less active. They are:

hydrogen-oxygen or water vapor reaction

$$FeO + 2H \rightarrow Fe + H_2O$$

carbon-oxygen reaction

$$FeO + C \rightarrow Fe + CO$$

### 2.4.4 Methods of Controlling Porosity

One of the best ways to control porosity is to reduce the amount of gas evolved during welding. The three major sources of gaseous producing elements in the welding process are the parent metal, the electrode and the atmosphere. Keeping the sulfur content low in the base metal will help eliminate the most harmful gas, $H_2S$, using low hydrogen electrodes and electrodes kept free of moisture will help reduce the amount of hydrogen present, and keeping the surfaces to be welded clean and free from contaminants will reduce the availability of hydrogen and oxygen.

The introduction of deoxidation elements during the welding or the casting of the base metal or filler metal will help control porosity by reducing available oxygen. Gases such as carbon monoxide (CO) and sulfur dioxide ($SO_2$) will be reduced in this way. Deoxidizing elements such as aluminum, manganese, and silicon can be introduced in the base metal or the welding atmosphere. Providing these elements to the base metal or filler metal produces killed or semi-killed steel, as opposed to rimmed steel, and thus helps minimize porosity.

Another important method of controlling porosity is to alter the welding procedure such that the distance a gas must travel to escape the weld pool is shortened or that the time the gas has to travel through the weld pool is lengthened. A slow steady cooling rate will help lengthen the time to a maximum. High heat input and preheat can help to produce

the desired reduction in cooling rate. Although too high a heat input produced by excessive current or voltage can cause excessive penetration into the base metal and result in the gases having too long a distance to travel. Therefore, the heat input must be kept within a range that will provide optimal conditions. Another parameter which affects the escape of the gases from the weld pool is the welding speed. High speeds produce excessive amounts of porosity. If the speed is kept down, the heat input is increased thus reducing the cooling rate.

The general relationships between the variables responsible for porosity and the methods that help control porosity are summarized in the flow diagram shown in Figure 2.10.

## 2.5 Slag Inclusions

### 2.5.1 Introduction

Slag inclusions are non-metallic materials which are trapped in a weld. They can range in size from very small globules to large long bands along the axis of the weld. Entrapment can be due to slag becoming mixed in the weld pool or due to surface slag not being completely removed and then being covered by succeeding passes.

### 2.5.2 Principal Factors Affecting Slag Inclusions

During welding a non-metallic slag is deposited on the weld surface. This slag comes from the electrode covering in shielded metal-arc welding, or from the flux used in other welding processes such as submerged arc and flux-core arc welding. Various factors can cause slag to be deposited in locations which may be hard to clean. If the electrode is too large to reach the bottom of a groove, or if the angle of the groove is too small to ensure good fusion at the bottom, slag may fall to the bottom and become trapped below the weld bead. Also, if unusual weld bead geometries are produced, such as V-shaped or overly convex weld bead or exaggerated weaves in the weld path, the slag can become trapped within the weld bead geometry.

Heat input also affects the formation of slag inclusions. Low arc energies result in fast cooling rates which allow less time for slag to escape from the weld, hence the slag becomes trapped. High arc energies cause higher temperatures and more stirring, which may mean more slag will be melted and mixed into the weld.

Another source of inclusions is the reaction of oxidizing gases produced during welding. These gases react with elements such as iron, aluminum, silicon, and manganese. When excessive amounts of these elements are present, harmful inclusions can be formed.

### 2.5.3 Phenomenon of Slag Inclusion Formation

Once slag is introduced into the weld, high temperatures cause the slag to melt and stirring of the arc mixes the slag with the weld metal. After the arc passes, the slag begins to float to the surface of the weld. At the same time, the weld metal begins to cool. As it cools, the weld metal becomes more viscous and restricts movement of the slag. If insufficient time is provided for the slag to escape, it remains in the weld as an inclusion.

### 2.5.4 Methods of Controlling Slag Inclusions

The most important consideration in controlling the presence of slag inclusions, especially in multi-pass welding, is to be sure all slag is removed from the weld surface. Slag on the weld surface should be removed by backchipping, wire brushing, grinding, or air-arc gouging. Also, proper size electrodes and smooth continuous welding processes and procedures should be used so that unusual configurations are not formed to trap surface slag.

For slag that becomes mixed within the weld bead, sufficient cooling time must be provided to allow the slag to float to the surface. High enough preheat or heat input must be used to avoid rapid cooling in the weld. Too high a heat input must also be avoided or more slag may become mixed in the weld.

To control inclusions from oxide-gas reactions, excessive amounts of the reactive elements should be avoided in the base metal composition.

The flow chart shown in Figure 2.11 indicates the relationship between many of the factors that cause and help control slag inclusions.

## 2.6 Lack of Fusion

### 2.6.1 Introduction

Lack of fusion is the term used to describe voids or lack of bonding which occur at the weld bead or weld-base metal interfaces. These voids occur due to the failure of the deposited weld metal and the underlying base metal or weld metal (multipass welds) to completely fuse together. Lack of fusion (LOF) discontinuities are usually elongated in the direction of welding, with either sharp or rounded edges depending on the conditions of formation.

### 2.6.2 Principal Factors Affecting Lack of Fusion

The two major factors affecting LOF are the heat applied to the surface being welded and the condition of that surface.

The heat applied to the surface depends on the arc energy and the welder's ability to properly manipulate the arc. Low arc energies do not provide enough heat to melt the underlying metal. Insufficient root opening, poor bead shape and poor welder technique may not allow the full arc energy to be directed properly to the surface.

The amount of heat absorbed by the underlying metal depends on the condition of the surface. Dirty surfaces due to mill scale, rust, grease. or other contaminants may prevent the arc heat from reaching the underlying metal.

### 2.6.3 Phenomenon of Lack of Fusion

During welding, the filler metal is melted and deposited on the underlying metal to form the weld bead. When insufficient heat is being absorbed by the underlying metal, it does not melt. As noted, this can be due to insufficient arc heat or poor surface conditions. If the underlying metal does not melt, it does not fuse completely with the weld bead and a void

is formed between the two.

### 2.6.4 Methods of Controlling Lack of Fusion

To prevent LOF, the underlying metal must be provided with enough heat to allow complete fusion with the weld deposit. The arc energy must therefore be high enough to melt the underlying metal and provide acceptable weld bead shapes. Joint geometry must allow proper control of the arc. Narrow root openings, for example, are to be avoided. In addition, surfaces to be welded should be cleaned of mill scale, rust, grease, or any other contaminant which would shield the underlying metal from the arc heat.

The flow diagram shown in Figure 2.12 indicates the relationship between many of the factors that cause and help control LOF.

# 3.0 DEVELOPMENT OF TEST PROGRAM

## 3.1 Purpose of Test Program

A test program was established, based on a set of preliminary welding requirements that were developed from the work of Bailey[6] and Coe[5]. The purpose of the tests was to assess the validity of the proposed requirements. To be valid, compliance with the requirements also should produce welds with minimum discontinuities and adequate strength and ductility.

The test program included the fabrication of test welds, groove welds and fillet welds, using various welding procedures. To determine the quality of the welded test specimens, the following tests were performed:

1) Metallographic studies - to detect discontinuities which might be present.

2) Radiographic studies - to detect discontinuities which might be present.

3) Hardness Tests - to determine the microstructural hardness of the weldments (hardness gives indication of susceptibility to cold cracking).

4) Tension Tests - to determine the strength of the welded specimens.

5) Bend Tests - to determine the ductility of the welds and to detect discontinuities which might be present.

Specific details of how the tests were conducted are discussed in Sections 5.1 thru 5.5.

## 3.2 Welding Procedures for Test Specimens

A large number of different welding procedures is possible. However, since it was not within the limits of the study to check a large number of procedures, a systematic approach to varying the welding procedures was used.

Fifty test specimens were fabricated from mild (similar to A36), low alloy (A441), and quenched and tempered (A514) base metals, using E6010, E7018, E7024, E7028 and E11018 covered electrodes, and systemically varying preheat temperature, arc energy, travel speed, TSN, restraint, electrode, and joint type. For example, the welding procedures for the mild steel specimen included the following:

1) Specimens A1A, A1B, and A1C to show the effect of preheat.

2) Specimens A1A and A2A to show the effect of arc energy.

3) Specimens A3A, A1A, A3B, and A3C to show the effect of TSN.

4) Specimens A2A and A4A to show the effect of electrode hydrogen level.

5) Specimens A1A, D1A, A1B, D1B, A1C, and D1C to show the effect of restraint.

6) Specimens A3B, E1A, and F1A to show the effect of joint type.

7) Specimens A1B and A1D to show the effect of plate length.

The welding procedures for the specimen listed above form a matrix of welding procedures from which welding requirements will be developed. The same systematic approach has been used to develop the test welding procedures for the low alloy (A441) and quenched and tempered (A514) steels. The details of the welding procedures used for the fifty specimens are listed in Tables 3.1 through 3.3. Fabrication details are discussed in Sections 4.1 through 4.3.

# 4.0 PREPARATION OF TEST SPECIMENS

## 4.1 Equipment and Materials

The equipment used to weld the specimens is shown in Figure 4.1a.

Welds were made using a 570 amp capacity power source equiped with voltage and current meters for both AC and DC power. These meters were used to obtain the voltage and current output of the machine during welding.

Welding travel speed was monitored using the speed indicator system shown in Figure 4.1b. The system consisted of variable speed guide mechanism normally used for automatic welding or flame-cutting. A pointer was attached to the mechanism for the welder to follow. By calibrating the variable speed motor, accurate control of welding speed was achieved.

Asbestos sheets were placed under the specimen. The purpose of these sheets was to prevent the metal table from acting as a heat sink and thus altering the cooling rates of the welds. It was observed during welding that only minimal heat transfer to the table occurred.

Preheats were applied to the base metal within 3-inches (76.2mm) of the weld using an oxy-acetylene flame. A pyrocon was used to measure the preheat temperature at a distance of 3-inches (76.2mm) from the weld.

The specimens were fabricated from a 1-inch (25.4mm) mild steel plate, a 1-inch (25.4mm) A441 steel plate and a 3/4-inch (19.1mm) A514 steel plate. Mechanical and chemical properties of these steels are listed in Table 4.1. The steel chemistries listed were determined by check analysis.

Commercially available E6010, E7018, E7024, E7028 and E11018 covered electrodes were used to weld the specimens. Typical current ranges[16] and required mechanical and chemical properties are listed in Table 4.2. All low-hydrogen electrodes were stored at 300°F (149°C) for a minimum of 3 hours in a holding oven to comply with AWS specifications.

## 4.2 Specimen Geometries

Several specimen geometries were used to achieve the desired thermal severity (TSN) and degree of restraint. For easier reference, these various specimen geometries are designated as "type 1" through "type 6".

The geometry type of each test specimen is listed in Tables 3.1 through 3.3.

The type 1 specimen geometry is shown in Figure 4.2. The specimen consists of two plates joined by a double-level (AWS B-U5a) welded joint. Plate lengths varied as required for gripping of the tension test specimen. This geometry provides a TSN of 8t and low restraint on the weld.

Types 2 and 3 specimen geometries are shown in Figure 4.3. A type 2 specimen consists of two perpendicular plates joined by a double-level. (AWS TC-U5b) weld. The TSN for this joint is 12t. A type 3 specimen is made by joining a second plate to the completed type 2 (tee) specimen with another double-level (AWS TC-U5b) weld. The TSN for this joint is 16t. Low restraint is imposed on both welds. The surfaces of the tee plate to be welded were hand ground clean of mill scale.

The type 4 specimen geometry is shown in Figure 4.4. A plate was machined to provide for a double-level (AWS B-U5a) joint. This geometry provides a TSN of 8t and high restraint on the weld.

Types 5 and 6 specimen geometries are shown in Figure 4.5. These specimens consist of two plates joined by two fillet welds. The first weld is a type 5 specimen and the second a type 6. All weld passes of the type 5 specimen were completed before welding of the type 6 specimen was started. The TSN for both geometry types is 12t. Low restraint is imposed on the first weld; a higher restraint is imposed on the second weld. Surfaces of the plates to be welded were hand ground clean of mill scale.

## 4.3 Welding of Specimens

The specimens were welded using the following sequence:

1) Plates tack welded together at ends. (This was not required for type 4 specimen geometry).

2) Specimen placed on asbestos sheets in alignment with speed indicator.

3) Specified preheat applied.

4) Weld pass deposited following weld speed indicator.

5) During welding, voltage and current read from meters by an observer. These readings fluctuated rapidly within a range. The median was taken as the representative value.

6) Slag covering back-chipped and brushed. (First pass also hand ground and brushed on bottom side to remove slag covering).

7) Specimen allowed to cool to proper preheat-interpass temperature.

8) Next weld pass deposited.

9) Process (steps 4-8) repeated until weld completed.

## 4.4 Sectioning of Specimens for Testing

After welding had been completed, a minimum of 48 hours was allowed for any possible delayed cracking to occur. The specimens were then photographed, radiographed and sectioned for further testing.

Types 1 and 4 specimens were sectioned as shown in Figure 4.6. Types 2 and 3 specimens were sectioned as shown in Figure 4.7. These specimens were machined to provide one metallurigical specimen of each weld, one reduced-section tension specimen and two side bend specimen.

Types 5 and 6 specimens were sectioned as shown in Figure 4.8. These specimen were machined to provide one metallurgical specimen of each weld.

# 5.0 DESCRIPTION AND RESULTS OF TESTS

## 5.1 Metallographic Studies

Metallographic studies were conducted on the specimens to detect discontinuities which might be present on the cut section. One face of the metallurgical specimens was polished and then etched with 2% nital. A photomacrograph was taken at 3.2 magnification to show the larger discontinuities that might be present. To detect smaller discontinuities not visible in the photomacrograph, the entire weld area was scanned at a 214.4 magnification. Photomicrographs were taken of the typical microstructures at 214.4 magnification and typical discontinuities at 53.6, 107.2 or 214.4 magnification. These photomicrographs are shown in Figs. A1.1 through A1.51.

The number of occurrences of each discontinuity present at the cross section of the weld scanned has been described as follows:

| | | | |
|---|---|---|---|
| None | (N) | = | 0 |
| Few | (F) | = | 1-5 |
| Several | (S) | = | 6-25 |
| Considerable | (C) | = | 26 or more |

Results for all the specimens are given in Tables 5.1 through 5.3.

## 5.2 Radiographic Studies

Radiographic studies were conducted on many of the test specimens to detect the presence of discontinuities throughout the length of the weld. Types 1, 2, 3, and 4 specimens were radiographed after the weld reinforcement had been ground flush with the plates. All radiograph exposures were sensitive to 2% of the plate thickness.

The frequency of the discontinuities detected on the radiographs has been described by the term discontinuity ratio. The discontinuity ratio is defined as the ratio of the area of discontinuity visible on the radiograph to the cross-sectional area of the weld, expressed in percent. Typical radiographs of specimens with relatively high, medium, and low discontinuity ratios are shown in Figure 5.1. Results for all specimens are listed in Tables 5.1 through 5.3.

## 5.3 Hardness Tests

The purpose of the hardness tests was to determine the microstructural hardness of the welded joint. As noted previously hardness gives an indication of the susceptibility to cracking. Vickers diamond hardness surveys using a 200 gram load were taken on the polished and etched metallurgical specimens at the locations shown in Figure 5.2. Additional readings were taken as required in the base metal HAZ near the last weld pass. The data from these surveys are summarized in Tables 5.1 through 5.3. Typical hardness values are plotted in Figures 5.3 through 5.8 for specimens A1A, A1C, B1A, B1C, C1A and C1C.

## 5.4 Tension Tests

The purpose of the tension tests was to determine the strength of the welded specimens. Reduced-section tension tests were conducted on types 1, 2, 3 and 4 specimens. Dimensions of the typical tension coupon specimens were in accordance with Figure 5.10.1.3F of the AWS Structural Welding Code[1]. The computed ultimate stress and locations of failure of these specimens are listed in Tables 5.1 through 5.3. Photos of the tension-test failure surfaces are shown in Figure 5.9.

## 5.5 Bend Tests

The purpose of the bend tests was to determine the soundness and ductility of the welds. Guided side bend tests were performed on type 1, 2, 3 and 4 specimens. Dimensions of the bend test specimens and testing were in accordance with Figures 5.10.1.3H and 5.27.1A, respectively, of the AWS Structural Welding Code[1]. Results of these tests were evaluated by criteria outlined in Section 5.12.2 of the AWS Structural Welding Code[1]. These criteria are as follows:

> "Any specimen in which a crack or other open discontinuity exceeding 1/8-inch (3.2mm) measured in any direction shall be considered as having failed. Cracks occuring on the corners of the specimen during testing shall not be considered."

When more than one open discontinuity occurred, the sum of these were considered in the evaluation. The results of these tests are summarized in Tables 5.1 through 5.3. Photos of the tested bend specimen are shown in Figure 5.10.

# 6.0 DISCUSSION AND ANALYSIS OF TEST RESULTS

## 6.1 Effect of Plate Length

As stated in Section 3.2, specimens A1B and A1D show the effect of specimen plate length (perpendicular to the weld). During the initial phase of specimen fabrication, it was thought that a 5-inch plate length might not provide enough metal to model an infinite heat sink; the available metal would become saturated with the welding heat and not cool the weld properly. To investigate this possibility, specimens A1B (5-inch plate length) and A1D (20-inch plate length) were fabricated first. The test results for these specimens are summarized in Table 5.1. The hardness values (a function of the cooling rate) are approximately the same; it was concluded that the 5-inch plate length used for several of the specimens would provide an adequate heat sink to represent a longer plate. This conclusion is in agreement with Linnert[15], who has stated the following: "The cooling of the heat-affected zone is determined largely by the volume of base metal within a 3-inch radius of the weld. The base metal outside of this radius is too far removed to be influential in determining the rate at which heat is withdrawn from the relatively narrow heat-affected zone, at least during the early important stages of cooling."

## 6.2 Cold Cracking

As discussed in Sections 5.1 and 5.3, hardness tests were conducted to determine the susceptibility of the test specimens to cold cracking and metallographic studies were conducted to determine what cold cracking had occurred. Following is a discussion and analysis of the results of these tests.

Results of the hardness surveys of specimens A1A, A1C, B1A, B1C, C1A, and C1C (plotted in Figs. 5.3 through 5.8) show the following. First, specimens A1A (341HV) and B1A (490HV) had greater maximum hardnesses than specimens A1C (232 HV) and B1C (294 HV), respectively. Thus, for the mild and low-alloy steels, preheat temperatures of 225°F and 300°F had a beneficial effect in reducing hardness. However, specimens C1A (457 HV)

and C1C (457 HV) had the same maximum HAZ hardness even though C1C had been preheated to 300°F. Thus, for the quenched and tempered steel, preheat did not have a beneficial effect in reducing HAZ hardness. Second, for specimens A1C, B1A, B1C, C1A, and C1C (multipass welds), the maximum HAZ hardness occurred near the fusion line of the last weld pass. The portion of the base metal HAZ formed by the other weld passes was tempered by the subsequent weld passes. However, for specimen A1A (see Figure A1.21g), the last weld pass occurred at the top-center of the weld cross section and tempered all of the base metal HAZ. Thus, for specimen A1A a lower maximum hardness was measured than would have occurred if the last weld pass had been adjacent to the base metal.

The effects of the various welding variables included in this study on the HAZ hardness are illustrated in Figs. 6.1 through 6.3. In these figures, the ranges of measured HAZ hardness have been plotted for the various specimens; they have been grouped to show the effect of preheat, arc energy, thermal severity number, electrode and joint type. Based on the data and these figures the following observations can be made. For the mild steel specimens (see Fig. 6.1) and the low-alloy steel specimens (see Fig. 6.2), an increase in preheat, an increase in arc energy, and a decrease in TSN (factors which reduce cooling rate) resulted in a reduced maximum HAZ hardness. It is noted that for specimens A1A (Fig. A1.2- top center of weld cross-section), D1A (Fig. A1.30 - bottom right of weld) and A3C (Fig. A1.9 - bottom center of weld) the last pass was deposited on the weld metal and not base metal. Consequently, it has been concluded, for reasons discussed in the preceding paragraph, that all of the HAZ was softened. For the quenched and tempered steels (see Fig. 6.3) the effects of preheat, arc energy, and TSN were small, although specimens C2B and D2C (high arc energy) and C3A (low TSN) had slightly reduced maximum hardnesses.

The type of electrode in general had little effect on hardness; this is to be expected. It is noted that for specimen B4B, the last weld pass (bottom of weld cross-section in Fig. A1.21g) did not form base metal HAZ but retempered the portion of the HAZ formed by the underlying weld pass. This probably accounts for the lower hardness (412 HV) as compared to

specimen B2A (473HV). The effect of joint type was also small; the full penetration (TC-U5a) joints had only slightly greater maximum hardnesses than the fillet welds. Finally, the effect of type of welding current was small; specimens E4A and F4A (DCEP-reverse polarity) had, on the average only slightly higher maximum hardnesses than specimens E4B and F4B (DCEN-straight polarity).

In summary, factors which reduced the cooling rate (increased preheat, increased arc energy, or decreased TSN) reduced the maximum HAZ hardness for the mild steel and low-alloy steel specimens, but did not have a significant effect on the maximum HAZ hardness of the quenched and tempered steel specimens. Also, the electrode type, joint type, and type of current did not affect the maximum HAZ hardness.

The relationship between the welding procedures used for this study and the welding requirements suggested by Coe[5], Bailey[12] and Bradstreet[13] to minimize HAZ cold cracking are shown in Figs. 6.3 through 6.6 Plotted in these figures are curves which represent the suggested preheat temperatures as a function of TSN for a given arc energy and hydrogen level. As discussed in Section 2.2.4.2, these suggested preheat temperatures are based on HAZ hardness control. Thus, a welding procedure which plots above a given curve should, according to the reference indicated, produce a maximum HAZ hardness which is lower than the critical hardness for which the curves have been developed. Conversely, a welding procedure which plots below a given curve should produce a maximum HAZ hardness which is higher than the critical hardness. The current AWS Structural Welding Code[1] minimum preheat temperatures are shown, assuming that two equal sized plates are being welded as is the case for the test specimens.

Also plotted in Figs. 6.4 through 6.6 are the welding conditions for the test specimens which are indicated by the specimen identification, maximum measured HAZ hardness (number in parenthesis), and symbols which refer to the type of cold cracking found in the specimens (W=weld metal cracking, C = HAZ cracking). Based on these figures, the following observations have been made.

First, for the mild steel specimens (see Fig. 6.4) and the low-alloy steel specimens (see Fig. 6.5), the hardness values indicate that curves which fall about midway between those suggested by Bailey[12] and Coe[5] would best predict the critical HAZ hardness. All mild and low-alloy steel specimens which plotted above the Bailey curves had maximum measured HAZ hardnesses that were less than the critical hardness. However, for the quenched and tempered steel specimens (see Fig. 6.6), the AWS[1] and Coe[5] curves do not appear to provide an adequate means of controlling hardness. As discussed in the preceding paragraphs, cooling rate (basis of the curves) did not appear to have a significant effect on maximum hardness of the quenched and tempered steel specimens and hence hardness control by this method does not appear possible; Graville[4] has come to the same conclusion.

Second, no HAZ cracks occurred in any of the low restraint (types 1, 2, 3, and 5 geometry) or medium restraint (type 6 geometry) mild or low-alloy steel specimens, even though several of these specimens had hardnesses which were greater than the critical hardness. This suggests that under conditions of low restraint, higher critical hardnesses than those suggested can probably be tolerated without HAZ cracking. However, under conditions of very high restraint (type 4 geometry), specimen D1C (Figs. A1.32 and 5.10) cracked even though the maximum measured HAZ hardness was well below the suggested critical hardness (232 HV<<350HV). Graville[4] has also observed HAZ cracks in soft microstructures in very highly restrained butt welds. This suggests that under conditions of very high restraint, either lower critical hardnesses than those suggested or some other form of treatment must be used to minimize HAZ cracking. Thus, it is apparent that restraint should play a significant role in the establishment of a critical HAZ hardness.

Weld metal microcracks occurred in many of the test specimens welded with E6010 electrodes, but were not observed in welds produced with E7024, E7028, E7018, or E11018 electrodes. The microcracks were often associated with small inclusions (see Figs. A1.2 through A1.9, A1.30, A1.31, A1.38, and A1.39); Graville[4] has suggested that the inclusions provide sites for initiation of cracking. The microcracks which appear in the retempered

weld zones probably occurred in the weld metal and remained when the surrounding metal was retempered by a succeeding weld pass. Hardness readings taken near weld metal microcracks in several of the specimens ranged from 187 HV to 238 HV. Furthermore, it was observed that the cracks did not always occur in the hardest portion of the weld metal.

The effects of various welding variables on weld metal microcracking are illustrated in Figure 6.7. Increased preheat temperature, increased arc energy, and decreased TSN (factors which reduce cooling rate) reduced the occurrence of microcracks, as did the use of low-hydrogen electrodes. Thus it is apparent that these variables play an important role in much the same way as in HAZ cracking. In fact, inspection of Fig. 6.4 shows that test procedures using EG010 electrodes which are above the Bailey[12] curves (developed for HAZ cracking) did not produce microcracking, and test procedures which are below the Bailey curves did produce microcracking. It is apparent that even though the Bailey curves were not developed for weld metal microcracking, they do give a good indication of the welding requirements necessary to minimize the microcracking.

## 6.3 Hot Cracking

Preliminary welding requirements to minimize hot cracking were developed in Section 2.3.4. Figures 6.8 through 6.10 show the relationship between the proposed welding requirements (plotted as curves) and the test welding procedures. A welding procedure which plots to the left of the curves should not produce hot cracking. Conversely, a welding procedure which plots to the right of the appropriate curve (depending on degree of penetration) should produce hot cracking.

The presence of hot cracking was detected in several specimens in the metallographic inspections. These specimens are indicated by the symbol "H" (Figs. 6.8-6.10), and photos of typical hot cracks are shown in Appendix A. Although only a limited number of data points are available, some trends do develop. For the mild steel specimens (see Fig. 6.8), there is a fairly good agreement between predicted and actual behavior, but some adjustment appears to be necessary for the Group 2 electrodes. For the low-alloy steel specimens (see Fig. 6.9), the

preliminary requirements appear to be too conservative. For the quenched and tempered steels (see Fig. 6.10), there is good agreement between predicted and actual behavior, but again only a limited number of data points are available for comparison.

## 6.4 Porosity, Slag Inclusions and Lack of Fusion

The effects of various welding variables on the radiographic discontinuity ratio are shown in Figs. 6.11 through 6.13. From these figures, it is difficult to detect definite trends between discontinuity ratio and the welding variables. However, it appears that in general an increase in arc energy reduces the discontinuity ratio. It would also be expected from the discussion in Section 2, that an increase in preheat temperature and a decrease in TSN (factors which reduce cooling rate) would also reduce the discontinuity ratio, but this cannot be shown conclusively on the basis of the test results.

For the mild steel specimens which were welded with E6010 electrodes (see Fig. 6.11), the discontinuity ratio varied from 17 to 56%. The specimens were welded with an arc energy ranging from 21 to 34 KJ/in. and a current ranging from 108 to 133 Amps (see Table 3.1). The recommended current range for this electrode is 140-225 Amps. (see Table 4.2). The welding conditions selected for the mild steel specimens welded with E6010 electrodes were based on a desire to produce cold cracking. To insure this, low currents were selected to limit the arc energy. Thus, by using a current below the recommended current range a relatively high discontinuity ratio was produced.

For the low-alloy steel specimens which were welded with E7018 electrodes (see Fig. 6.12), the discontinuity ratio varied from 1 to 16% which is on the average considerably lower than for the mild steel E6010 specimen group. The specimens were welded with an arc energy ranging from 31 to 56 KJ/in. and a current ranging from 189 to 289 Amps. (see Table 3.2). The recommended current range for this electrode is 170-280 Amps. (see Table 4.2). Thus, the test welding currents ranged from within to slightly above the recommended range. Comparison of this specimen group to the mild steel E6010 specimen group shows that by staying within the

recommended electrode current range, a lower discontinuity ratio is produced.

For the quenched and tempered steel specimens which were welded with E11018 electrodes (see Fig. 6.13), the discontinuity ratio varied from 1 to 7% which is on the average somewhat lower than for the low alloy steel E7018 specimen group. The specimens were welded with an arc energy ranging from 32 to 69 KJ/in. and a current ranging from 187 to 291 Amps (see Table 3.3). The recommended current range for this electrode is 160-280 Amps (see Table 4.2). Thus the test welding currents were within to slightly above the recommended range. In general, the arc energies were higher, the TSN was lower, and the preheat temperatures were slightly higher than for the low alloy E7018 specimen group.

In summary, the use of increased arc energy and maintaining proper current reduced the discontinuity ratio. Increased preheat temperature and reduced TSN would also be expected to reduce the occurrence of discontinuities but the test results do not show this latter effect conclusively.

## 6.5 Tensile Strength

The effects of various welding variables on joint efficiency are shown in Figs. 6.14 through 6.16. These figures show that the major influence of the welding variables is their effect on the development of weld discontinuities. Significant reductions in joint efficiency occurred only in the presence of weld discontinuities such as weld metal microcracks, HAZ cracks, slag inclusions, and lack of fusion. For instance, specimen A1A had a 12% reduction in joint efficiency due to the combined effects of slag, LOF, and weld metal microcracks. Specimen D1A had a 30% reduction in joint efficiency due to the combined effects of slag, LOF, weld metal microcracks, and HAZ cracking. Specimen D2C had a 27% reduction due to the combined effects of hot cracking and slag. It is apparent that discontinuities can result in significant reductions in joint efficiency; the various welding variables are important factors in the formation of the discontinuities.

## 6.6 Ductility

Side bend tests were conducted to determine the ductility of the welded specimens. The results of the tests are summarized in Tables 5.1 through 5.3.

Of the mild steel specimens (see Table 5.1 and Fig. 5.10), only specimen A3A passed the bend tests. Specimens A1C and A4A failed during bending due to the formation of cracks which initiated at discontinuities. The other specimens of this group failed prior to bending due to discontinuities which exceeded the testing criteria outlined in Section 5.5.

Of the low-alloy steel specimens (see Table 5.2 and Fig. 5.10), only specimens B2B and D3A passed the bend tests. It is noted that specimen B2B was welded using the highest arc energy and had the lowest discontinuity ratio of this specimen group. Specimens B1C, B4B, and D3B failed prior to bending due to discontinuities which exceeded the testing criteria. The other specimens of this group failed during bending due to the formation of cracks which initiated at discontinuities.

Of the quenched and tempered steel specimens (see Table 5.3 and Fig. 5.10), only specimen C3A passed the bend tests. Specimen D2C failed prior to bending due to discontinuities which exceeded the testing criteria. The other specimens of this group failed during bending due to the formation of cracks in the HAZ. It was observed that the cracks initiated in areas of the HAZ which had experienced necking deformations; no noticeable deformations occurred in the weld metal or base metal. It is further noted that many of the quenched and tempered steel specimen HAZ's were softened by the welding (see Fig. 6.3), thus reducing the yield strength. Linnert[15] observed failures in bend tests of quenched and tempered steel specimens welded with electrodes which over-matched the base metal yield strength. Linnert suggests that excessive localized elongation occurs in the lower-yield-strength steel. Based on the observation that excessive deformations occurred in the HAZ's, it has been concluded that one or both of the factors discussed above contributed to the failure of the quenched and tempered bend test specimens.

In summary, the test results of the mild and low-alloy steel specimens further demonstrates the importance of minimizing discontinuities. Many of the specimens were not able to deform sufficiently due to stress concentrations caused by the discontinuities. For the quenched and tempered steel, the test results show that the weld metal should not overmatch the base metal strength excessively and the arc energy must be properly controlled to avoid softening in the HAZ.

# 7.0 CONCLUSIONS AND RECOMMENDATIONS

## 7.1 Cold Cracking

As discussed in Section 6.2, the test results show that the preheat temperatures recommended by Bailey[12] give a slightly conservative prediction of maximum HAZ hardness. The test results also show that a greater HAZ hardness can be tolerated without HAZ cracking under conditions of reduced restraint. For example, Bailey[12] and Coe,[5] among others, suggest critical hardnesses of 350HV (other-than-low hydrogen) and 400HV (low hydrogen) for conditions of medium restraint (see Fig. 2.4). However, low restraint specimens A3B (other-than-low hydrogen) and B3C (low hydrogen) tolerated hardnesses of 399HV and 509HV respectively, without HAZ cracking. Furthermore, it was observed that the preheat temperatures recommended by Bailey[12] to minimize HAZ cracking in medium restraint joints were sufficient to minimize weld metal microcracking even in the test specimens welded with E6010 electrodes.

Based on the above findings, Table 7.1 has been developed which summarizes the preheat temperatures recommended to produce HAZ hardnesses which are less than the critical hardnesses. The critical hardnesses selected for the various welding conditions are summarized in Table 7.2.

Table 7.1 has been consolidated to some extent to produce Table 7.3, which lists the recommended preheat temperature for a given TSN, arc energy, CE, and hydrogen level. Linear interpolations may be made for conditions which fall between those tabulated.

A comparison of the recommended preheat temperatures to the current AWS Structural Welding Code[1] requirements is shown in Figure 7.1. In plotting the AWS Structural Welding Code requirements, it has been assumed that two equal thickness plates are being joined. For a typical mild steel (see Fig. 7.1a), the recommended preheat temperatures are for the most part below those specified by the AWS Structural Welding Code. For a typical low-alloy steel (see Fig. 7.1b), however, the recommended preheat temperatures are for the most part above those specified by the AWS Structural Welding Code.[1]

In addition to the application of the recommended preheats, the general procedural steps outlined in Section 2.2 should be taken. These steps include cleaning and drying of surfaces to be welded and proper baking of electrodes.

Since the above recommendations are based on a study of a limited number of test welds, further study of cold cracking is recommended. These studies should include a wider range of electrodes, steel chemistries, and joint types. The critical hardnesses for a wider range of hydrogen level, joint geometry, and restraint need to be established also.

## 7.2 Hot Cracking

As discussed in Section 6.3, the test results of the mild and quenched and tempered steel specimens show fairly good agreement with the behavior predicted by the preliminary welding requirements developed in section 2.3.4. However, the test results of the low-alloy steel specimens do not show the same type of agreement to the predicted behavior; the preliminary welding requirements are overconservative for the low-alloy steel specimens.

The preliminary welding requirements to minimize hot cracking are all based on the control of weld metal carbon content. However, other elements have also been shown[14] to have an effect on hot cracking. Thus, other elements may also have to be considered in the formulating welding requirements.

On the basis of the study presented herein, no specific recommendations can be made to minimize hot cracking. It has been shown in the tests, however, that combinations of high welding speed and high arc energy can produce hot cracking. Thus, such situations should be avoided. Further study of hot cracking is recommended to evaluate further the preliminary welding requirements and, if necessary, to establish more valid or effective requirements.

## 7.3 Porosity, Slag Inclusions, and Lack of Fusion

As discussed in Section 6.4, the test results show that increased arc energy reduced the occurrence of porosity, slag inclusions, and lack

of fusion. Staying within the recommended current range has also been shown to be an important consideration.

In addition to maintaining proper welding current and arc energy, the steps outlined in Sections 2.4 through 2.6 should also be followed. These steps include cleaning of surfaces to be welded, proper removal of slag covering between passes, providing proper joint geometry, and use of proper electrode size.

On the basis of the study presented herein, no specific recommendations can be made regarding suitable arc energies. Furthermore, it is recommended that further testing be conducted to establish appropriate arc energy ranges for the various electrodes. The suggested arc energy ranges could then be incorporated along with the suggested current ranges into the appropriate welding codes or specifications.

## List of References


1. AWS Structural Welding Code (D1.1-81).

2. Marshalla, R. and Munse, W. H., "Welding Requirements to Minimize Cold Cracking in Bridge Steels", Draft Report for IHR-304, Feb. 1978.

3. Handel, W. and Munse, W. H., "Welding Requirements to Minimize Hot Cracking, Porosity and Slag Inclusions in Bridge Steels", Draft Report for IHR-304, June 1971.

4. Graville, B. A., The Principles of Cold Cracking Control in Welds, Dominion Bridge Company, Limited, 1975.

5. Coe, F. R., Welding Steels Without Hydrogen Cracking, The Welding Institute (England) 1973.

6. Bailey, N., "The Establishment of Safe Welding Procedures for Steels", Welding Journal, April 1972, p. 169s-177s.

7. Winterton, K., "Weldability Prediction from Steel Composition to Avoid HAZ Cracking", Welding Journal, June 1961, p. 253s-258s.

8. Cottrell, C. L. M., Bradstreet, B. J., "A Method for Calculating the Effect of Preheat on Weldability", British Welding Journal, July 1955, p. 305-309.

9. Blodgett, O., Design of Welded Structures, p. 7.2-11 - 7.2-18.

10. Rosenthal, D., "Mathematical Theory of Heat Distribution During Welding and Cutting", Welding Journal, May 1941, p. 220s-234s.

11. Stout, R. D., Doty, W. D., Weldability of Steels, Welding Research Council, 1978, Third Edition.

12. Bailey, N., "Welding Carbon: Manganese Steels", Metal Construction, 2(10), 1970, pp. 442-446.

13. Bradstreet, B. J., "Methods to Establish Procedures for Welding Low Alloy Steels", Engineering Journal, Vol. 46, No. 11, 1963, pp. 37-41.

14. Borland, J. C., "Suggested Explanation of Hot Cracking in Mild and Low Alloy Steel Welds", British Welding Journal, Aug. 1961, pp. 526-540.

15. Linnert, G. E., Welding Metallurgy, Volume 2, American Welding Society, 1967, Third Edition.

16. AWS Electrode Specifications (A5.1, A5.5) 1969.

17. Jackson, C. E. and Goodwin, W. J., "Effect of Variations of Welding Technique on the Transition Behavior of Welded Specimens", Welding Journal 27(5), pp. 253s-266s, (1948).

18. Lancaster, J. F., The Metallurgy of Welding Brazing and Soldering, American Elsevier Publishing Co., Inc., p. 76, (1965).

19. Bowman, Mark D., and Munse, W. H., "The Effect of Discontinuities on the Fatigue Behavior of Transverse Butt Welds in Steel", University of Illinois, Department of Civil Engineering, Structural Research Series No. 491, Illinois Cooperative Highway and Transportation Research Program Series No. 189, April 1981.

20. Houldcroft, P. T., British Welding Journal, 1954, 1, 470.

Table 2.1

Estimated Percentage Dilution at Various Weld Speeds and Arc Energies

| ARC ENERGY (KJ/IN) | WELD SPEED (IN/MIN) / Penetration | 4 | 6 | 8 | 10 | 12 | 14 | 16 | 18 | 20 |
|---|---|---|---|---|---|---|---|---|---|---|
| 20 | High | 2 | 5 | 11 | 17 | 17 | 21 | 21 | 23 | 29 |
| | Medium | 1 | 4 | 8 | 12 | 13 | 15 | 15 | 17 | 22 |
| | Low | 1 | 2 | 4 | 6 | 6 | 8 | 7 | 9 | 11 |
| 30 | High | 8 | 17 | 27 | 32 | 37 | 38 | 43 | 48 | 49 |
| | Medium | 6 | 12 | 20 | 24 | 27 | 28 | 32 | 36 | 37 |
| | Low | 3 | 6 | 10 | 12 | 14 | 14 | 16 | 13 | 18 |
| 40 | High | 13 | 27 | 41 | 47 | 50 | 51 | 59 | 59 | 59 |
| | Medium | 10 | 20 | 30 | 35 | 37 | 38 | 44 | 44 | 44 |
| | Low | 5 | 10 | 15 | 17 | 19 | 19 | 22 | 22 | 22 |
| 45 | High | 32 | 40 | 47 | 51 | 56 | 59 | 62 | 66 | 66 |
| | Medium | 24 | 30 | 35 | 38 | 42 | 44 | 46 | 50 | 50 |
| | Low | 12 | 15 | 18 | 19 | 21 | 22 | 23 | 25 | 25 |
| 50 | High | 28 | 41 | 51 | 56 | 61 | 63 | 66 | 66 | 66 |
| | Medium | 21 | 31 | 38 | 42 | 45 | 47 | 50 | 50 | 50 |
| | Low | 10 | 15 | 19 | 21 | 23 | 23 | 25 | 25 | 25 |
| 60 | High | 37 | 53 | 63 | 67 | 75 | 75 | 77 | 74 | 69 |
| | Medium | 28 | 38 | 47 | 50 | 56 | 56 | 57 | 55 | 51 |
| | Low | 14 | 19 | 24 | 25 | 28 | 29 | 29 | 27 | 26 |
| 65 | High | 44 | 60 | 74 | 79 | 86 | 83 | 79 | 77 | 69 |
| | Medium | 33 | 45 | 55 | 59 | 65 | 62 | 59 | 57 | 51 |
| | Low | 16 | 22 | 28 | 30 | 33 | 31 | 30 | 29 | 27 |

Table 2.2

Grouping of Electrodes

| Manual Shielded Metal Arc Welding | Electrode Group |
|---|---|
| **Mild Steel Electrodes** | |
| E4510* | 1 |
| E4520* | 1 |
| E6010 | 1 |
| E6011 | 1 |
| E6012* | 1 |
| E6013 | 2 |
| E6020* | 2 |
| E6027 | 2 |
| E7014 | 2 |
| E7015 | 2 |
| E7016 | 2 |
| E7018 | 2 |
| E7024 | 2 |
| E7028 | 2 |
| **Low-Alloy Steel Electrodes** | |
| E70XX-AX* | 1 |
| E80XX-B1 | 3 |
| E80XX-B2 | 1 |
| E80XX-CX | 1 |
| E90XX-B3 | 3 |
| E90XX-D1 | 1 |
| E100XX-D2 | 3 |
| EXXXX-BXL | 1 |
| EXXXX-G | 1 |

*Because of the low manganese contents of the deposited weld metal for electrodes E4510, E4520, E6012, E6020, E7011-A1, E7010-A1, these electrodes should not be used at arc levels less than 35,000 Joules/in.

Table 3.1

Fabrication Data for Mild Steel Test Specimens

| Specimen Designation | Steel Type | Geometry Type(1) | Plate Thickness | TSN (inches) | Restraint | Preheat (°F) | Number of Weld Passes | Travel Speed (in/min) | | Electrode | | | Test Ave. Current (amps) | | Test Ave. Current (volts) | | Arc Energy (kJ/in) | Power Type(2) |
|---|---|---|---|---|---|---|---|---|---|---|---|---|---|---|---|---|---|---|
| | | | | | | | | Root Passes | Outer Passes | Type | Root Passes | Outer Passes | Root Passes | Outer Passes | Root Passes | Outer Passes | | |
| A1A | mild | 1 | 1" | 8 | low | 70° | 14 | 6 | 8 | E6010 | 1/8" | 3/16" | 80 | 108 | 28 | 25 | 21 | DCEP |
| A1B | mild | 1 | 1" | 8 | low | 150° | 15 | 6 | 8 | E6010 | 1/8" | 3/16" | 93 | 130 | 28 | 26 | 25 | DCEP |
| A1C | mild | 1 | 1" | 8 | low | 225° | 14 | 6 | 8 | E6010 | 1/8" | 3/16" | 100 | 130 | 26 | 26 | 25 | DCEP |
| A1D | mild | 1 | 1" | 8 | low | 150° | 14 | 6 | 8 | E6010 | 1/8" | 3/16" | 90 | 123 | 28 | 27 | 25 | DCEP |
| A2A | mild | 1 | 1" | 8 | low | 70° | 12 | 5 | 6 | E6010 | 1/8" | 3/16" | 98 | 130 | 29 | 26 | 34 | DCEP |
| A3A | mild | 1 | 1/2" | 4 | low | 70° | 6 | 6 | 8 | E6010 | 1/8" | 3/16" | 98 | 133 | 28 | 26 | 27 | DCEP |
| A3B | mild | 2 | 1" | 12 | low | 70° | 13 | 6 | 8 | E6010 | 1/8" | 3/16" | 103 | 125 | 28 | 27 | 25 | DCEP |
| A3C | mild | 3 | 1" | 16 | low | 70° | 12 | 6 | 8 | E6010 | 1/8" | 3/16" | 95 | 121 | 28 | 26 | 24 | DCEP |
| A4A | mild | 1 | 1" | 8 | low | 70° | 10 | 4 | 8 | E7018 | 1/8" | 3/16" | 120 | 184 | 22 | 22 | 32 | DCEP |
| A4B | mild | 1 | 1" | 8 | low | 70° | 8 | 6 | 8 | E7028 | 5/32" | 3/16" | 198 | 268 | 30 | 30 | 59 | DCEP |
| D1A | mild | 4 | 1" | 8 | high | 70° | 14 | 6 | 8 | E6010 | 1/8" | 3/16" | 98 | 128 | 27 | 26 | 25 | DCEP |
| D1B | mild | 4 | 1" | 8 | high | 150° | 12 | 6 | 8 | E6010 | 1/8" | 3/16" | 110 | 129 | 25 | 26 | 25 | DCEP |
| D1C | mild | 4 | 1" | 8 | high | 225° | 12 | 6 | 8 | E6010 | 1/8" | 3/16" | 95 | 130 | 29 | 26 | 26 | DCEP |
| E1A | mild | 5 | 1" | 12 | low | 70° | 3 | - | 8 | E6010 | - | 3/16" | - | 115 | - | 23 | 20 | DCEP |
| F1A | mild | 6 | 1" | 12 | med | 70° | 3 | - | 8 | E6010 | - | 3/16" | - | 127 | - | 21 | 20 | DCEP |
| E4A | mild | 5 | 1" | 12 | low | 70° | 3 | - | 8 | E7024 | - | 3/16" | - | 167 | - | 30 | 38 | DCEP |
| F4A | mild | 6 | 1" | 12 | med | 70° | 3 | - | 8 | E7024 | - | 3/16" | - | 173 | - | 28 | 37 | DCEP |
| E4B | mild | 5 | 1" | 12 | low | 70° | 3 | - | 8 | E7024 | - | 3/16" | - | 160 | - | 32 | 38 | DCEN |
| F4B | mild | 6 | 1" | 12 | med | 70° | 3 | - | 8 | E7024 | - | 3/16" | - | 163 | - | 29 | 36 | DCEN |
| E4C | mild | 5 | 1" | 12 | low | 70° | 3 | - | 8 | E7024 | - | 3/16" | - | 245 | - | 38 | 70 | AC |
| F4C | mild | 6 | 1" | 12 | med | 70° | 3 | - | 8 | E7024 | - | 3/16" | - | 243 | - | 38 | 70 | AC |

(1) See Figures 4.2 through 4.5 for sketches of specimen geometries.
(2) Welding polarity; DCEP = reverse polarity, DCEN = straight polarity, AC = alternating polarity.

Table 3.2

Fabrication Data for Low-Alloy Steel Test Specimens

| Specimen Designation | Steel Type | Geometry Type(1) | Plate Thickness | TSN (inches) | Restraint | Preheat (°F) | Number of Weld Passes | Travel Speed (in/min) | | Electrode | | | Test Ave. Current (amps) | | Test Ave. Current (volts) | | Arc Energy (kJ/in) | Power Type(2) |
|---|---|---|---|---|---|---|---|---|---|---|---|---|---|---|---|---|---|---|
| | | | | | | | | Root Passes | Outer Passes | Type | Root Passes | Outer Passes | Root Passes | Outer Passes | Root Passes | Outer Passes | | |
| B1A | A441 | 1 | 1" | 8 | low | 70° | 10 | 5 | 8 | E7018 | 1/8" | 3/16" | 120 | 191 | 22 | 22 | 33 | DCEP |
| B1B | A441 | 1 | 1" | 8 | low | 200° | 12 | 5 | 8 | E7018 | 1/8" | 3/16" | 118 | 192 | 23 | 22 | 32 | DCEP |
| B1C | A441 | 1 | 1" | 8 | low | 300° | 10 | 5 | 8 | E7018 | 1/8" | 3/16" | 123 | 190 | 22 | 22 | 32 | DCEP |
| B2A | A441 | 1 | 1" | 8 | low | 70° | 9 | 4 | 6 | E7018 | 1/8" | 3/16" | 150 | 191 | 23 | 22 | 44 | DCEP |
| B2B | A441 | 1 | 1" | 8 | low | 70° | 8 | 4 | 8 | E7018 | 1/8" | 3/16" | 145 | 289 | 25 | 26 | 56 | DCEP |
| B3A | A441 | 1 | 1/2" | 4 | low | 200° | 4 | 5 | 8 | E7018 | 1/8" | 3/16" | 118 | 195 | 23 | 23 | 32 | DCEP |
| B3B | A441 | 2 | 1" | 12 | low | 200° | 12 | 5 | 8 | E7018 | 1/8" | 3/16" | 113 | 189 | 23 | 22 | 32 | DCEP |
| B3C | A441 | 3 | 1" | 16 | low | 200° | 12 | 5 | 8 | E7018 | 1/8" | 3/16" | 123 | 190 | 22 | 22 | 31 | DCEP |
| B4A | A441 | 1 | 1" | 8 | low | 200° | 10 | 5 | 8 | E6010 | 1/8" | 3/16" | 100 | 167 | 29 | 27 | 34 | DCEP |
| B4B | A441 | 1 | 1" | 8 | low | 70° | 8 | 7 | 8 | E7028 | 5/32" | 3/16" | 175 | 228 | 29 | 27 | 45 | DCEP |
| D3A | A441 | 4 | 1/2" | 4 | high | 200° | 4 | 5 | 8 | E7018 | 1/8" | 3/16" | 128 | 190 | 24 | 22 | 34 | DCEP |
| D3B | A441 | 4 | 1" | 8 | high | 200° | 12 | 5 | 8 | E7018 | 1/8" | 3/16" | 130 | 190 | 23 | 22 | 32 | DCEP |
| E3A | A441 | 5 | 1/2" | 6 | low | 200° | 1 | - | 8 | E7018 | - | 3/16" | - | 175 | - | 22 | 29 | DCEP |
| F3A | A441 | 6 | 1/2" | 6 | med | 200° | 1 | - | 8 | E7018 | - | 3/16" | - | 175 | - | 23 | 30 | DCEP |
| E3B | A441 | 5 | 1" | 12 | low | 200° | 3 | - | 8 | E7018 | - | 3/16" | - | 187 | - | 23 | 32 | DCEP |
| F3B | A441 | 6 | 1" | 12 | med | 200° | 3 | - | 8 | E7018 | - | 3/16" | - | 193 | - | 23 | 34 | DCEP |

1) See Figures 4.2 through 4.5 for sketches of specimen geometries.
2) Welding polarity; DCEP = reverse polarity, DCEN = straight polarity, AC = alternating polarity.

Table 3.3

Fabrication Data for Quenched and Tempered Steel Test Specimens

| Specimen Designation | Steel Type | Geometry Type(1) | Plate Thickness | TSN (inches) | Restraint | Preheat (°F) | Number of Weld Passes | Travel Speed (in/min) | | Electrode | | | Test Ave. Current (amps) | | Test Ave. Current (volts) | | Arc Energy (kJ/in) | Power Type(2) |
|---|---|---|---|---|---|---|---|---|---|---|---|---|---|---|---|---|---|---|
| | | | | | | | | Root Passes | Outer Passes | Type | Root Passes | Outer Passes | Root Passes | Outer Passes | Root Passes | Outer Passes | | |
| C1A | A514 | 1 | 3/4" | 6 | low | 150° | 6 | 4 | 6 | E11018 | 1/8" | 3/16" | 123 | 190 | 24 | 22 | 43 | DCEP |
| C1B | A514 | 1 | 3/4" | 6 | low | 225° | 6 | 4 | 6 | E11018 | 1/8" | 3/16" | 125 | 190 | 24 | 22 | 43 | DCEP |
| C1C | A514 | 1 | 3/4" | 6 | low | 300° | 6 | 4 | 6 | E11018 | 1/8" | 3/16" | 120 | 190 | 24 | 22 | 42 | DCEP |
| C2A | A514 | 1 | 3/4" | 6 | low | 225° | 6 | 5 | 8 | E11018 | 1/8" | 3/16" | 115 | 190 | 24 | 22 | 32 | DCEP |
| C2B | A514 | 1 | 3/4" | 6 | low | 225° | 6 | 4 | 7 | E11018 | 1/8" | 3/16" | 153 | 291 | 33 | 26 | 69 | DCEP |
| C3A | A514 | 1 | 3/8" | 3 | low | 225° | 4 | 5 | 7 | E11018 | 1/8" | 3/16" | 140 | 215 | 29 | 24 | 46 | DCEP |
| C3B | A514 | 2 | 3/4" | 9 | low | 225° | 6 | 5 | 7 | E11018 | 1/8" | 3/16" | 140 | 228 | 27 | 23 | 44 | DCEP |
| C3C | A514 | 3 | 3/4" | 12 | low | 225° | 6 | 5 | 7 | E11018 | 1/8" | 3/16" | 148 | 214 | 24 | 22 | 40 | DCEP |
| D2A | A514 | 4 | 3/4" | 6 | high | 225° | 6 | 5 | 8 | E11018 | 1/8" | 3/16" | 115 | 190 | 25 | 22 | 32 | DCEP |
| D2B | A514 | 4 | 3/4" | 6 | high | 225° | 6 | 4 | 6 | E11018 | 1/8" | 3/16" | 128 | 187 | 24 | 22 | 43 | DCEP |
| D2C | A514 | 4(3) | 3/4" | 6 | high | 225° | 11(3) | 4 | 7 | E11018 | 1/8" | 3/16" | 145 | 285 | 31 | 28 | 68 | DCEP |
| E2A | A514 | 5 | 3/4" | 9 | low | 225° | 3 | - | 7 | E11018 | - | 3/16" | - | 207 | - | 24 | 43 | DCEP |
| F2A | A514 | 6 | 3/4" | 9 | med | 225° | 3 | - | 7 | E11018 | - | 3/16" | - | 210 | - | 24 | 43 | DCEP |

(1) See Figures 4.2 through 4.5 for sketches of specimen geometries.
(2) Welding polarity; DCEP = reverse polarity, DCEN = straight polarity, AC = alternating polarity
(3) Machining error occured as shown in Figure 4.4. Burn-through occured on first five passes due to inadequate root land.

Table 4.1

Summary of Mechanical and Chemical Properties of Base Metals

| Steel Type | Plate Thickness | Ultimate Strength (KSI) | Hardness (HV)(1) | Chemical Composition - % by Weight | | | | | | | | | Carbon Equivalent (CE)(2) |
|---|---|---|---|---|---|---|---|---|---|---|---|---|---|
| | | | | Carbon (C) | Manganese (Mn) | Silicon (Si) | Chromium (Cr) | Molybdenum (Mo) | Vanadium (V) | Nickel (Ni) | Copper (Cu) | Sulphur (S) | |
| Mild | 1" | 61.6 | 145 | 0.17 | 0.44 | <0.01 | <0.02 | <0.01 | - | <0.01 | <0.04 | 0.035 | 0.25 |
| A441 | 1" | 86.3 | 187 | 0.18 | 1.16 | 0.22 | 0.02 | <0.01 | 0.057 | 0.02 | 0.22 | 0.025 | 0.44 |
| A514 | 3/4" | 129 | 341 | 0.15 | 0.85 | 0.27 | 0.51 | 0.49 | 0.057 | 0.86 | 0.25 | 0.017 | 0.62 |

(1) HV = Vickers hardness (200 gram load) - average value from test data.
(2) CE = C + (Mn + Si)/6 + (Cr + Mo + V)/5 + (Ni + Cu)/15.

See Figure A1.1 for photomicrographs of base metals.

Table 4.2

Summary of Electrode Current Ranges and Weld Metal Compositions

| Electrode | Min. Tensile Strength (KSI) | Min. Yield Point (KSI) | Current Range (1/8-inch dia.) | Current Range (5/32-inch dia.) | Current Range (3/16-inch dia.) | Chemical Composition | | | | | | | | | Remarks |
|---|---|---|---|---|---|---|---|---|---|---|---|---|---|---|---|
| | | | | | | Carbon (C) | Manganese (Mn) | Silicon (Si) | Chromium (Cr) | Molybdenum (Mo) | Vanadium (V) | Nickel (Ni) | Phosphorus (P) | Sulphur (S) | |
| E6010 | 62 | 50 | 75-125 | - | 140-215 | - | - | - | - | - | - | - | - | - | Ref. 16 |
| | | | 75-130 | - | 140-225 | - | - | - | - | - | - | - | - | - | Reported by manufacturer |
| E7018 | 72 | 60 | 115-165 | - | 200-275 | - | 1.25(1) | 0.90 | 0.20(1) | 0.30(1) | 0.08(1) | 0.30(1) | - | - | Max. percent - Ref. 16 |
| | | | 90-150 | - | 170-280 | 0.06 | 1.10 | 0.50 | - | 0.40-0.65 | - | - | 0.03 | 0.04 | Reported by manufacturer |
| E7024 | 72 | 60 | - | - | 230-305 | - | 1.25(1) | 0.90 | 0.20(1) | 0.30(1) | 0.08(1) | 0.30(1) | - | - | Max. percent - Ref. 16 |
| | | | - | - | 250-280 | - | - | - | - | - | - | - | - | - | Reported by manufacturer |
| E7028 | 72 | 60 | - | 180-250 | 230-305 | - | 1.25(1) | 0.90 | 0.20(1) | 0.30(1) | 0.08(1) | 0.30(1) | - | - | Max. percent - Ref. 16 |
| | | | - | 180-270 | 240-330 | - | - | - | - | - | - | - | - | - | Reported by manufacturer |
| E11018-M | 110 | 98-110 | - | - | - | 0.10 | 1.30-1.80 | 0.60 | 0.30-1.50 | 0.30-0.55 | 0.05 | 1.75-2.50 | 0.030 | 0.030 | Ref. 16 |
| | | | 95-155 | - | 160-280 | 0.06 | 1.53 | 0.27 | 0.31 | 0.42 | - | 1.88 | 0.030 | 0.030 | Reported by manufacturer |

(1) The sum total of these elements shall not exceed 1.50 percent.

Table 5.1

Summary of Test Results for Mild Steel Specimens

| Specimen Designation | Hardness (HV) | | | | | | Cracking | | | Porosity | Slag Inclusions | Small Inclusions | Lamellar Inclusions | Lack of Fusion | Discontinuity Ratio(2) | Tension Tests | | | Bend Tests | | |
|---|---|---|---|---|---|---|---|---|---|---|---|---|---|---|---|---|---|---|---|---|---|
| | BM | | HAZ | | WM, RT | | | | | | | | | | | | | | | | |
| | Minimum | Maximum | Minimum | Maximum | Mimimum | Maximum | HAZ Cracks | WM Microcracks | Hot Cracks | | | | | | | Ultimate Stress (KSI) | Joint(1) Efficiency (%) | Location of Failure | Result | % Elongation (1" gage) | Location of Failure |
| A1A | 154 | 205 | 172 | 341 | 168 | 244 | N | C | N | N | F | C | Y | S | 54 | 53.7 | 87 | WM, HAZ | F | - | LOF |
| A1B | 148 | 183 | 161 | 362 | 164 | 244 | N | F | N | N | F | C | Y | S | 27 | 59.5 | 97 | WM | F | - | LOF |
| A1C | 148 | 183 | 148 | 232 | 161 | 205 | N | N | N | N | N | C | Y | S | 24 | 62.8 | 100 | WM, HAZ | F | 11 | LOF |
| A1D | 145 | 192 | 145 | 341 | 168 | 238 | N | F | N | S | F | C | Y | S | 35 | 62.1 | 100 | BM | F | - | LOF |
| A2A | 175 | 215 | 179 | 264 | 179 | 226 | N | S | N | F | S | C | Y | F | 30 | 59.8 | 97 | WM, HAZ | F | - | LOF |
| A3A | 179 | 221 | 201 | 244 | 196 | 232 | N | N | N | N | F | C | Y | F | 17 | 62.3 | 100 | BM | P | 23 | - |
| A3B | 148 | 196 | 161 | 399 | 172 | 244 | N | C | N | C | F | C | Y | S | 43 | }44.7 | }73 | }BM(3) | F | - | LOF |
| A3C | 148 | 183 | 179 | 278 | 161 | 232 | N | C | N | F | F | C | Y | S | 56 | | | | F | - | LOF |
| A4A | 154 | 205 | 179 | 257 | 215 | 264 | N | N | N | N | S | C | Y | N | 15 | 61.6 | 100 | BM | F | 20 | HAZ |
| A4B | 154 | 179 | 168 | 215 | 196 | 264 | N | N | F | C | F | C | Y | N | 27 | 63.4 | 100 | WM, HAZ | F | - | slag |
| D1A | 148 | 192 | 175 | 374 | 175 | 232 | Y | S | N | N | N | C | Y | S | 19 | 42.9 | 70 | WM, HAZ | F | - | crack |
| D1B | 154 | 196 | 172 | 330 | 172 | 221 | Y | S | N | F | F | C | Y | S | 25 | 42.8 | 69 | WM, HAZ | F | - | crack |
| D1C | 140 | 168 | 175 | 232 | 175 | 232 | Y | N | N | F | F | C | Y | F | 19 | 42.6 | 69 | WM, HAZ | F | - | crack |
| E1A | 143 | 168 | 175 | 362 | 187 | 221 | N | C | N | N | F | C | Y | N | - | - | - | - | - | - | - |
| F1A | 154 | 175 | 187 | 374 | 192 | 215 | N | C | N | F | F | C | Y | N | - | - | - | - | - | - | - |
| E4A | 137 | 164 | 161 | 341 | 196 | 278 | N | N | N | N | S | C | Y | N | - | - | - | - | - | - | - |
| F4A | 143 | 175 | 164 | 386 | 179 | 257 | N | N | F | N | C | C | Y | N | - | - | - | - | - | - | - |
| E4B | 145 | 168 | 168 | 330 | 232 | 286 | N | N | F | N | C | C | Y | F | - | - | - | - | - | - | - |
| F4B | 140 | 164 | 151 | 351 | 215 | 244 | N | N | S | F | C | C | Y | N | - | - | - | - | - | - | - |
| E4C | 145 | 168 | 145 | 286 | 215 | 250 | N | N | F | N | C | C | Y | N | - | - | - | - | - | - | - |
| F4C | 137 | 175 | 161 | 271 | 148 | 244 | N | N | N | N | C | C | Y | N | - | - | - | - | - | - | - |

HV = Vickers hardness
BM = Base metal
HAZ = Heat-affected zone
WM = Weld metal
RT = Retempered zone

N = None
F = Few (1- 5)
S = Several (6-25)
C = Considerable (>25)
Y = Yes

(1) Joint efficiency is defined as the ratio of joint ultimate stress to base metal ultimate stress in percent.
(2) Discontinuity ratio is defined as the ratio of the area of discontinuity present on radiograph in 1-inch length of weld to the cross-sectional area of the weld, expressed in percent.
(3) Failed in thru-thickness direction of the vertical plate.

Table 5.2

Summary of Test Results for Low-Alloy Steel Specimens

| Specimen Designation | Hardness (HV) | | | | | | Cracking | | | Porosity | Slag Inclusions | Small Inclusions | Lamellar Inclusions | Lack of Fusion | Discontinuity Ratio(2) | Tension Tests | | | Bend Tests | | |
|---|---|---|---|---|---|---|---|---|---|---|---|---|---|---|---|---|---|---|---|---|---|
| | BM | | HAZ | | WM, RT | | | | | | | | | | | | | | | | |
| | Minimum | Maximum | Minimum | Maximum | Mimimum | Maximum | HAZ Cracks | WM Microcracks | Hot Cracks | | | | | | | Ultimate Stress (KSI) | Joint(1) Efficiency (%) | Location of Failure | Result | % Elongation (1" gage) | Location of Failure |
| B1A | 187 | 244 | 210 | 490 | 201 | 271 | N | N | N | N | S | C | Y | N | 7 | 88.1 | 100 | BM | F | 13 | slag |
| B1B | 175 | 215 | 201 | 426 | 183 | 238 | N | N | N | N | S | C | Y | N | 5 | 86.8 | 100 | WM, HAZ | F | 11 | slag |
| B1C | 192 | 232 | 187 | 294 | 187 | 244 | N | N | N | F | S | C | Y | F | 16 | 75.5 | 87 | WM, HAZ | F | - | slag |
| B2A | 175 | 201 | 210 | 473 | 210 | 244 | N | N | N | S | F | C | Y | N | 9 | 87.6 | 100 | WM, HAZ | F | 22 | HAZ |
| B2B | 183 | 210 | 205 | 386 | 201 | 232 | N | N | N | N | F | C | Y | N | 1 | 86.3 | 100 | BM | P | 23 | - |
| B3A | 192 | 232 | 192 | 286 | 210 | 215 | N | N | N | C | F | C | Y | N | 12 | 83.8 | 97 | HAZ | F | 23 | RT |
| B3B | 192 | 244 | 201 | 473 | 196 | 278 | N | N | N | F | F | C | Y | N | 8 | 80.0 | 93 | BM(3) | F | 8 | HAZ |
| B3C | 168 | 215 | 210 | 509 | 192 | 244 | N | N | N | S | S | C | Y | N | 8 | | | | F | 5 | HAZ |
| B4A | 192 | 210 | 192 | 426 | 161 | 215 | N | N | N | N | F | C | Y | F | 3 | 80.5 | 93 | WM, HAZ | F | 16 | HAZ |
| B4B | 183 | 201 | 201 | 412 | 210 | 271 | N | N | N | C | F | C | Y | F | 29 | 78.1 | 90 | WM, HAZ | F | - | slag |
| D3A | 187 | 210 | 196 | 286 | 221 | 226 | N | N | N | S | N | C | Y | N | 2 | 82.3 | 95 | BM | P | 22 | - |
| D3B | 196 | 232 | 210 | 412 | 196 | 264 | Y | N | N | S | N | C | Y | F | 5 | 85.4 | 99 | WM, HAZ | F | - | crack |
| E3A | 183 | 205 | 192 | 341 | 221 | 238 | N | N | N | S | F | C | Y | N | - | - | - | - | - | - | - |
| F3A | 179 | 201 | 192 | 362 | 232 | 238 | N | N | N | S | N | C | Y | N | - | - | - | - | - | - | - |
| E3B | 192 | 210 | 210 | 457 | 201 | 250 | N | N | N | C | F | C | Y | N | - | - | - | - | - | - | - |
| F3B | 183 | 210 | 210 | 457 | 232 | 257 | N | N | N | C | F | C | Y | N | - | - | - | - | - | - | - |

HV = Vickers hardness
BM = Base metal
HAZ = Heat-affected zone
WM = Weld metal
RT = Retempered zone

N = None
F = Few (1-5)
S = Several (6-25)
C = Considerable (>25)
Y = Yes

(1) Joint efficiency is defined as the ratio of joint ultimate stress to base metal ultimate stress in percent.
(2) Discontinuity ratio is defined as the ratio of the area of discontinuity present on radiograph in 1-inch length of weld to the cross-sectional area of the weld, expressed in percent.
(3) Failed in thru-thickness direction of the vertical plate.

Table 5.3

Summary of Test Results for Quenched and Tempered Steel Specimens

| Specimen Designation | Hardness (HV) | | | | | | Cracking | | | Porosity | Slag Inclusions | Small Inclusions | Lamellar Inclusions | Lack of Fusion | Discontinuity Ratio(2) | Tension Tests | | | Bend Tests | | |
|---|---|---|---|---|---|---|---|---|---|---|---|---|---|---|---|---|---|---|---|---|---|
| | BM | | HAZ | | WM, RT | | | | | | | | | | | | | | | | |
| | Minimum | Maximum | Minimum | Maximum | Mimimum | Maximum | HAZ Cracks | WM Microcracks | Hot Cracks | | | | | | | Ultimate Stress (KSI) | Joint(1) Efficiency (%) | Location of Failure | Result | % Elongation (1" gage) | Location of Failure |
| C1A | 286 | 341 | 278 | 457 | 250 | 362 | N | N | N | C | F | C | Y | N | 7 | 128 | 99 | WM, HAZ | F | 8 | HAZ |
| C1B | 321 | 374 | 271 | 473 | 286 | 330 | N | N | N | C | F | S | Y | N | 4 | 128 | 99 | WM, HAZ | F | 7 | HAZ |
| C1C | 286 | 351 | 264 | 457 | 271 | 330 | N | N | N | C | F | C | Y | N | 3 | 126 | 98 | WM, HAZ | F | 18 | HAZ |
| C2A | 303 | 330 | 257 | 457 | 321 | 341 | N | N | N | C | F | C | Y | N | 5 | 126 | 98 | WM, HAZ | F | 18 | HAZ |
| C2B | 312 | 330 | 257 | 426 | 286 | 303 | N | N | F | C | F | C | Y | N | 2 | 125 | 97 | WM, HAZ | F | 14 | HAZ |
| C3A | 286 | 321 | 271 | 426 | 312 | 312 | N | N | N | S | N | C | Y | N | 4 | 127 | 98 | WM, HAZ | P | 23 | - |
| C3B | 257 | 341 | 264 | 457 | 250 | 351 | N | N | N | S | N | S | Y | N | 2 | } 129 | }100 | } BM(3) | F | 19 | HAZ |
| C3C | 321 | 351 | 250 | 457 | 294 | 341 | N | N | N | S | F | S | Y | N | 1 | | | | F | 8 | HAZ |
| D2A | 321 | 351 | 274 | 457 | 321 | 341 | N | N | N | S | S | C | Y | F | 6 | 128 | 99 | WM, HAZ | F | 8 | HAZ |
| D2B | 278 | 351 | 264 | 457 | 232 | 362 | N | N | N | C | F | C | Y | F | 2 | 130 | 100 | WM, HAZ | F | 15 | HAZ |
| D2C | 312 | 341 | 264 | 412 | 257 | 286 | N | N | F | S | S | C | Y | N | 1 | 96 | 74 | WM, HAZ | F | - | slag |
| E2A | 321 | 341 | 294 | 457 | 303 | 362 | N | N | N | C | N | C | Y | N | - | - | - | - | - | - | - |
| F2A | 330 | 341 | 286 | 441 | 341 | 362 | Y | N | N | S | N | C | Y | N | - | - | - | - | - | - | - |

HV = Vickers hardness
BM = Base metal
HAZ = Heat-affected zone
WM = Weld metal
RT = Retempered zone

N = None
F = Few (1-5)
S = Several (6-25)
C = Considerable (>25)
Y = Yes

(1) Joint efficiency is defined as the ratio of joint ultimate stress to base metal ultimate stress in percent.
(2) Discontinuity ratio is defined as the ratio of the area of discontinuity present on radiograph in 1-inch length of weld to the cross-sectional area of the weld, expressed in percent.
(3) Failed in thru-thickness direction of the vertical plate.

Table 7.1

Summary of Preheat Temperatures to Minimize Cold Cracking in Mild and Low-Alloy Steels

| CE | | Minimum Preheat Temperature °F | | | | | | | | | | | | | | | |
|---|---|---|---|---|---|---|---|---|---|---|---|---|---|---|---|---|---|
| | | TSN=4 | | | | TSN=8 | | | | TSN=12 | | | | TSN=16 | | | |
| | | Arc Energy (KJ/in.) | | | | Arc Energy (KJ/in.) | | | | Arc Energy (KJ/in.) | | | | Arc Energy (KJ/in.) | | | |
| High Hydrogen | Low Hydrogen | 20 | 40 | 60 | 80 | 20 | 40 | 60 | 80 | 20 | 40 | 60 | 80 | 20 | 40 | 60 | 80 |
| 0.37 | 0.40 / 0.41 | 32 / 32 | 32 / 32 | 32 / 32 | 32 / 32 | 257 / 167 | 32 / 32 | 32 / 32 | 32 / 32 | 302 / 257 | 185 / 32 | 32 / 32 | 32 / 32 | 325 / 279 | 248 / 167 | 122 / 32 | 32 / 32 |
| 0.39 | 0.42 / 0.43 | 122 / 32 | 32 / 32 | 32 / 32 | 32 / 32 | 291 / 243 | 86 / 32 | 32 / 32 | 32 / 32 | 329 / 293 | 234 / 144 | 70 / 32 | 32 / 32 | 356 / 325 | 279 / 234 | 203 / 93 | 55 / 32 |
| 0.41 | 0.44 / 0.45 | 189 / 73 | 32 / 32 | 32 / 32 | 32 / 32 | 313 / 279 | 167 / 50 | 32 / 32 | 32 / 32 | 351 / 320 | 268 / 212 | 162 / 32 | 32 / 32 | 369 / 334 | 306 / 268 | 239 / 171 | 153 / 32 |
| 0.43 | 0.46 / 0.48 | 234 / 165 | 32 / 32 | 32 / 32 | 32 / 32 | 338 / 302 | 212 / 122 | 32 / 32 | 32 / 32 | 369 / 342 | 293 / 255 | 212 / 120 | 68 / 32 | 383 / 361 | 327 / 295 | 275 / 223 | 203 / 113 |
| 0.45 | 0.48 / 0.50 | 266 / 210 | 32 / 32 | 32 / 32 | 32 / 32 | 354 / 324 | 257 / 189 | 95 / 32 | 32 / 32 | 383 / 356 | 316 / 279 | 248 / 176 | 136 / 32 | 397 / 380 | 347 / 316 | 295 / 257 | 234 / 167 |
| 0.47 | 0.50 / 0.52 | 284 / 246 | 32 / 32 | 32 / 32 | 32 / 32 | 369 / 340 | 279 / 226 | 145 / 45 | 32 / 32 | 396 / 370 | 334 / 302 | 271 / 217 | 185 / 90 | 406 / 385 | 361 / 336 | 316 / 279 | 266 / 212 |
| 0.49 | 0.53 / 0.55 | 302 / 271 | 68 / 32 | 32 / 32 | 32 / 32 | 378 / 358 | 295 / 257 | 189 / 104 | 32 / 32 | 410 / 383 | 347 / 320 | 293 / 257 | 212 / 156 | 424 / 401 | 374 / 349 | 334 / 302 | 288 / 248 |
| 0.51 | 0.55 / 0.57 | 322 / 284 | 122 / 32 | 32 / 32 | 32 / 32 | 387 / 369 | 313 / 279 | 219 / 145 | 86 / 32 | 418 / 396 | 358 / 334 | 306 / 271 | 248 / 185 | 433 / 406 | 383 / 361 | 347 / 316 | 302 / 366 |
| 0.53 | 0.57 / 0.59 | 329 / 302 | 167 / 68 | 32 / 32 | 32 / 32 | 401 / 378 | 324 / 295 | 248 / 189 | 131 / 32 | 426 / 410 | 367 / 347 | 322 / 293 | 266 / 212 | -- / 424 | 392 / 374 | 356 / 334 | 320 / 288 |
| 0.55 | 0.59 / 0.62 | 347 / 322 | 198 / 122 | 32 / 32 | 32 / 32 | 410 / 387 | 338 / 313 | 271 / 219 | 174 / 86 | 437 / 418 | 378 / 358 | 333 / 306 | 286 / 248 | -- / 433 | 403 / 383 | 363 / 347 | 333 / 302 |
| 0.57 | 0.61 / -- | 356 / 329 | 212 / 167 | 32 / 32 | 32 / 32 | 414 / 401 | 347 / 324 | 279 / 248 | 189 / 131 | -- / 426 | 383 / 367 | 345 / 322 | 298 / 266 | -- / -- | 412 / 392 | 372 / 356 | 342 / 320 |

$°C = 5/9 \times (°F-32°)$

$$CE = C + \frac{Mn+Si}{6} + \frac{Cr+Mo+V}{5} + \frac{Ni+Cu}{15}$$

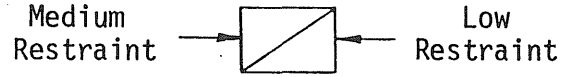


(See Fig. 2.4 for examples of restraint conditions.)

TABLE 7.2

HARDNESS VALUES USED TO DEVELOP RECOMMENDED PREHEAT TEMPERATURES TO MINIMIZE COLD CRACKING

| | Medium Restraint | Low Restraint |
|---|---|---|
| Other-than-low hydrogen | 350 HV | 400 HV |
| Low hydrogen | 400 HV | 450 HV |

Table 7.3

Recommended Preheat Temperatures to Minimize Cold Cracking in Mild and Low-Alloy Steels

| CE | | Minimum Preheat Temperature °F | | | | | | | | | | | | | | | |
|---|---|---|---|---|---|---|---|---|---|---|---|---|---|---|---|---|---|
| | | TSN=4 | | | | TSN=8 | | | | TSN=12 | | | | TSN=16 | | | |
| | | Arc Energy (KJ/in.) | | | | Arc Energy (KJ/in.) | | | | Arc Energy (KJ/in.) | | | | Arc Energy (KJ/in.) | | | |
| High Hydrogen | Low Hydrogen | 20 | 40 | 60 | 80 | 20 | 40 | 60 | 80 | 20 | 40 | 60 | 80 | 20 | 40 | 60 | 80 |
| 0.37 | 0.40 / 0.41 | 32 / 32 | 32 / 32 | 32 / 32 | 32 / 32 | 250 / 175 | 32 / 32 | 32 / 32 | 32 / 32 | 300 / 250 | 200 / 32 | 32 / 32 | 32 / 32 | 325 / 275 | 250 / 175 | 125 / 32 | 32 / 32 |
| 0.41 | 0.44 / 0.45 | 200 / 75 | 32 / 32 | 32 / 32 | 32 / 32 | 325 / 275 | 175 / 50 | 32 / 32 | 32 / 32 | 350 / 325 | 275 / 225 | 175 / 32 | 32 / 32 | 375 / 350 | 300 / 275 | 250 / 175 | 150 / 32 |
| 0.45 | 0.48 / 0.50 | 275 / 225 | 32 / 32 | 32 / 32 | 32 / 32 | 350 / 325 | 250 / 200 | 100 / 32 | 32 / 32 | 400 / 375 | 325 / 275 | 250 / 175 | 150 / 32 | 400 / 375 | 350 / 325 | 300 / 250 | 250 / 175 |
| 0.49 | 0.53 / 0.55 | 300 / 275 | 75 / 32 | 32 / 32 | 32 / 32 | 375 / 350 | 300 / 250 | 200 / 100 | 32 / 32 | 425 / 400 | 350 / 325 | 300 / 250 | 225 / 150 | 425 / 400 | 375 / 350 | 350 / 300 | 300 / 350 |
| 0.53 | 0.57 / 0.59 | 325 / 300 | 175 / 75 | 32 / 32 | 32 / 32 | 400 / 375 | 325 / 300 | 250 / 200 | 125 / 32 | 425 / 425 | 375 / 350 | 325 / 300 | 275 / 225 | -- / 425 | 400 / 375 | 375 / 350 | 325 / 300 |
| 0.57 | 0.61 / -- | 350 / 325 | 225 / 175 | 32 / 32 | 32 / 32 | 425 / 400 | 350 / 325 | 275 / 250 | 200 / 125 | -- / 425 | 400 / 375 | 350 / 325 | 300 / 275 | -- / -- | 425 / 400 | 375 / 350 | 350 / 325 |

$°C = 5/9 \times (°F-32°)$

$$CE = C + \frac{Mn+Si}{6} + \frac{Cr+Mo+V}{5} + \frac{Ni+Cu}{15}$$

Medium Restraint → / ← Low Restraint

(See Fig. 2.4 for examples of restraint conditions.)

1) With E6010 electrodes, always use preheat recommended for medium restraint. (This will minimize weld metal microcracking.)
2) For conditions of high restraint, the above preheats may not be adequate. Some other form of joint treatment may be necessary.
3) For conditions of low restraint, the above preheats may be reduced if shown through joint tests that cracking will be avoided.

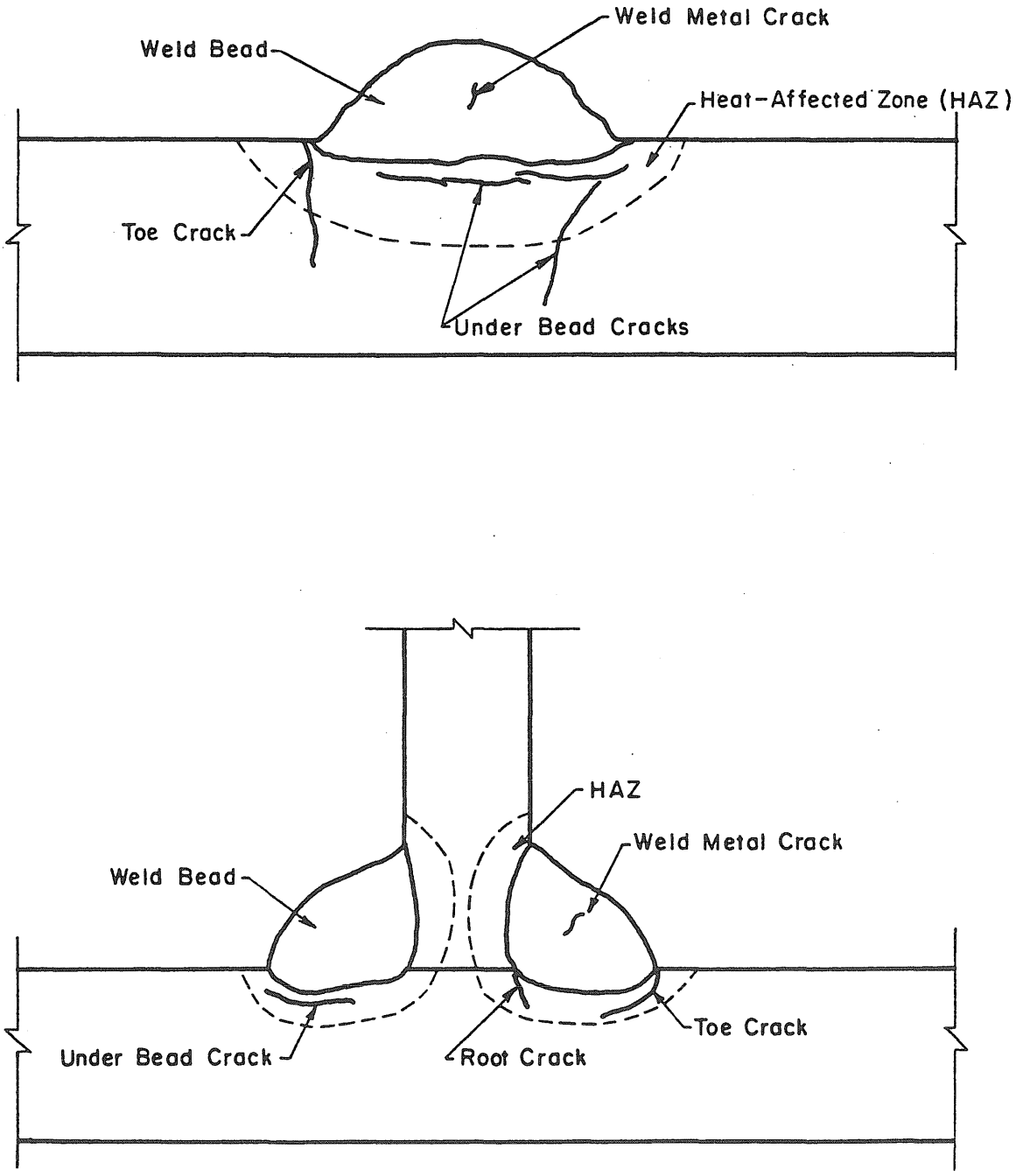


Fig. 2.1 Locations of Various Types of Cold Cracks.

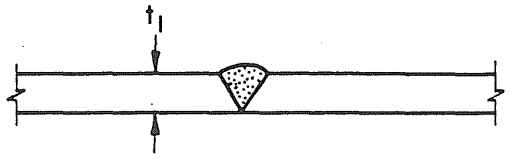


$$TSN = 4(t + t) = 8t$$

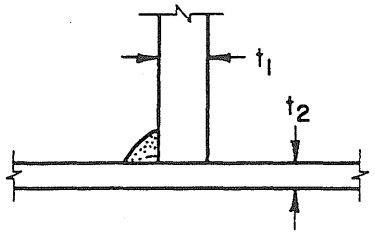


$$TSN = 4(t_1 + 2t_2)$$

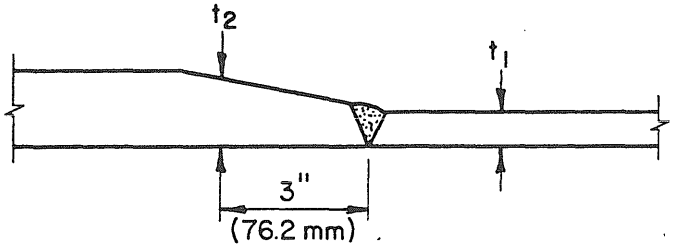


$$TSN = 4\left(t_1 + \frac{t_1 + t_2}{2}\right)$$

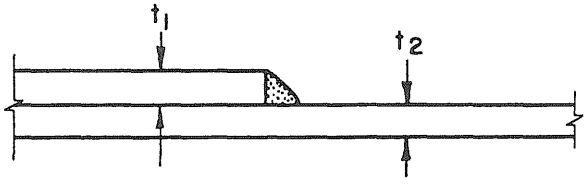


$$TSN = 4(t_1 + 2t_2)$$

Note: TSN Has the Same Dimensional Unit As t

Fig. 2.2 Thermal Severity Numbers for Typical Joints.

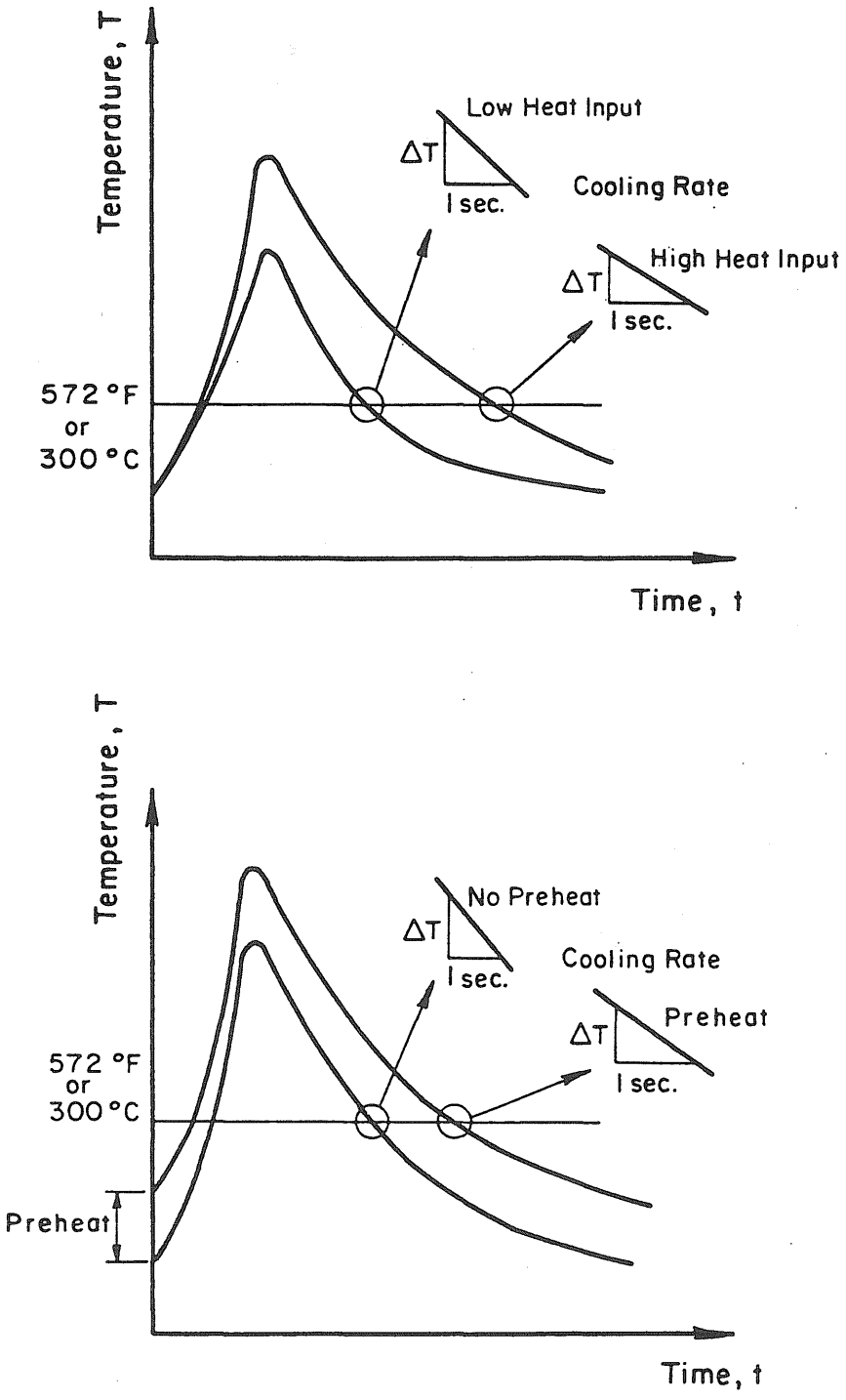


Note That A Higher Heat Input or Preheat Gives A Lower Cooling Rate At 572 °F (300 °C)

Fig. 2.3 Relationship of Heat Input and Preheat to Cooling Rate at 572°(300°C).

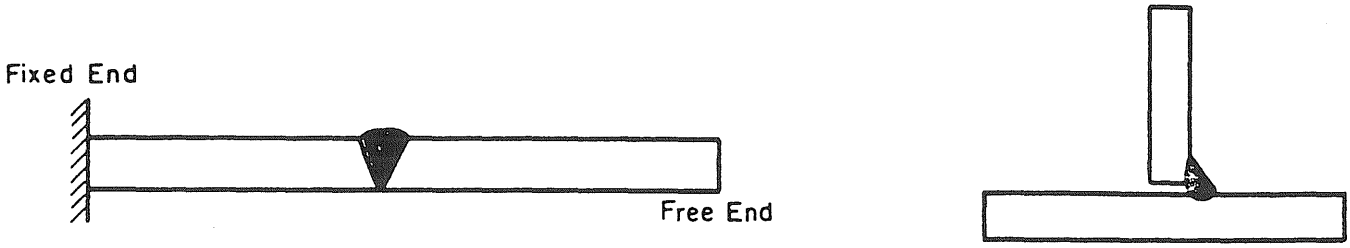


(a) Low Restraint

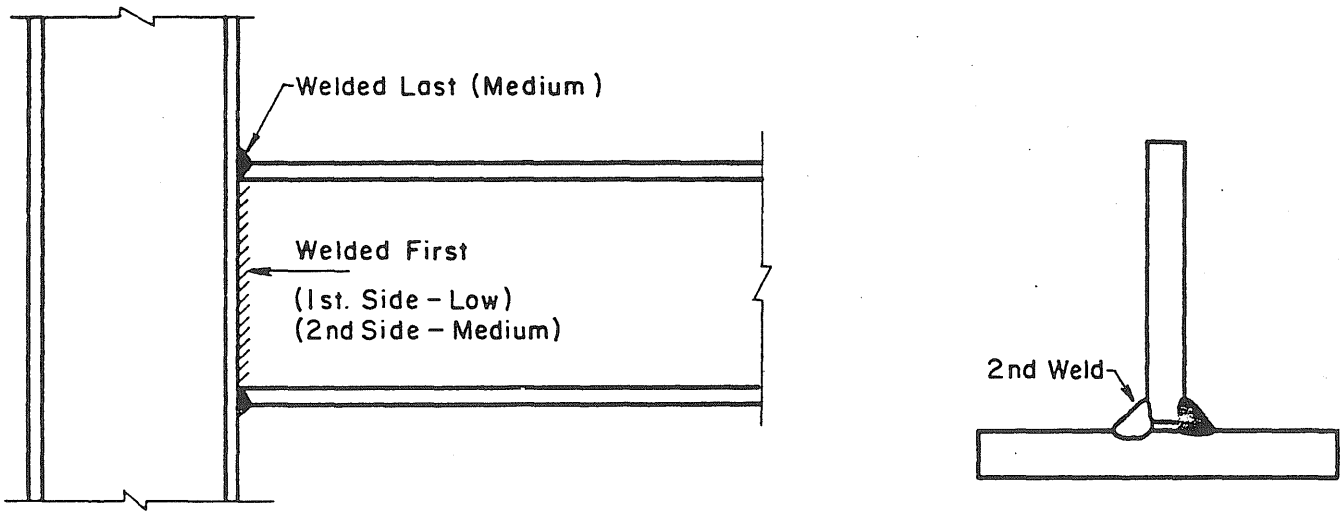


(b) Medium Restraint


(c) High Restraint

Fig. 2.4 Examples of Various Degrees of Restraint.

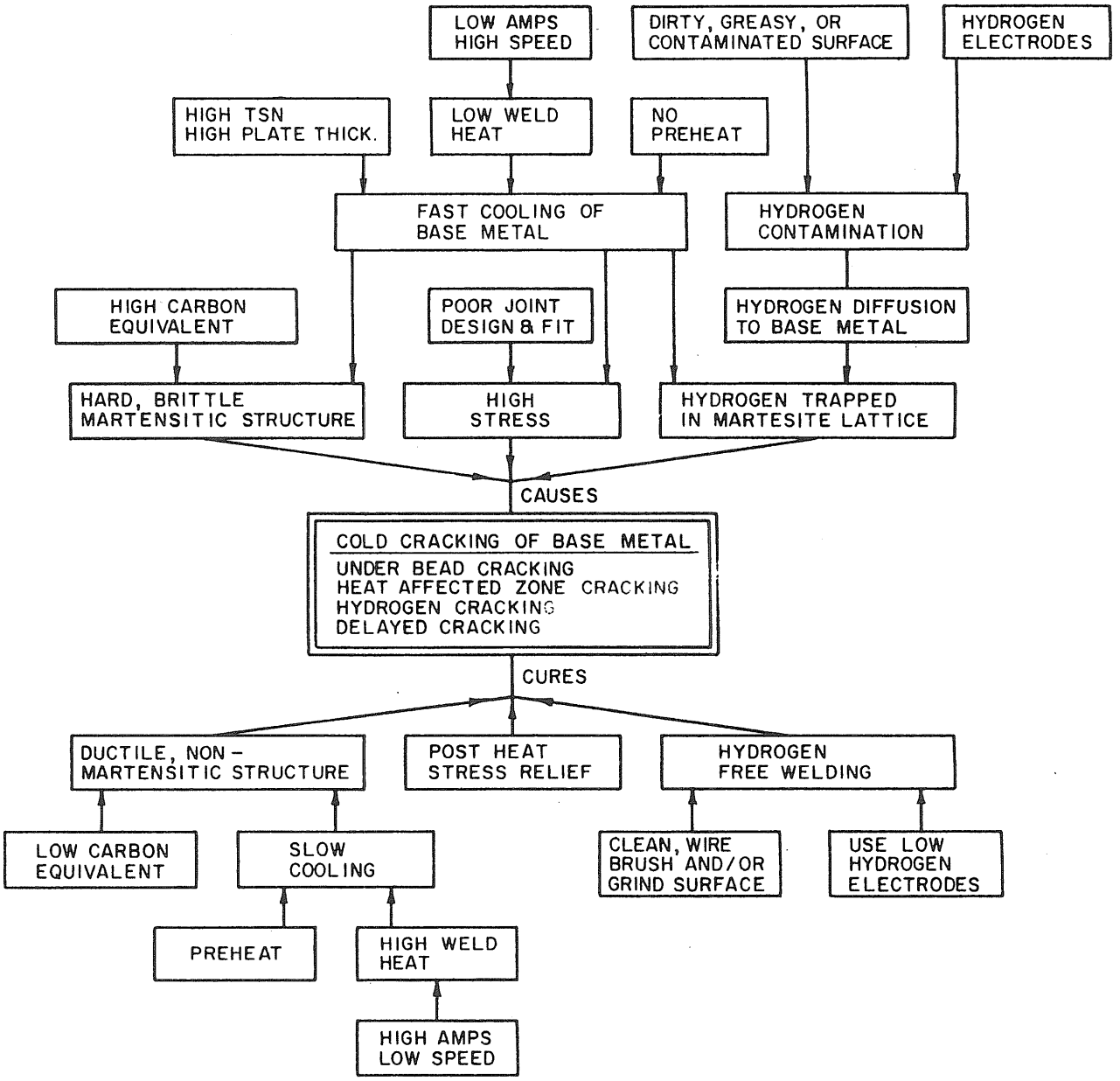


Fig. 2.5 Factors Affecting Cold Cracking in the Base Metal Heat-Affected Zone.

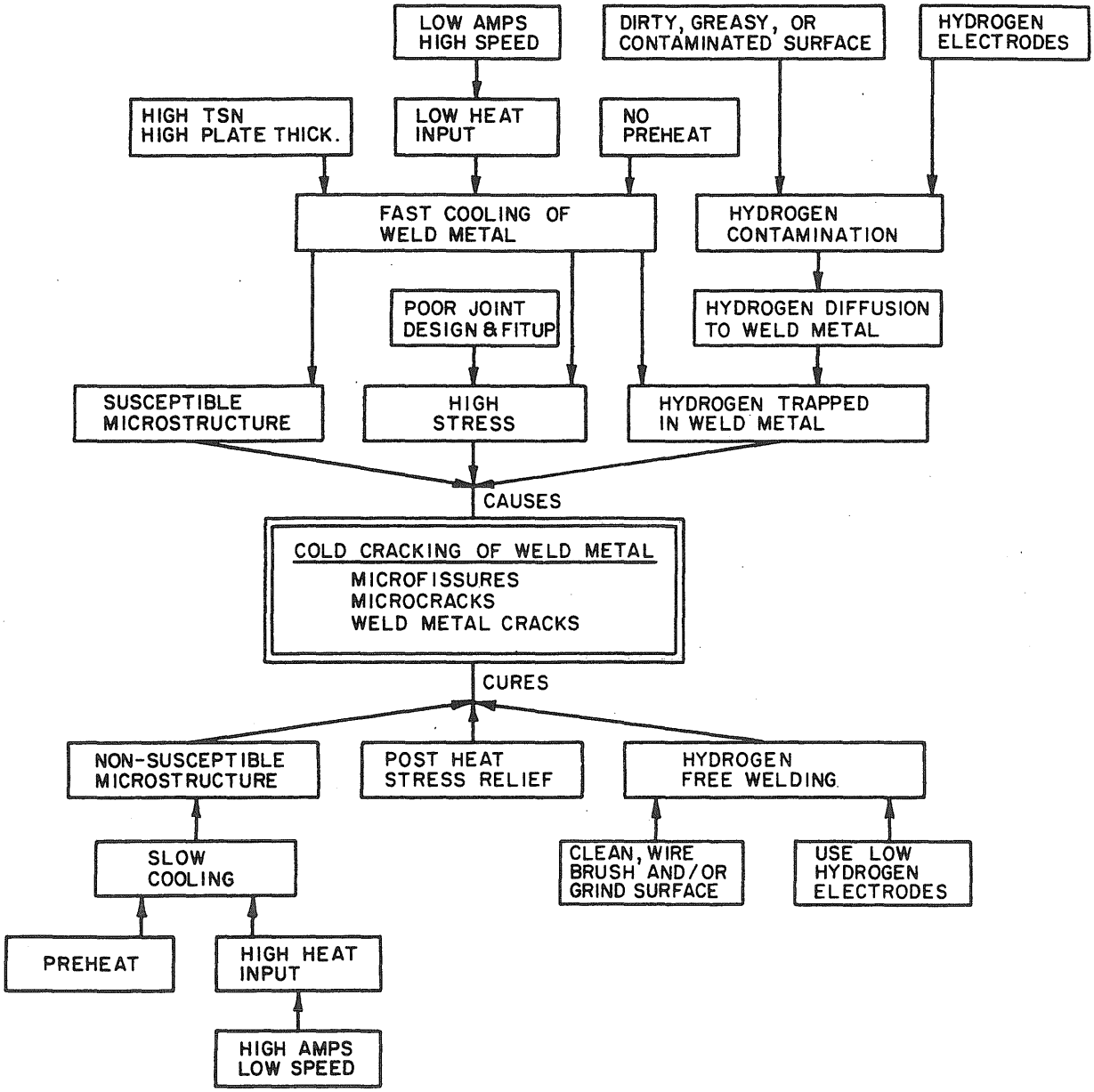


Fig. 2.6 Factors Affecting Cold Cracking in the Weld Metal.

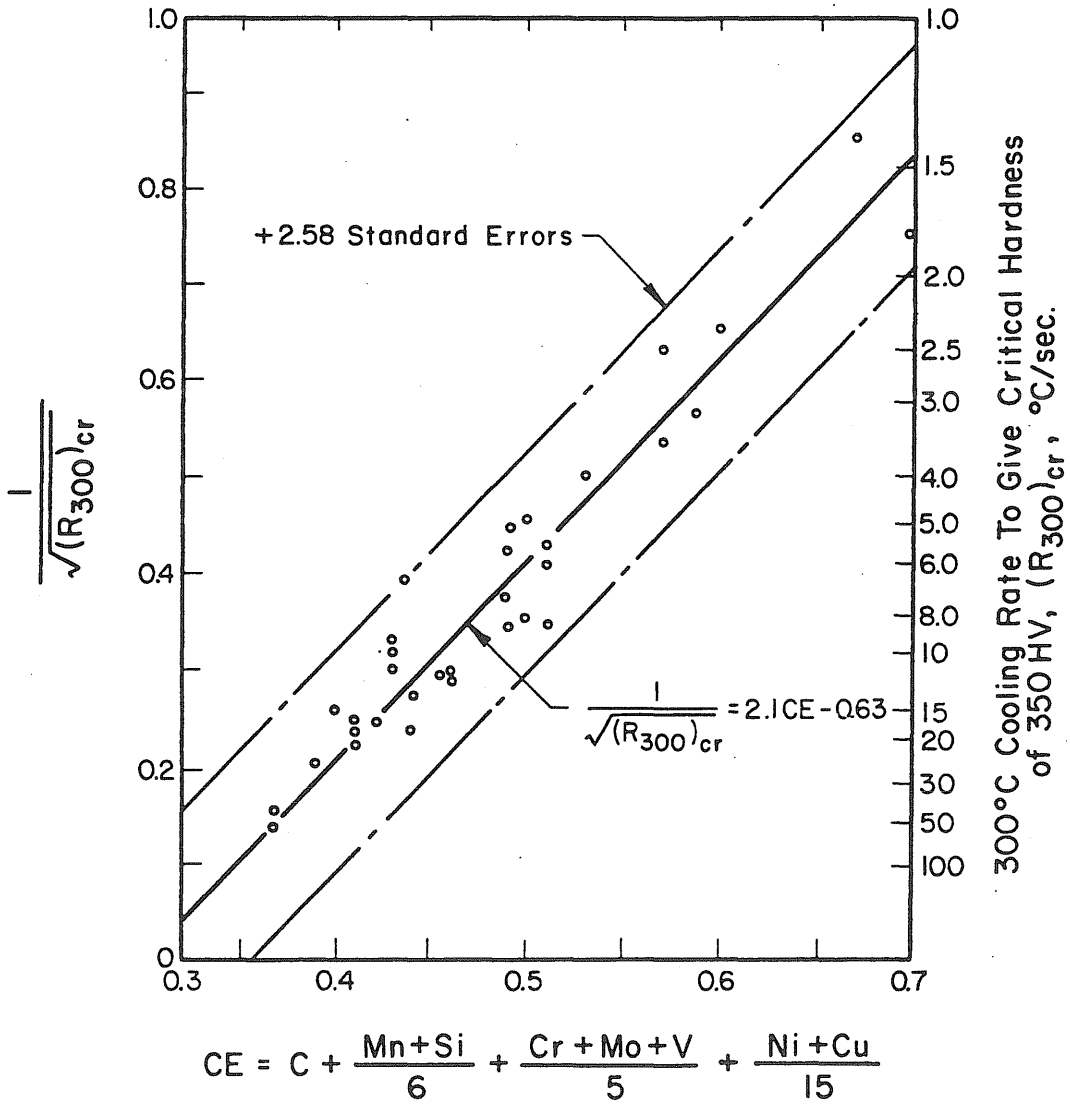


Fig. 2.7 Relationship Between Cooling Rate and Carbon Equivalent to Produce a Heat-Affected Zone Hardness of 350 HV. (2)

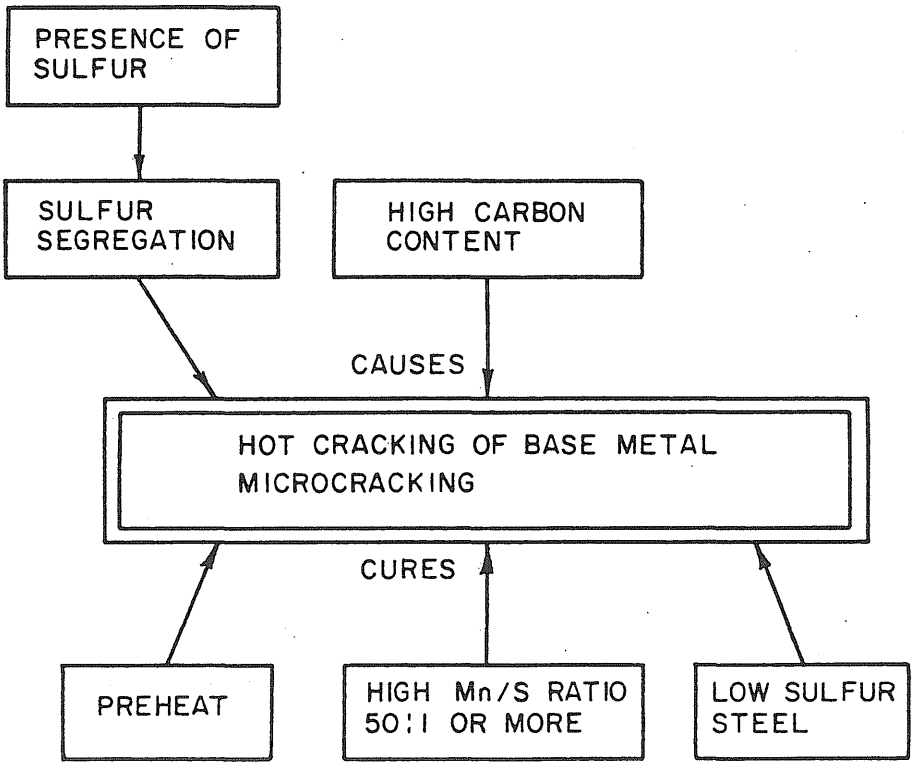


Fig. 2.8 Factors Affecting Hot Cracking in the Base Metal Heat-Affected Zone.

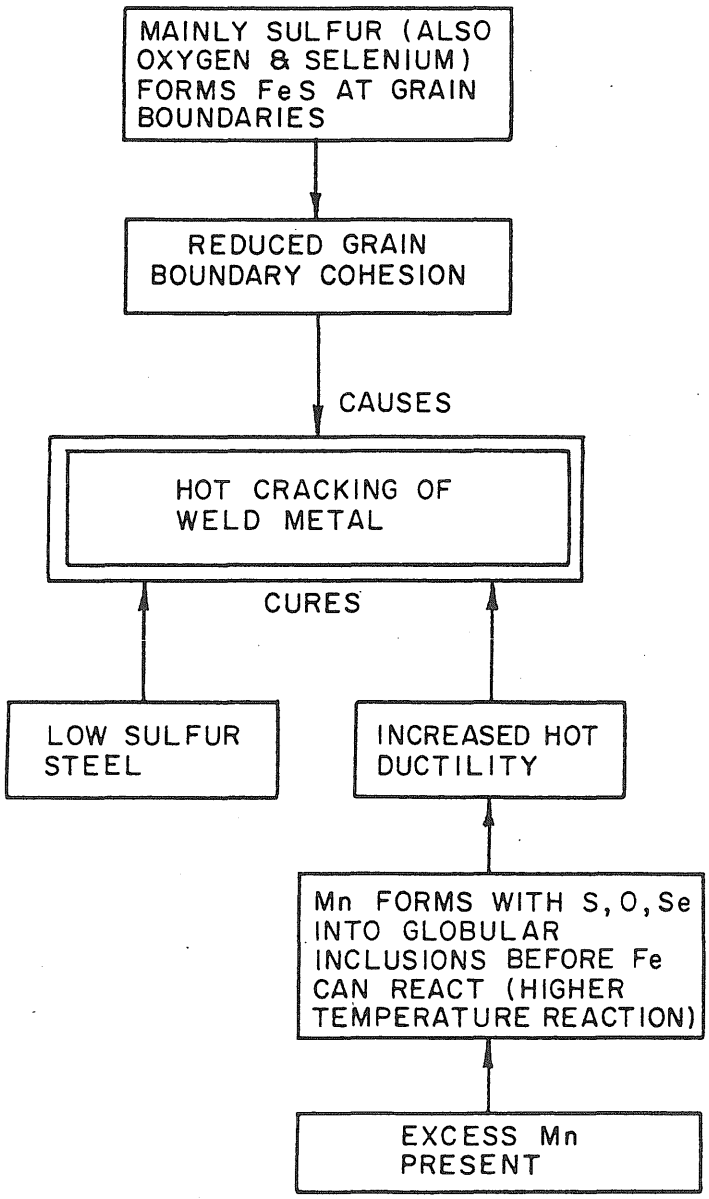


Fig. 2.9 Factors Affecting Hot Cracking in the Weld Metal.

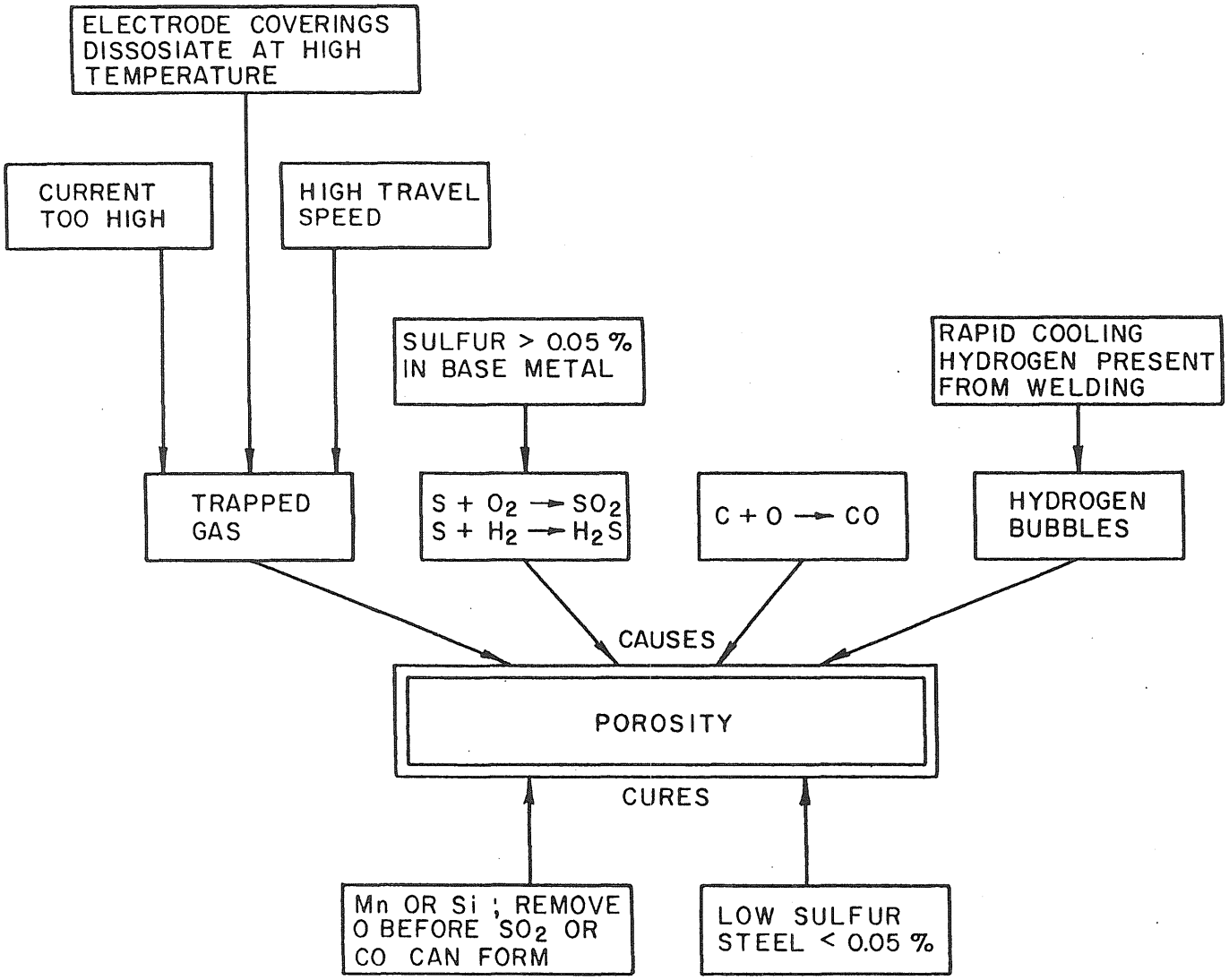


Fig. 2.10 Factors Affecting Porosity.

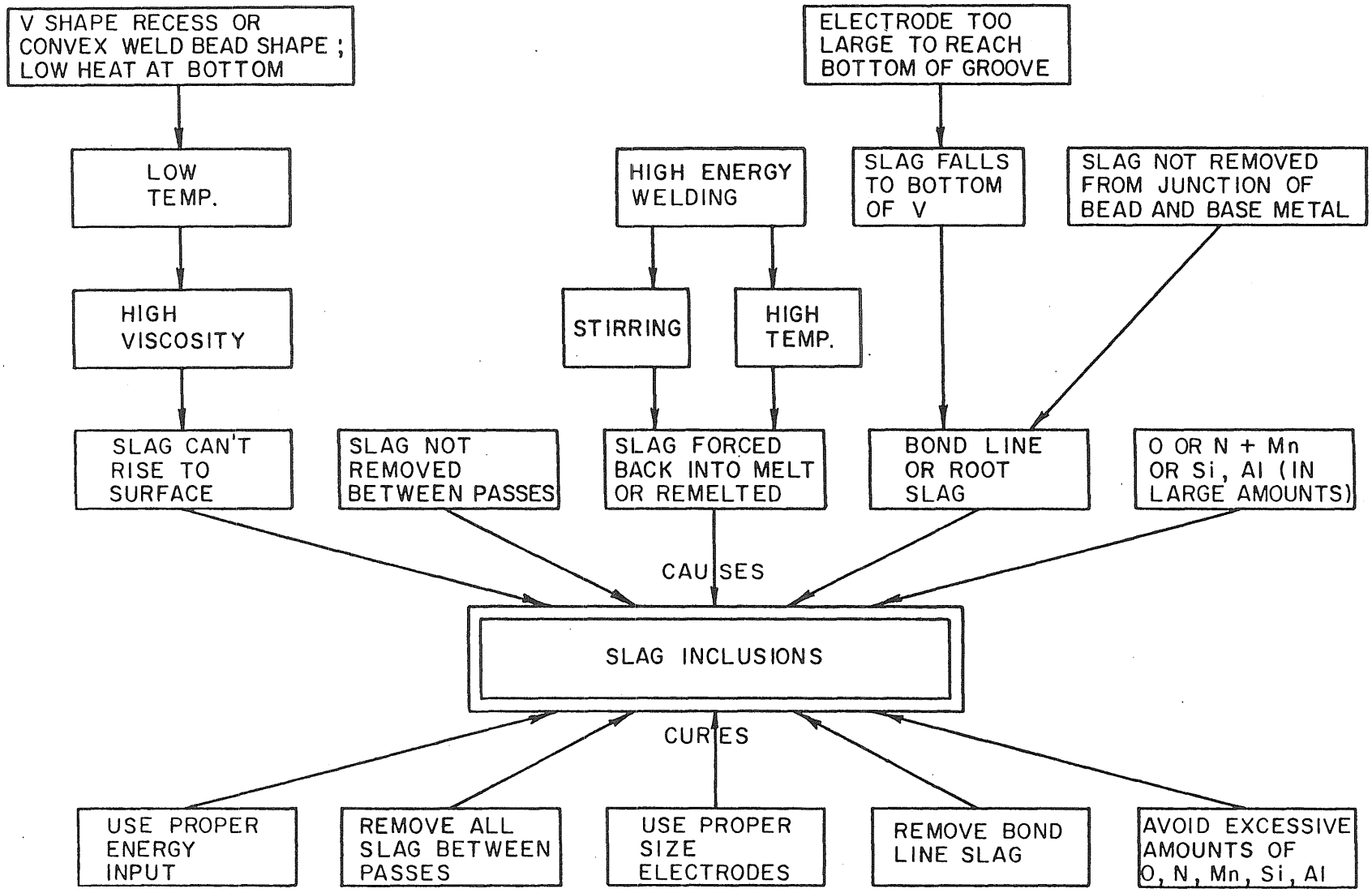


Fig. 2.11 Factors Affecting Slag Inclusions.

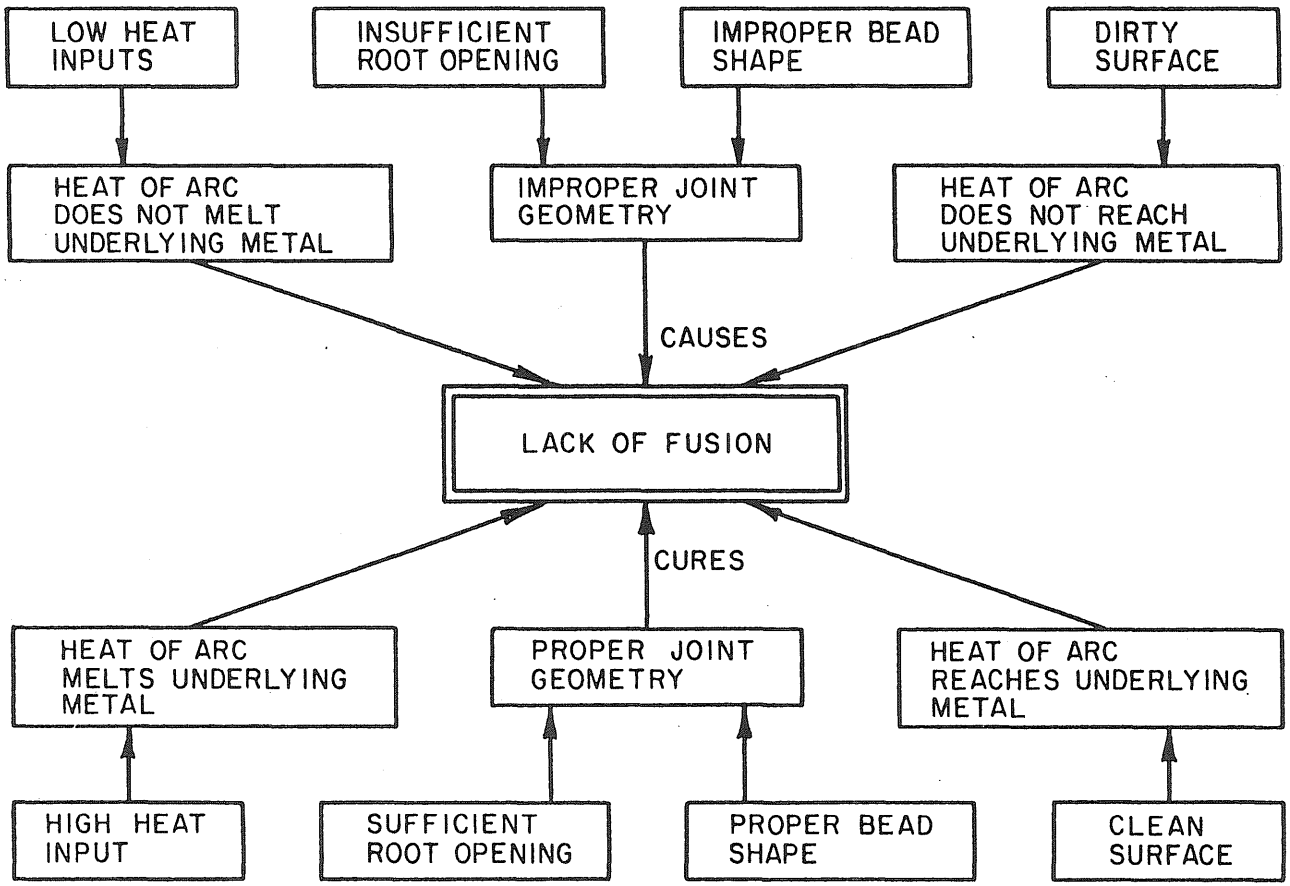


Fig. 2.12 Factors Affecting Lack of Fusion.

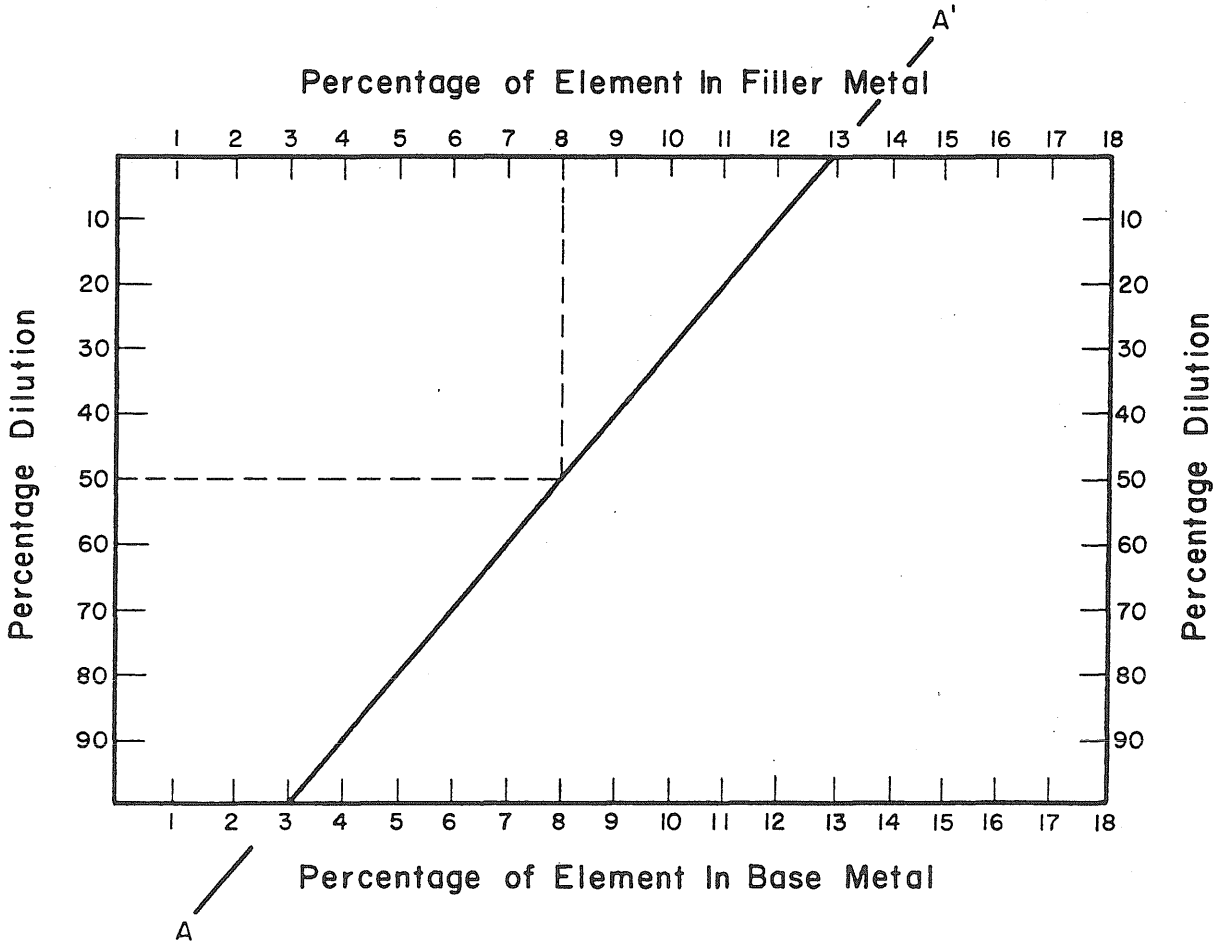


(From P. T. Houldcroft, Brit. Welding J. 1954, 1, 470) (20)

Fig. 2.13 Dilution Nomogram. (18)

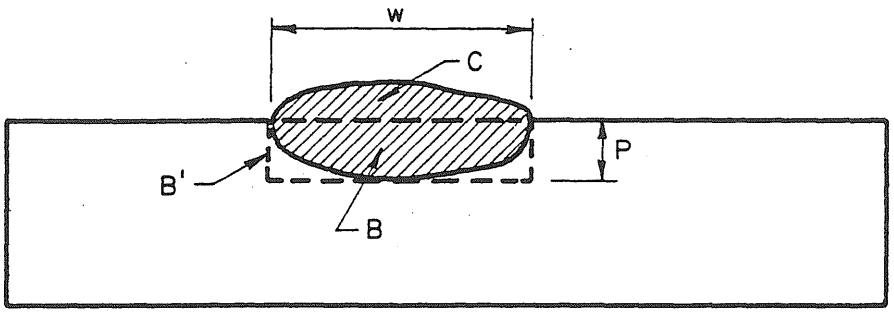


Weld 1 - Base Weld

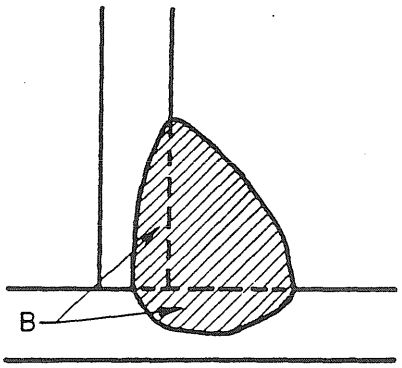


Weld 2 - Fillet Weld
High Penetration

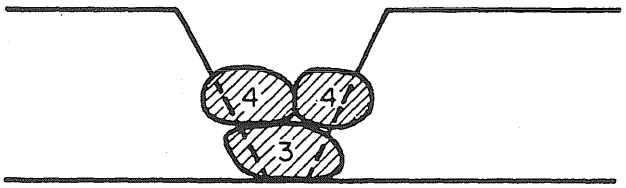


Weld 3 - Groove Weld
First Pass Medium Penetration
Weld 4 - Groove Weld
Additional Passes Low Penetration

Fig. 2.14 Weld Configurations.

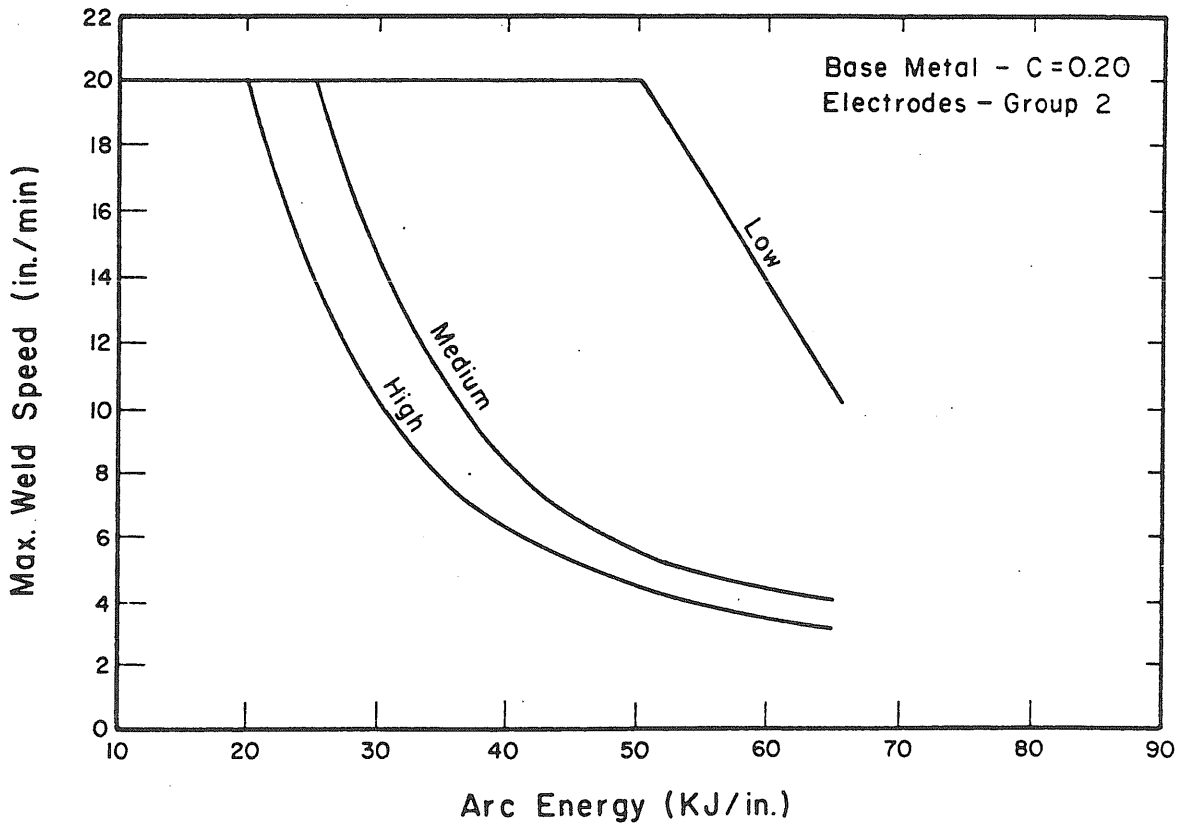


Fig. 2.15 Typical Plot of Preliminary Welding Requirements to Minimize Hot Cracking.

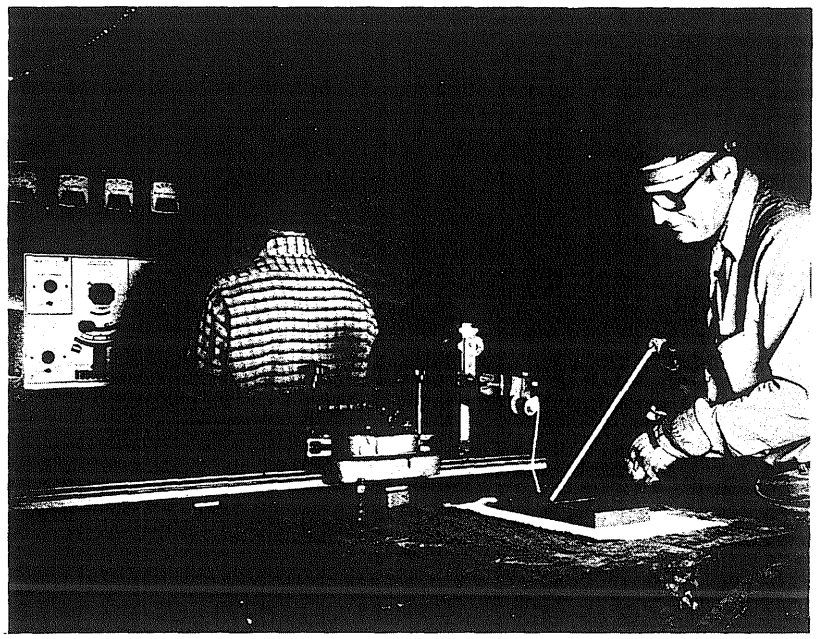

a) Setup of Welding Equipment

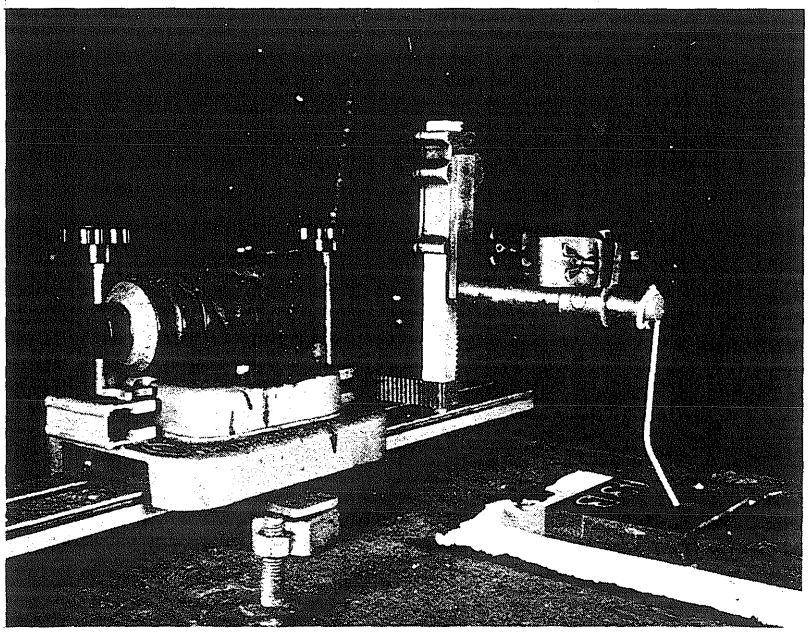

b) Speed Indicator System

Fig. 4.1 Welding Equipment

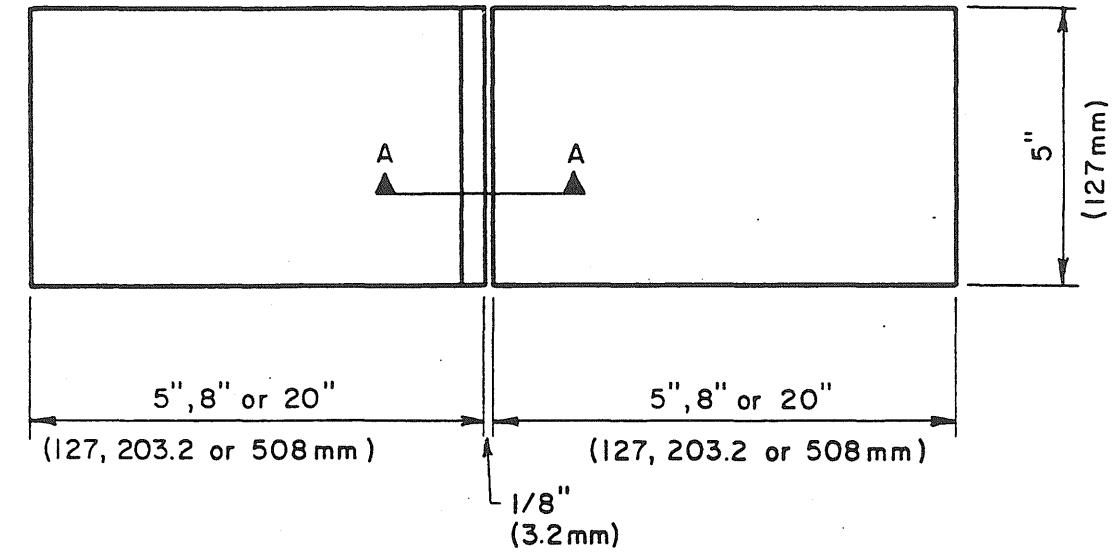


TOP VIEW

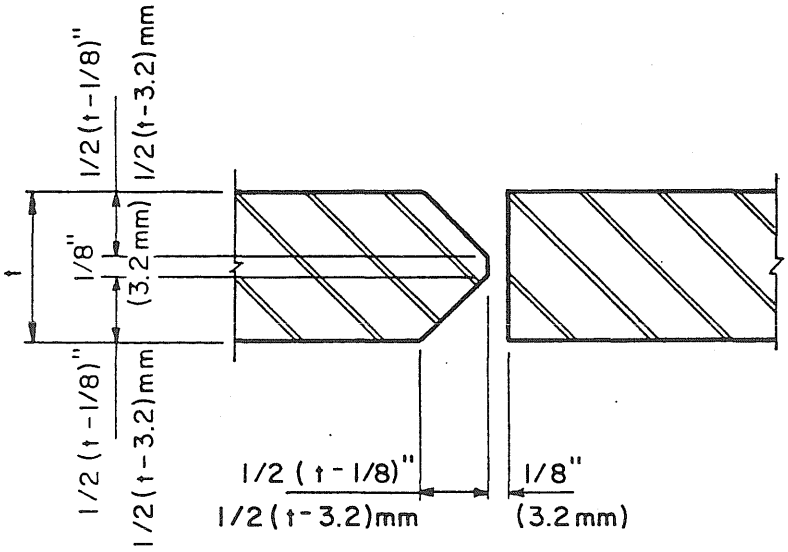


SECTION A–A

AWS B-U5a Joint
TSN = 8t

Fig. 4.2 Type "1" Specimen Geometry.

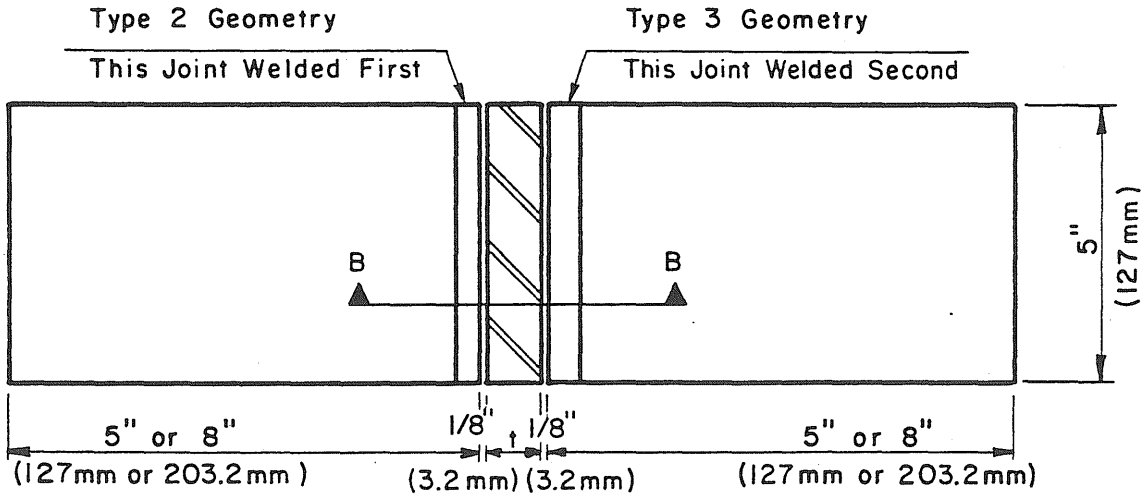


TOP VIEW

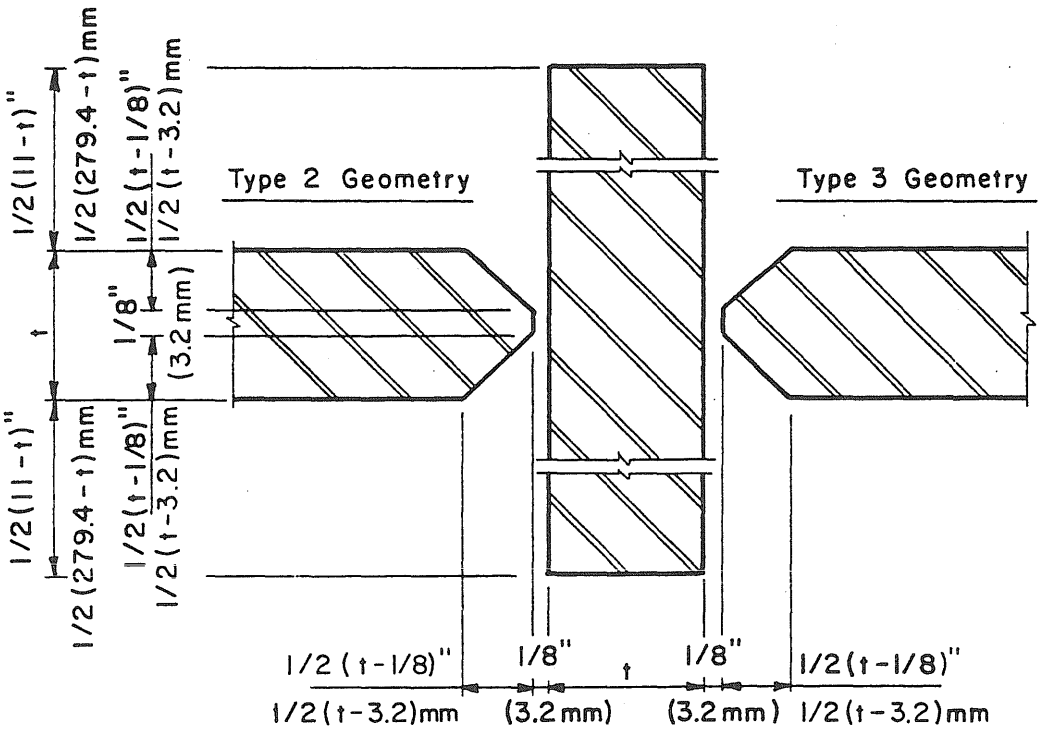


SECTION B-B

AWS TC-U5b Joints
TSN = 12 t For Type 2 Geometry
TSN = 16 t For Type 3 Geometry

Fig. 4.3 Types "2" and "3" Specimen Geometry.

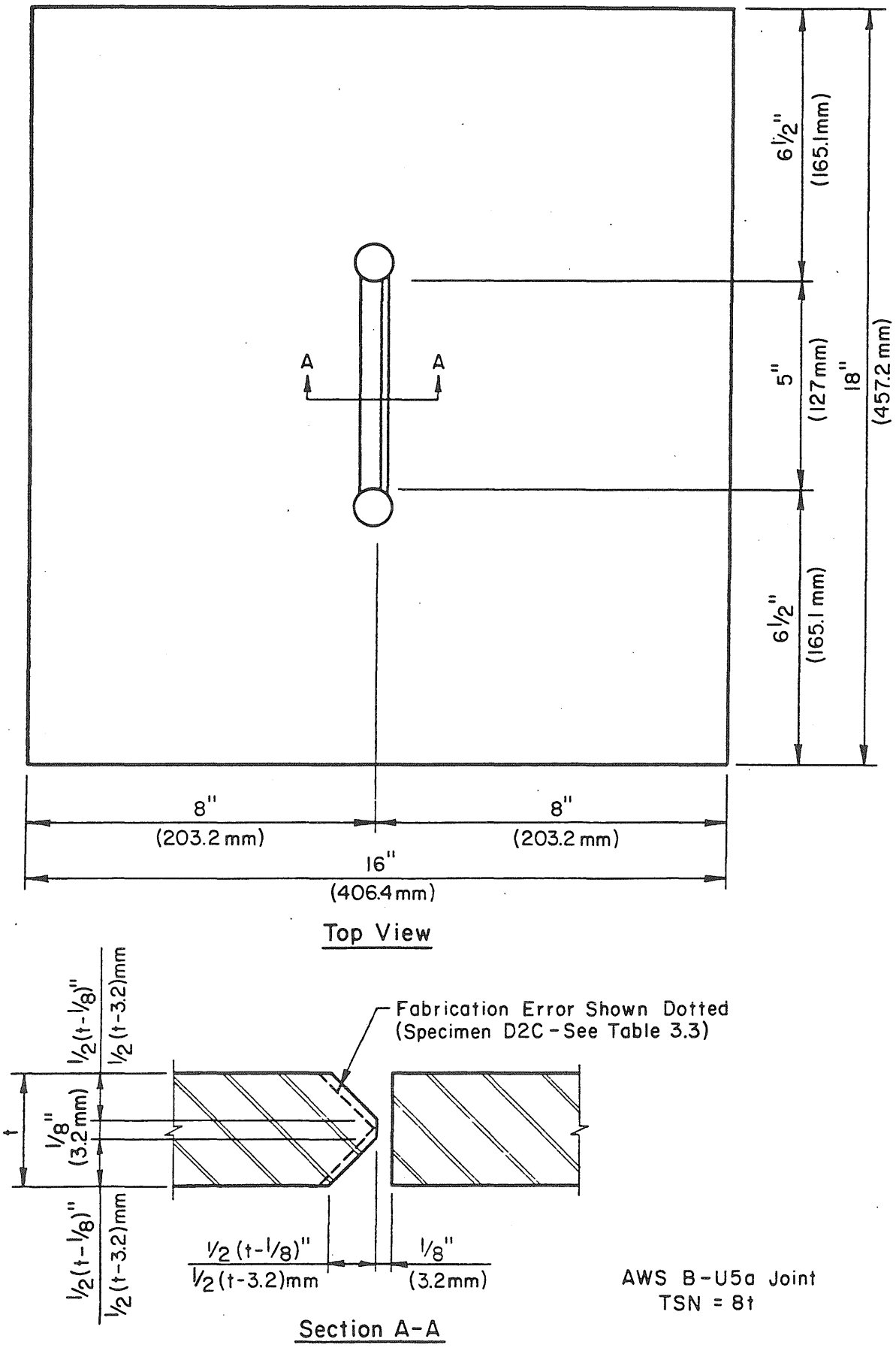


Fig. 4.4 Type "4" Specimen Geometry.

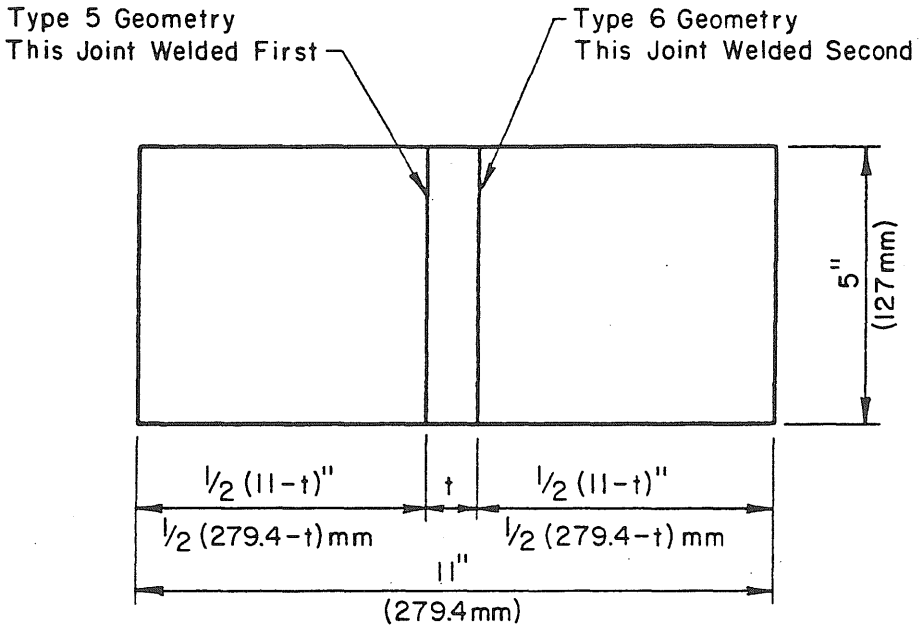


Top View

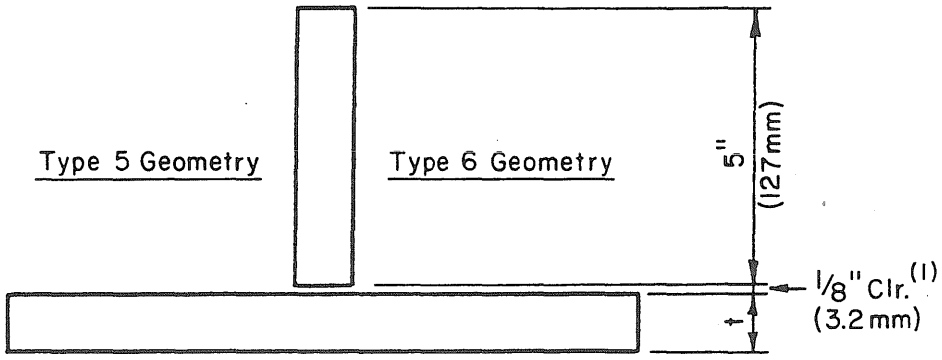


Side View

Fillet Welds
TSN = 12t For Type 5 and Type 6 Geometries

(1) Max. Clearance Permitted By AWS Specs. (D1.1-81) Was Used For All Specimens.

Fig. 4.5 Types "5" and "6" Specimen Geometry.

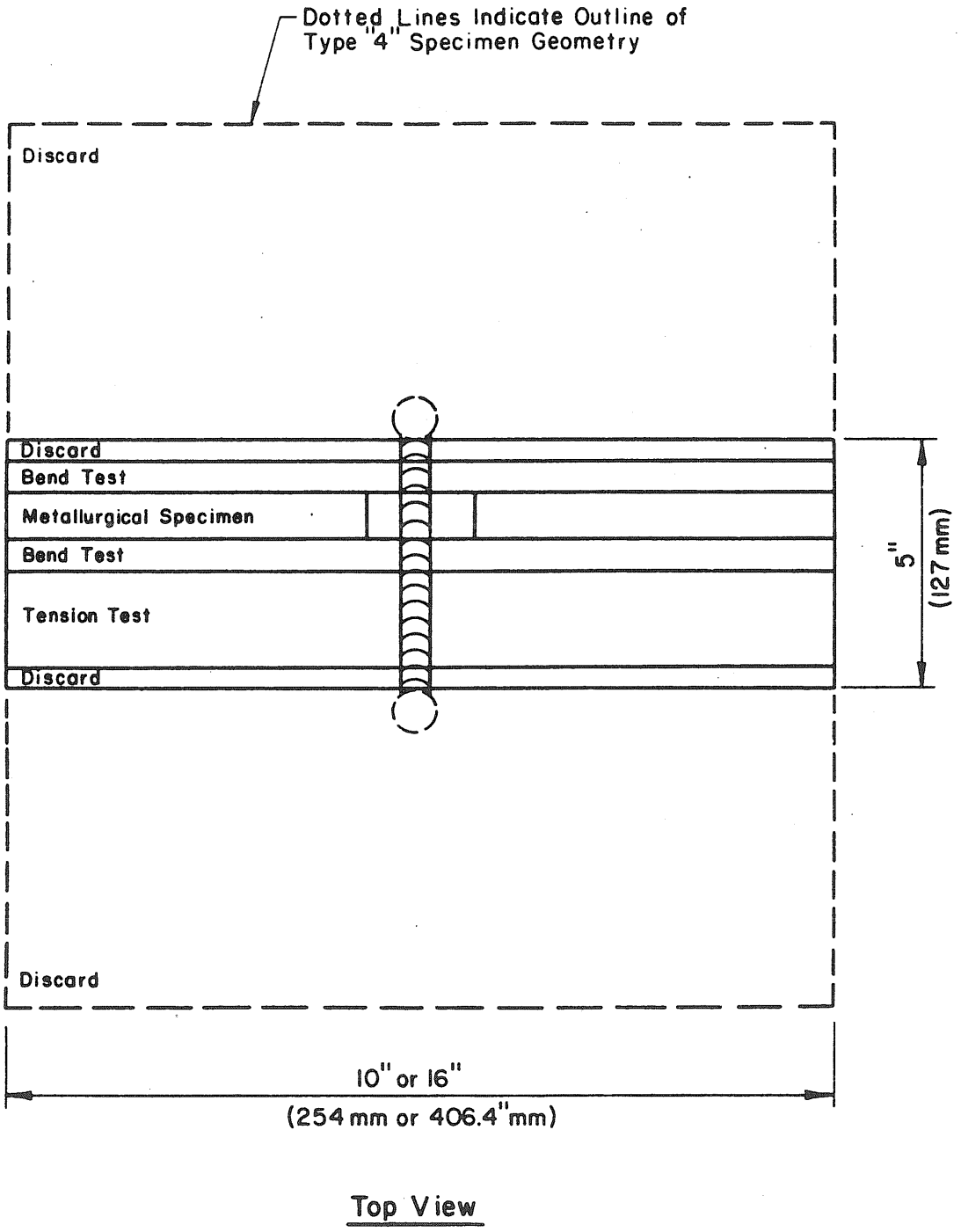


Fig. 4.6 Sectioning of Types "1" and "4" Specimens for Testing.

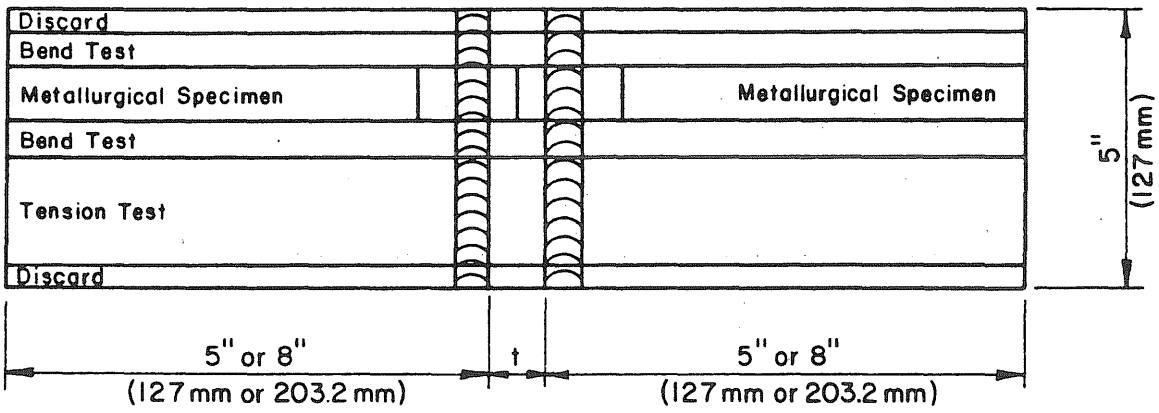


Top View

Fig. 4.7 Sectioning of Types "2" and "3" Specimens for Testing.

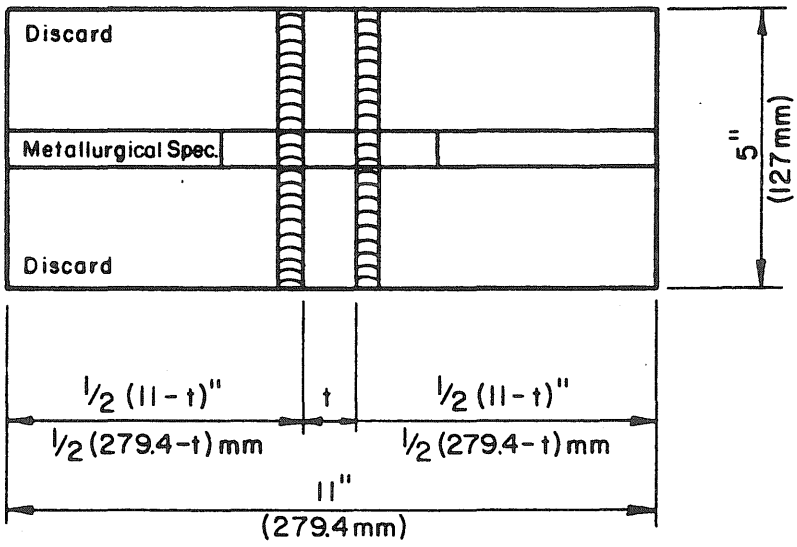


Top View

Fig. 4.8 Sectioning of Types "5" and "6" Specimens for Testing.

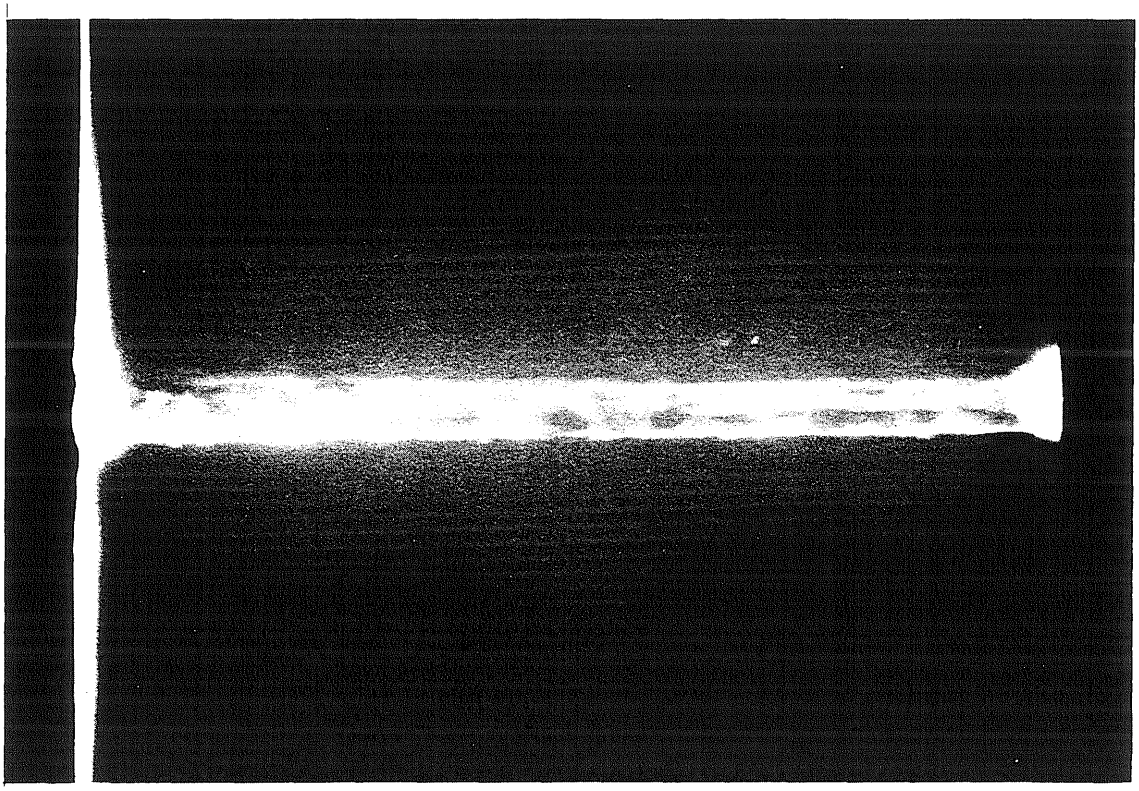

a) Specimen A1A - High discontinuity ratio (56%)

Fig. 5.1 Typical Radiographs of Specimens with High, Medium, and Low Discontinuity Ratios.

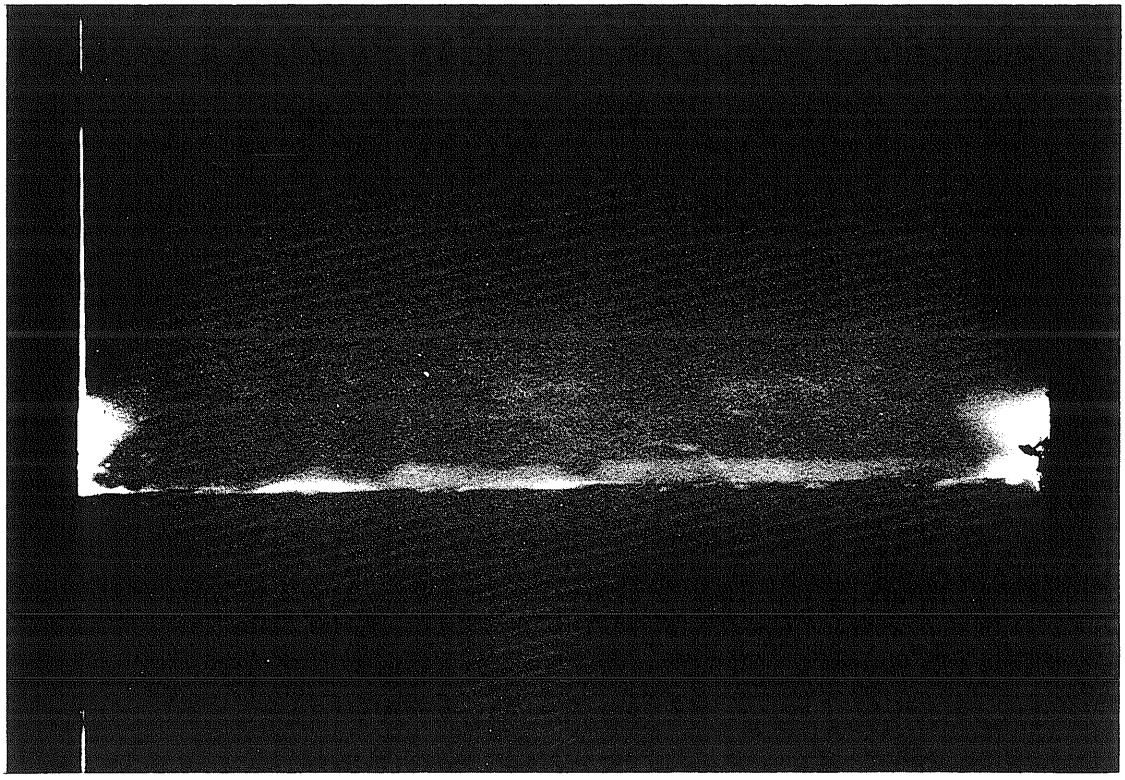

b) Specimen B1C - Medium discontinuity ratio (16%)

Fig. 5.1 Continued

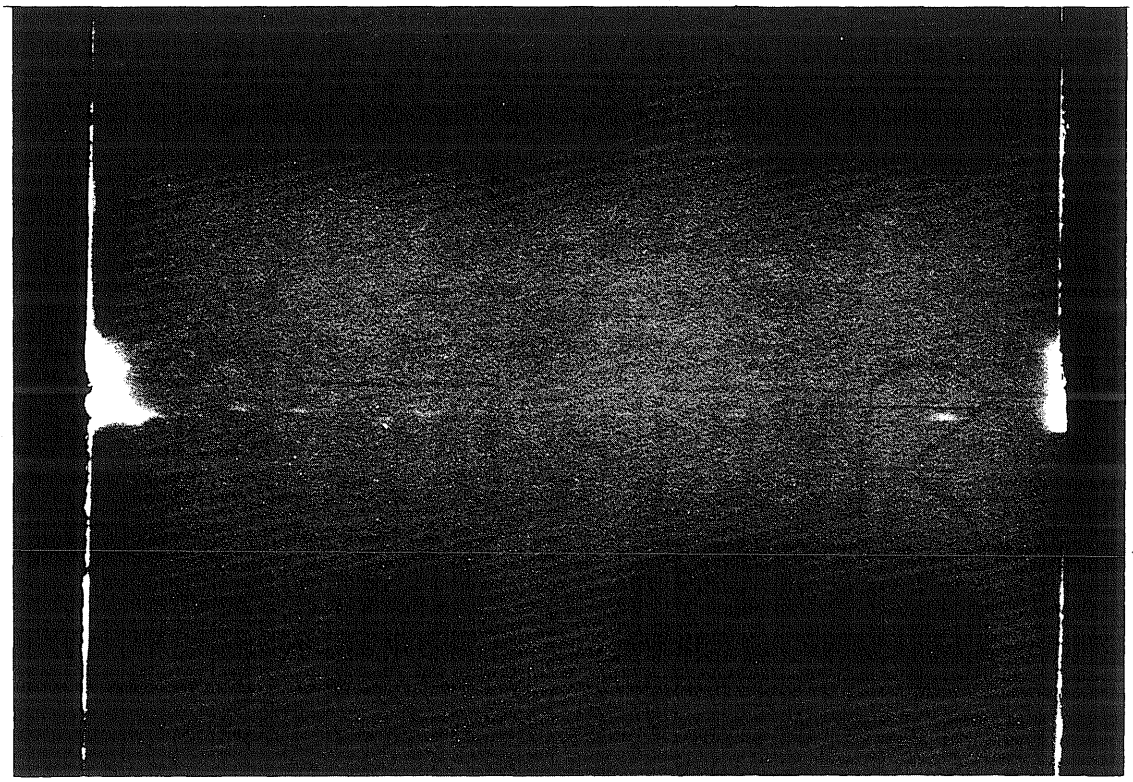

c) Specimen C1C - Low discontinuity ratio (3%)

Fig. 5.1 Continued

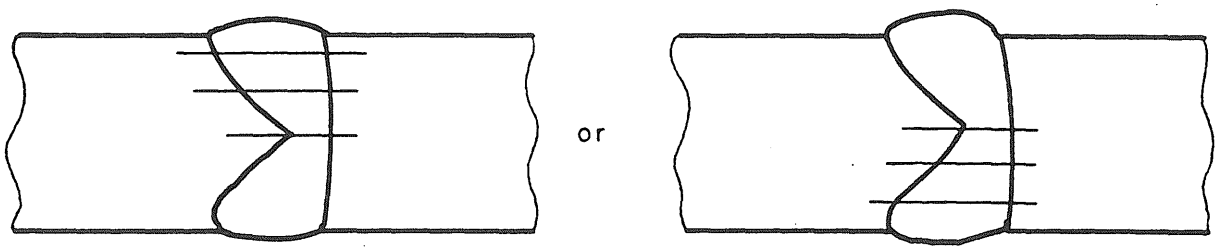


(a) Butt Weld ($t > 1/2"$)

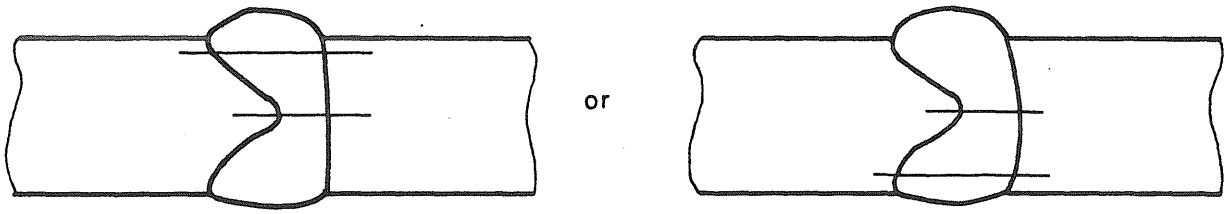


(b) Butt Weld ($t \leq 1/2"$)

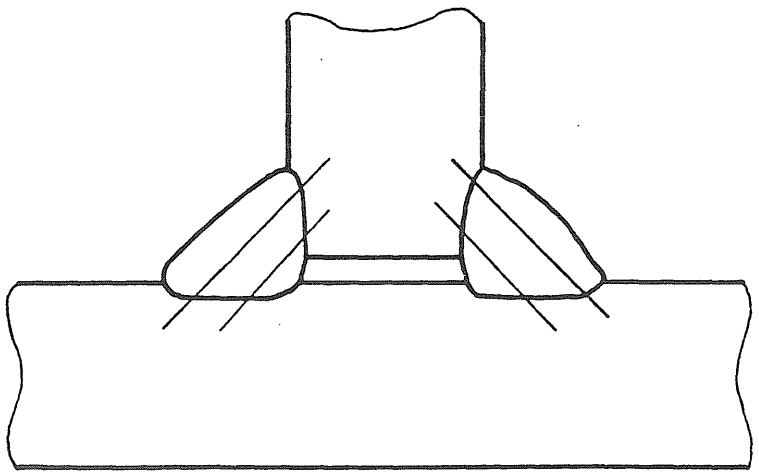

(c) Fillet Weld

Fig. 5.2 Typical Locations of Hardness Surveys.

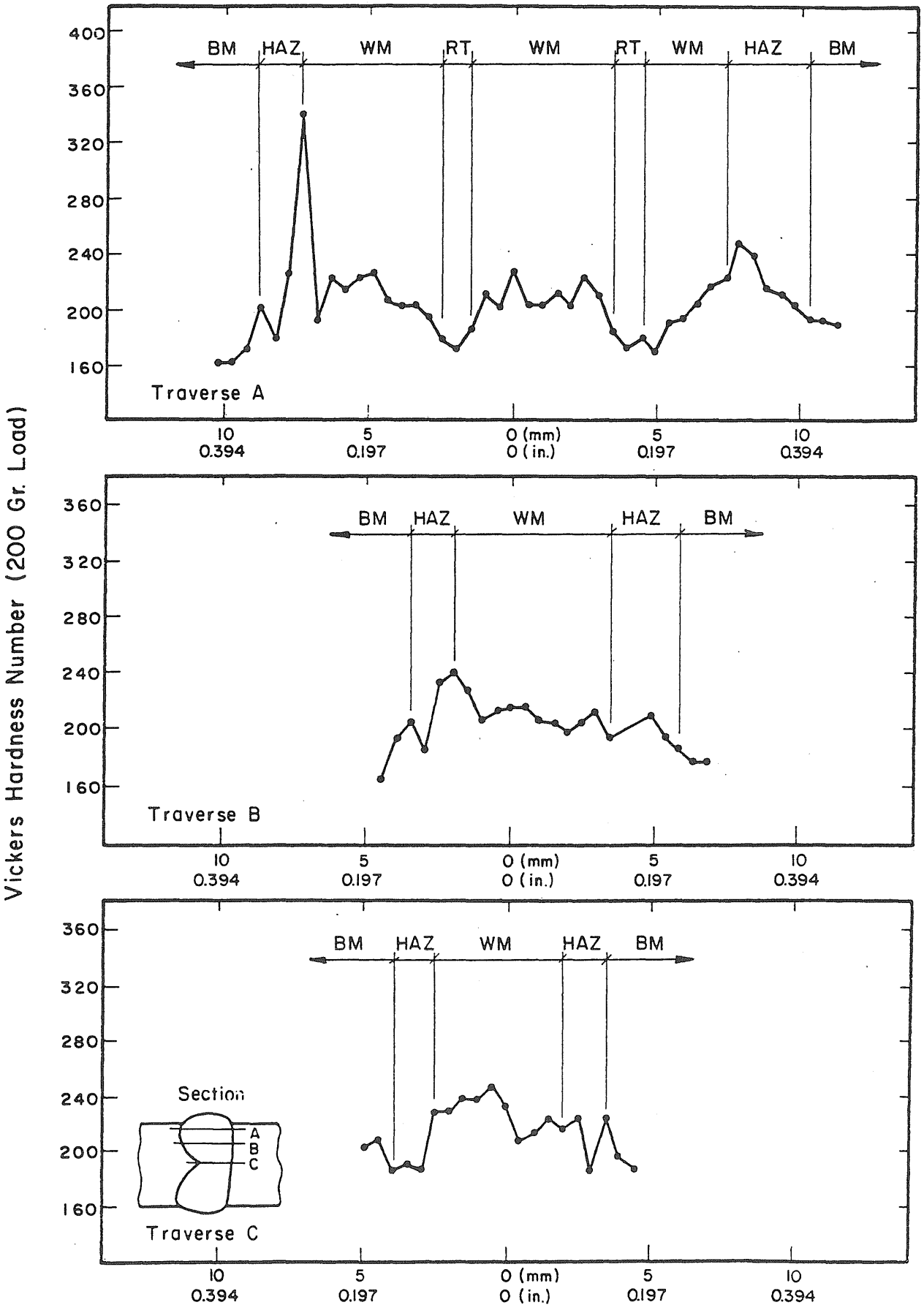


Fig. 5.3 Hardness Surveys for Specimen A1A.

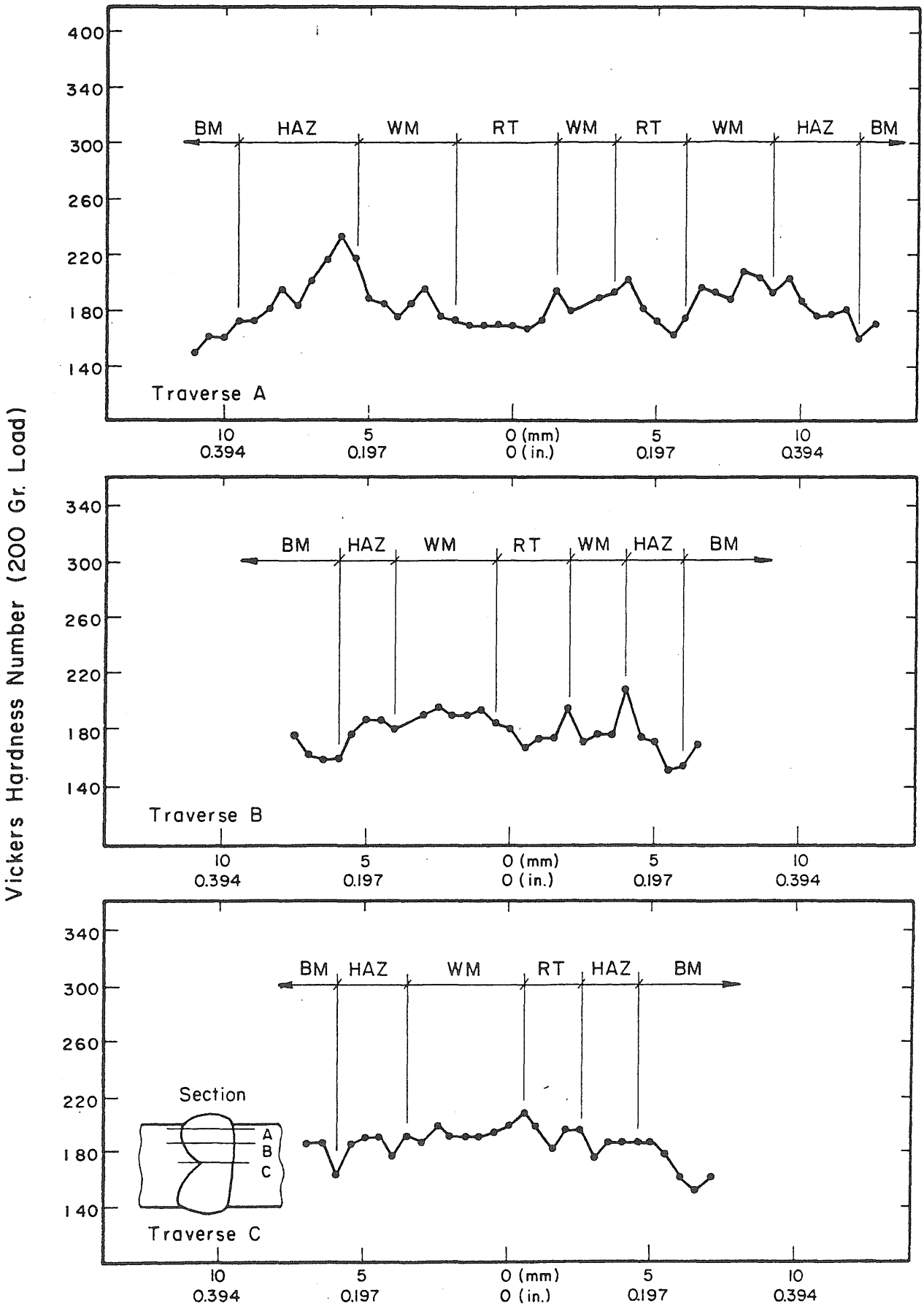


Fig. 5.4 Hardness Surveys for Specimen A1C.

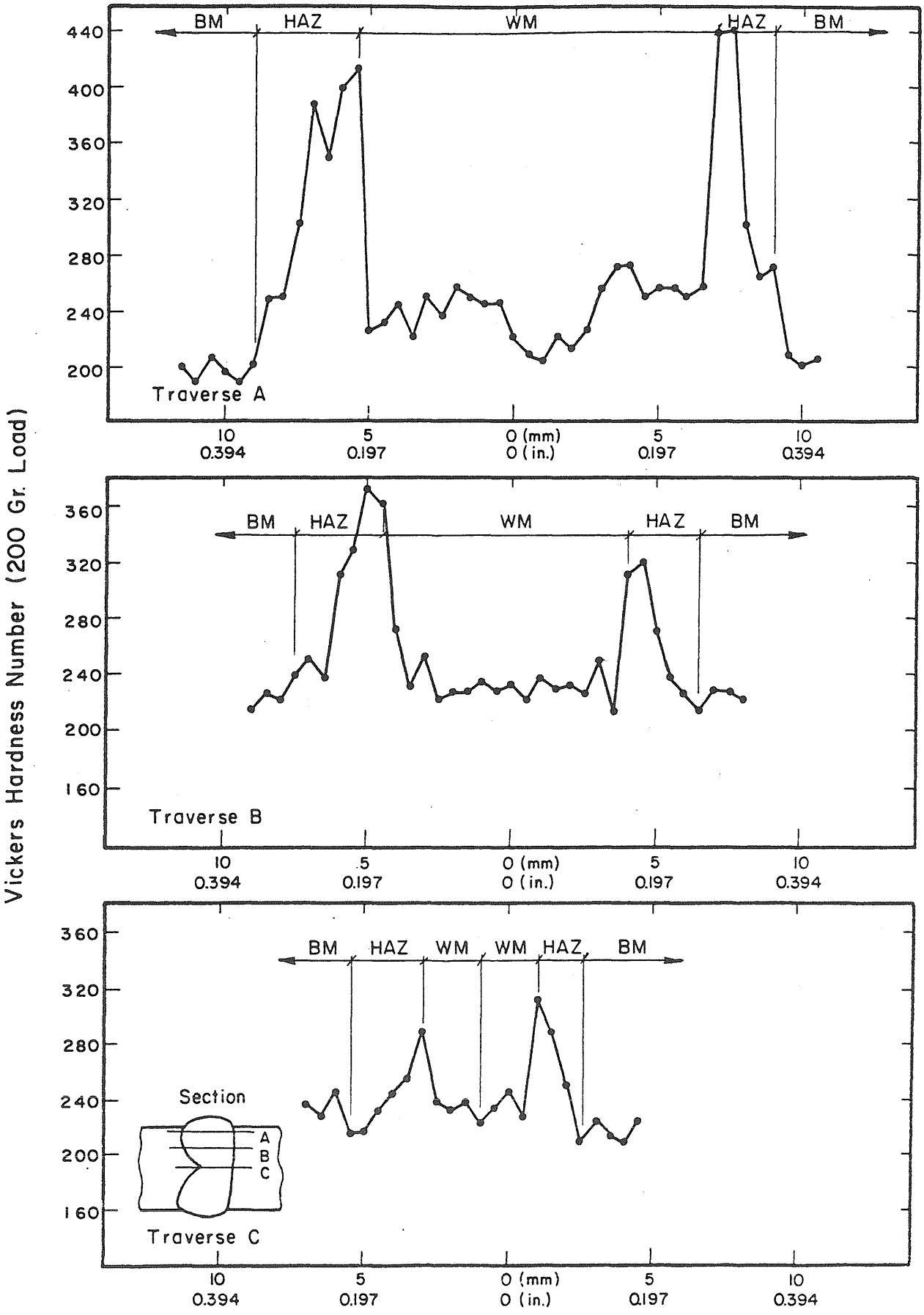


Fig. 5.5 Hardness Surveys for Specimen B1A.

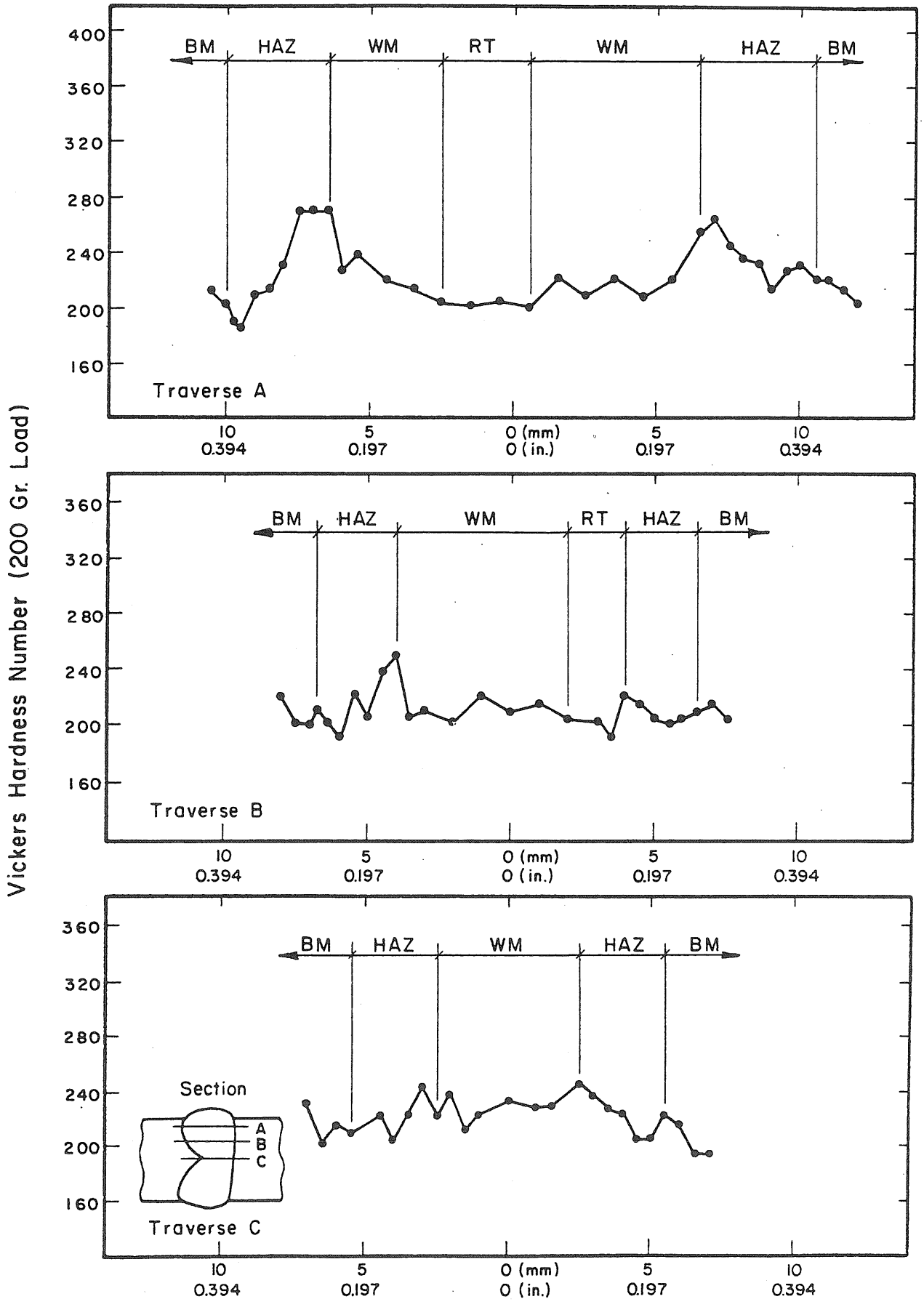


Fig. 5.6 Hardness Surveys for Specimen B1C.

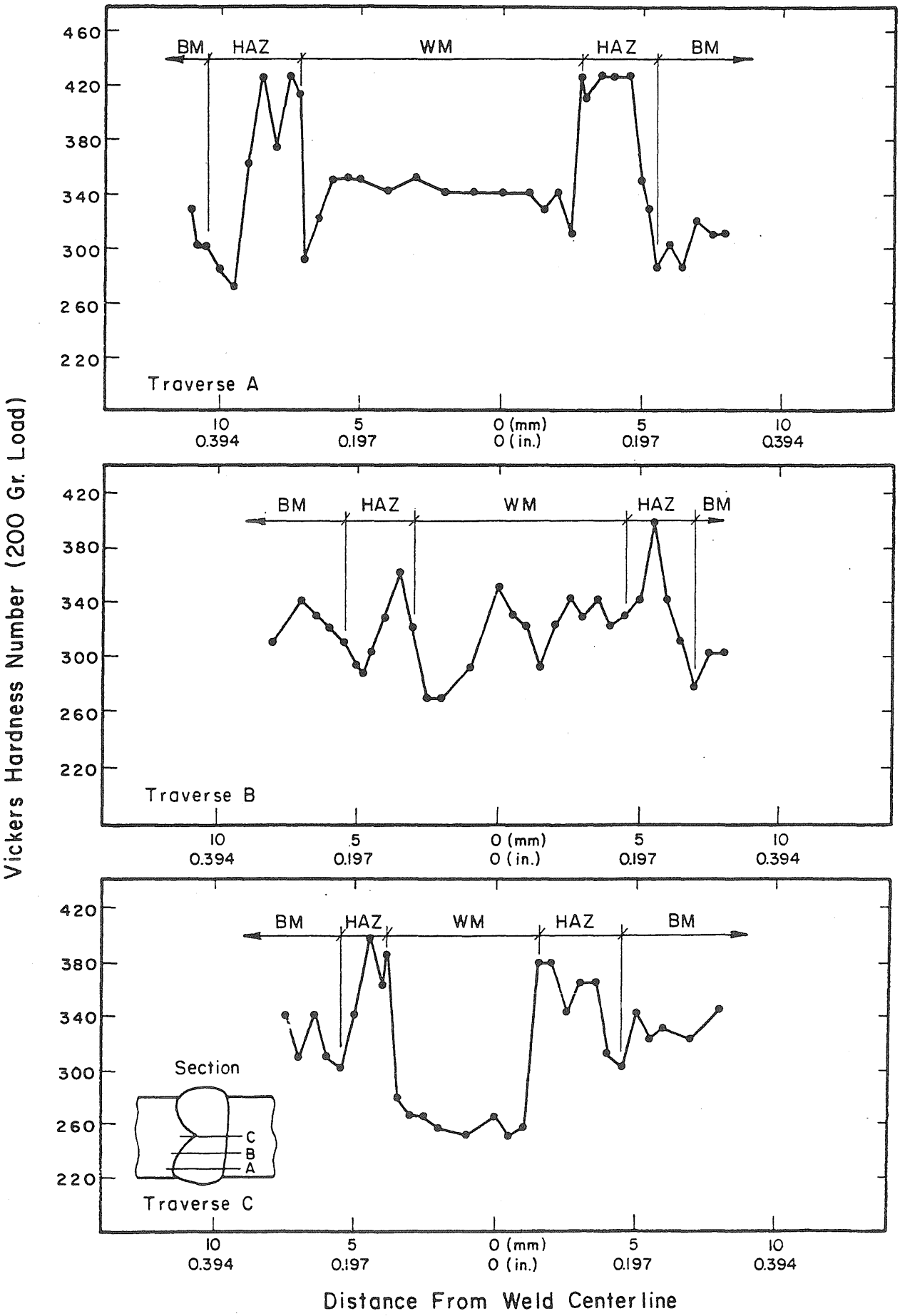


Fig. 5.7 Hardness Surveys for Specimen C1A.

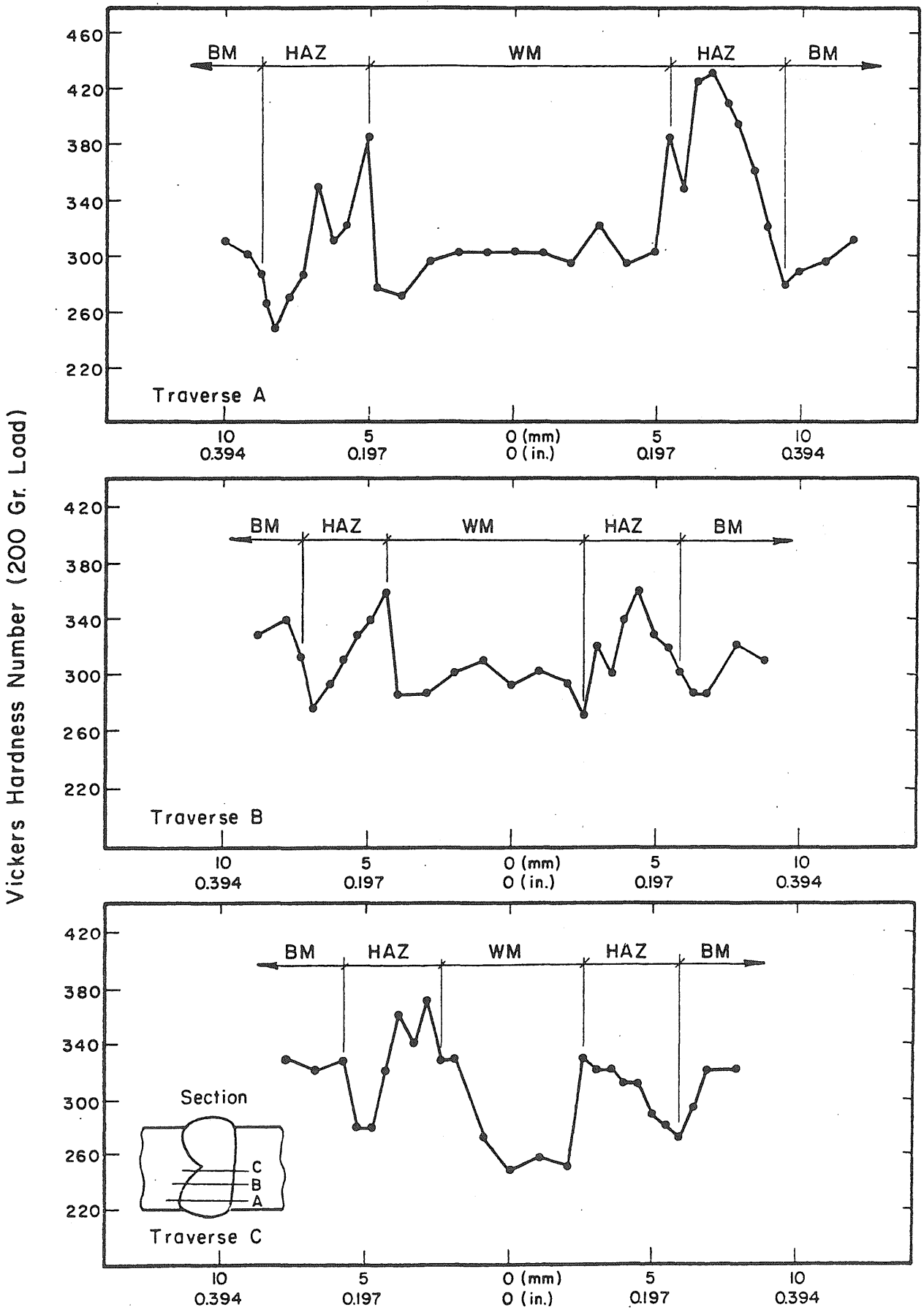


Fig. 5.8 Hardness Surveys for Specimen C1C.

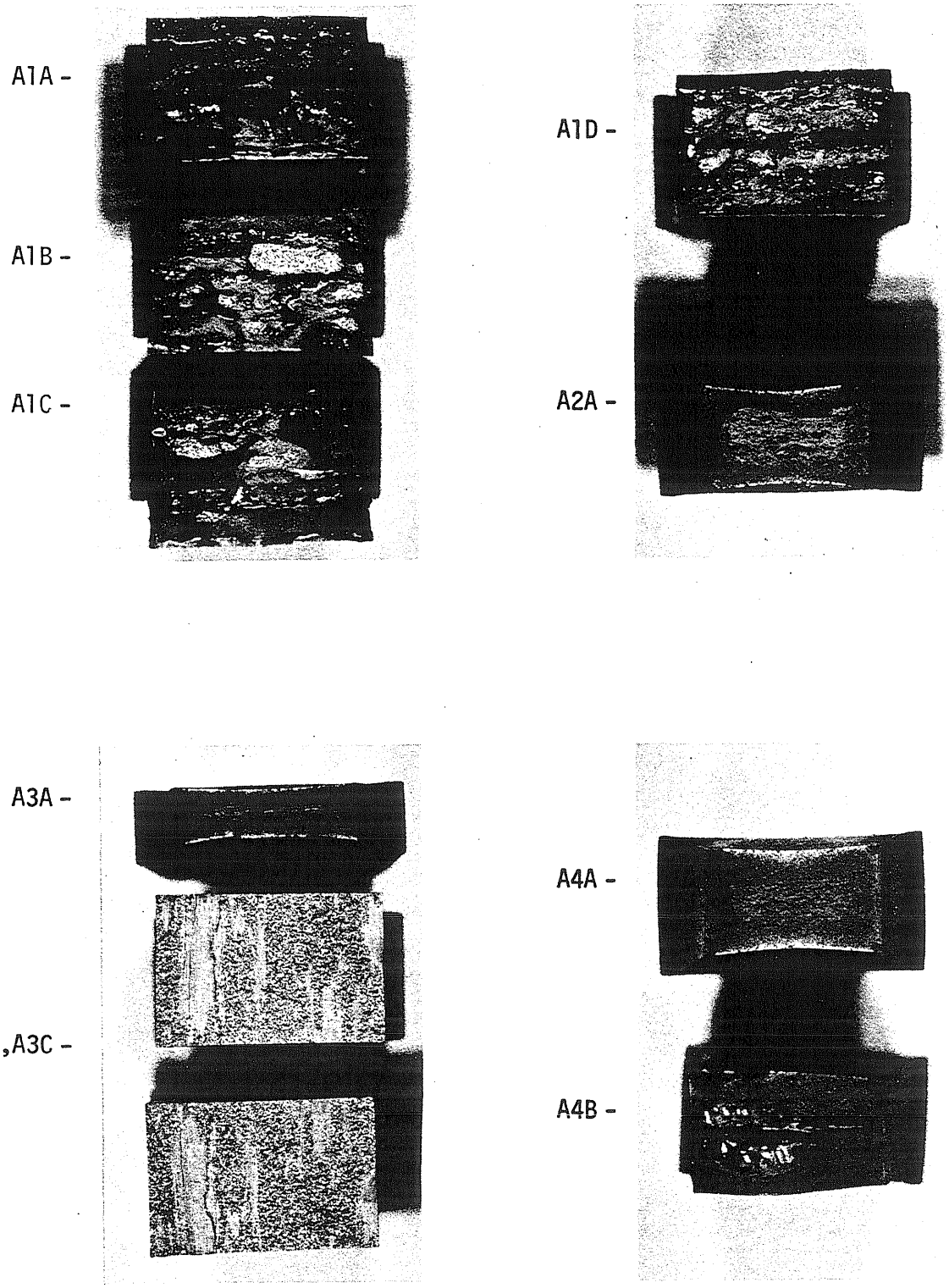


Fig. 5.9 Tension Test Failure Surfaces

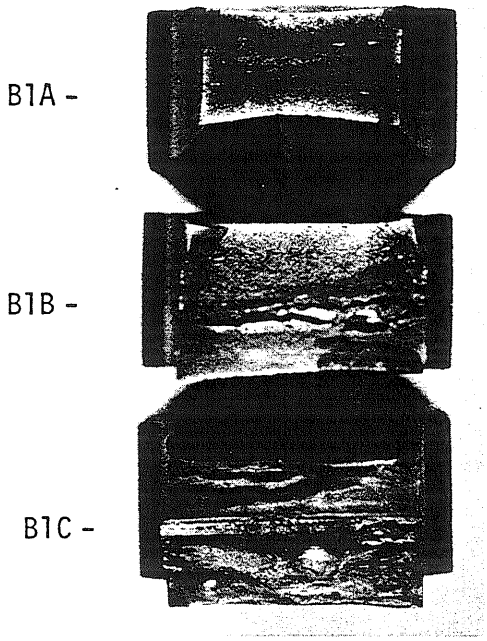


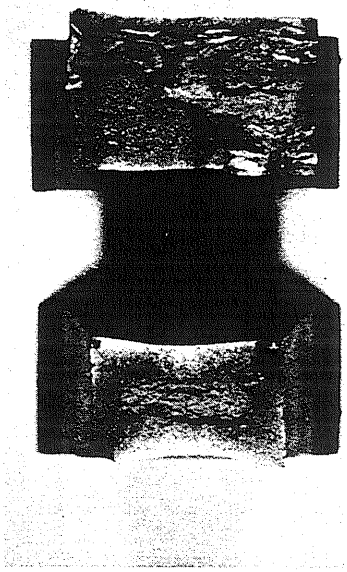


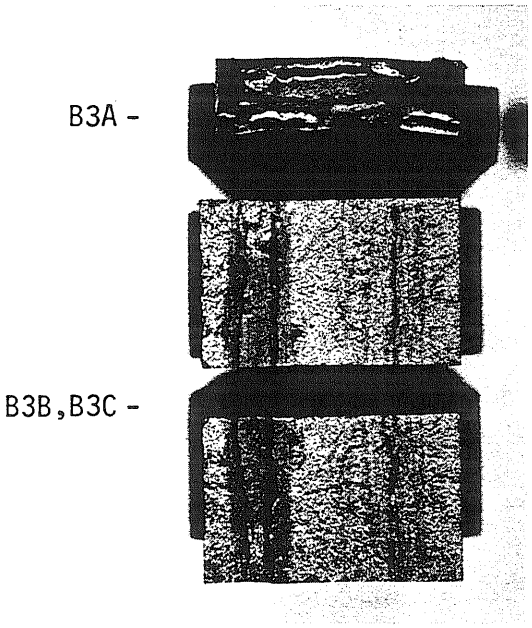


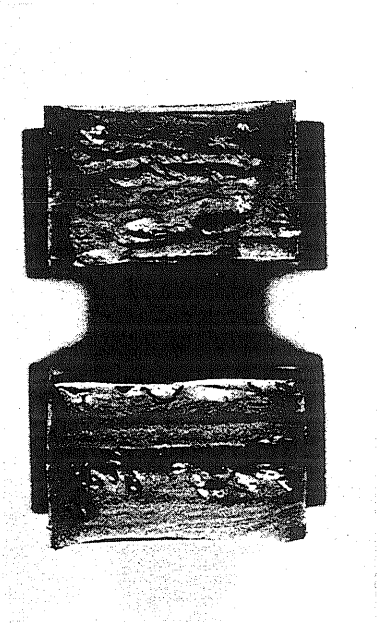


Fig. 5.9 Continued

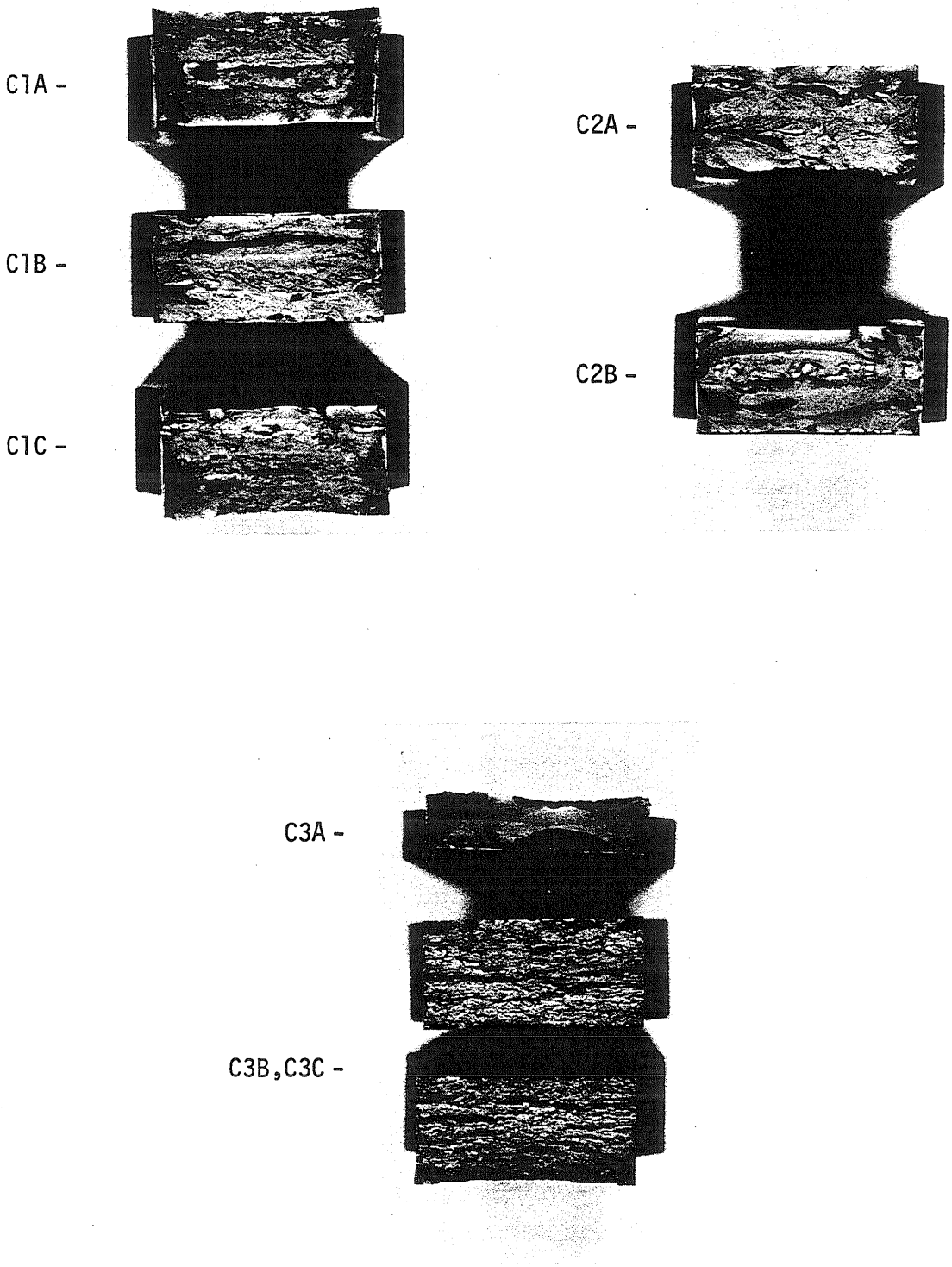


Fig. 5.9 Continued

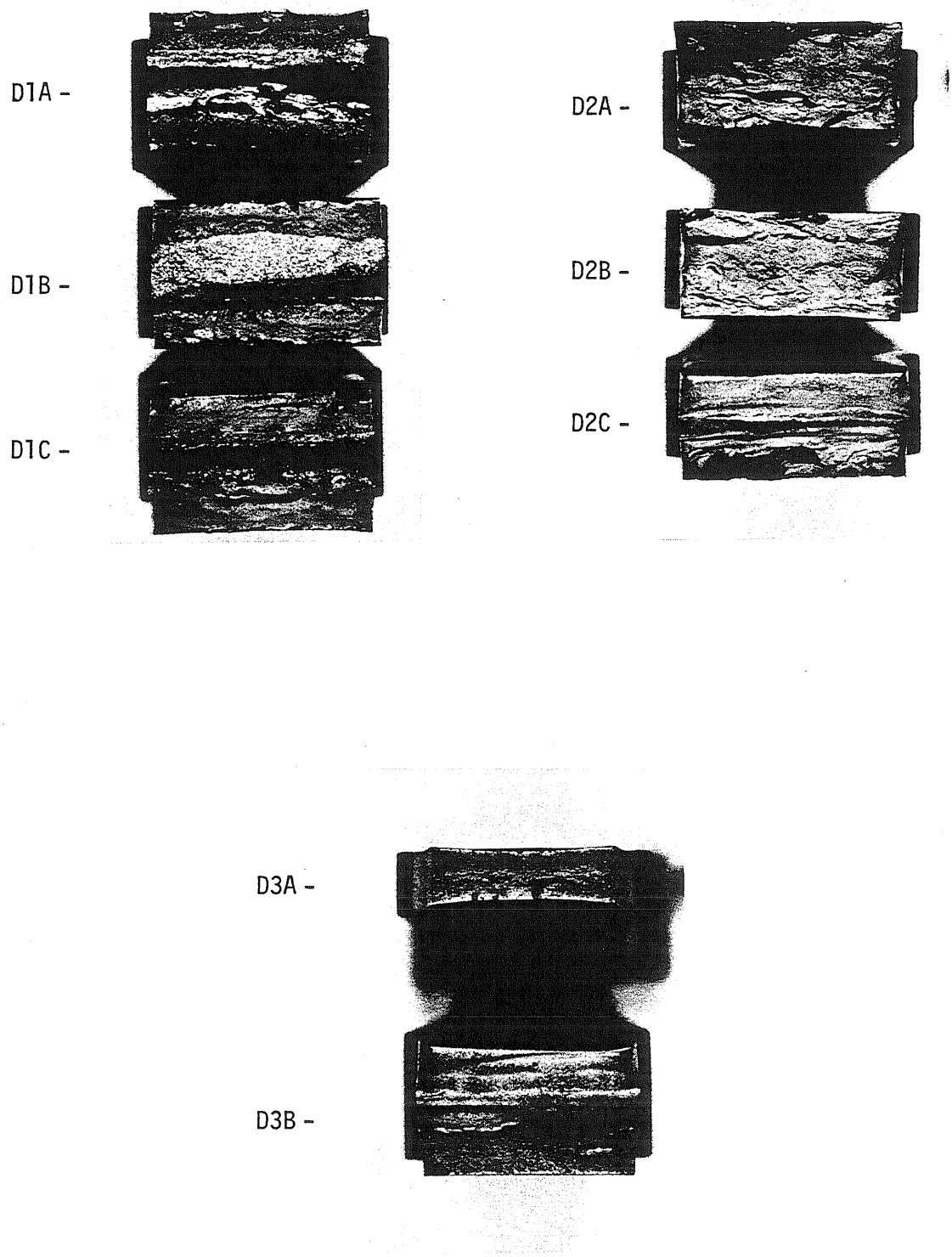


Fig. 5.9 Continued

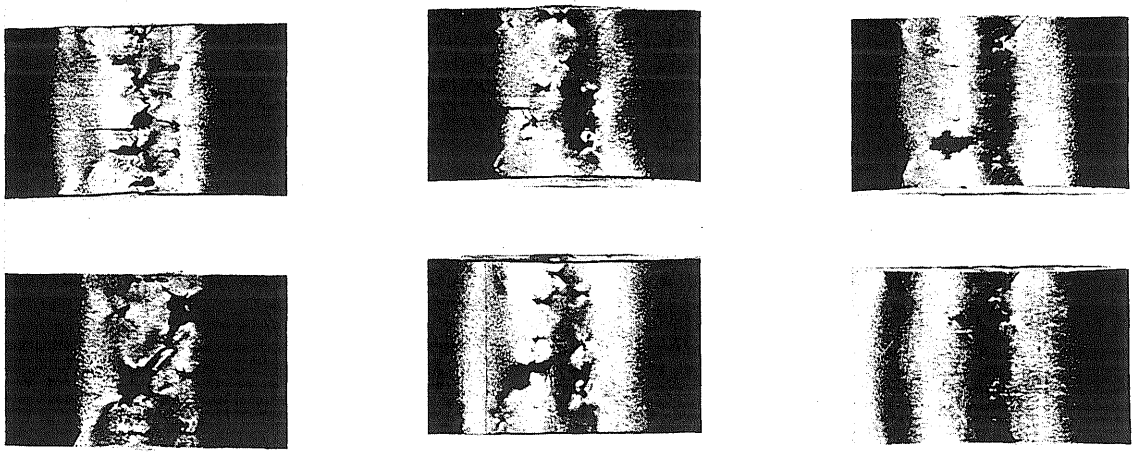

A1A A1B A1C

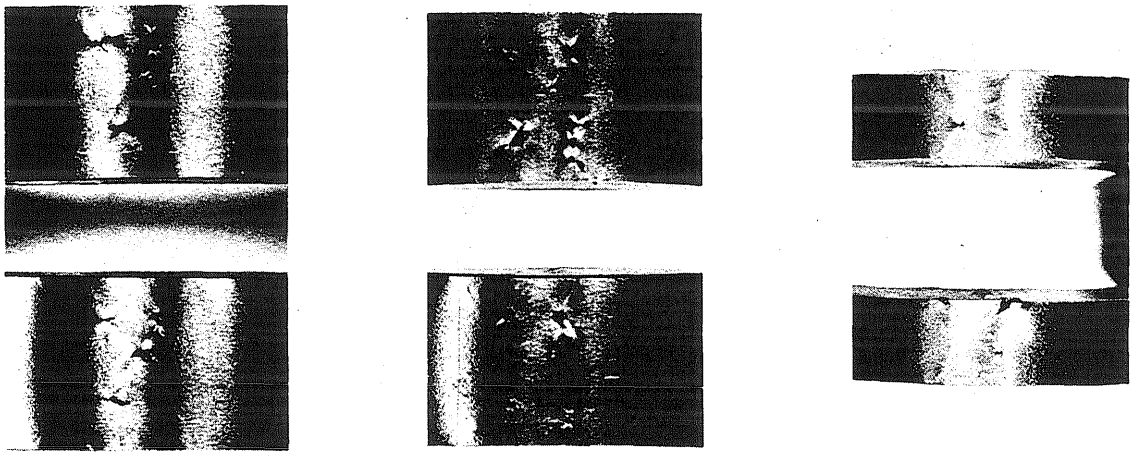

A1D A2A A3A

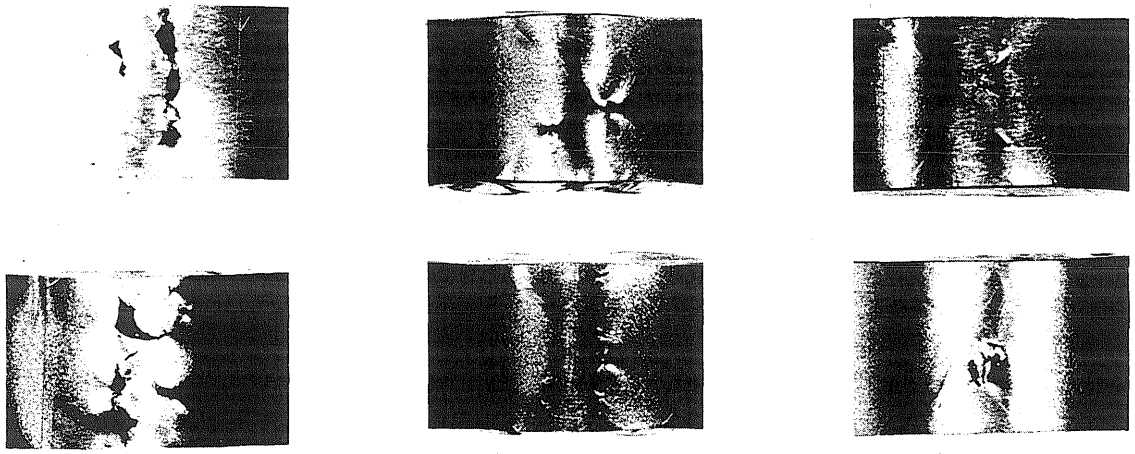

A3B
A3C A4A A4B

Fig. 5.10 Bend Test Specimens

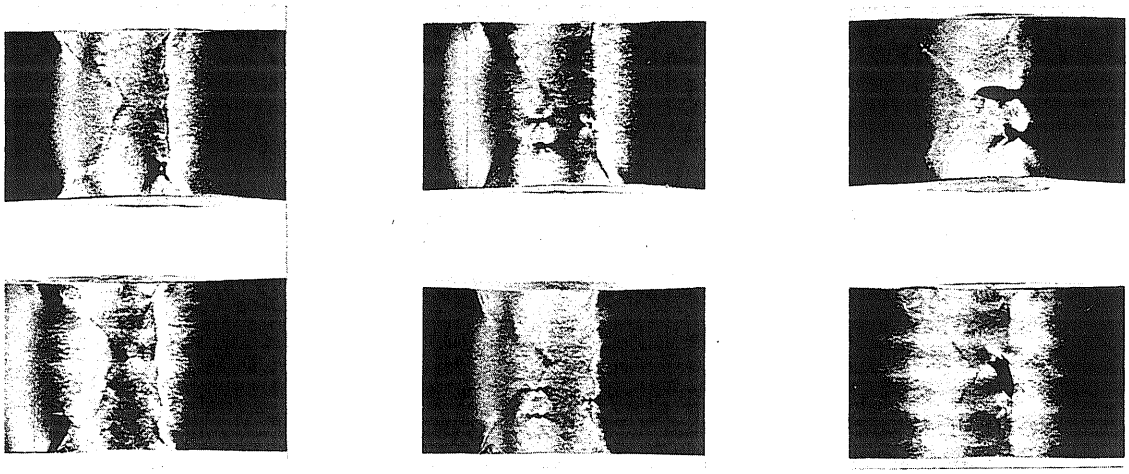

B1A B1B B1C

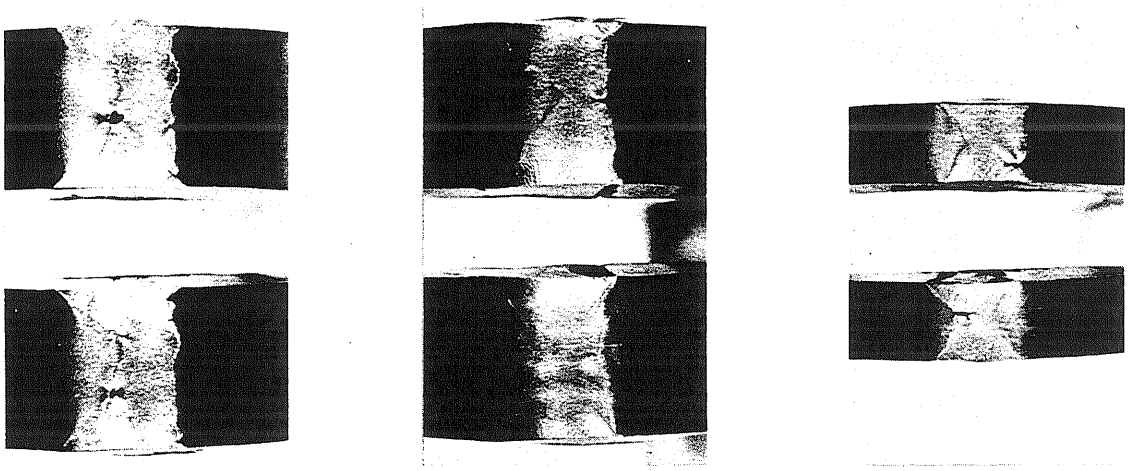

B2A B2B B3A

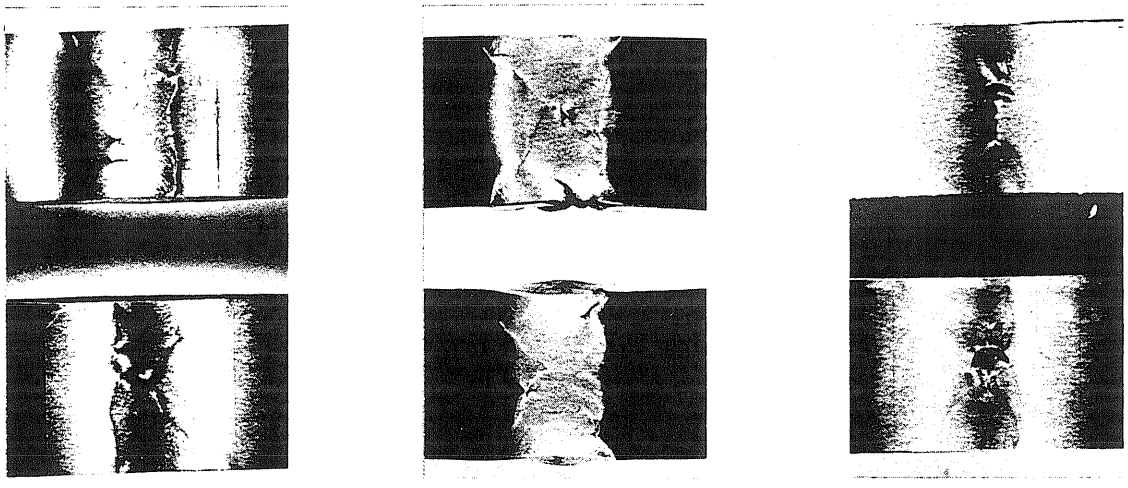

B3B
B3C B4A B4B

Fig. 5.10 Continued

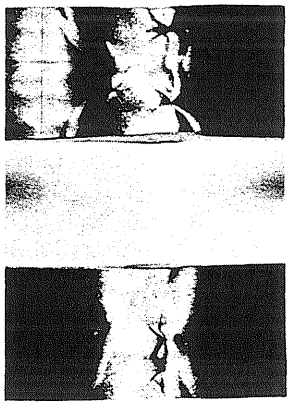

C1A

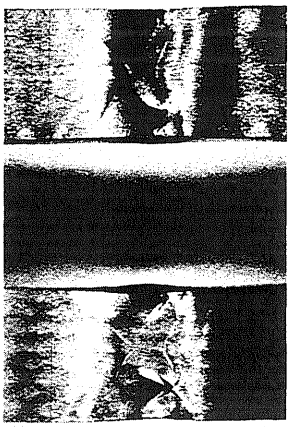

C1B

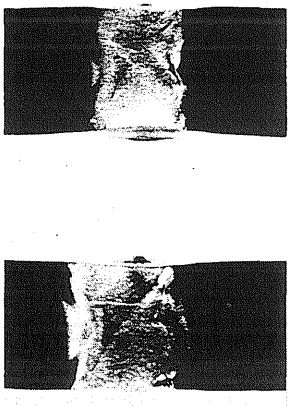

C1C

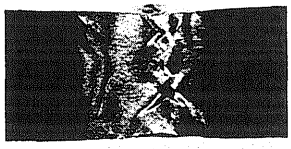

C2A

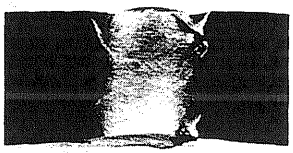

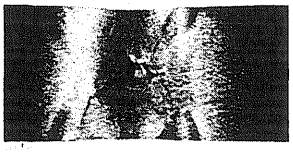

C2B

C3A

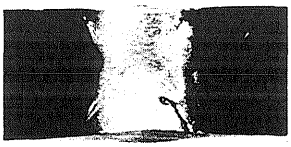

C3B
C3C

Fig. 5.10 Continued

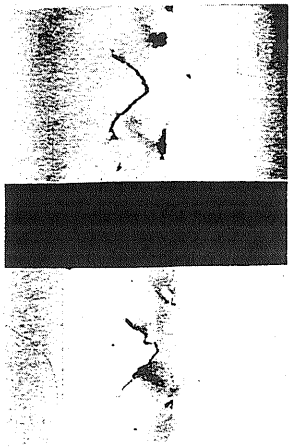

D1A

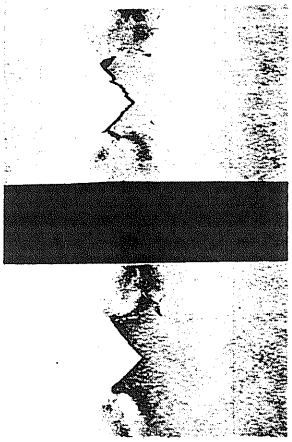

D1B

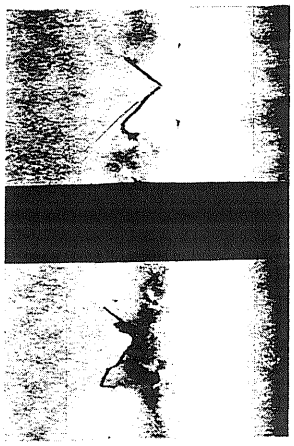

D1C

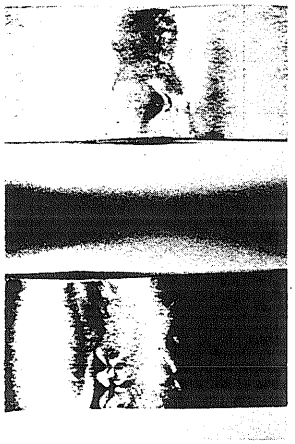

D2A

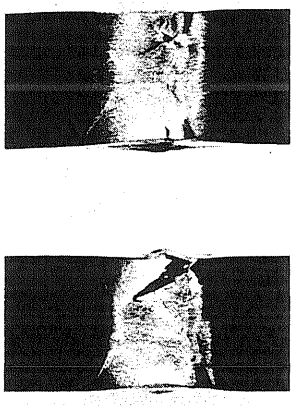

D2B

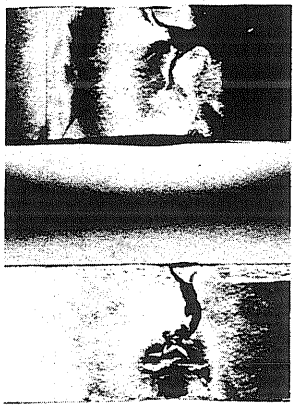

D2C

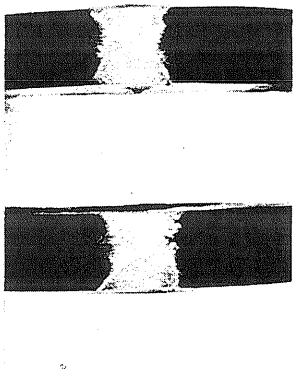

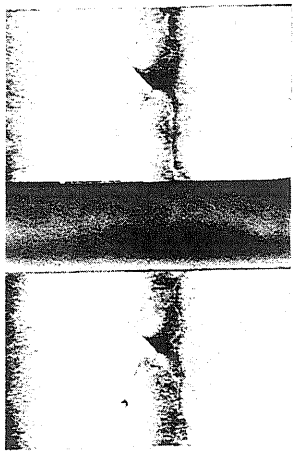

D3A D3B

Fig. 5.10 Continued

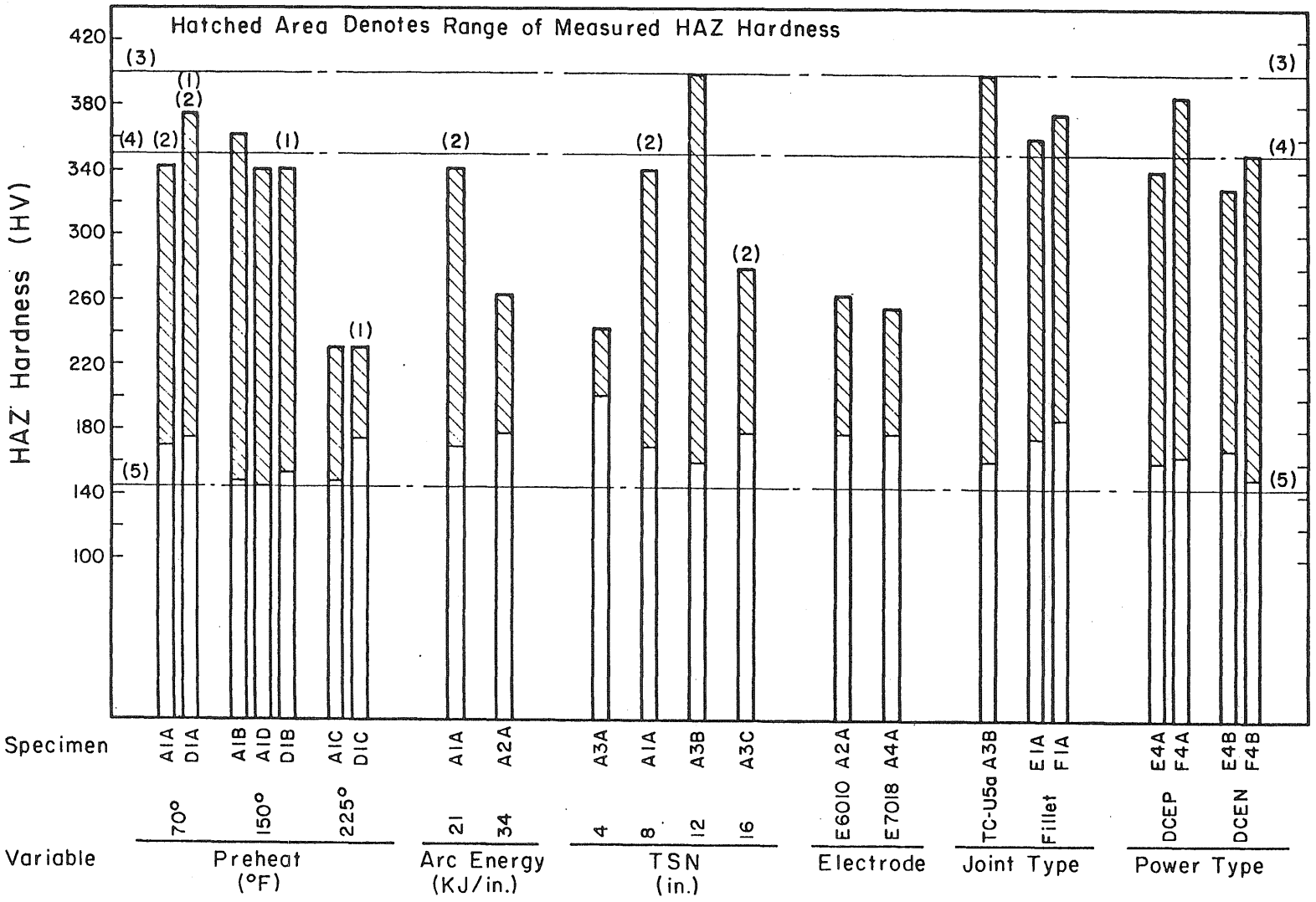


(1) HAZ cracking occurred at inner passes. See Figure 5.10.
(2) Last pass did not occur adjacent to base metal.
(3) Critical hardness for low hydrogen process to prevent HAZ cracking. (Ref. 5,12)
(4) Critical hardness for other-than-low hydrogen process to prevent HAZ cracking. (Ref. 5,12)
(5) Base metal hardness.

Fig. 6.1 Effects of Various Welding Variables on HAZ Hardness Range of Mild Steel Specimens.

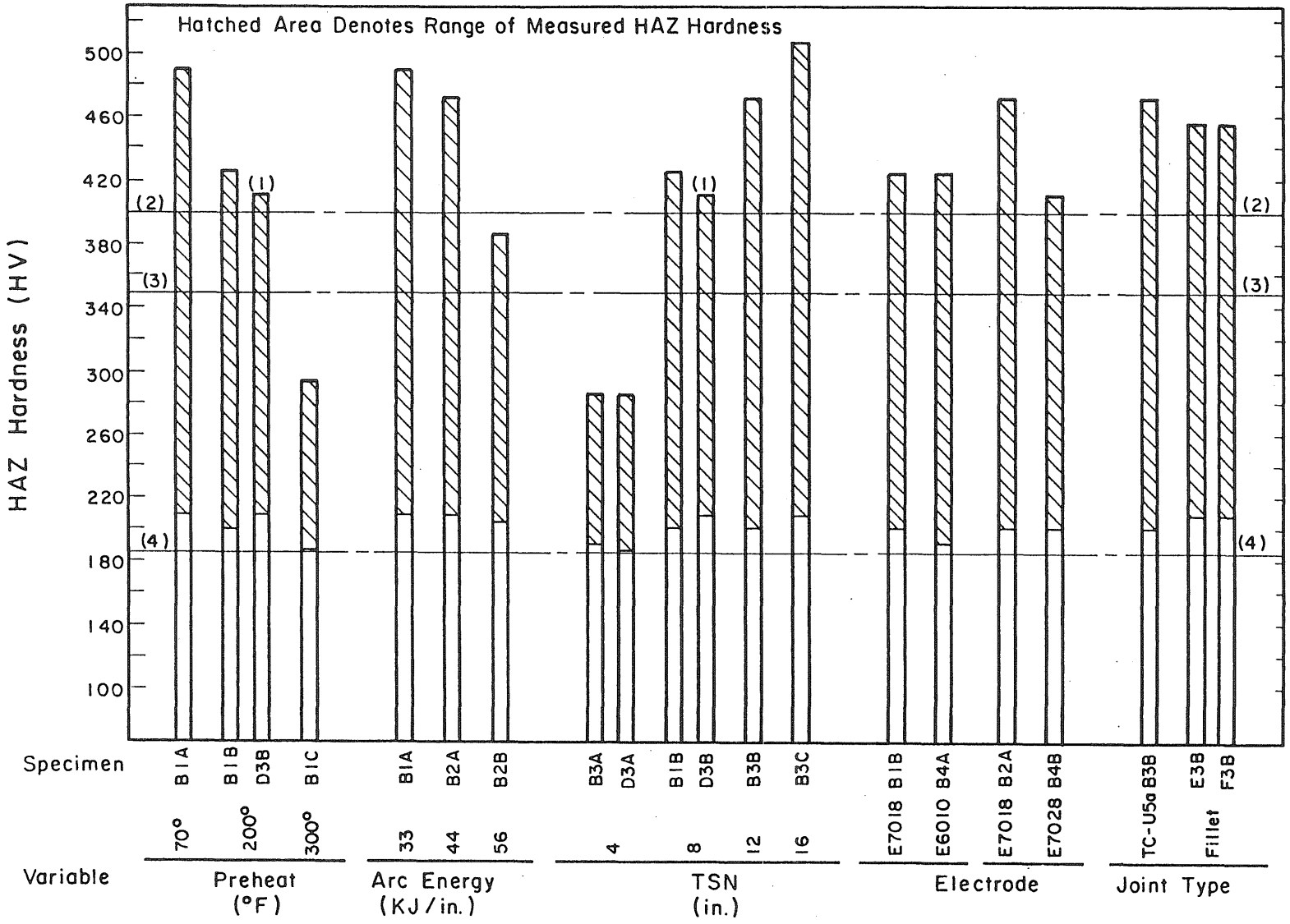


(1) HAZ cracking occurred at inner passes. See Figure 5.10.
(2) Critical hardness for low hydrogen process to prevent HAZ cracking. (Ref. 5,12)
(3) Critical hardness for other-than-low hydrogen process to prevent HAZ cracking. (Ref. 5,12)
(4) Base metal hardness.

Fig. 6.2 Effects of Various Welding Variables on HAZ Hardness Range of Low-Alloy Steel Specimens.

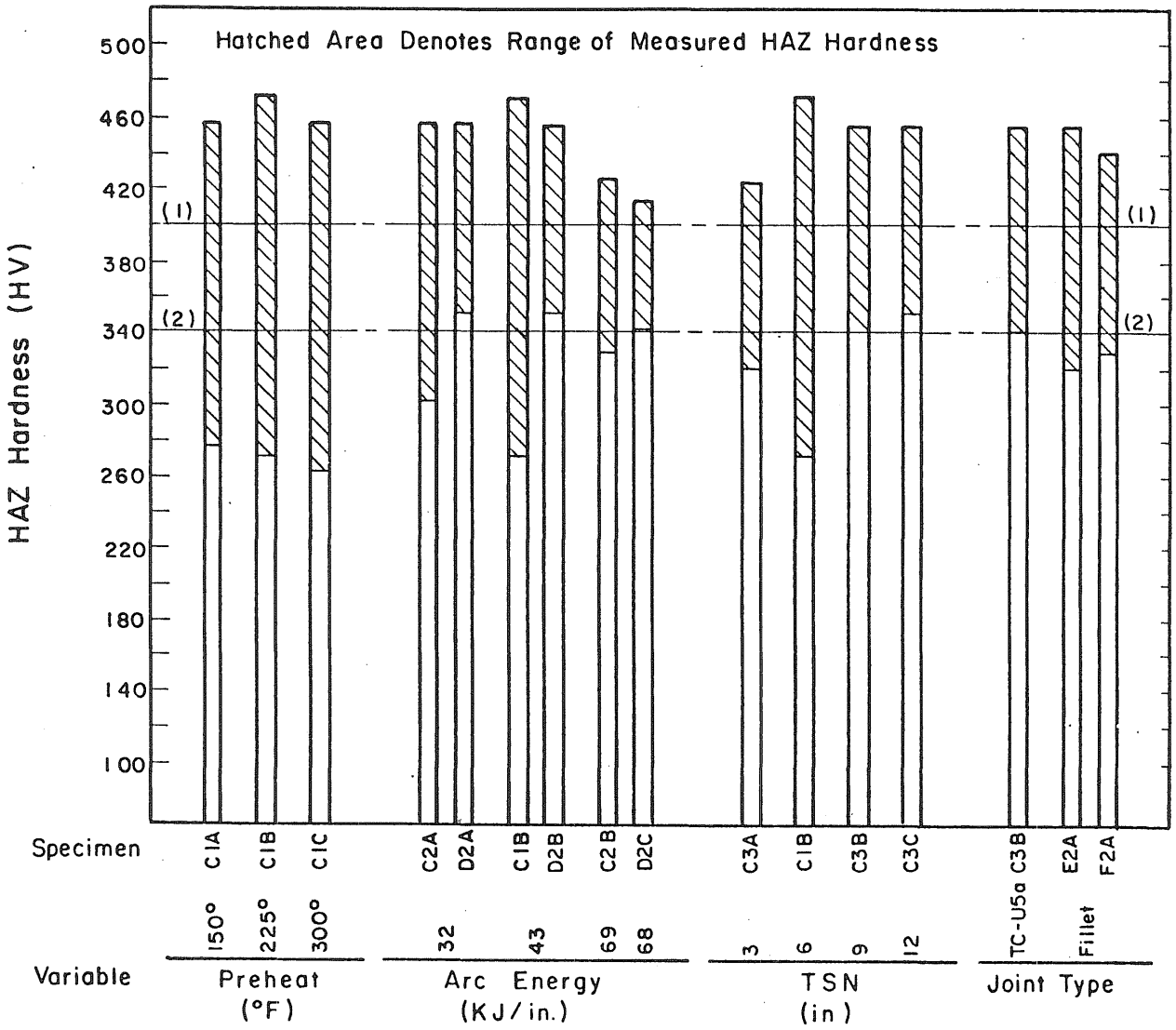


(1) Critical hardness for low hydrogen process to prevent HAZ cracking. (Ref. 5,12)
(2) Base metal hardness.

Fig. 6.3 Effects of Various Welding Variables on HAZ Hardness Range of Quenched and Tempered Steel Specimens.

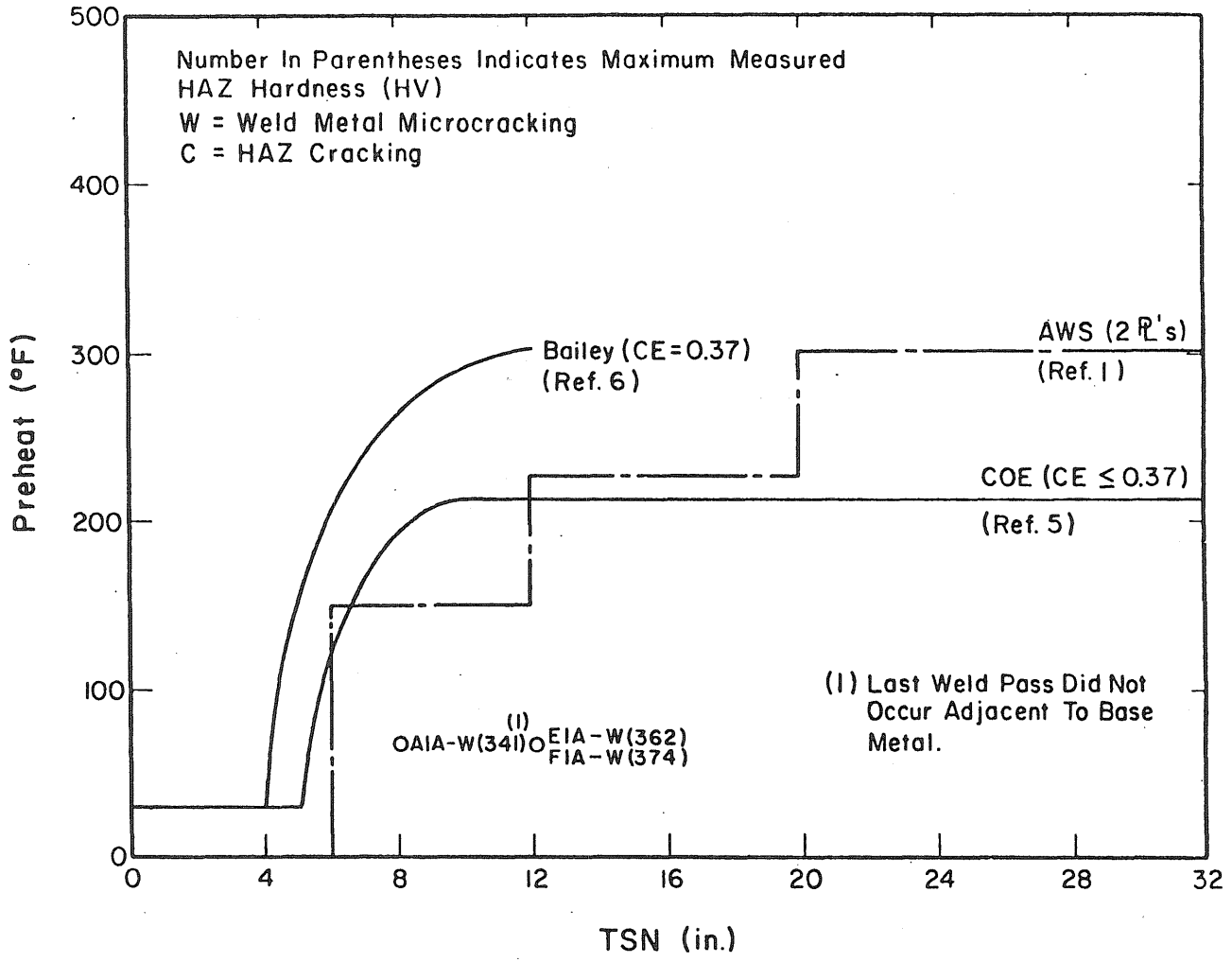


(a) Hydrogen = Other Than Low Arc Energy = 20 KJ/in.
Critical Hardness = 350 HV

Fig. 6.4 Relationship Between Test Welding Procedures and Welding Requirements to Control HAZ Cracking in Mild Steels.

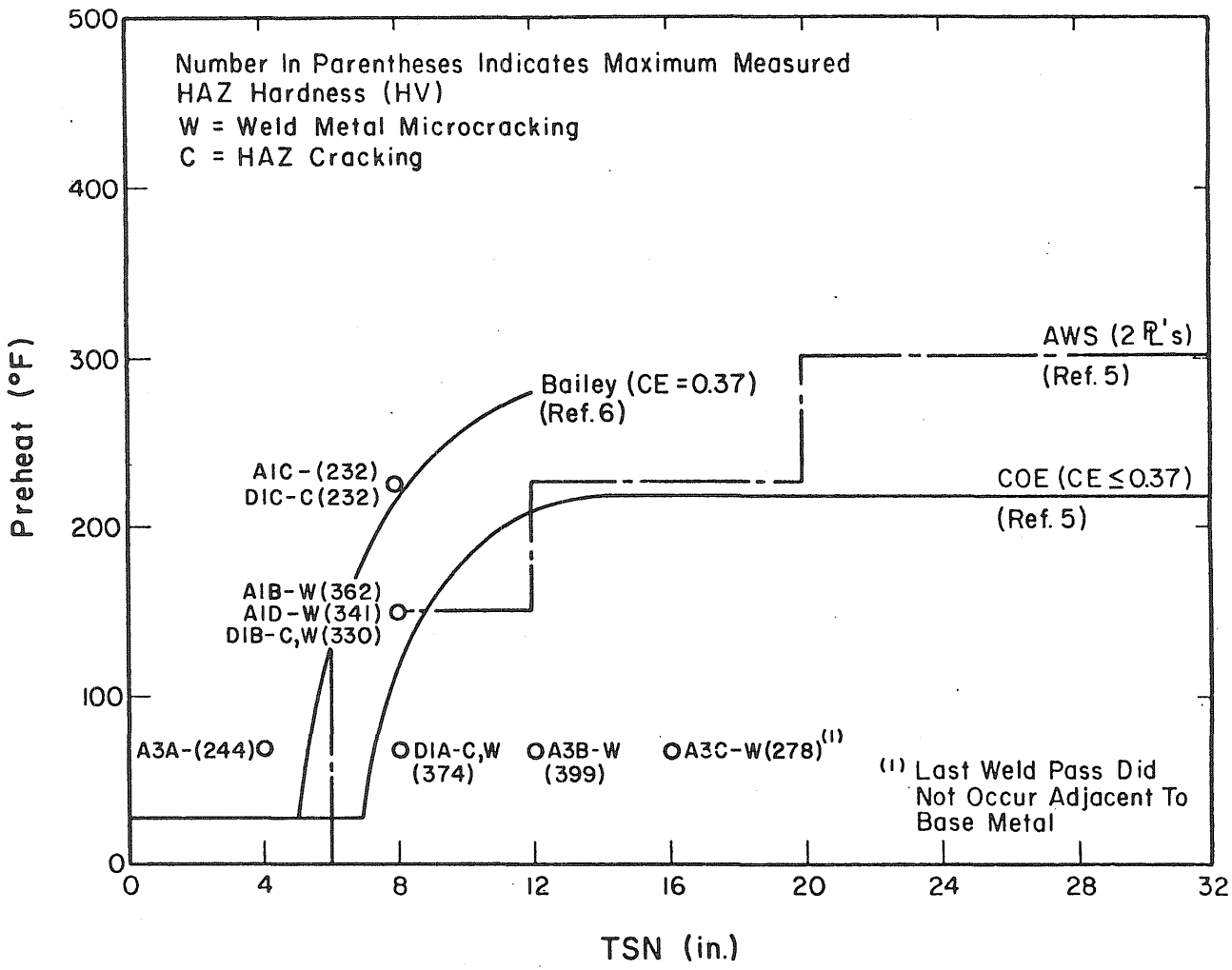


(b) Hydrogen = Other Than Low  Arc Energy = 25 KJ/in.
Critical Hardness = 350 HV

Fig. 6.4 Continued

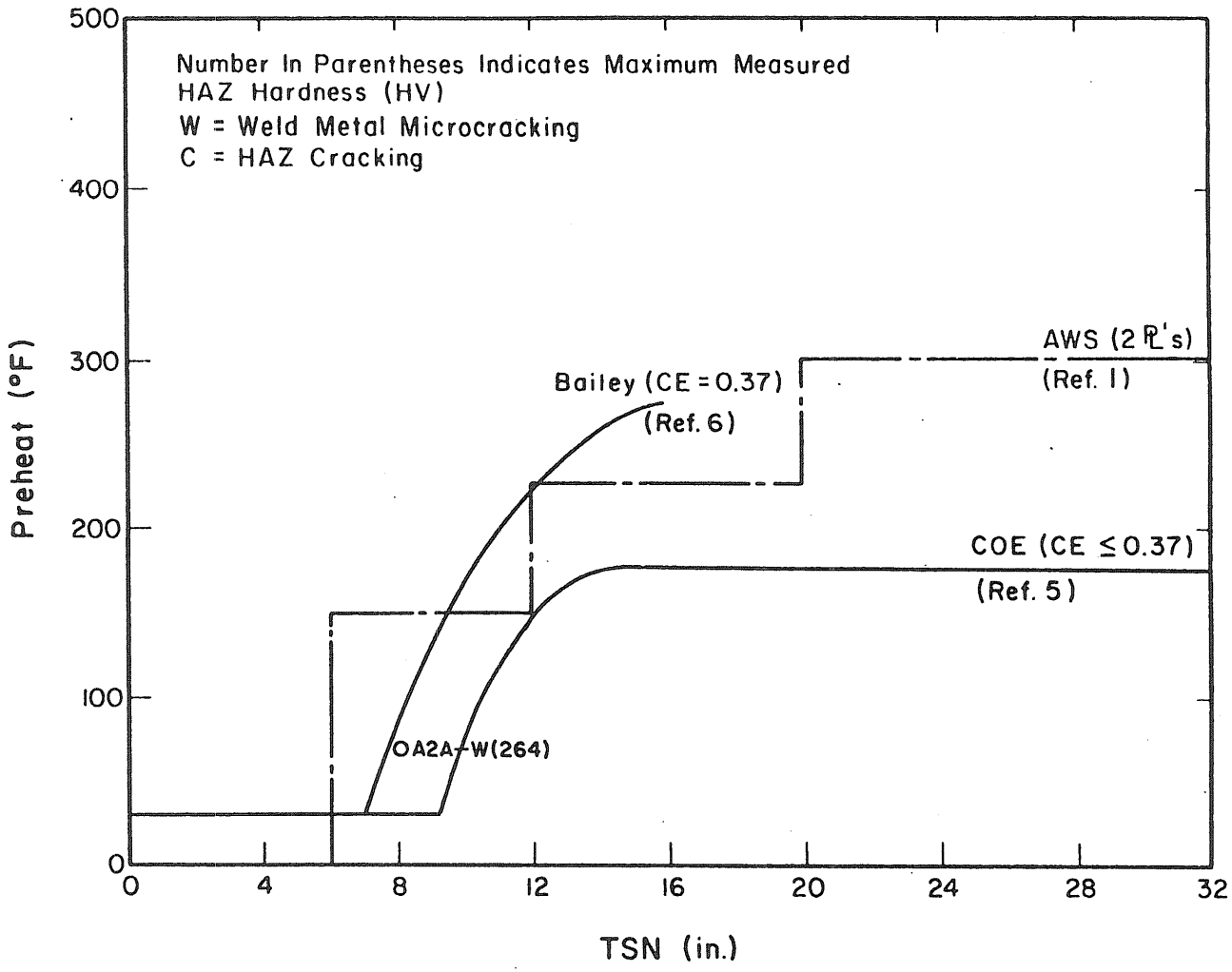


(c) Hydrogen = Other Than Low Arc Energy = 35 KJ/in.
Critical Hardness = 350 HV

Fig. 6.4 Continued

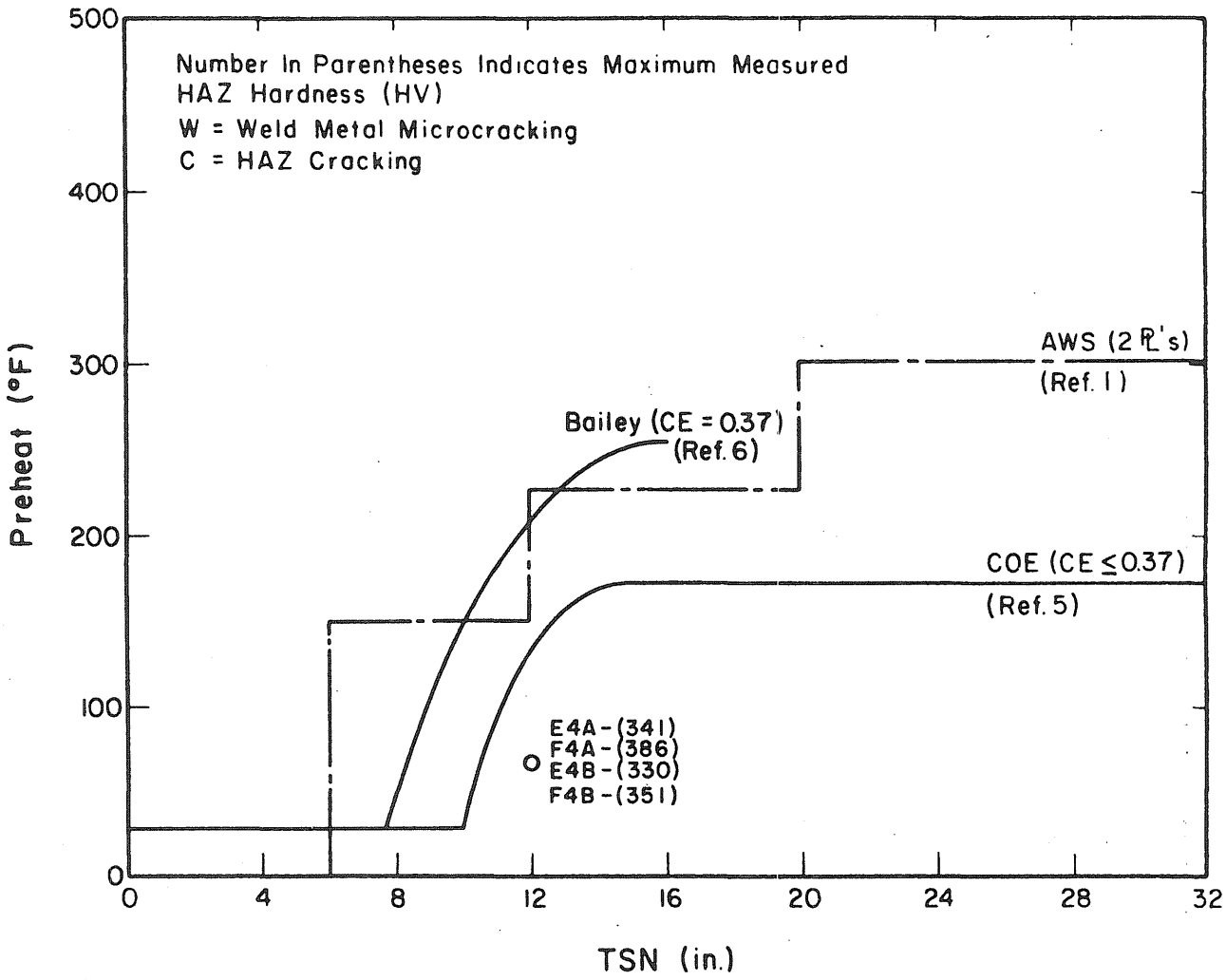


(d) Hydrogen = Other Than Low Arc Energy = 37 KJ/in.
Critical Hardness = 350 HV

Fig. 6.4 Continued

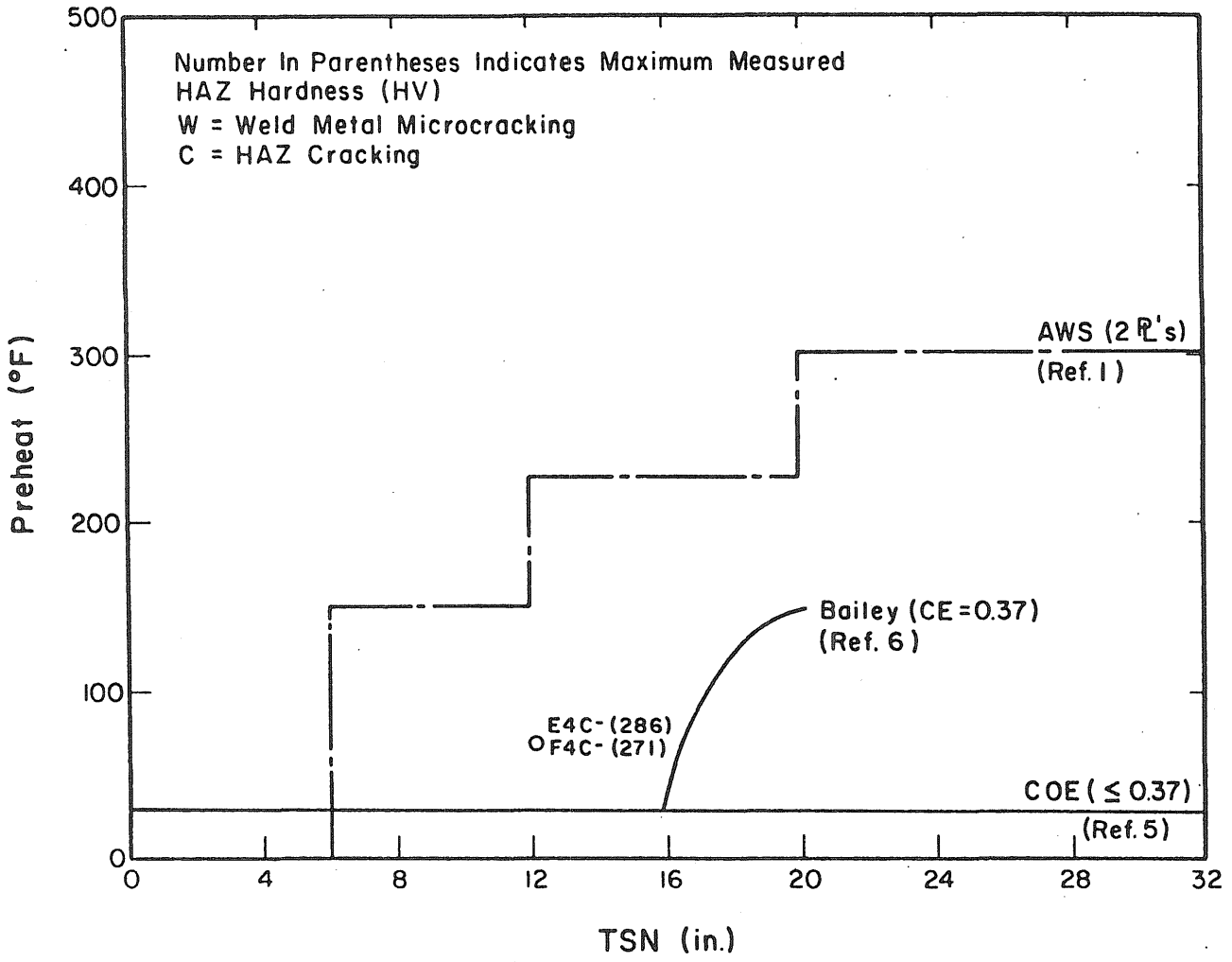


(e) Hydrogen = Other Than Low Arc Energy = 70 KJ/in.
Critical Hardness = 350 HV

Fig. 6.4 Continued

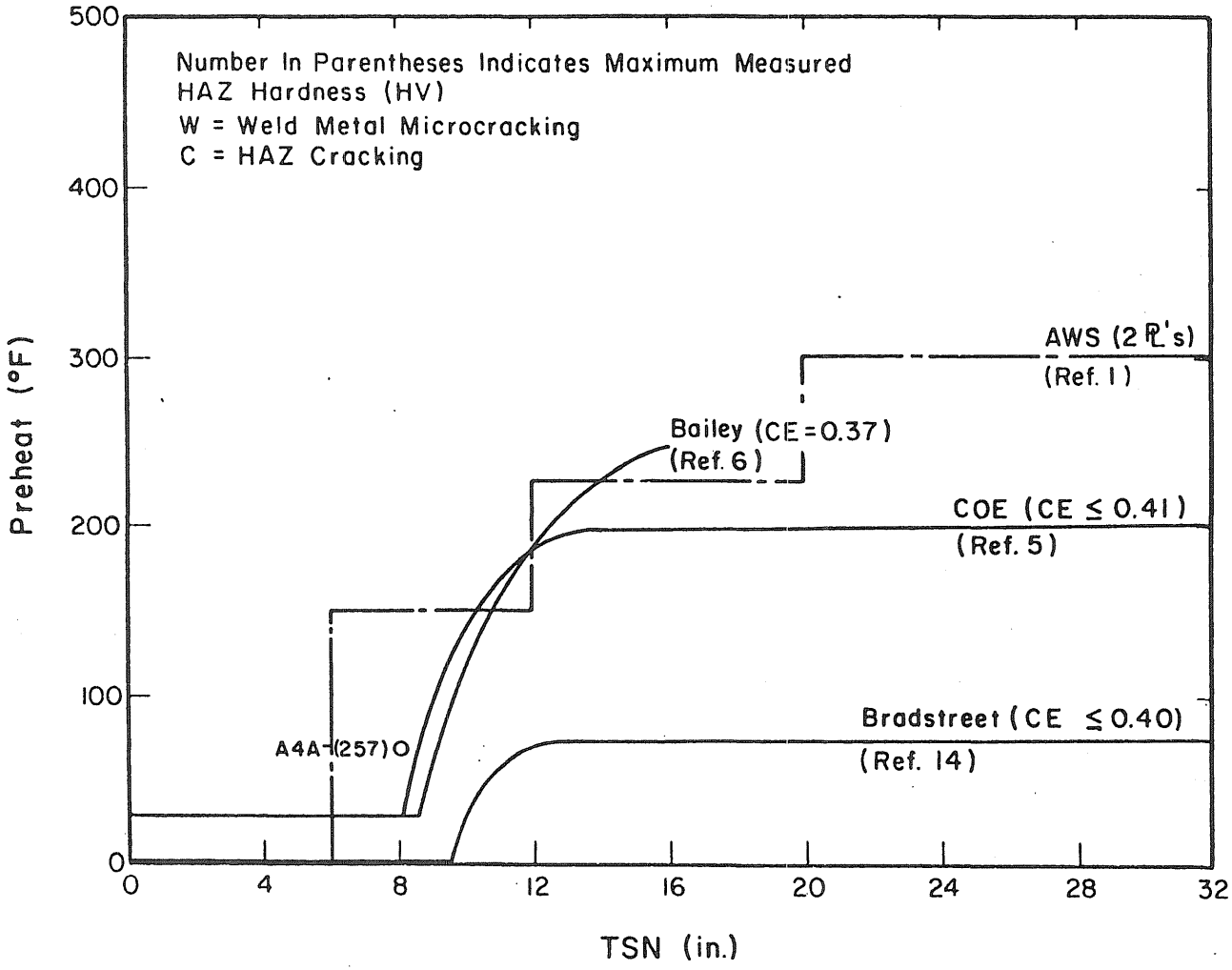


(f) Hydrogen = Low Arc Energy = 30 KJ/in.
Critical Hardness = 400 HV

Fig. 6.4 Continued

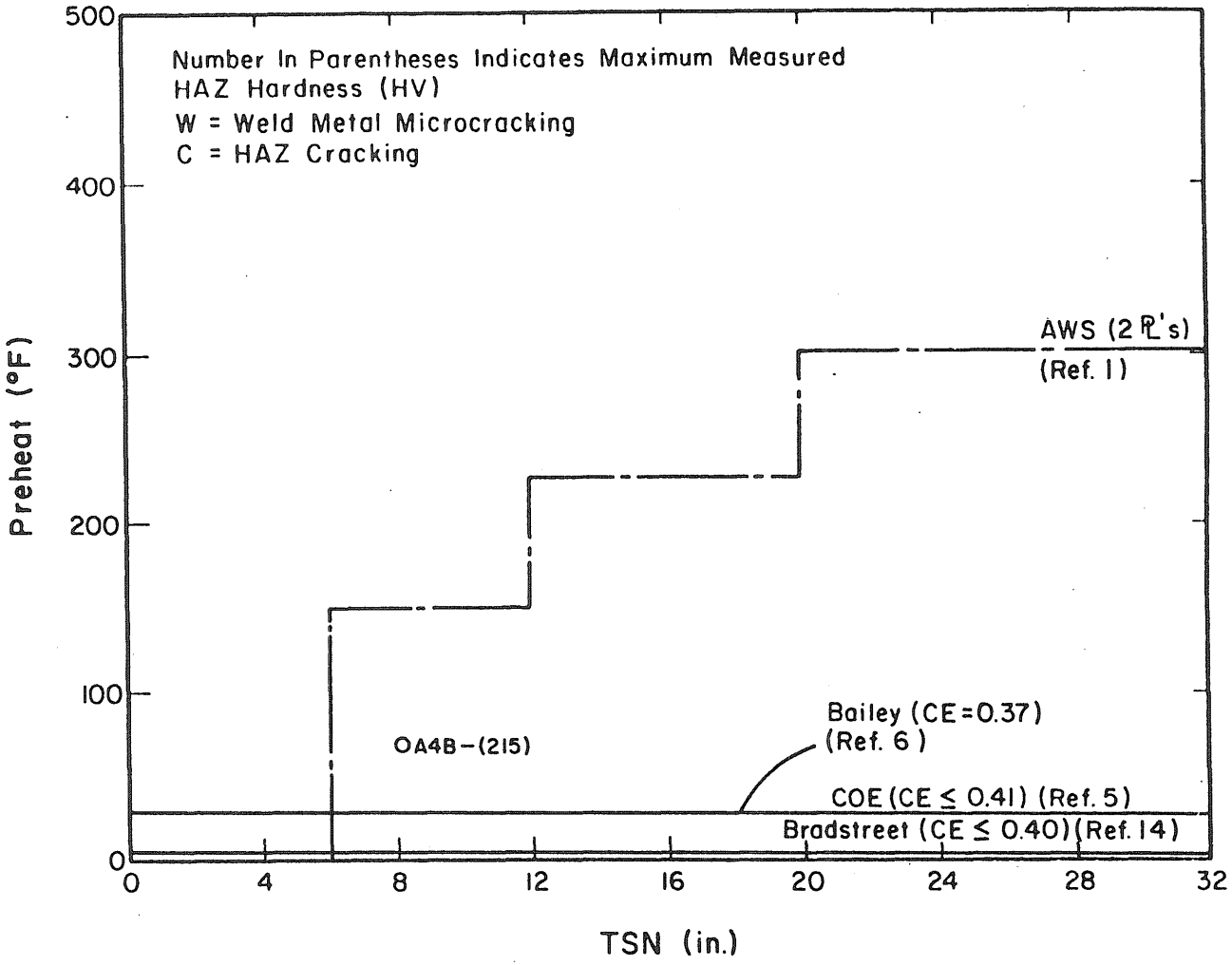


(g) Hydrogen = Low Arc Energy = 60 KJ/in.
Critical Hardness = 400 HV

Fig. 6.4 Continued

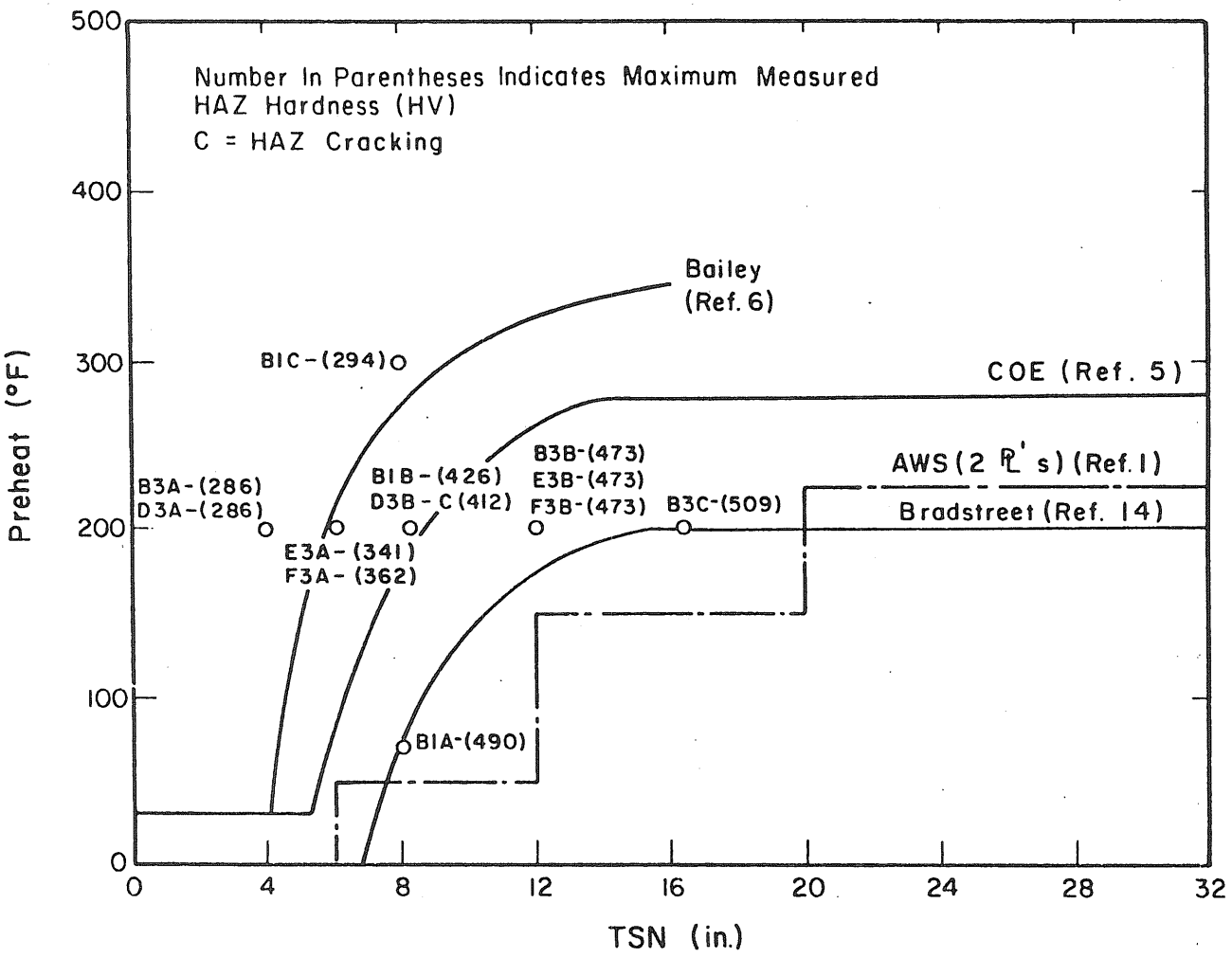


(a) Hydrogen = Low; Arc Energy = 30 KJ/in.
Critical Hardness = 400 HV; CE = 0.45

Fig. 6.5 Relationship Between Test Welding Procedures and Welding Requirements to Control HAZ Cracking in Low-Alloy Steels.

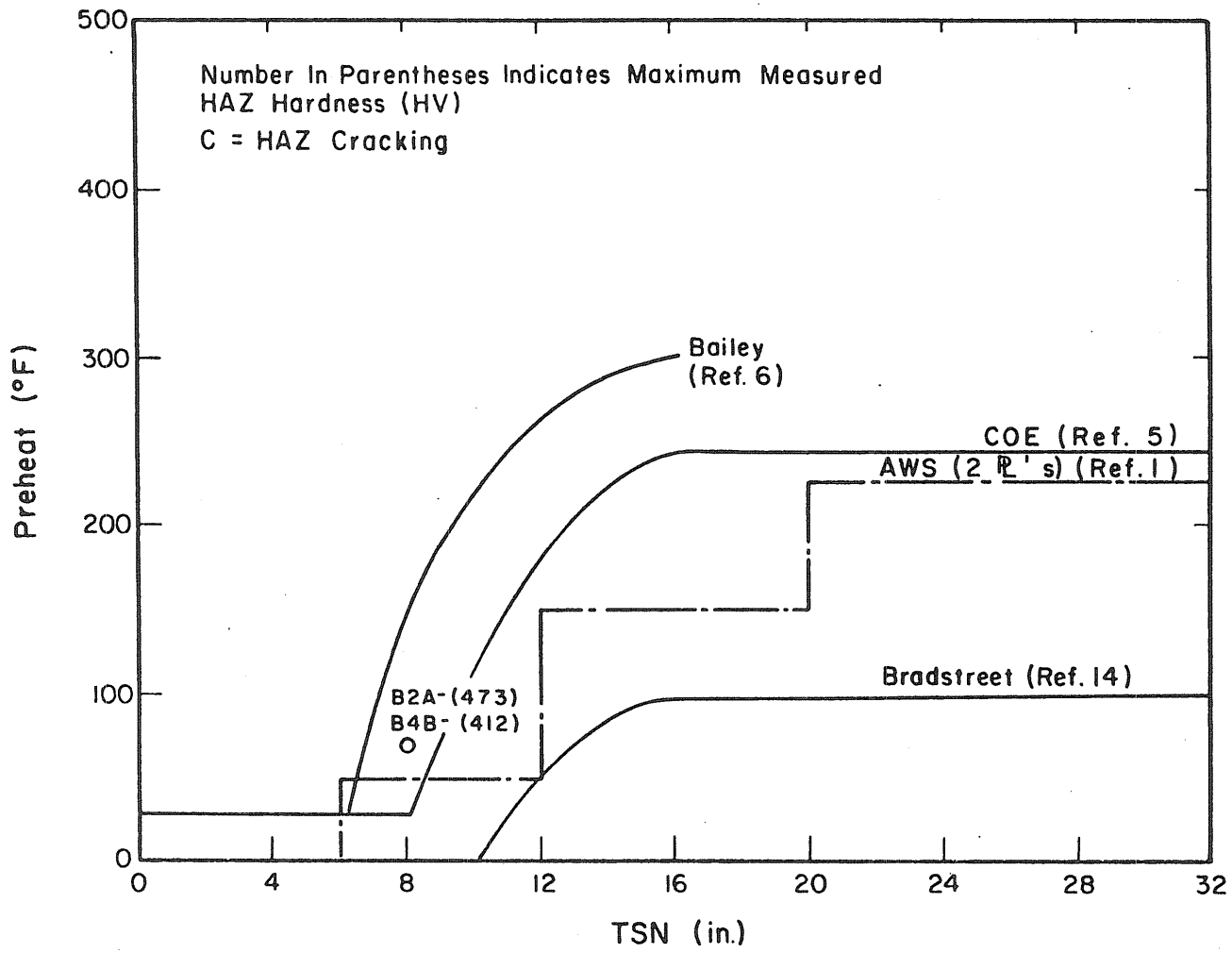


(b) Hydrogen = Low Arc Energy = 45 KJ/in.
Critical Hardness = 400 HV CE = 0.45

Fig. 6.5 Continued

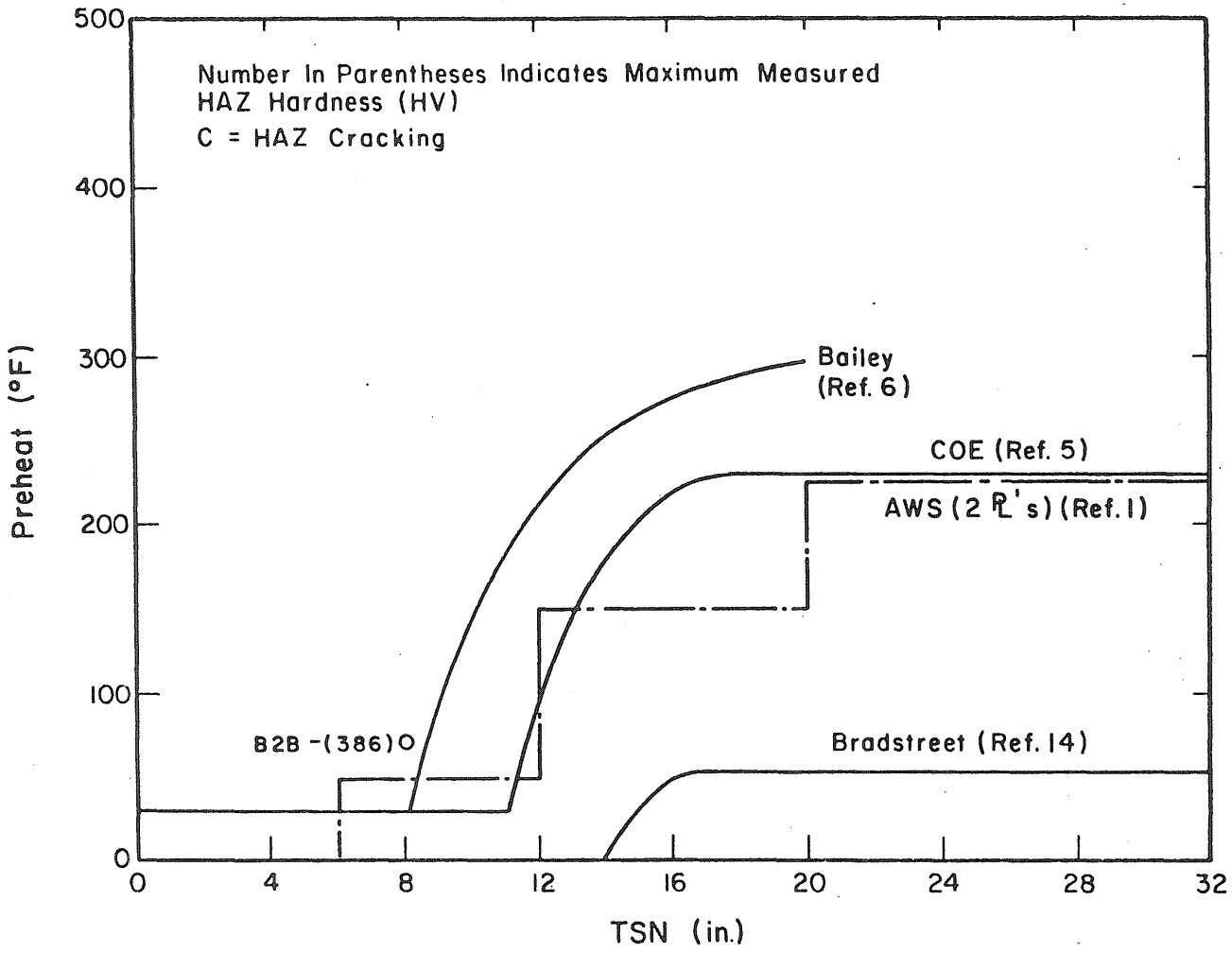


(c) Hydrogen = Low Arc Energy = 55 KJ/in.
Critical Hardness = 400 HV CE = 0.45

Fig. 6.5 Continued

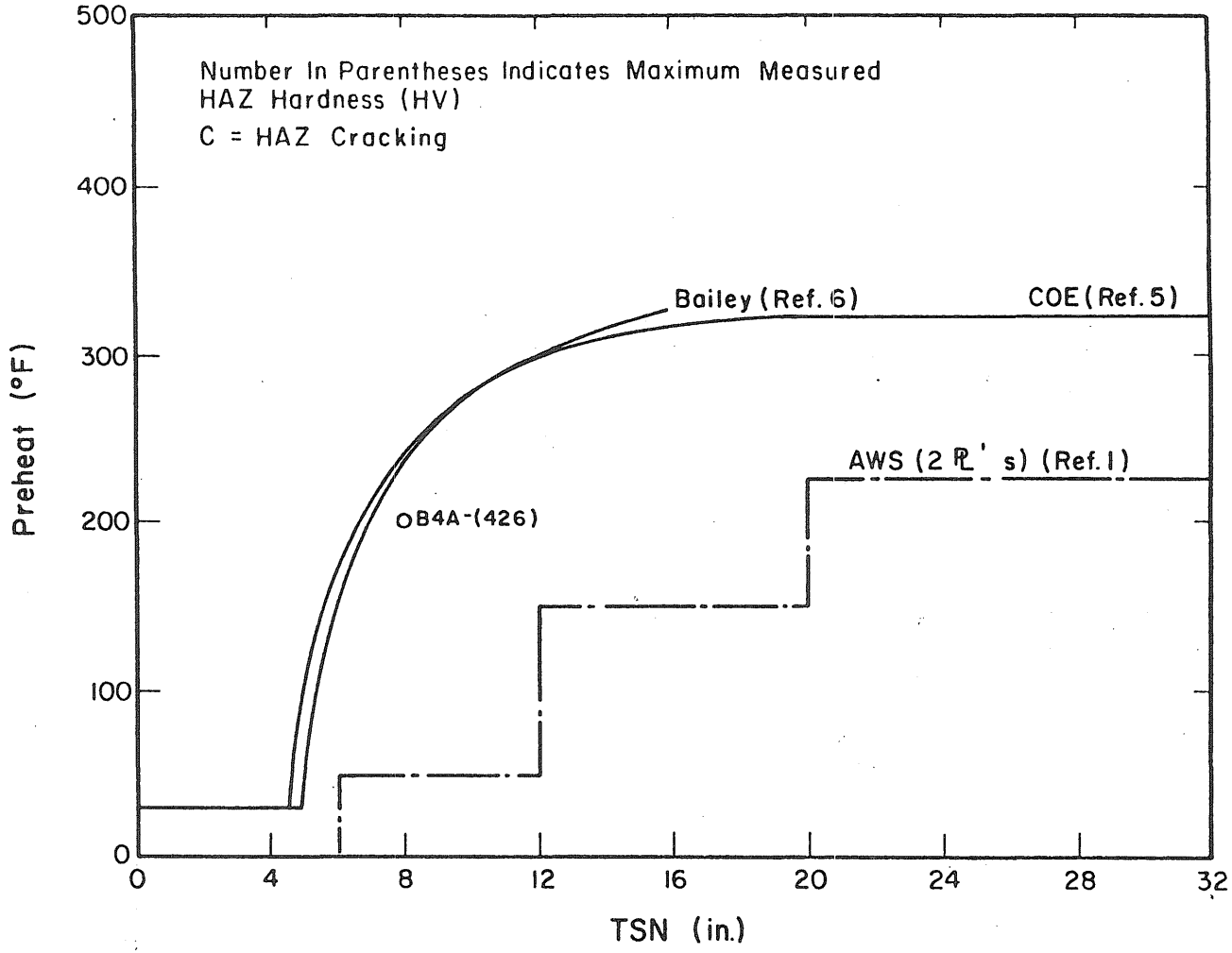


(d) Hydrogen = Low Arc Energy = 35 KJ/in.
Critical Hardness = 400 HV CE = 0.45

Fig. 6.5 Continued

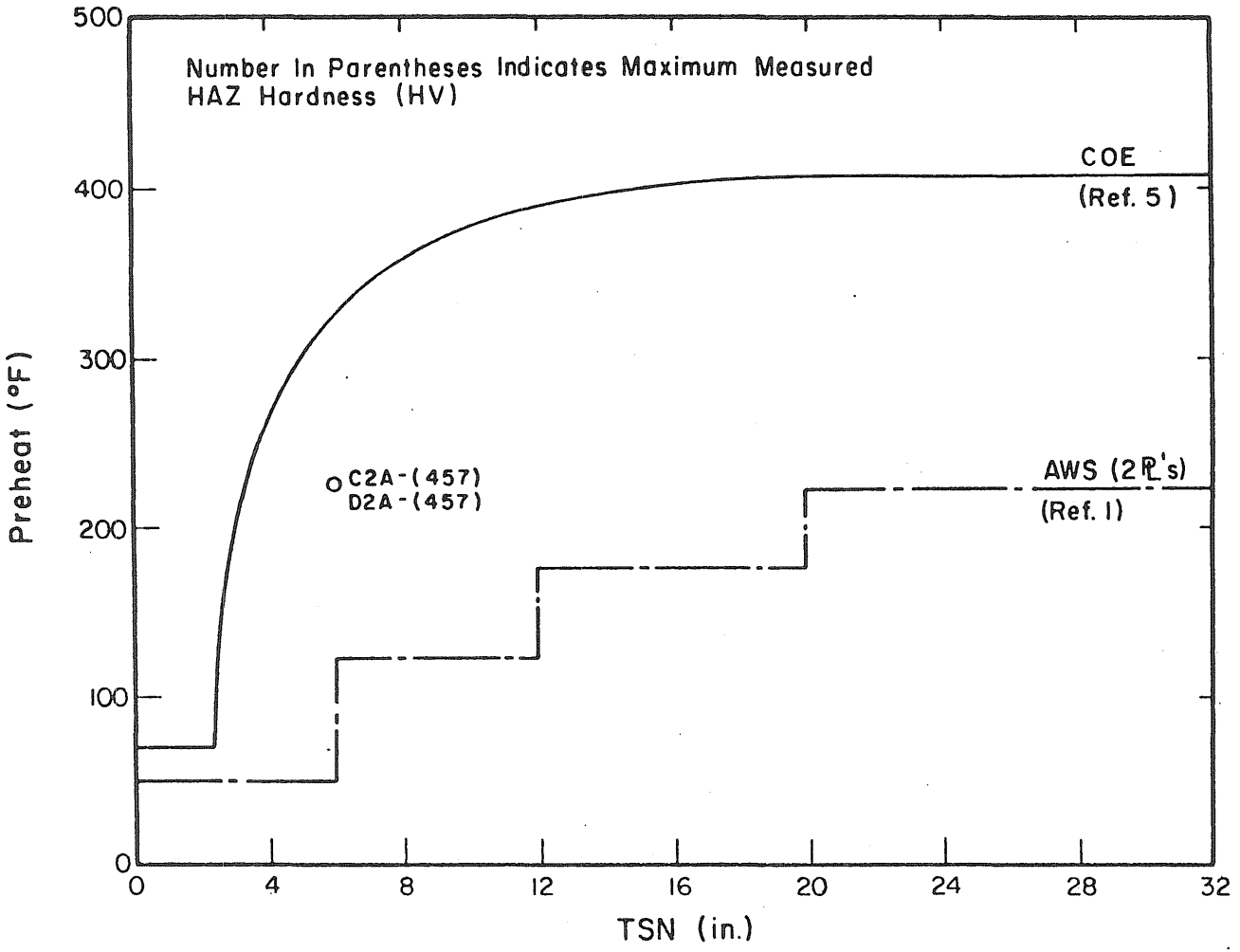


(a) Hydrogen = Low; Arc Energy = 32 KJ/in.; Critical Hardness = 400 HV; CE = 0.62

Fig. 6.6 Relationship Between Test Welding Procedures and Welding Requirements to Control HAZ Cracking in Quenched and Tempered Steels.

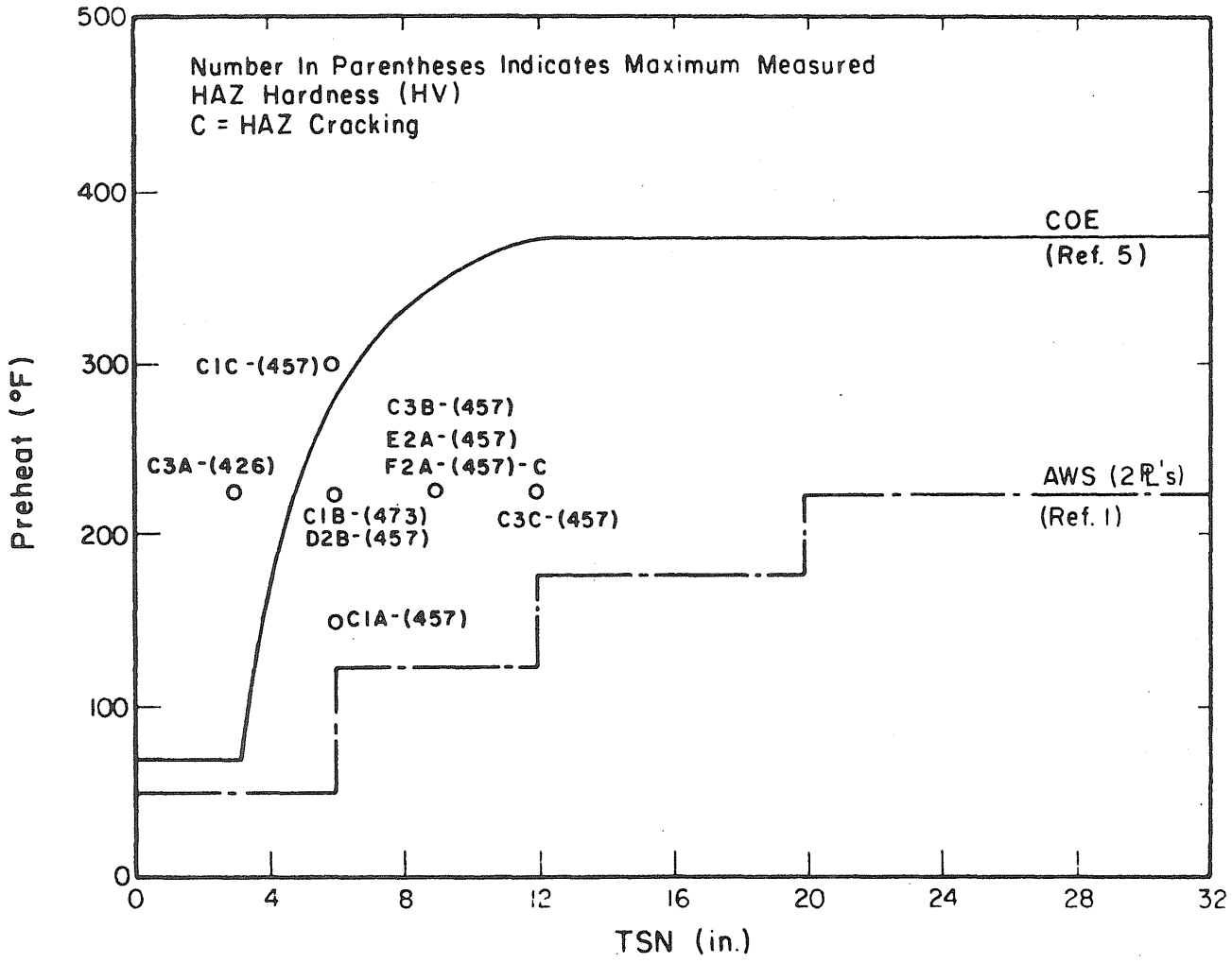


(b) Hydrogen = Low Arc Energy = 43 KJ/in.
Critical Hardness = 400 HV CE = 0.62

Fig. 6.6 Continued

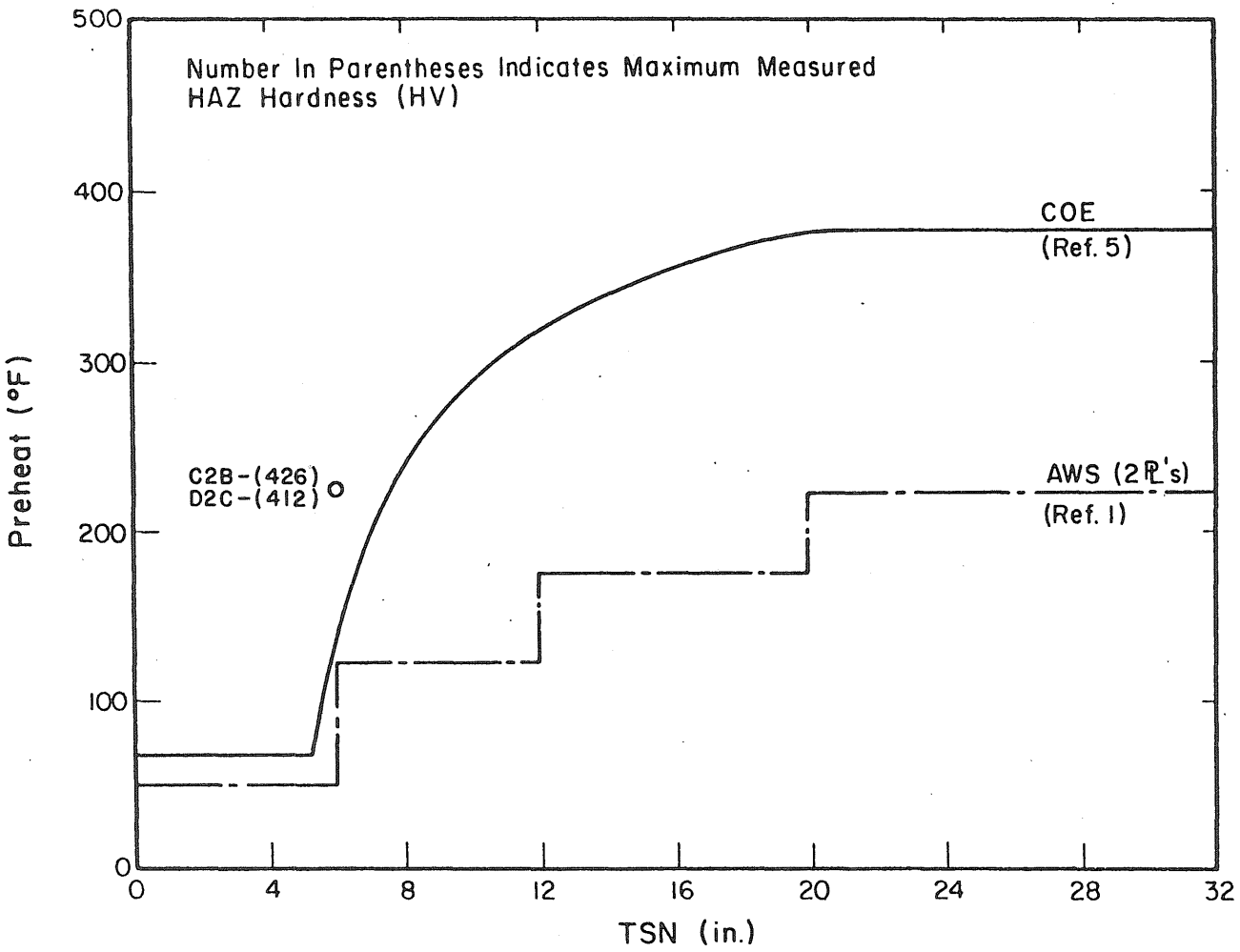


(c) Hydrogen = Low Arc Energy = 68 KJ/in.
Critical Hardness = 400 HV CE = 0.62

Fig. 6.6 Continued

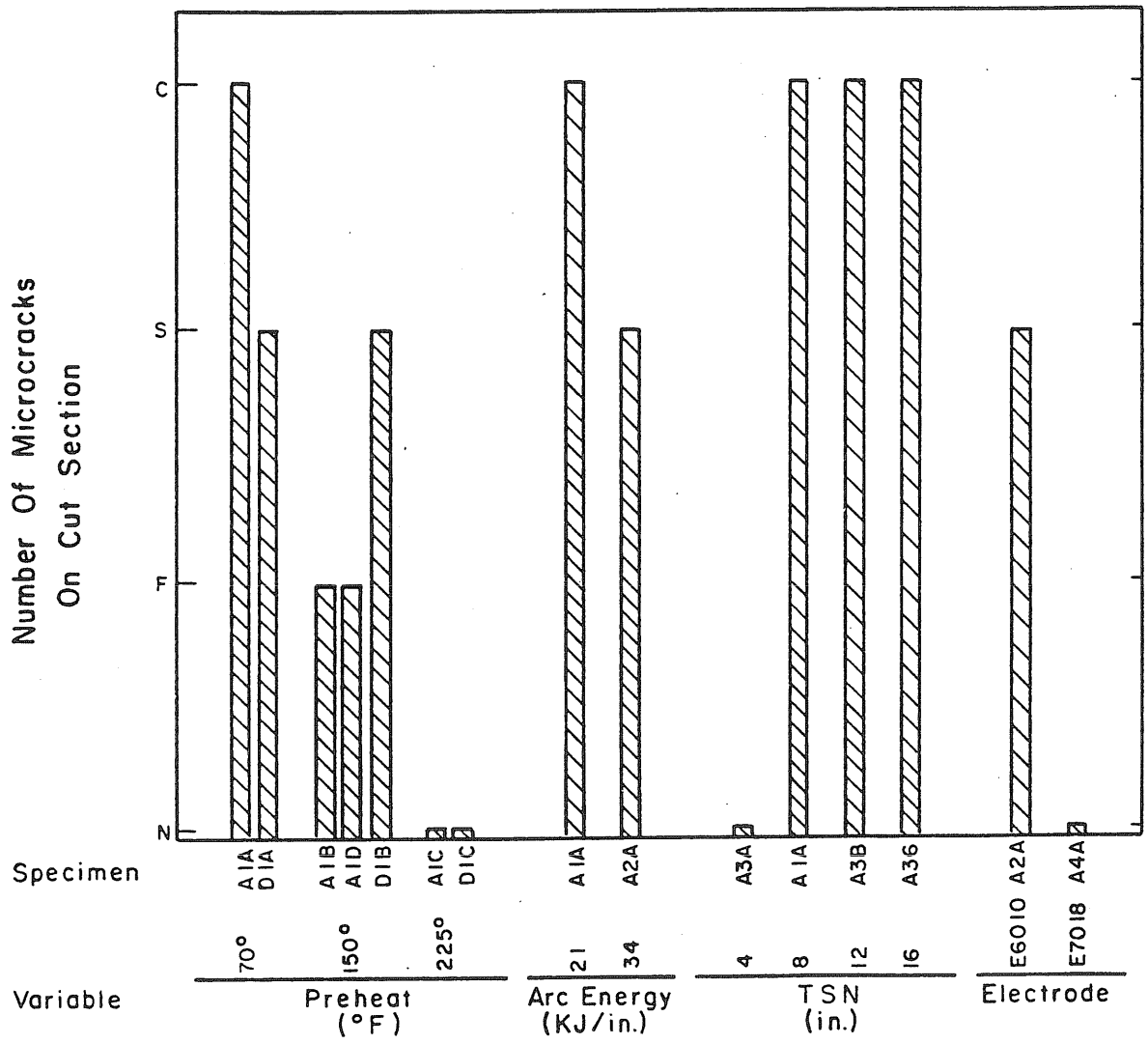


Fig. 6.7 Effects of Various Welding Variables on the Occurrence of Weld Metal Microcracking.

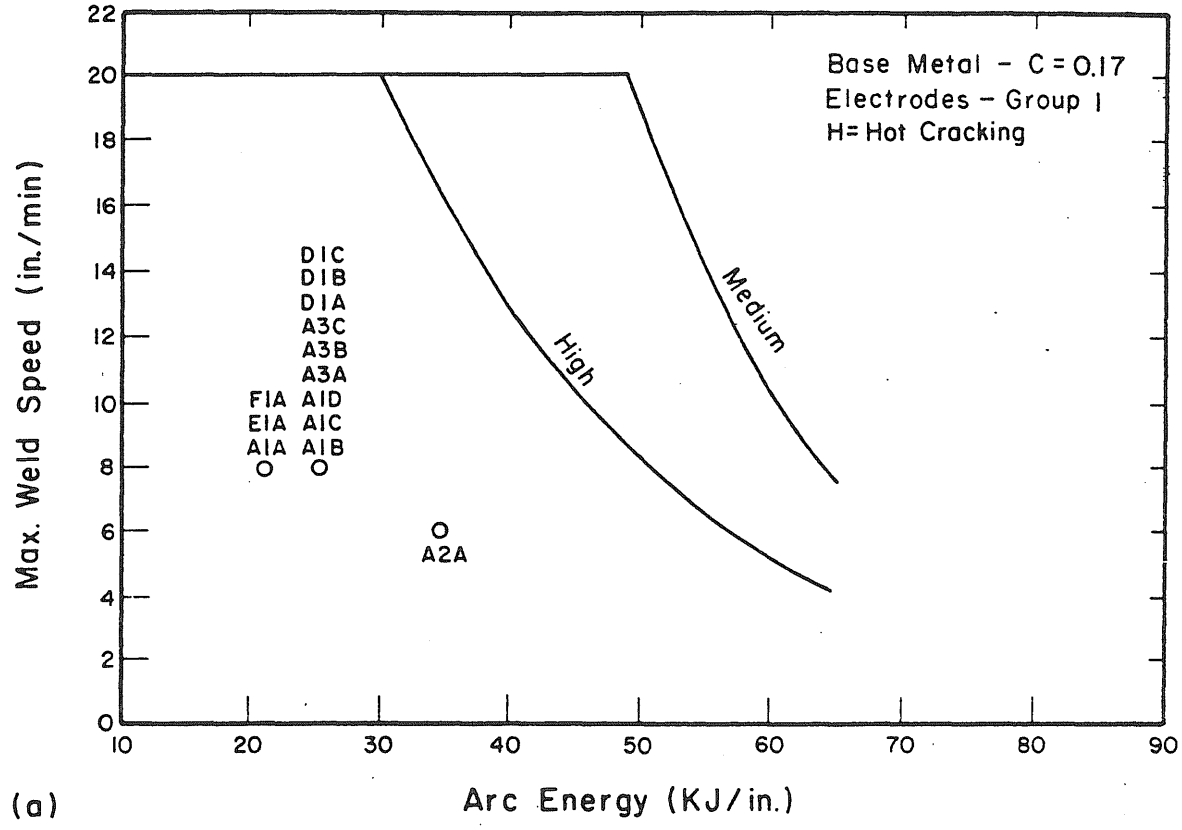


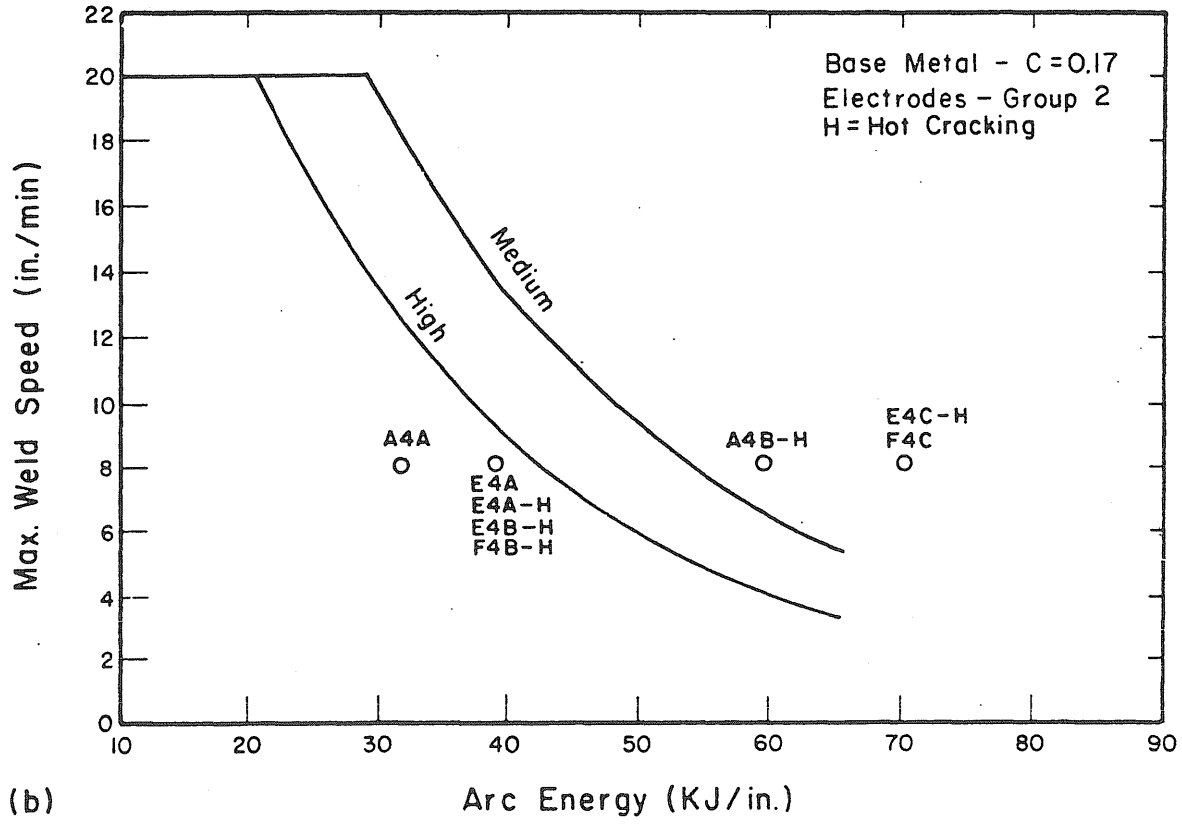


Fig. 6.8 Relationship Between Test Welding Procedures and Welding Requirements to Control Hot Cracking in Mild Steels.

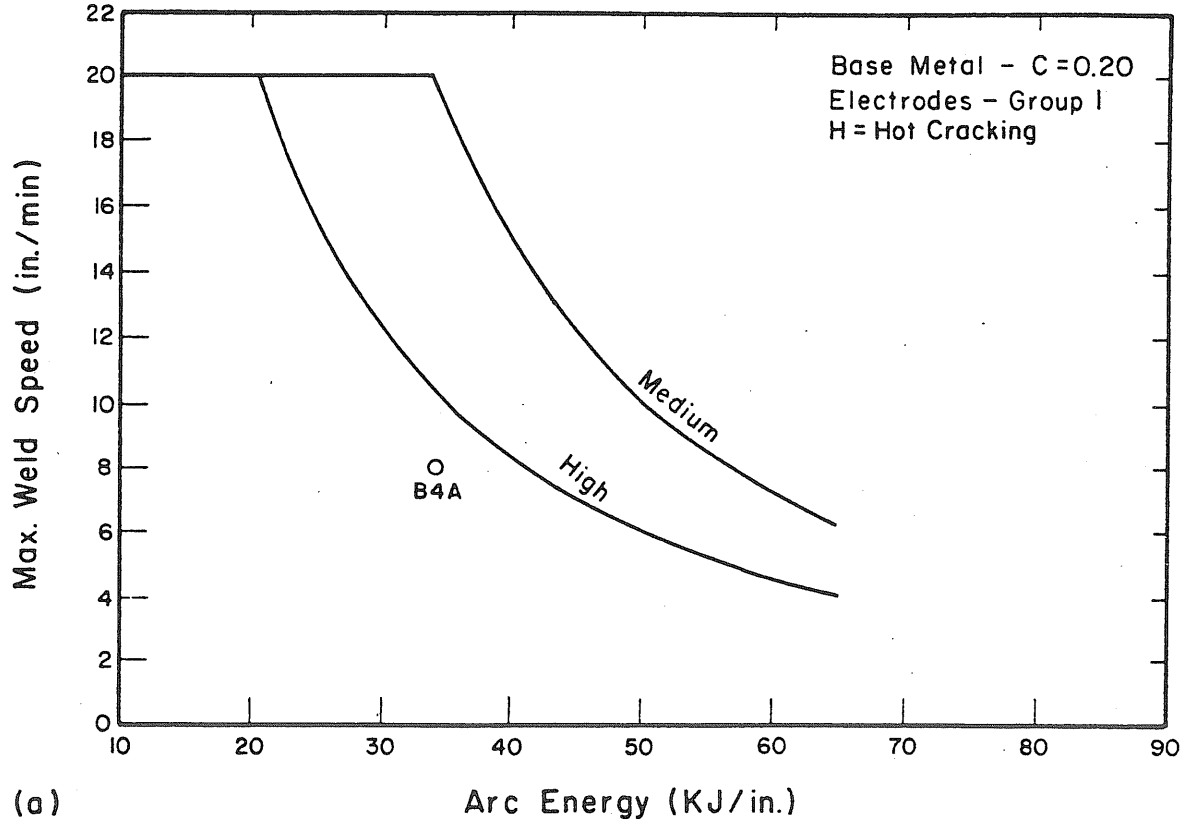


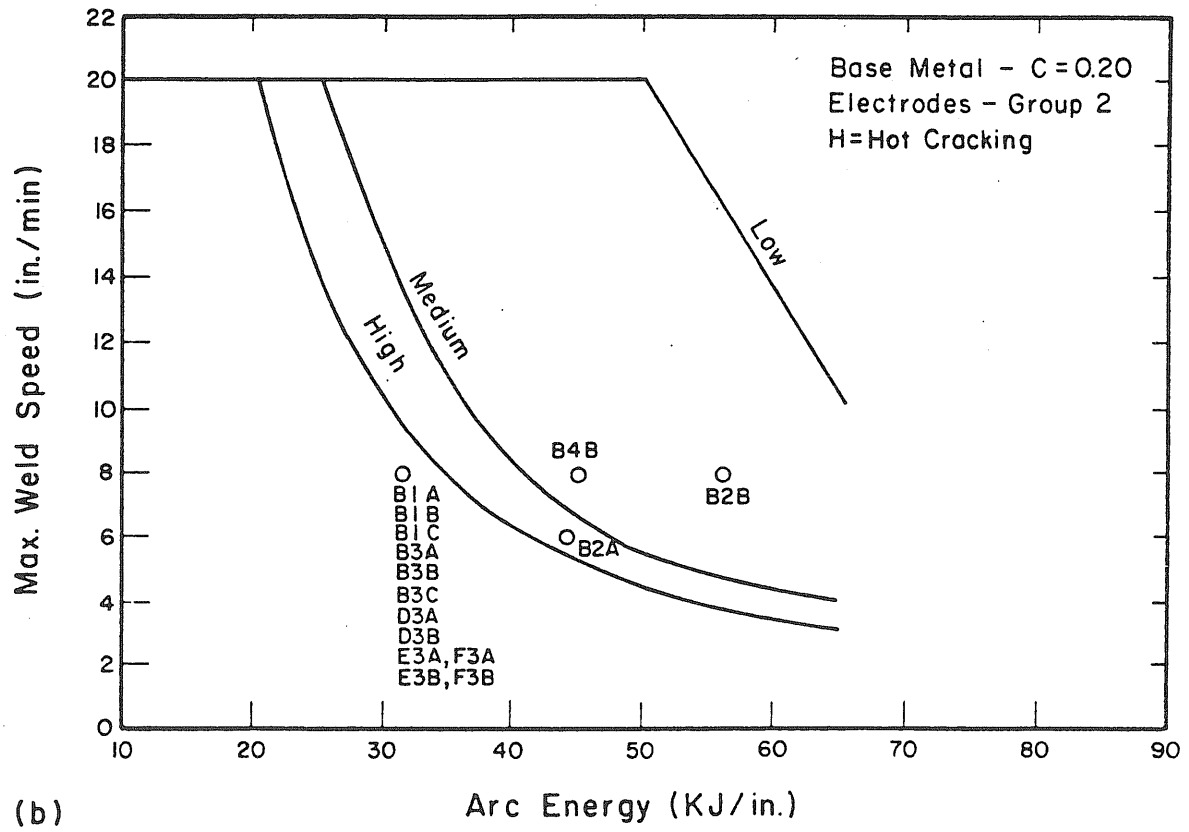


Fig. 6.9 Relationship Between Test Welding Procedures and Welding Requirements to Control Hot Cracking in Low-Alloy Steels.

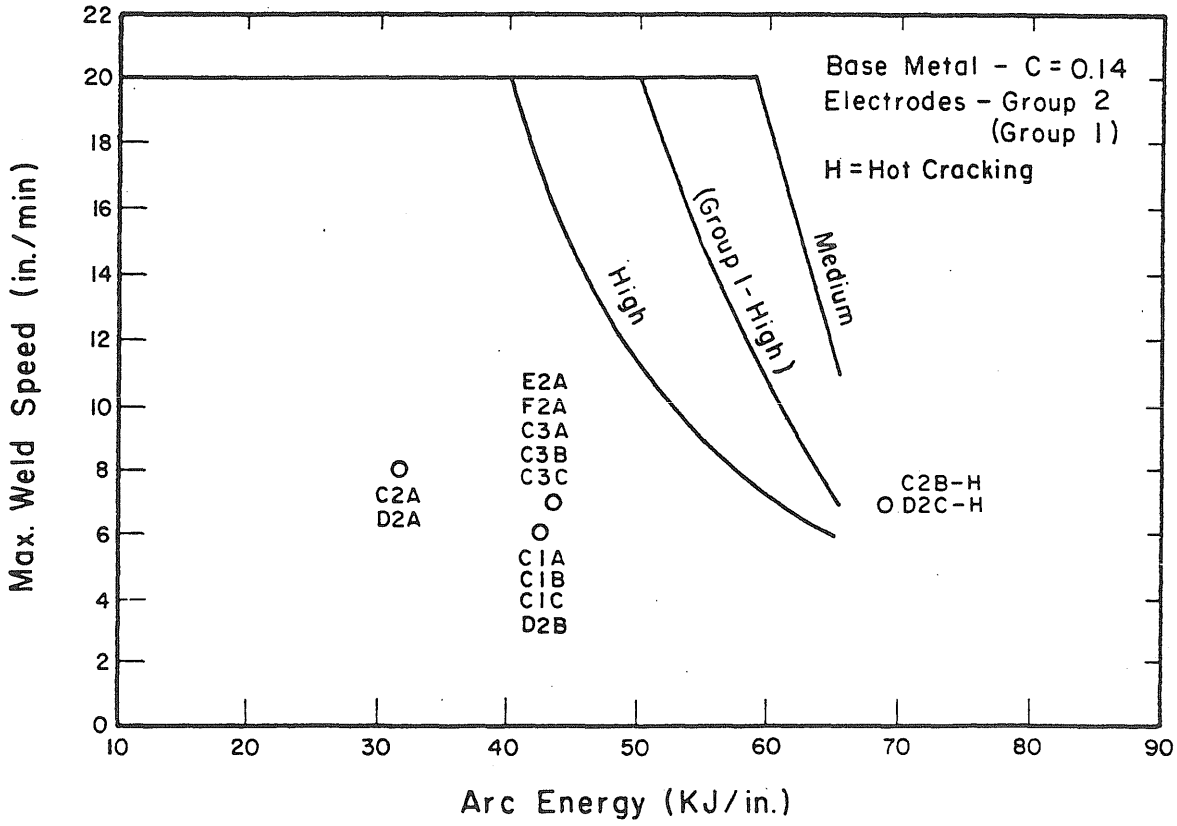


Fig. 6.10 Relationship Between Test Welding Procedures and Welding Requirements to Control Hot Cracking in Quenched and Tempered Steels.

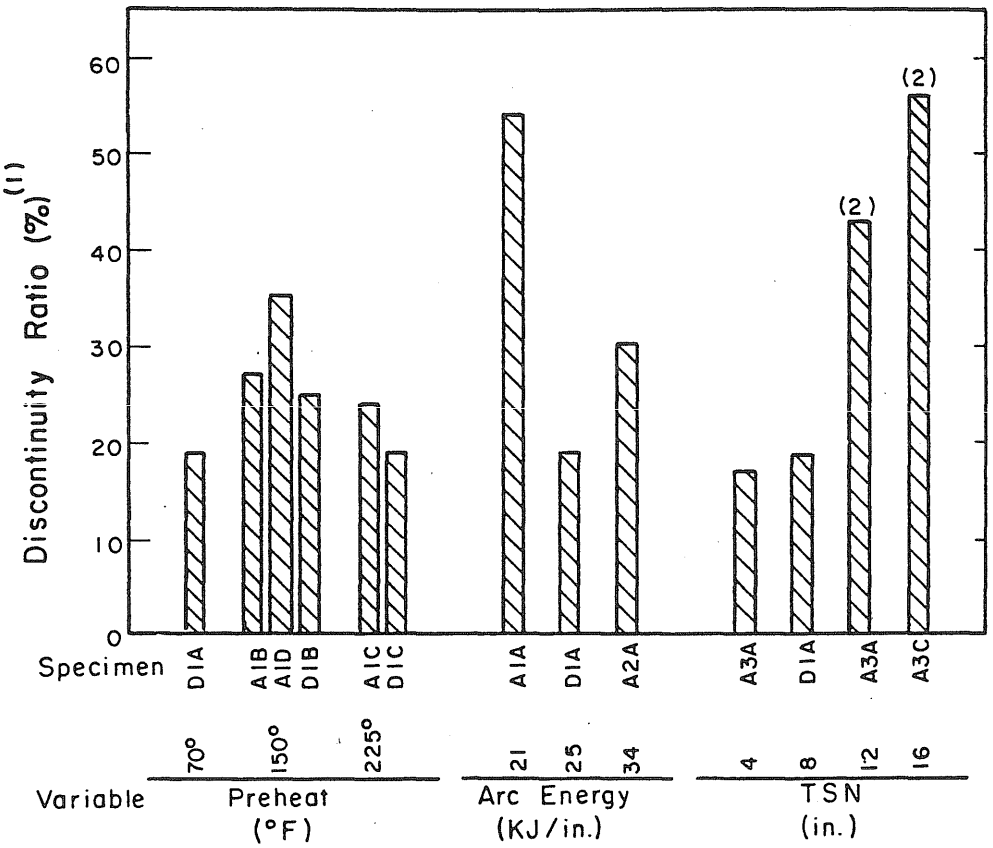


(1) Discontinuity ratio is defined as the ratio of the area of discontinuity present on radiograph in 1-inch length of weld to the cross-sectional area of the weld, expressed in percent.
(2) Type TC-U5a joint.

E6010 Electrode

Fig. 6.11 Effects of Various Welding Variables on Discontinuity Ratio of Mild Steel Specimens.

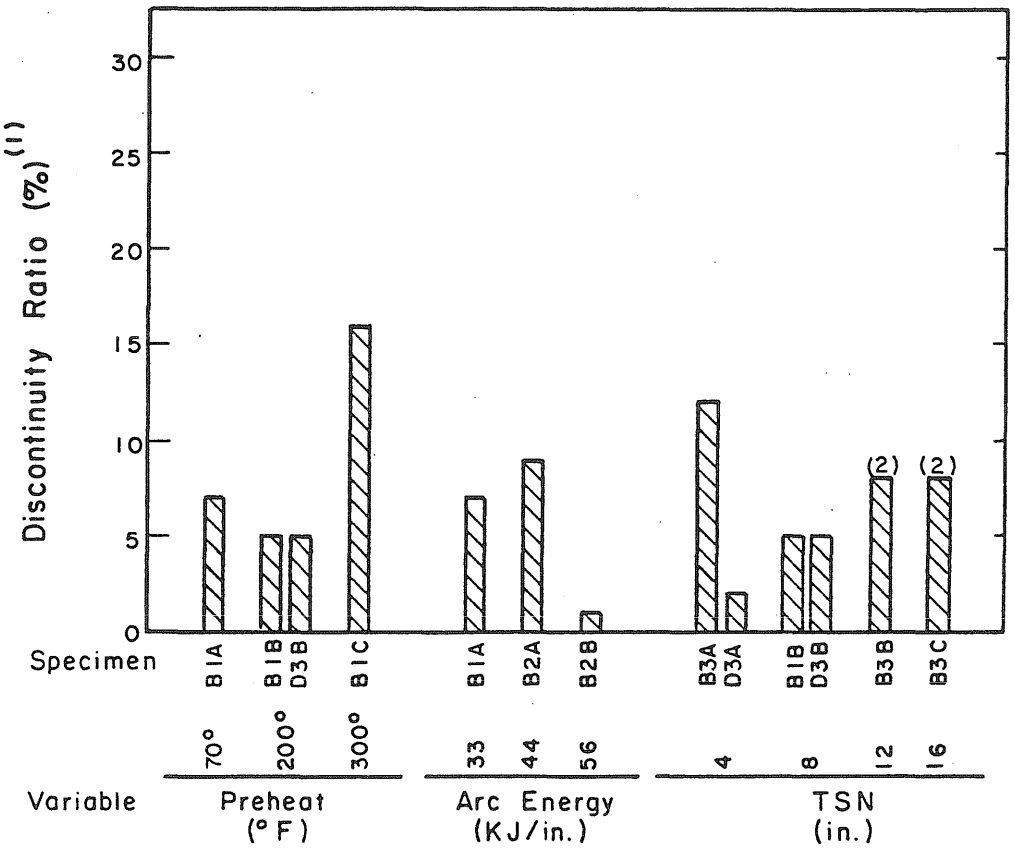


(1) Discontinuity ratio is defined as the ratio of the area of discontinuity present on radiograph in 1-inch length of weld to the cross-sectional area of the weld, expressed in percent.
(2) Type TC-U5a joint.

E7018 Electrode

Fig. 6.12 Effects of Various Welding Variables on Discontinuity Ratio of Low-Alloy Steel Specimens.

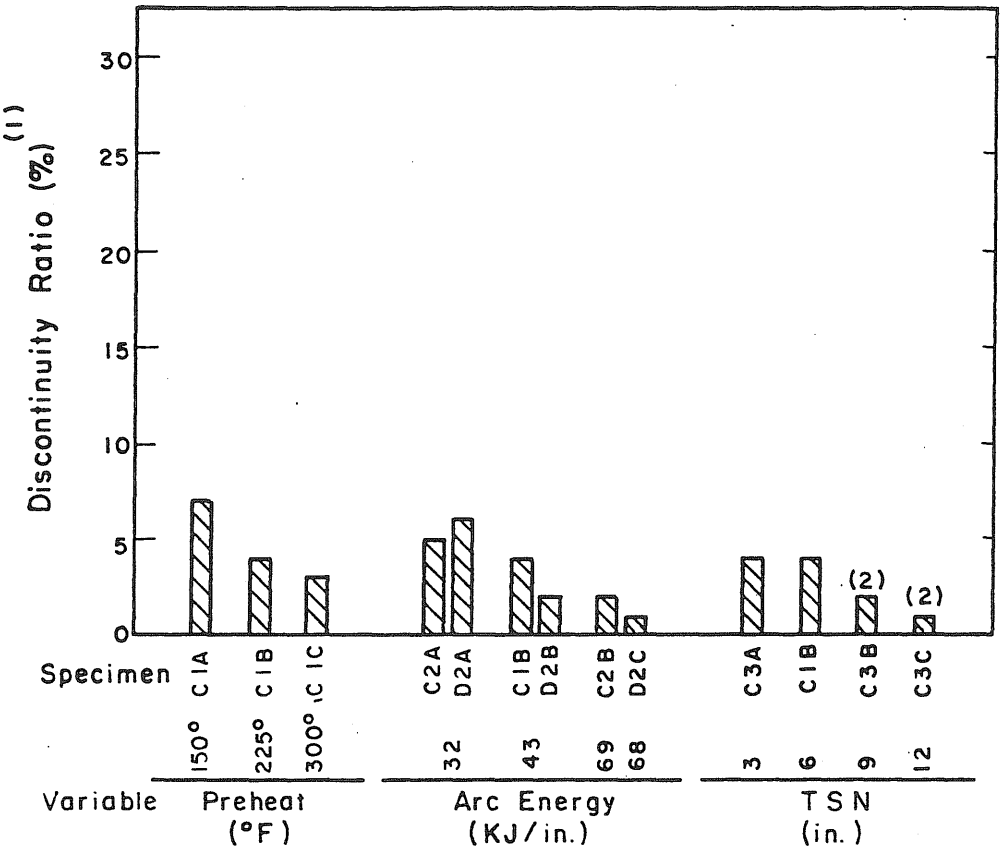


(1) Discontinuity ratio is defined as the ratio of the area of discontinuity present on radiograph in 1-inch length of weld, expressed in percent.
(2) Type TC-U5a joint.

E11018 Electrode

Fig. 6.13 Effects of Various Welding Variables on Discontinuity Ratio of Quenched and Tempered Steel Specimens.

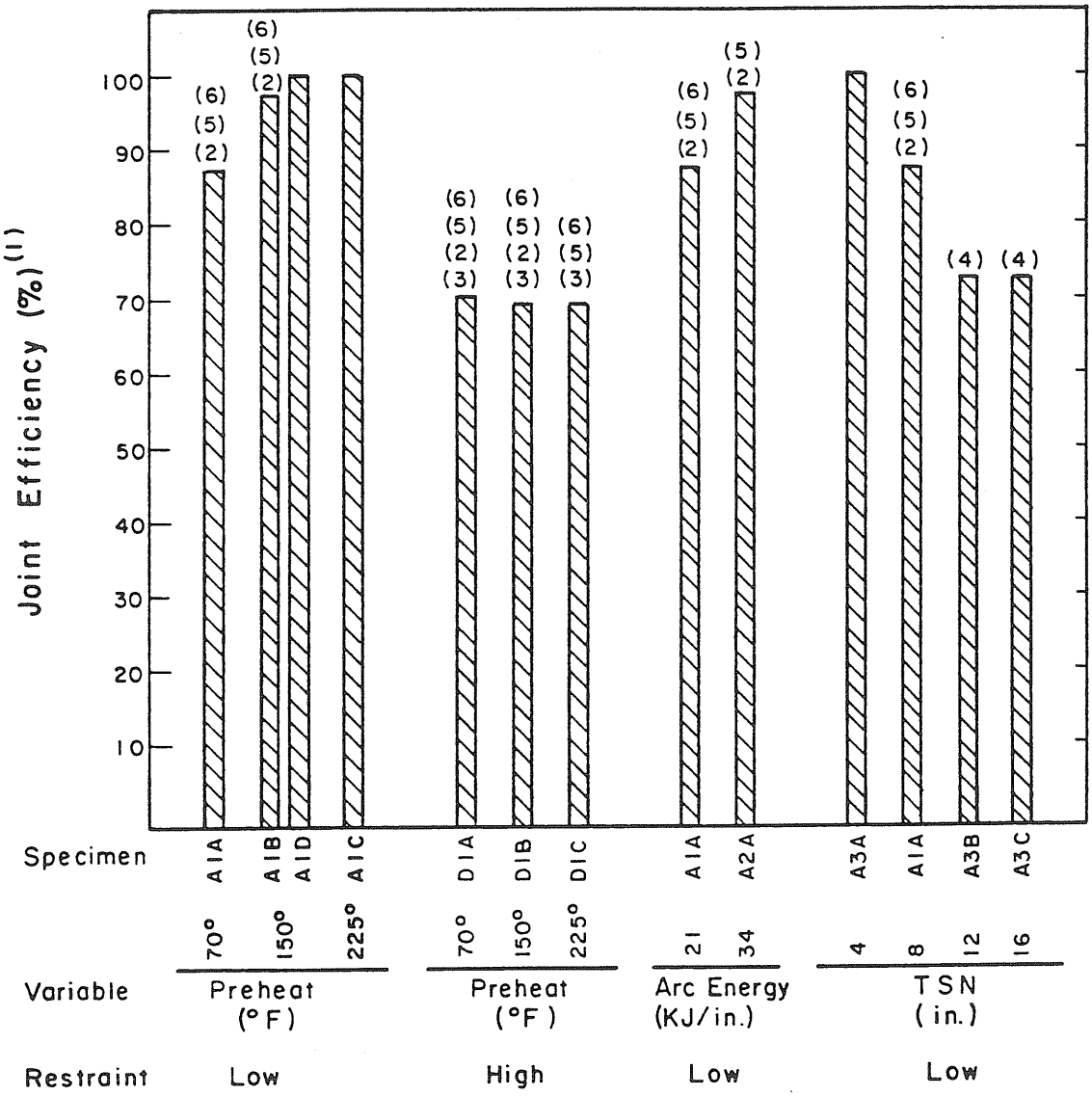


(1) Joint efficiency is defined as the ratio of joint ultimate stress to base metal ultimate stress in percent.
(2) Weld metal microcracking occurred. (See Appendix A)
(3) HAZ cracking occurred. (See Appendix A and Fig. 5.10)
(4) Failed in thru-thickness direction of base metal.
(5) LOF occurred. (See Appendix A)
(6) Slag occurred. (See Appendix A)

Fig. 6.14 Effects of Various Welding Variables on Joint Efficiency of Mild Steel Specimens.

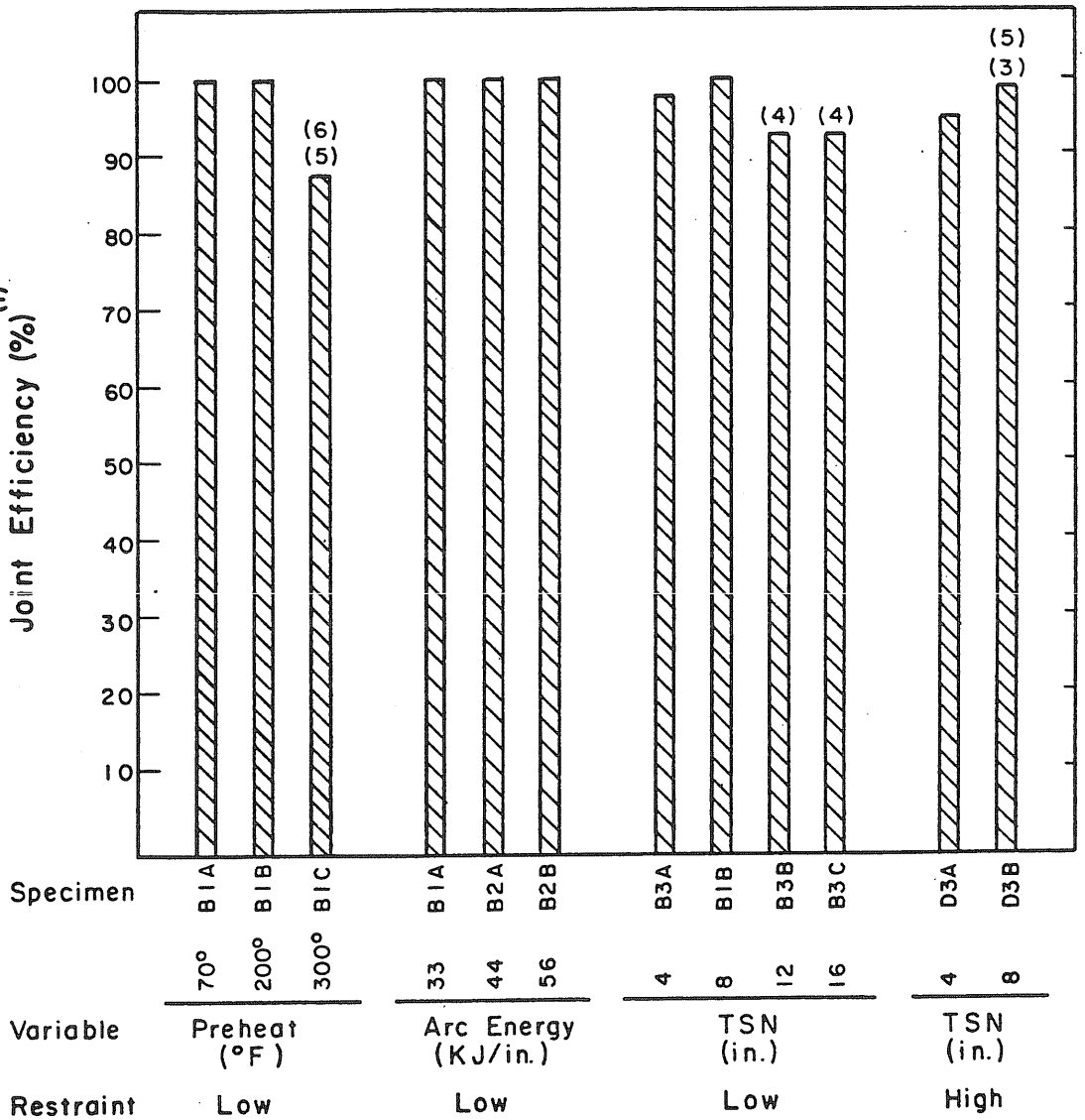


(1) Joint efficiency is defined as the ratio of joint ultimate stress to base metal ultimate stress in percent.
(2) Weld metal microcracking occurred. (See Appendix A)
(3) HAZ cracking occurred. (See Appendix A and Fig. 5.10)
(4) Failed in thru-thickness direction of base metal.
(5) LOF occurred. (See Appendix A)
(6) Slag occurred. (See Appendix A)

Fig. 6.15 Effects of Various Welding Variables on Joint Efficiency of Low-Alloy Steel Specimens.

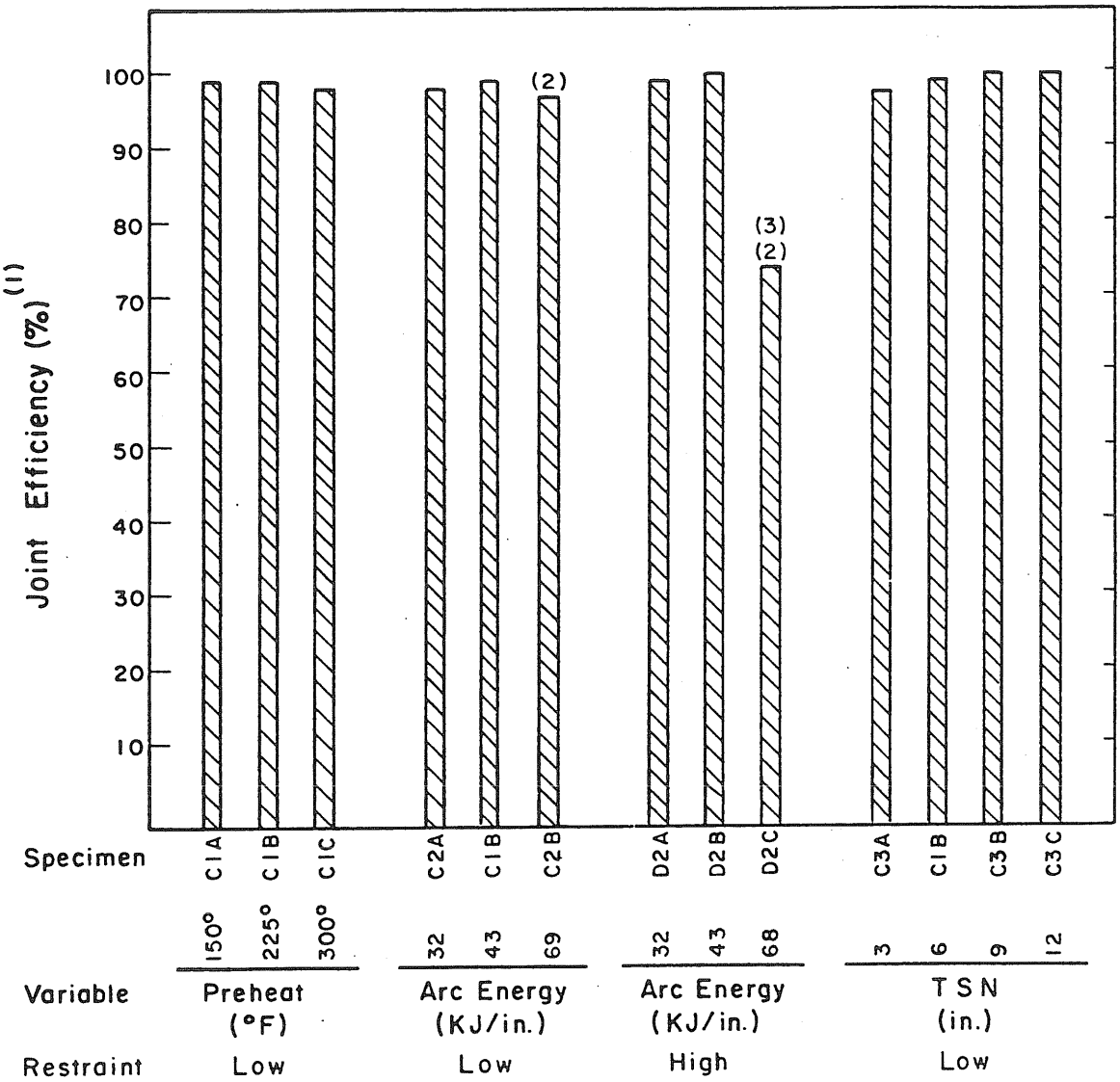


(1) Joint efficiency is defined as the ratio of joint ultimate stress to base metal ultimate stress in percent.
(2) Hot cracking occurred. (See Appendix A)
(3) Slag occurred. (See Appendix A)

Fig. 6.16 Effects of Various Welding Variables on Joint Efficiency of Quenched and Tempered Steel Specimens.

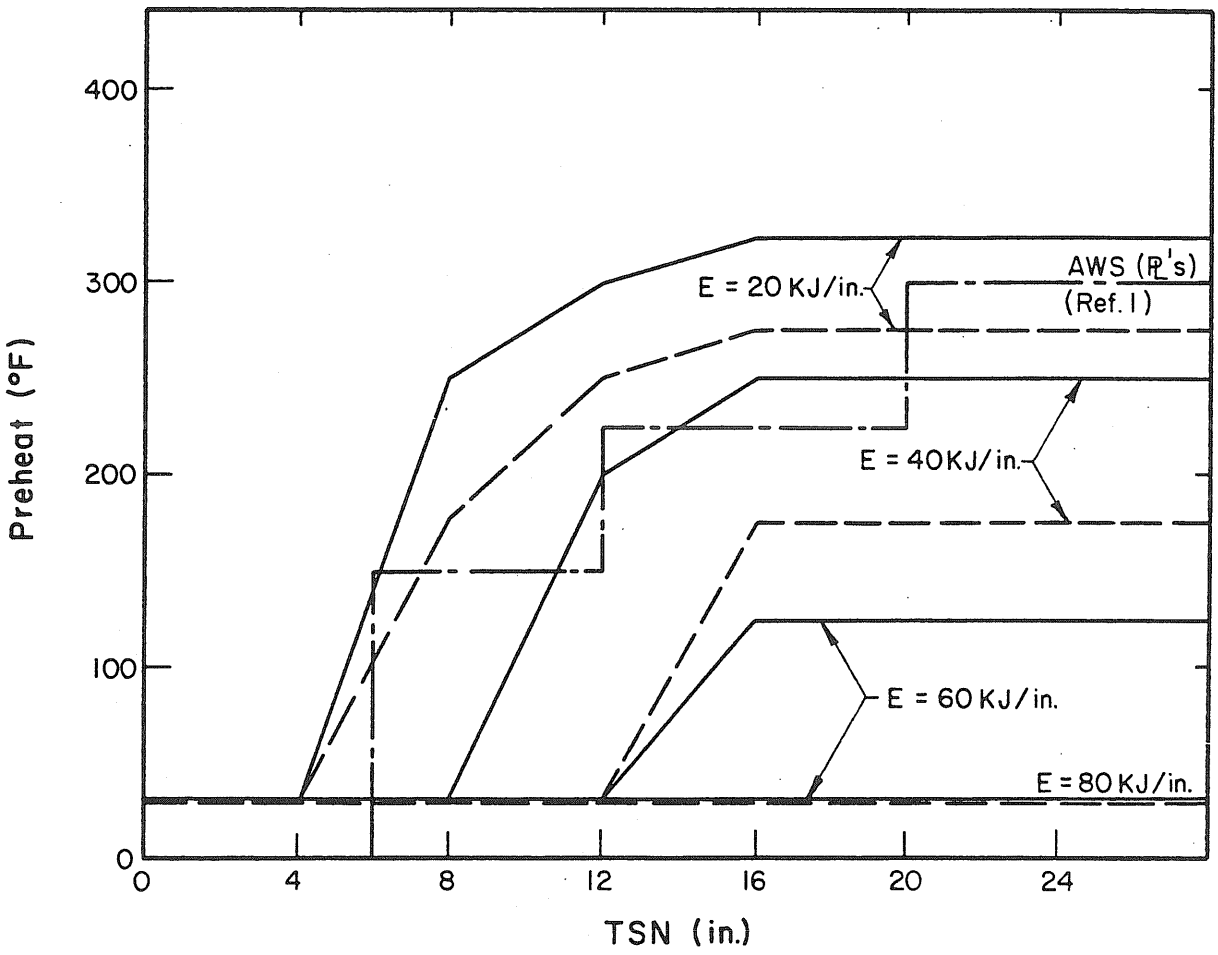


a) CE ≤ 0.37 Mild Steel
Hydrogen = Other Than Low
Critical Hardness = 350 HV (Med. Restraint) ———
= 400 HV (Low Restraint) — — —

Fig. 7.1 Comparison of Recommended Preheat Temperatures to Minimize Cold Cracking to Current AWS Structural Welding Code (1) Specified Preheat Temperatures.

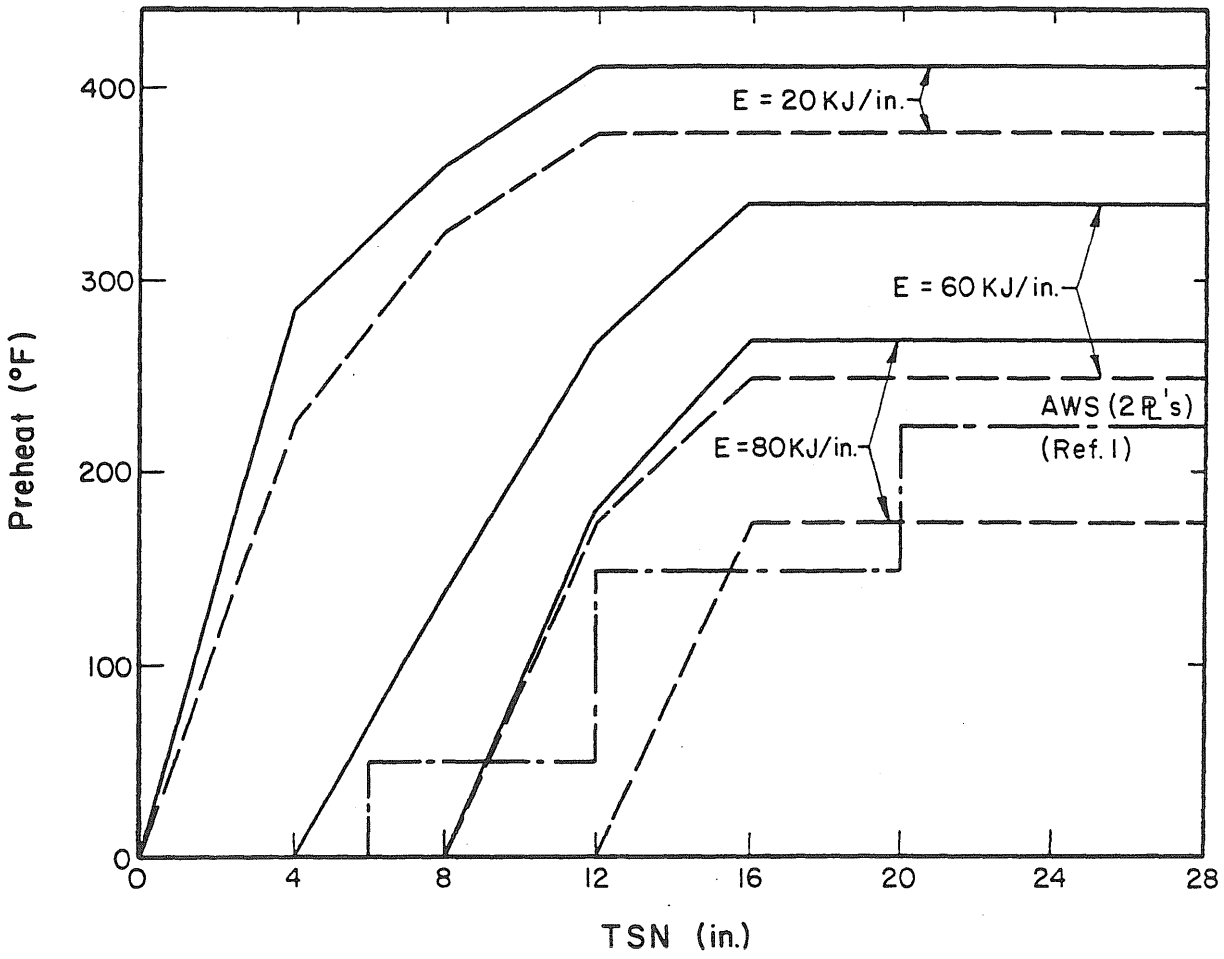


b) CE = 0.50 Low-Alloy Steel
Hydrogen = Low
Critical Hardness = 400 HV (Med. Restraint) ———
= 450 HV (Low Restraint) — — —

Fig. 7.1 Continued

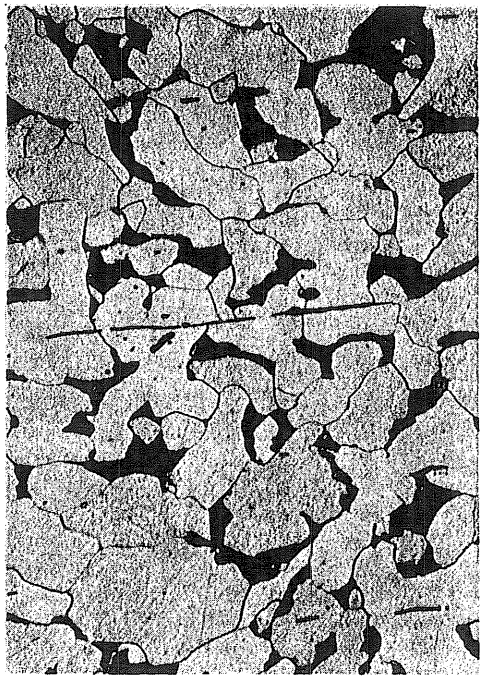

a) Mild Steel

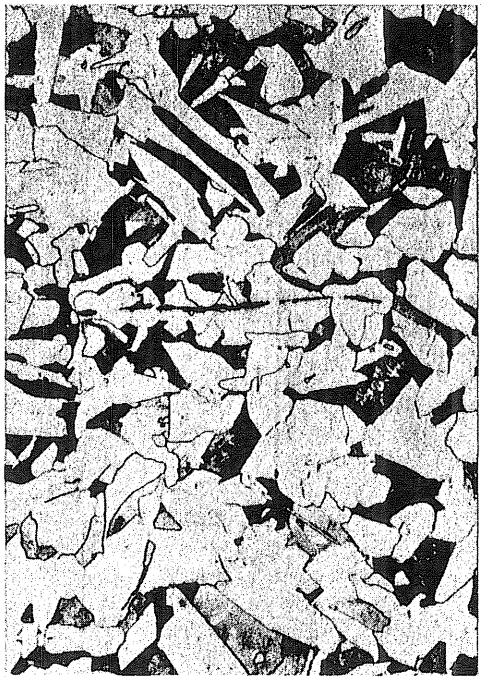

b) Low-Alloy Steel
(A441)

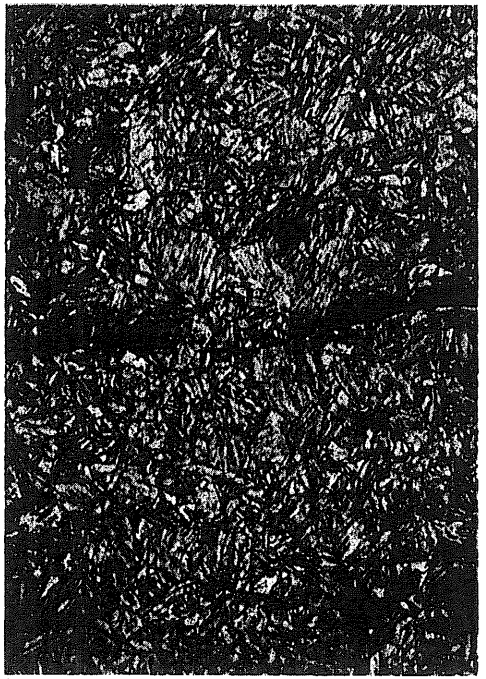

c) Quenched & Tempered Steel
(A514)

Fig. A1.1 Photomicrographs of Base Metals (214.4x, 2% Nital)

DURING REPRODUCTION FIGURES A1.2 THROUGH A1.51 (PAGES 134-183) WERE REDUCED BY 10%. THEY APPEAR HERE AT THAT REDUCTION.

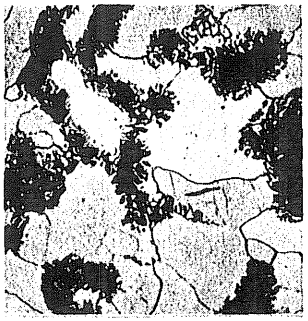

a) Spheroidized
(214.4x)

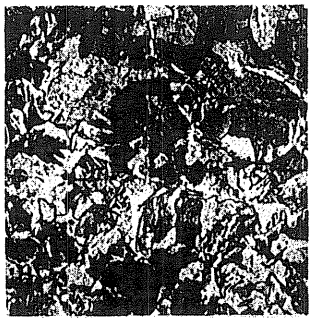

b) Refined
Lamellar inclusion
(214.4x)

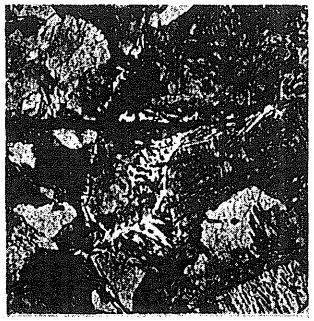

c) Coarsened
Lamellar inclusion
(214.4x)

d) Weld Metal
Small inclusions
(214.4x)

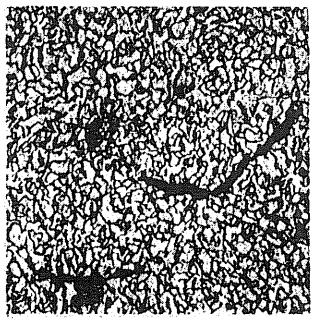

e) Retempered
Microcrack
(214.4x)

f) Weld Metal - Microcrack
(214.4x)

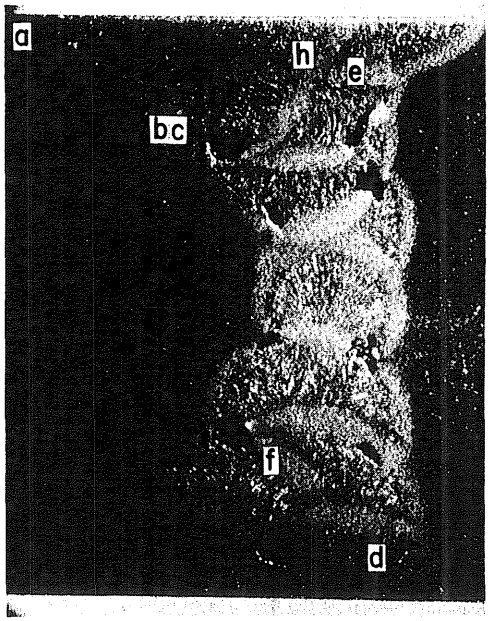


g) Photomacrograph
(3.2x)

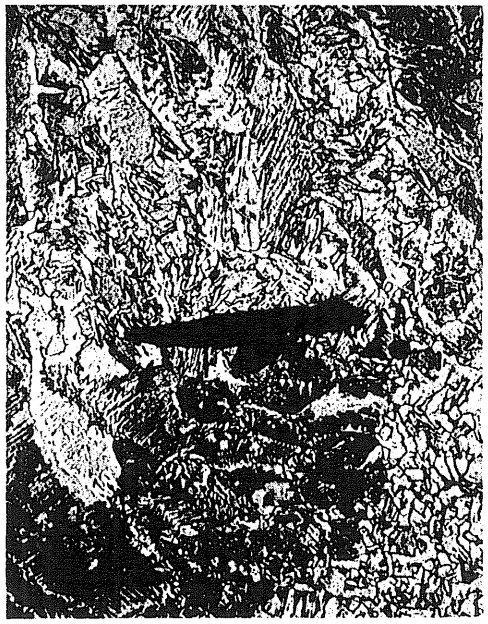

h) Weld Metal - Retempered slag
(214.4x)

Fig. A1.2 Photomacrograph and Photomicrographs of Specimen A1A. (2% Nital)

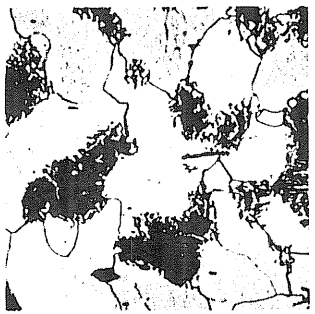

a) Spheroidized
(214.4x)

b) Refined
Lamellar inclusion
(214.4x)

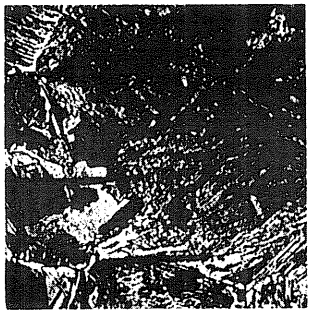

c) Coarsened
Lamellar inclusion
(214.4x)

d) Weld Metal
Small inclusions
(214.4x)

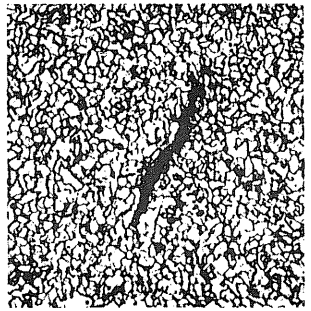

e) Retempered
Microcrack
(214.4x)

f) Weld Metal - Microcrack
(214.4x)

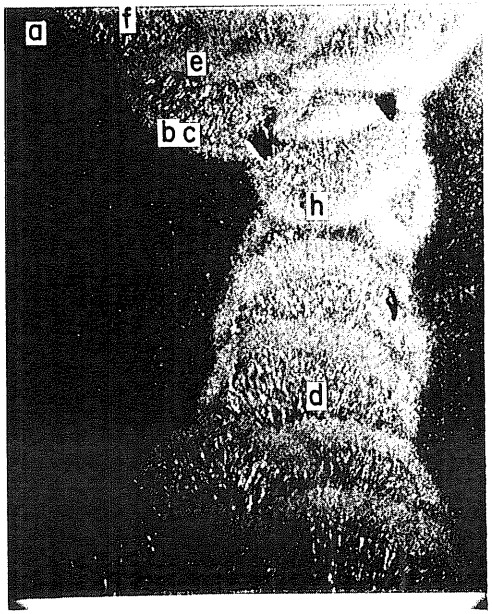


g) Photomacrograph
(3.2x)

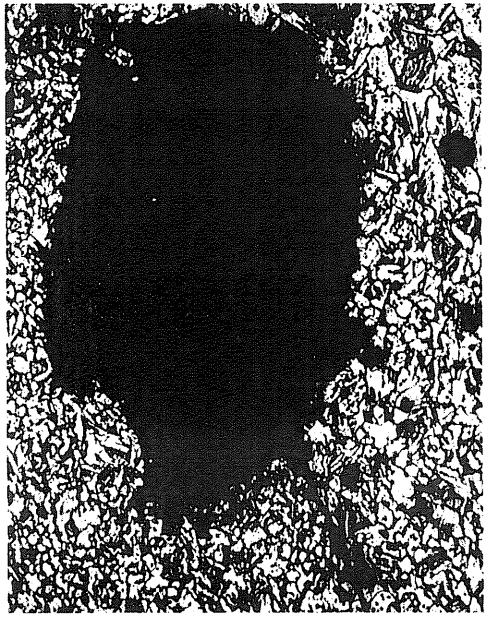

h) Weld Metal - Retempered slag
(214.4x)

Fig. A1.3 Photomacrograph and Photomicrographs of Specimen A1B. (2% Nital)

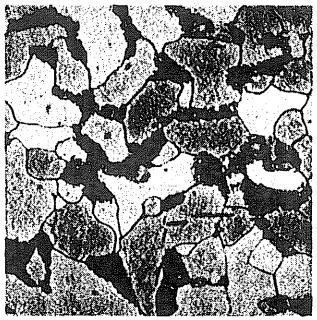

a) Spheroidized
Lamellar inclusion
(214.4x)

b) Refined
Lamellar inclusion
(214.4x)

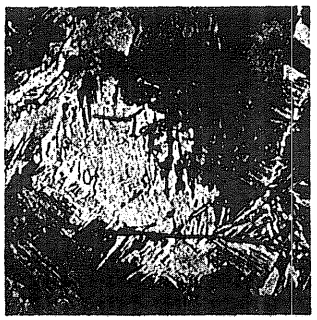

c) Coarsened
Lamellar inclusions
(214.4x)

d) Weld Metal
Small inclusion
(214.4x)

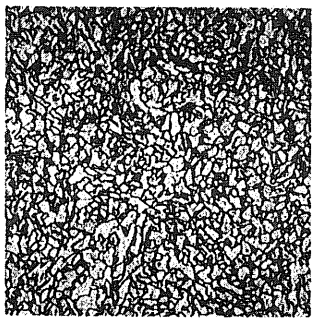

e) Retempered
(214.4x)

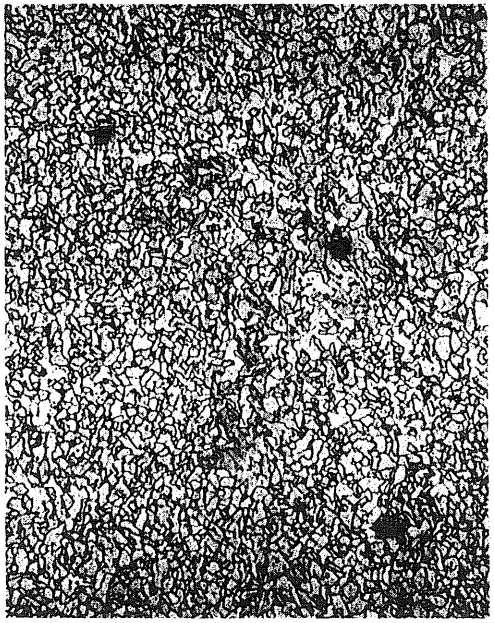

f) Retempered
Small inclusions
(214.4x)

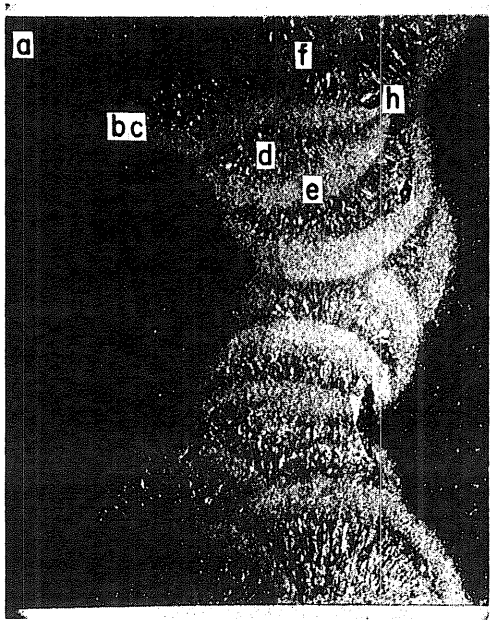


g) Photomacrograph
(3.2x)

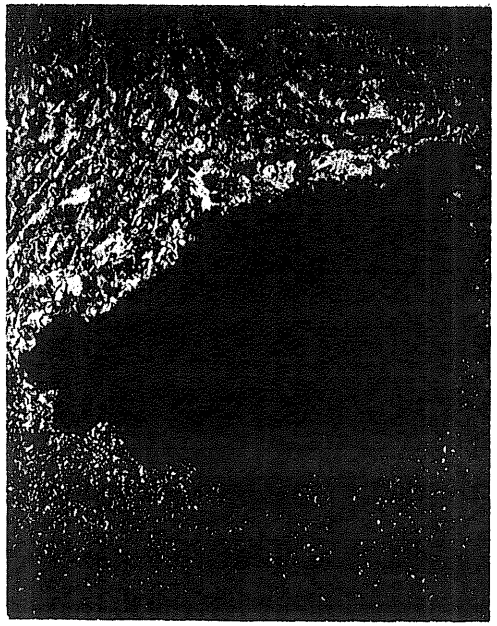

h) Weld Metal - Retempered
Lack of fusion
(53.6x)

Fig. A1.4 Photomacrograph and Photomicrographs of Specimen A1C. (2% Nital)

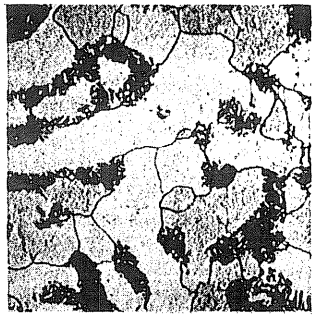

a) Spheroidized
(214.4x)

b) Refined
Lamellar inclusion
(214.4x)

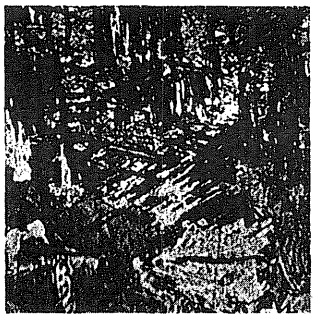

c) Coarsened
Lamellar inclusion
(214.4x)

d) Weld Metal
Porosity
(214.4x)

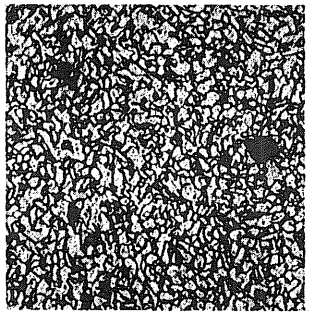

e) Retempered
Small inclusions
(214.4x)

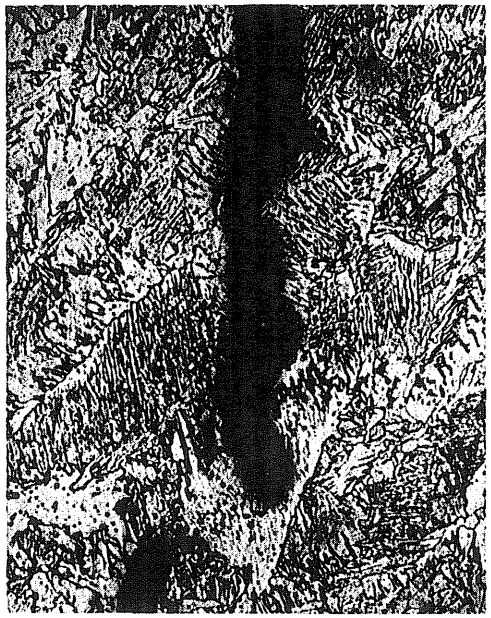

f) Weld Metal - Mircocrack
(214.4x)

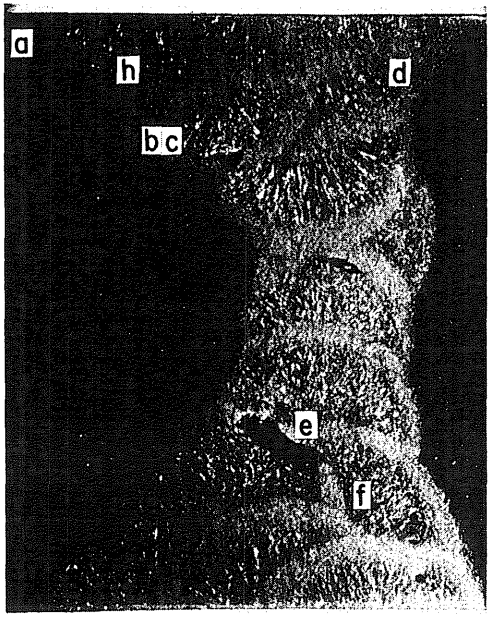


g) Photomacrograph
(3.2x)

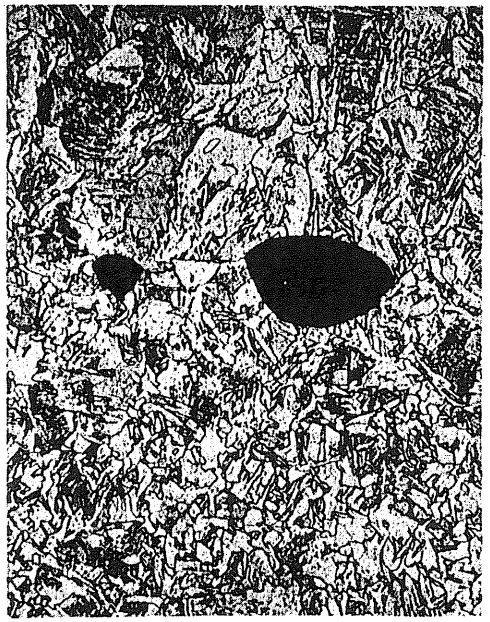

h) Weld Metal - Retempered slag
(214.4x)

Fig. A1.5 Photomacrograph and Photomicrographs of Specimen A1D. (2% Nital)

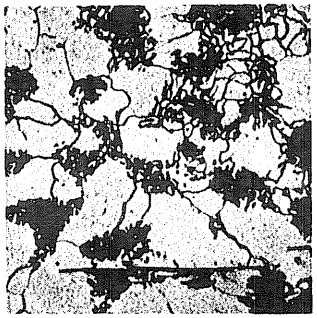

a) Spheroidized Lamellar inclusion (214.4x)

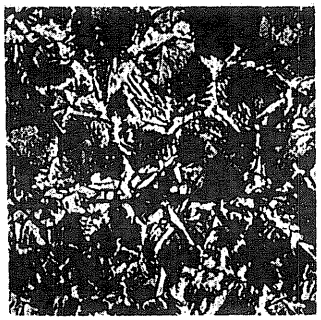

b) Refined Lamellar inclusion (214.4x)

c) Coarsened (214.4x)

d) Weld Metal Small inclusions (214.4x)

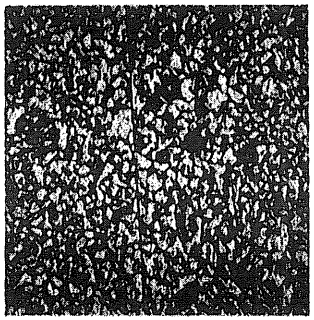

e) Retempered Porosity (214.4x)

f) Weld Metal - Microcrack (214.4x)

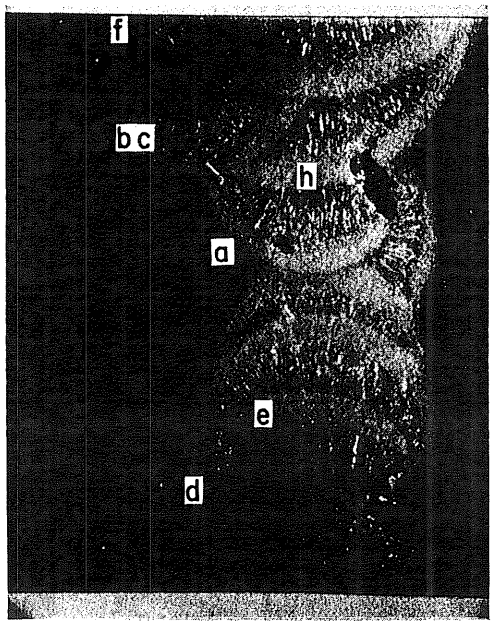


g) Photomacrograph (3.2x)

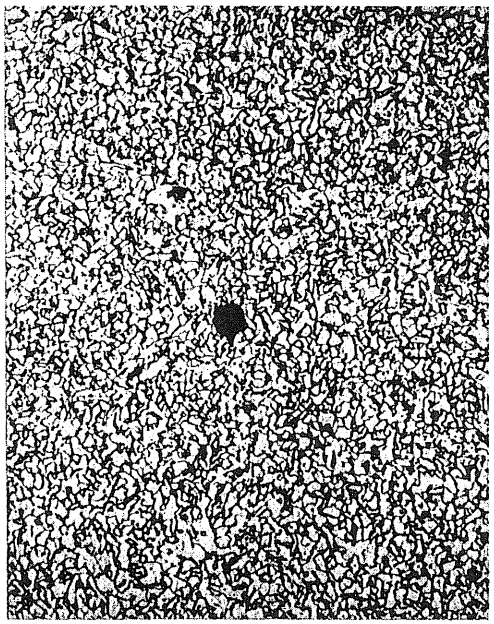

h) Retempered slag (214.4x)

Fig. A1.6 Photomacrograph and Photomicrographs of Specimen A2A. (2% Nital)

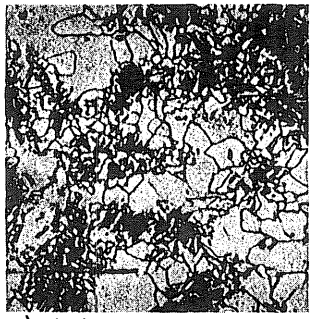

a) Spheroidized Lamellar inclusion (214.4x)

b) Refined (214.4x)

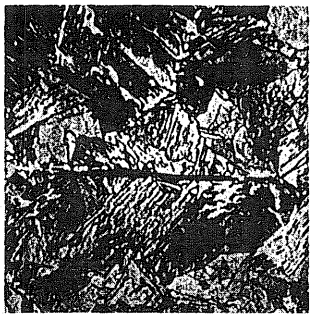

c) Coarsened Lamellar inclusion (214.4x)

d) Weld Metal (214.4x)

e) Retempered (214.4x)

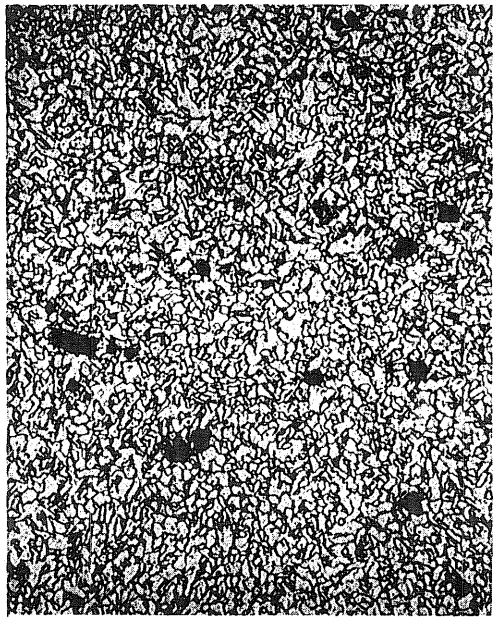

f) Retempered small inclusions (214.4x)

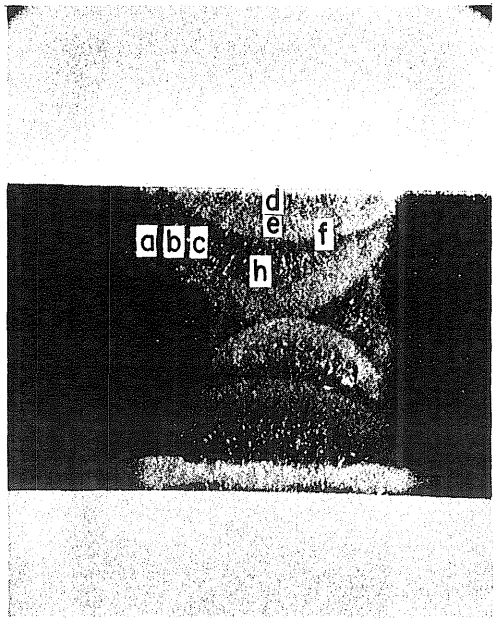


g) Photomacrograph (3.2x)

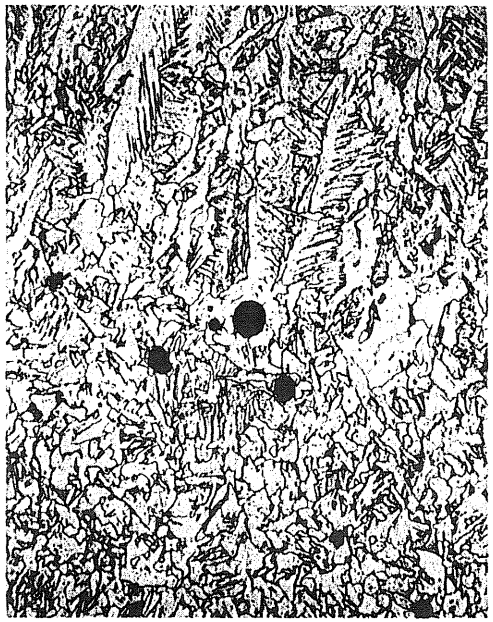

h) Weld Metal - Retempered slag (214.4x)

Fig. A1.7 Photomacrograph and Photomicrographs of Specimen A3A. (2% Nital)

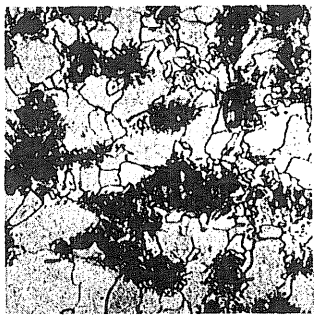

a) Spheroidized
(214.4x)

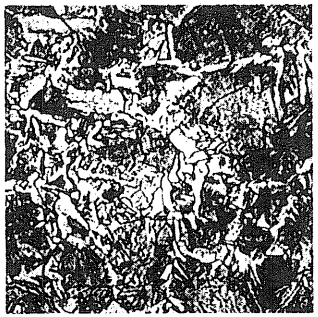

b) Refined
(214.4x)

c) Coarsened
(214.4x)

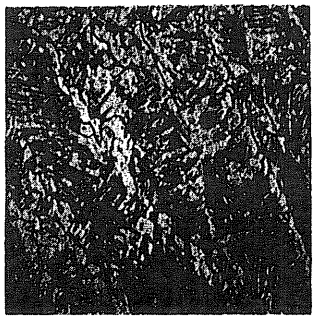

d) Weld Metal
Porosity
(214.4x)

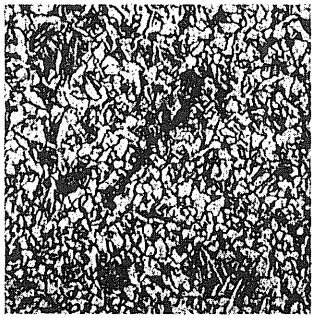

e) Retempered
Microcrack
(214.4x)

f) Weld Metal - Microcrack
(214.4x)

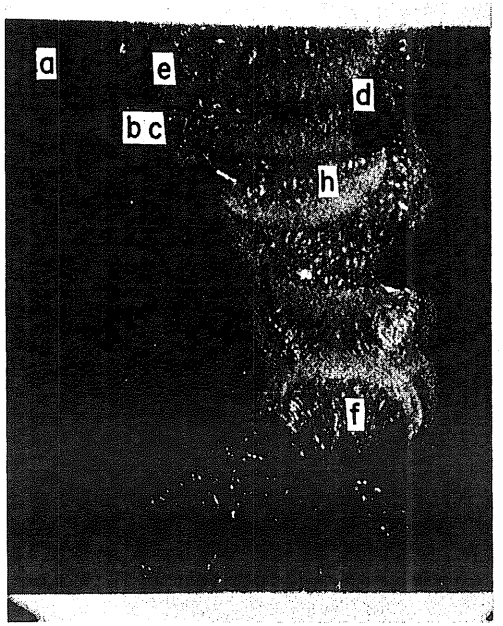


g) Photomacrograph
(3.2x)

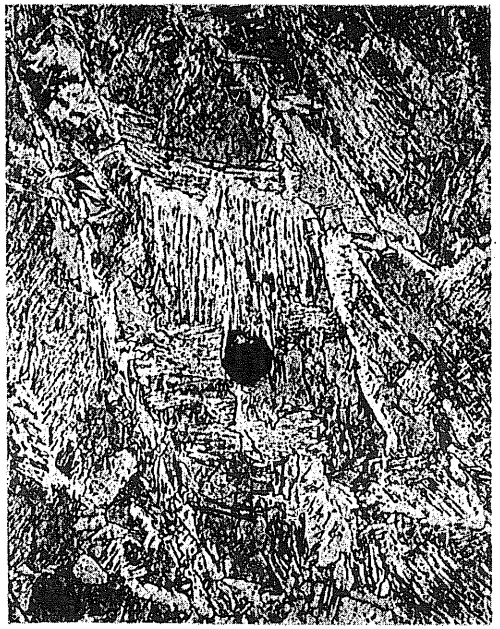

h) Weld Metal - Slag
(214.4x)

Fig. A1.8 Photomacrograph and Photomicrographs of Specimen A3B. (2% Nital)

a) Spheroidized (214.4x)

b) Refined (214.4x)

c) Coarsened (214.4x)

d) Weld Metal Porosity (214.4x)

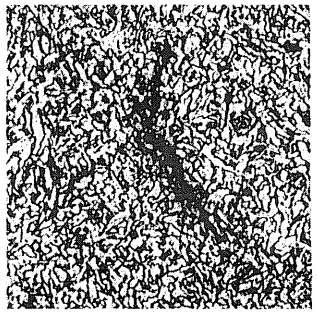

e) Retempered Microcrack (214.4x)

f) Weld Metal - Microcrack (214.4x)

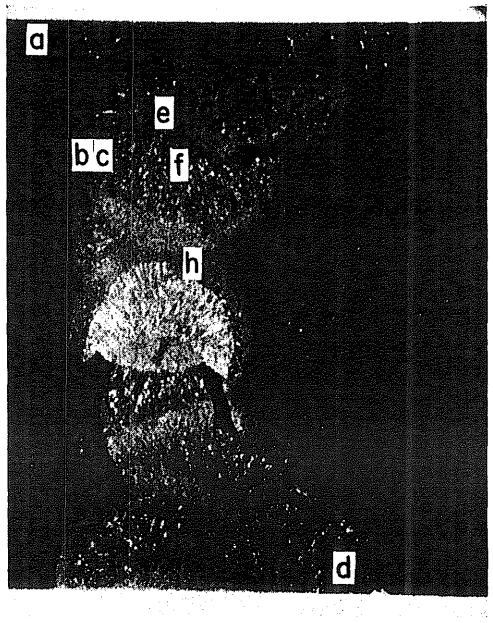


g) Photomacrograph (3.2x)

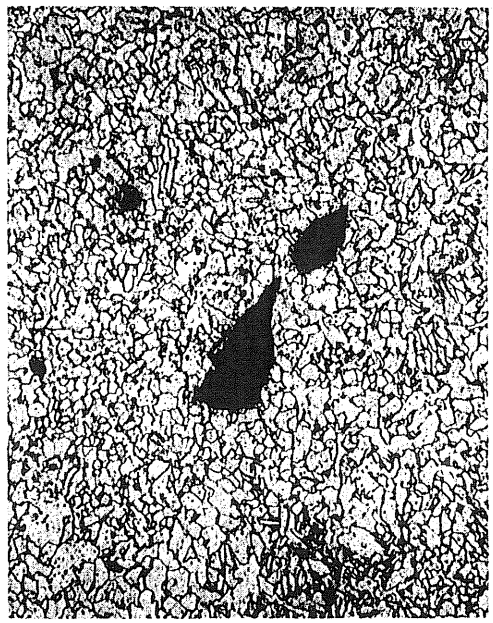

h) Retempered slag (214.4x)

Fig. A1.9 Photomacrograph and Photomicrographs of Specimen A3C. (2% Nital)

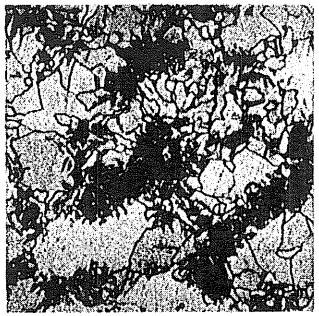

a) Spheroidized
(214.4x)

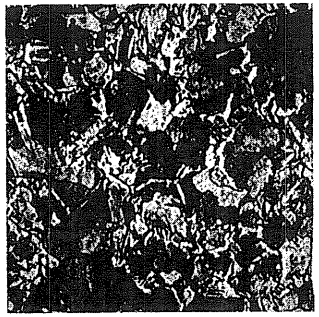

b) Refined
(214.4x)

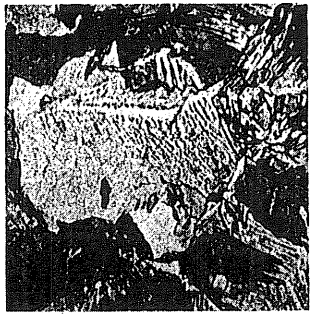

c) Coarsened
(214.4x)

d) Weld Metal
(214.4x)

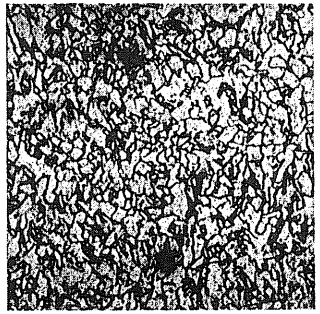

e) Retempered
Small inclusions
(214.4x)

f) Weld Metal
Small inclusions
(214.4x)

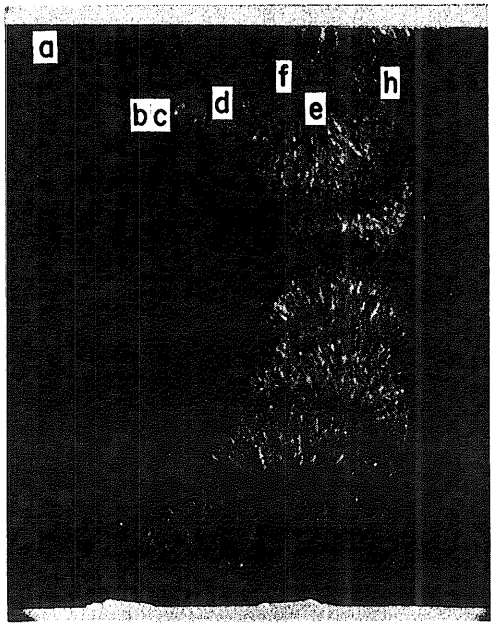


g) Photomacrograph
(3.2x)

h) Weld Metal - Retempered slag
(214.4x)

Fig. A1.10 Photomacrograph and Photomicrographs of Specimen A4A. (2% Nital)

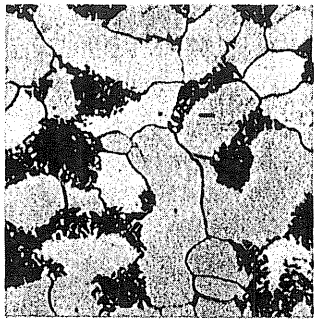

a) Spheroidized
(214.4x)

b) Refined
(214.4x)

c) Coarsened
Lamellar inclusion
(214.4x)

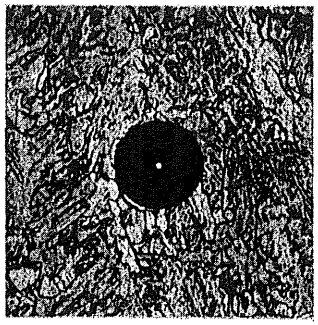

d) Weld Metal
Porosity
(214.4x)

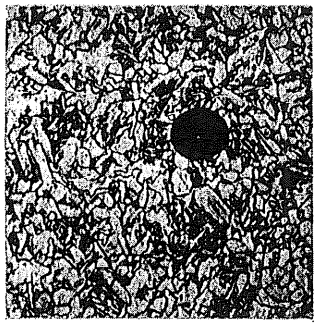

e) Retempered
Porosity
(214.4x)

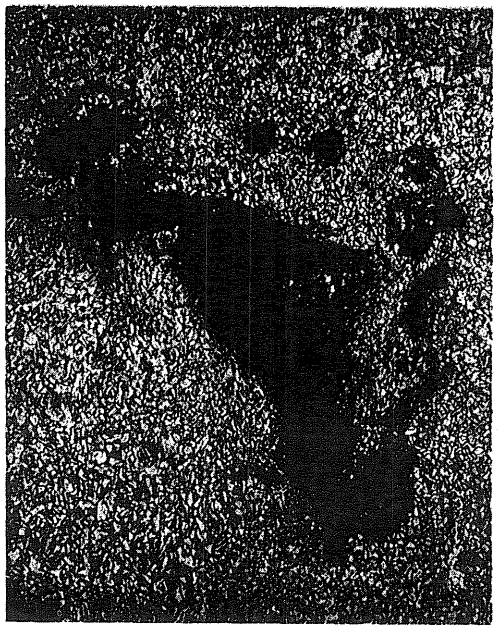

f) Retempered hot crack
(107.2x)

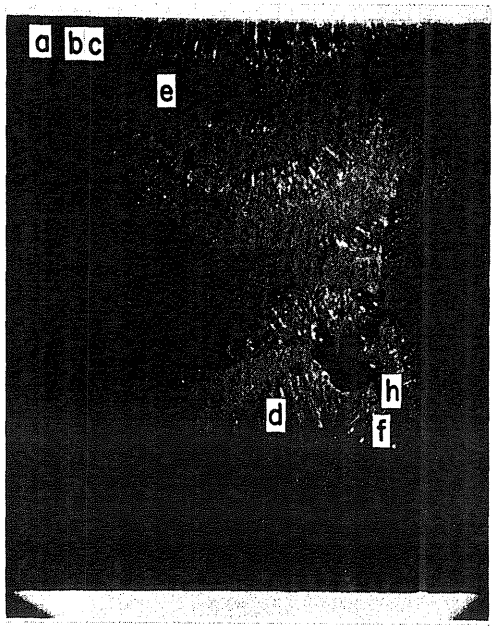


g) Photomacrograph
(3.2x)

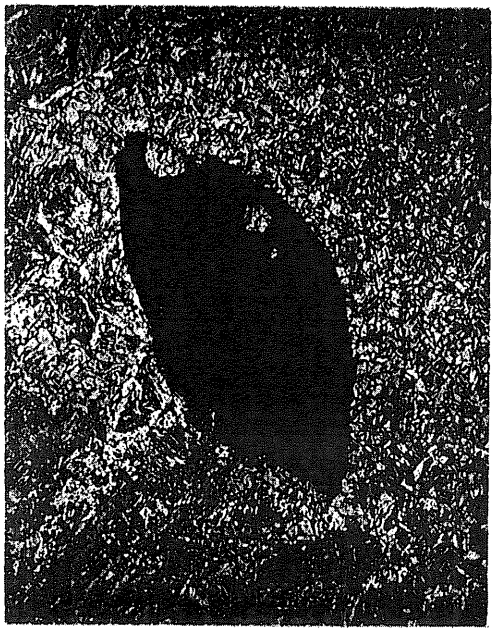

h) Weld Metal - Retempered slag
(107.2x)

Fig. A1.11 Photomacrograph and Photomicrographs of Specimen A4B. (2% Nital)

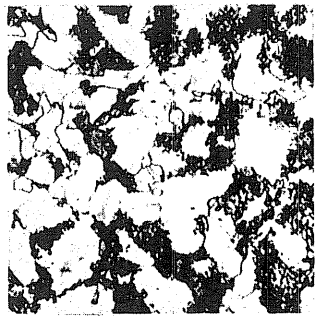

a) Spheroidized
(214.4x)

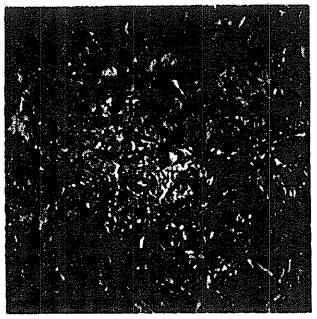

b) Refined
Lamellar inclusion
(214.4x)

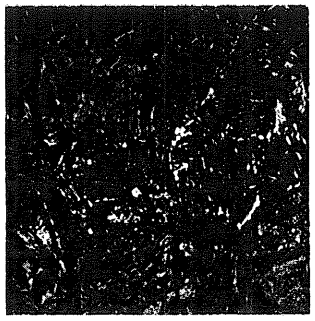

c) Coarsened
(214.4x)

d) Weld Metal
Small inclusion
(107.2x)

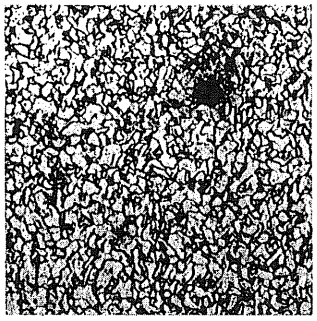

e) Retempered
Small inclusion
(214.4x)

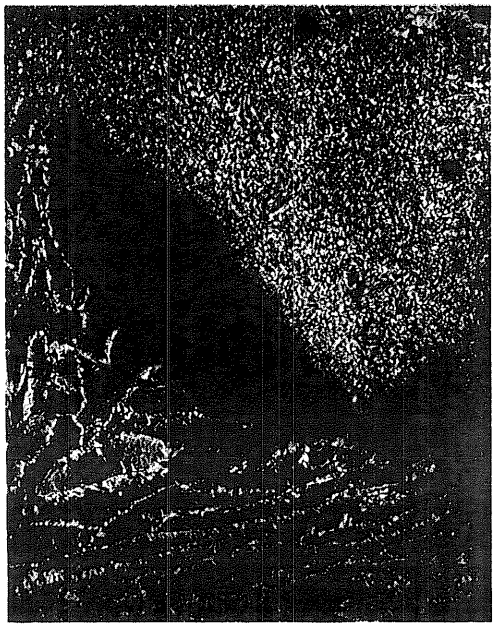

f) Weld Metal - Retempered slag
(53.6x)

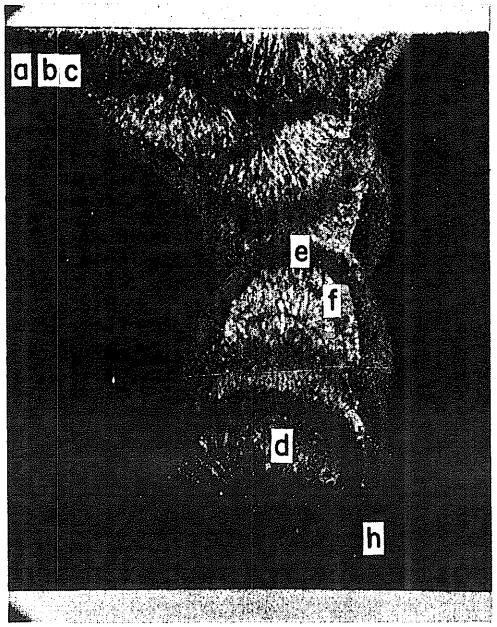


g) Photomacrograph
(3.2x)

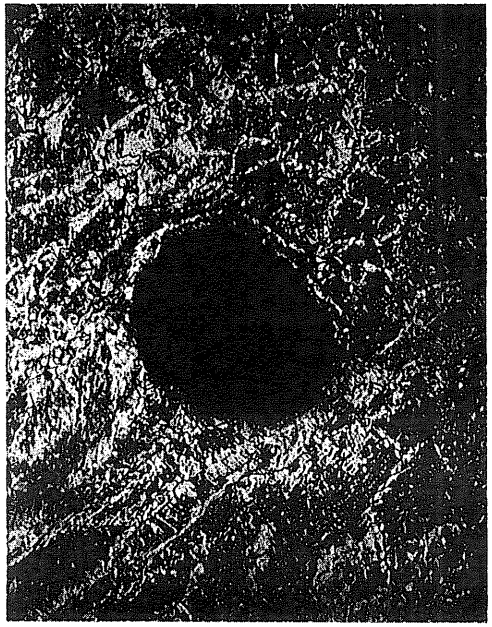

h) Weld Metal - Slag
(107.2x)

Fig. A1.12 Photomacrograph and Photomicrographs of Specimen B1A. (2% Nital)

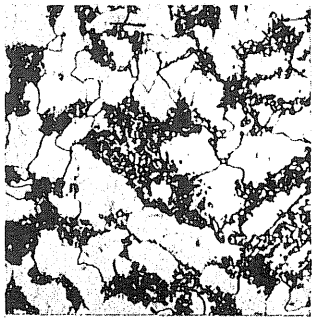

a) Spheroidized
(214.4x)

b) Refined
(214.4x)

c) Coarsened
Lamellar inclusion
(214.4x)

d) Weld Metal
(214.4x)

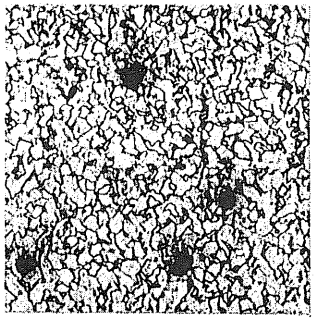

e) Retempered
Small inclusions
(214.4x)

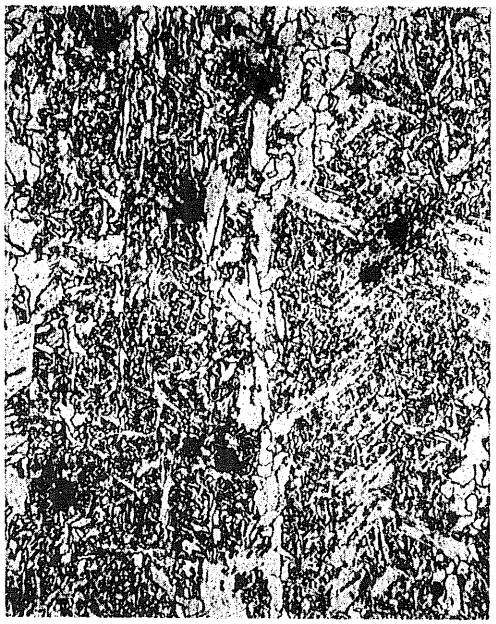

f) Weld Metal - Small inclusions
(214.4x)

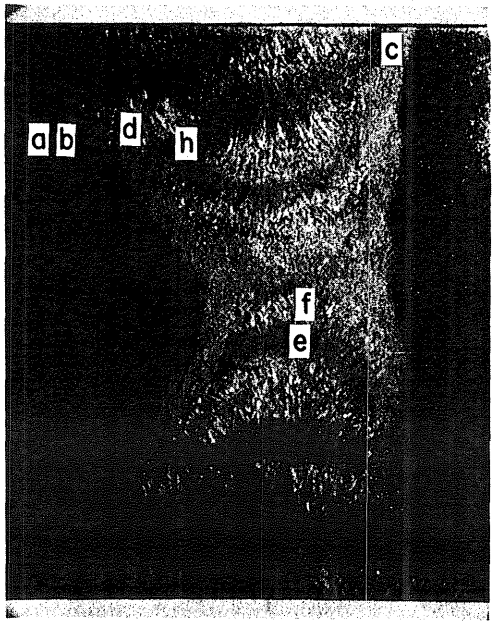


g) Photomacrograph
(3.2x)

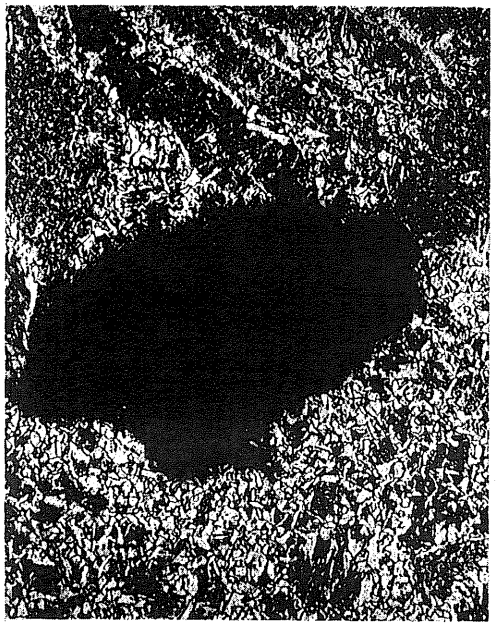

h) Weld Metal - Retempered slag
(107.2x)

Fig. A1.13 Photomacrograph and Photomicrographs of Specimen B1B. (2% Nital)

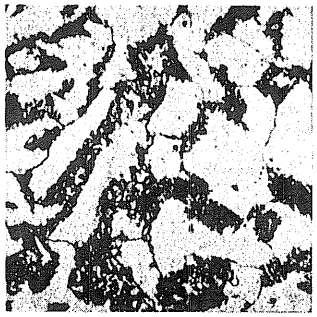

a) Sheroidized
(214.4x)

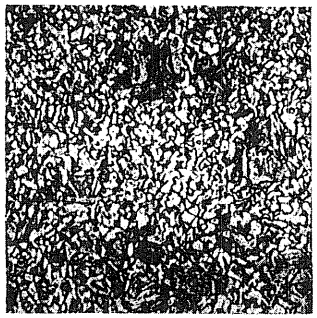

b) Refined
(214.4x)

c) Coarsened
(214.4x)

d) Weld Metal
Small inclusion
(214.4x)

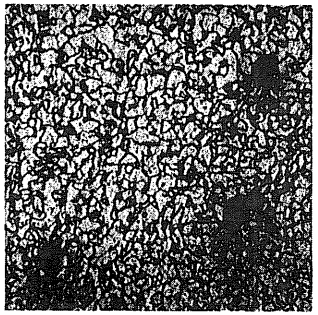

e) Retempered
Small inclusions
(214.4x)

f) Weld Metal - Porosity
(214.4x)

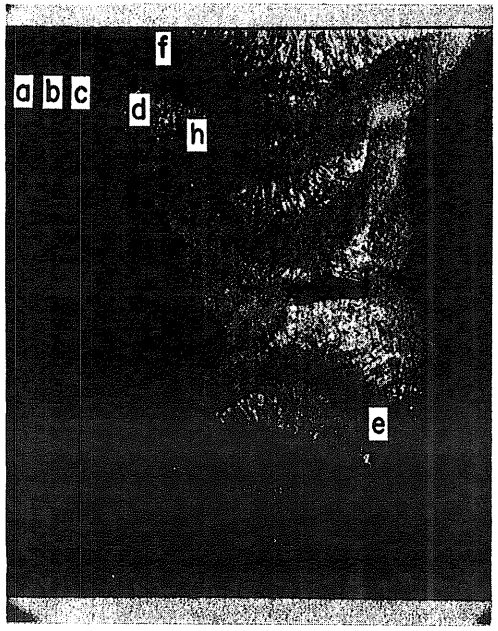


g) Photomacrograph
(3.2x)

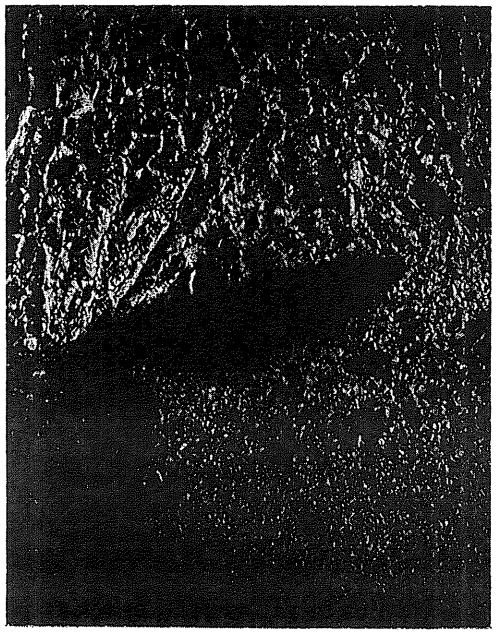

h) Weld Metal - Retempered slag
(53.6x)

Fig. A1.14 Photomacrograph and Photomicrographs of Specimen B1C. (2% Nital)

a) Spheroidized (214.4x)



b) Refined (214.4x)



c) Coarsened (214.4x)



d) Weld Metal Porosity (214.4x)



e) Retempered Small inclusion (214.4x)



f) Retempered slag (214.4x)




g) Photomacrograph (3.2x)



h) Weld Metal - Coarsened slag (53.6x)

Fig. A1.15 Photomacrograph and Photomicrographs of Specimen B2A. (2% Nital)

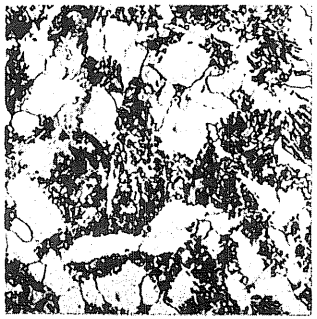

a) Spheroidized
(214.4x)

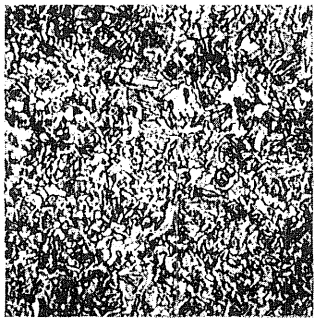

b) Refined
(214.4x)

c) Coarsened
(214.4x)

d) Weld Metal
Small inclusion
(214.4x)

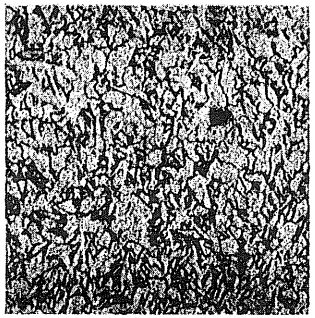

e) Retempered
Small inclusion
(214.4x)

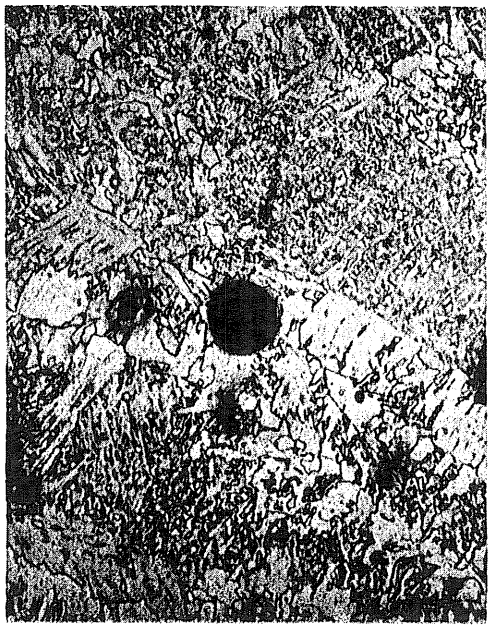

f) Weld Metal - Slag
(214.4x)

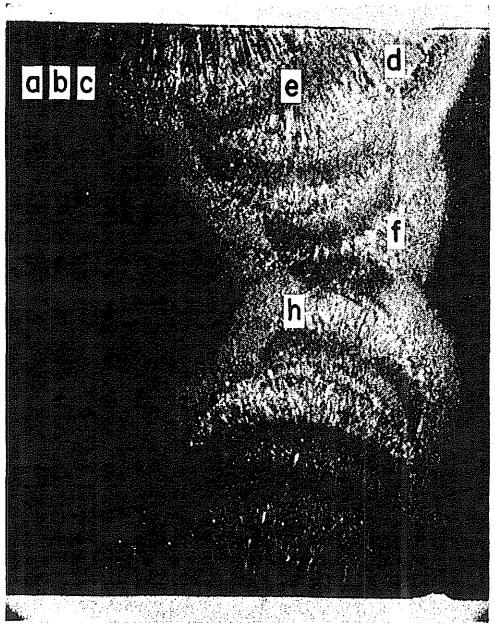


g) Photomacrograph
(3.2x)

h) Weld Metal - Crack
(214.4x)

Fig. A1.16 Photomacrograph and Photomicrographs of Specimen B2B. (2% Nital)

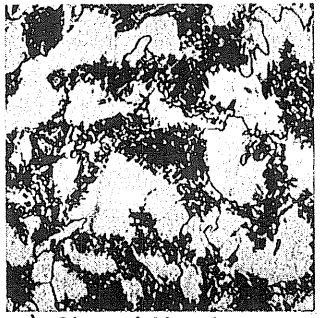

a) Sheroidized
(214.4x)

b) Refined
Lamellar inclusion
(214.4x)

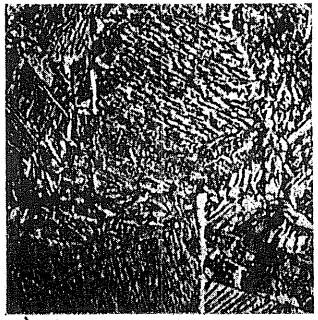

c) Coarsened
(214.4x)

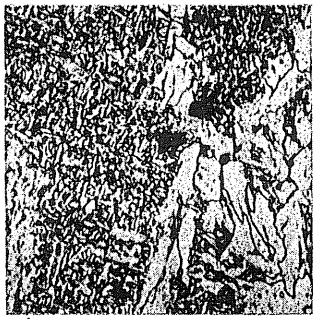

d) Weld Metal
Small inclusions
(214.4x)

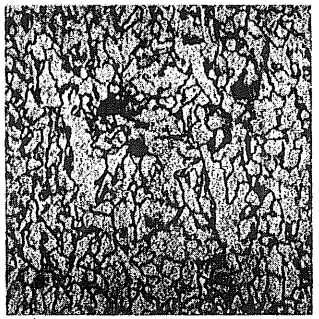

e) Retempered
Small inclusions
(214.4x)

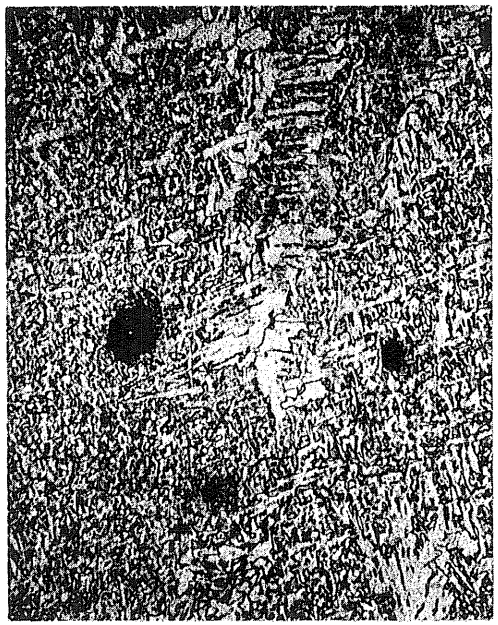

f) Weld Metal - Porosity
(214.4x)

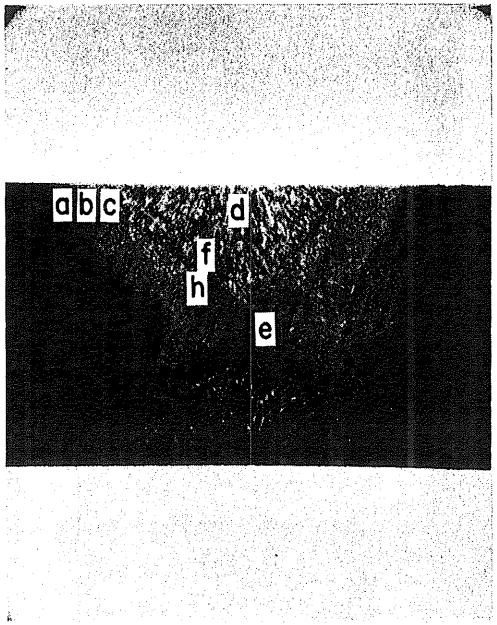


g) Photomacrograph
(3.2x)

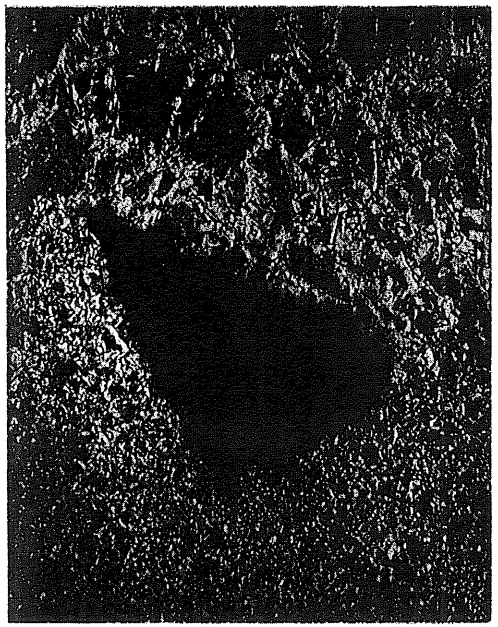

h) Weld Metal - Retempered slag
(53.6x)

Fig. A1.17 Photomacrograph and Photomicrographs of Specimen B3A. (2% Nital)

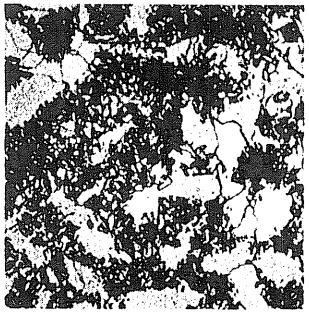

a) Spheroidized
(214.4x)

b) Refined
(214.4x)

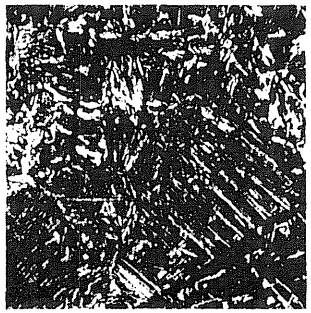

c) Coarsened
(214.4x)

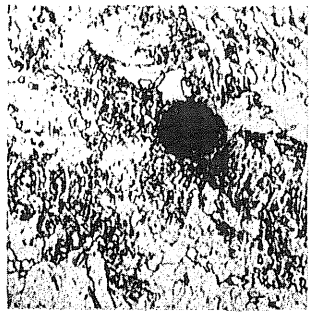

d) Weld Metal
Porosity
(214.4x)

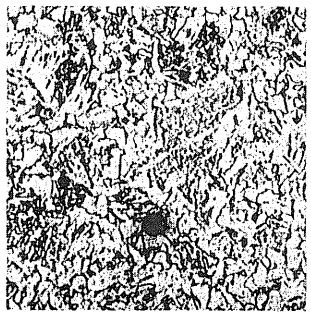

e) Retempered –
Small inclusions
(214.4x)

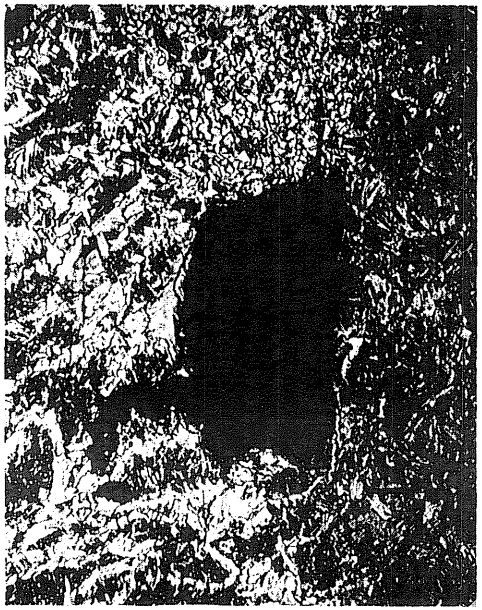

f) Weld Metal - Retempered Slag
(107.2x)

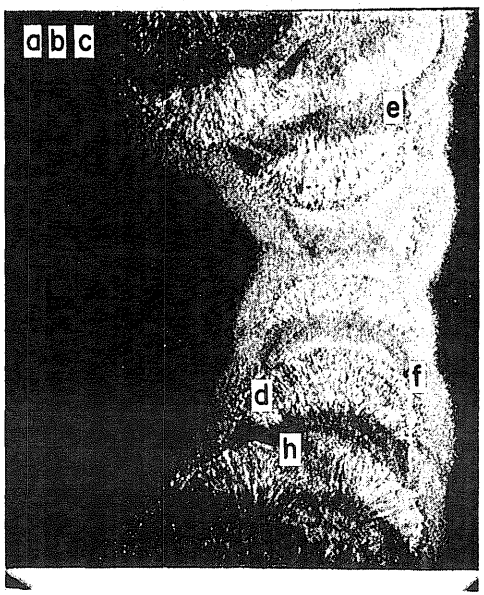


g) Photomacrograph
(3.2x)

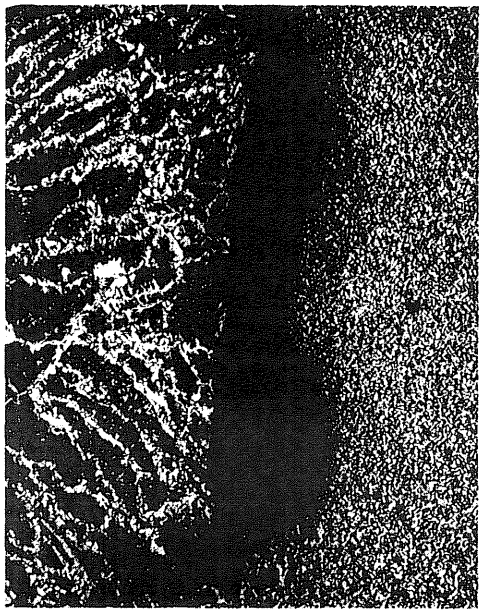

h) Weld Metal - Retempered slag
(53.6x) - Photo rotated 90°

Fig. A1.18 Photomacrograph and Photomicrographs of Specimen B3B. (2% Nital)

a) Spheroidized
(214.4x)

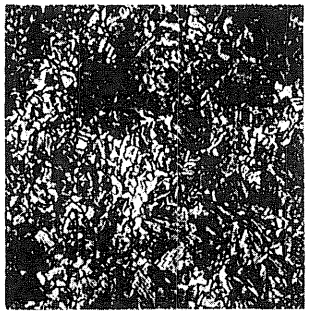

b) Refined
(214.4x)

c) Coarsened
(214.4x)

d) Weld Metal
Small inclusions
(214.4x)

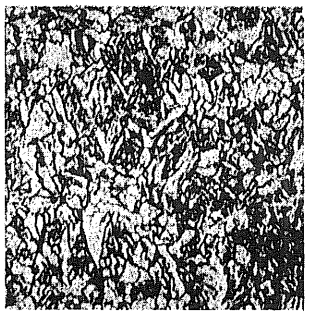

e) Retempered
Small inclusion
(214.4x)

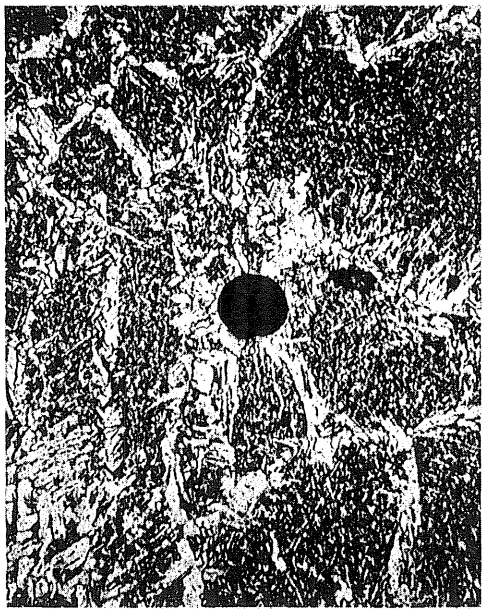

f) Weld Metal - Porosity
(214.4x)

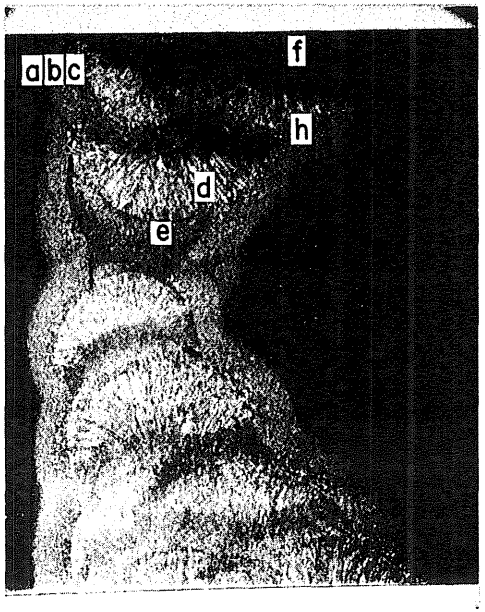


g) Photomacrograph
(3.2x)

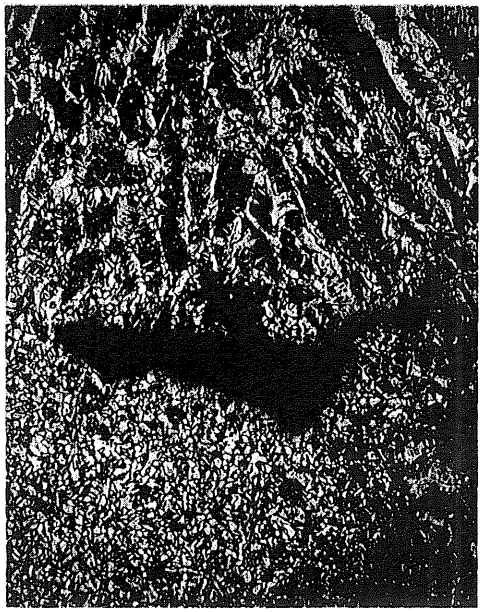

h) Weld Metal - Retempered slag
(107.2x)

Fig. A1.19 Photomacrograph and Photomicrographs of Specimen B3C. (2% Nital)

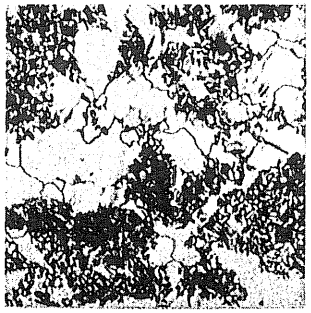

a) Spheroidized
(214.4x)

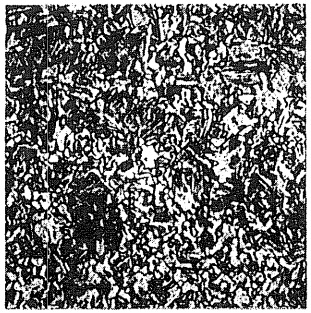

b) Refined
(214.4x)

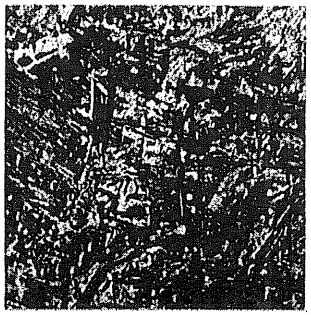

c) Coarsened
(214.4x)

d) Weld Metal
(214.4x)

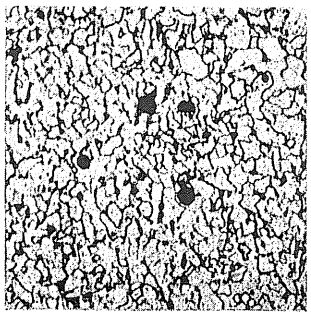

e) Retempered
Small inclusions
(214.4x)

f) Retempered slag
(214.4x)

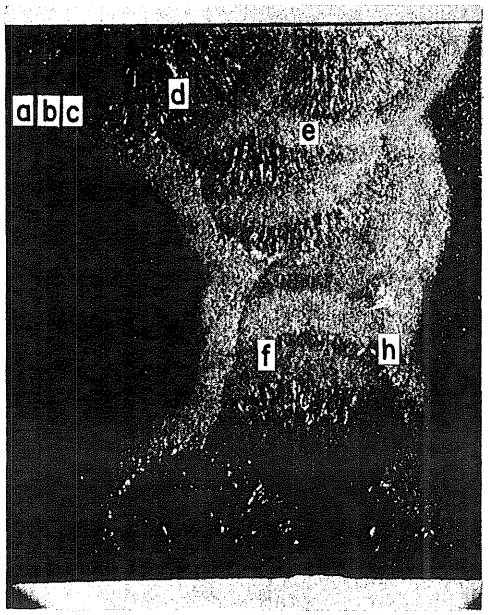


g) Photomacrograph
(3.2x)

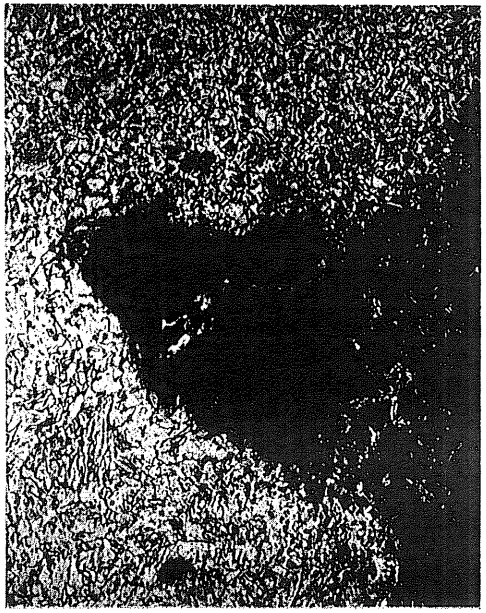

h) Weld Metal - Retempered
LOF - Slag
(107.2x)

Fig. A1.20 Photomacrograph and Photomicrographs of Specimen B4A. (2% Nital)

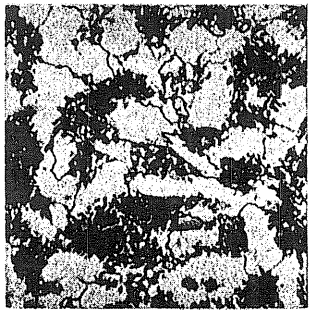

a) Spheroidized
(214.4x)

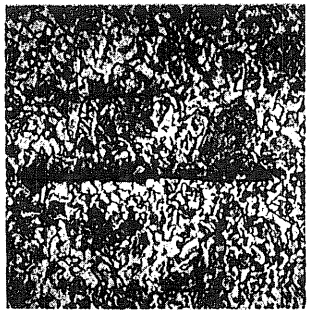

b) Refined
Lamellar inclusions
(214.4x)

c) Coarsened
(214.4x)

d) Weld Metal
(214.4x)

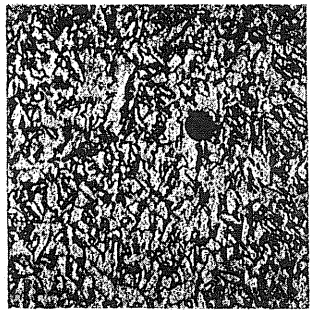

e) Retempered
Porosity
(214.4x)

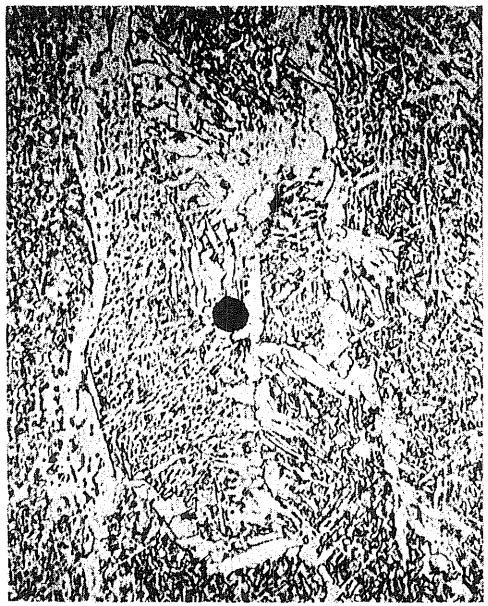

f) Weld Metal - Porosity
(214.4x)

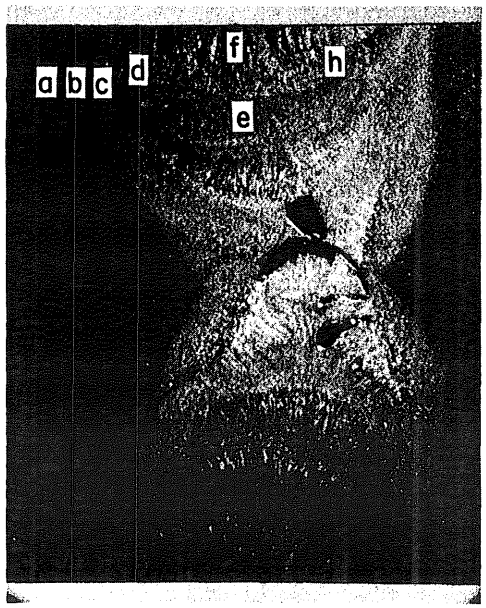


g) Photomacrograph
(3.2x)

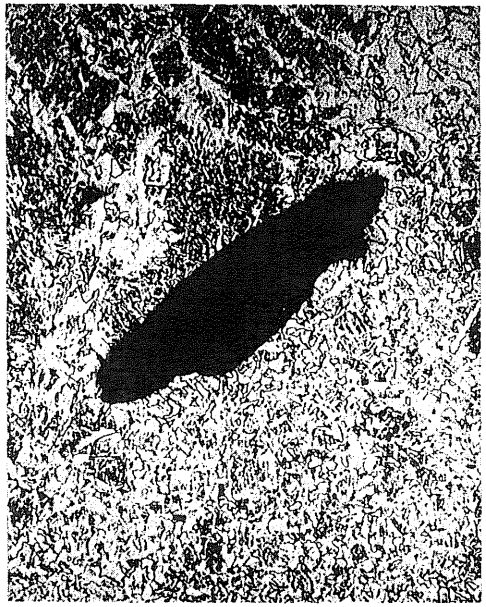

h) Weld Metal - Retempered slag
(107.2x)

Fig. A1.21 Photomacrograph and Photomicrographs of Specimen B4B. (2% Nital)

a) Spheroidized
(214.4x)

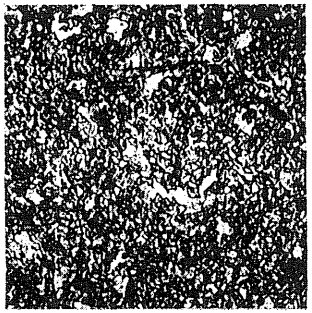

b) Refined
Lamellar inclusion
(214.4x)

c) Coarsened
(214.4x)

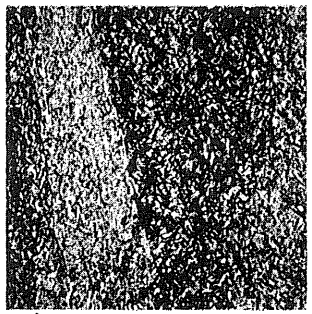

d) Weld Metal
(214.4x)

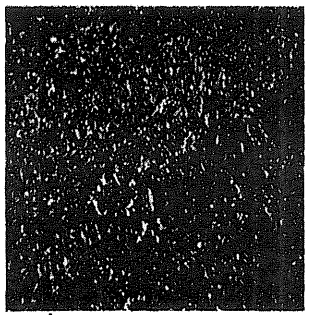

e) Weld Metal
Porosity
(214.4x)

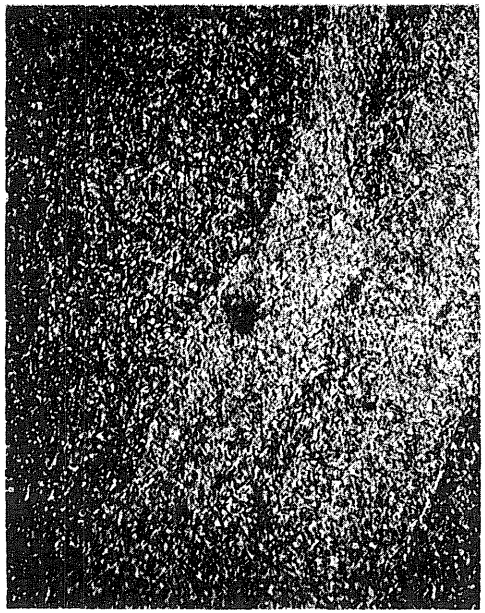

f) Weld Metal - Small inclusion
(214.4x)

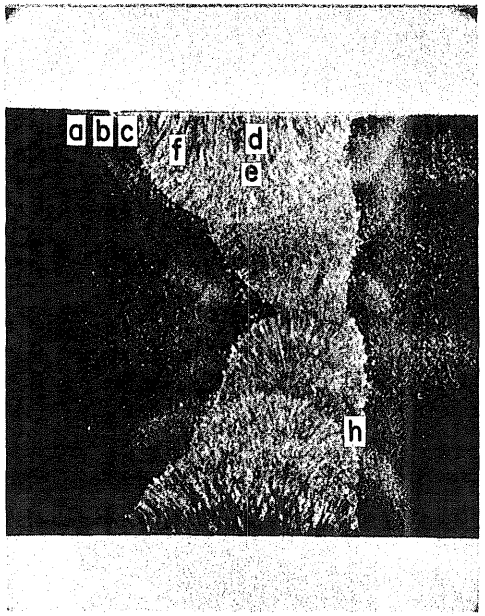


g) Photomacrograph
(3.2x)

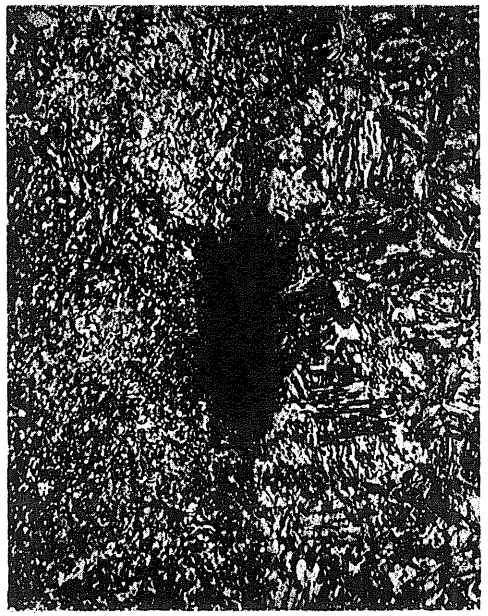

h) Weld Metal - Coarsened slag
(214.4x)

Fig. A1.22 Photomacrograph and Photomicrographs of Specimen C1A. (2% Nital)

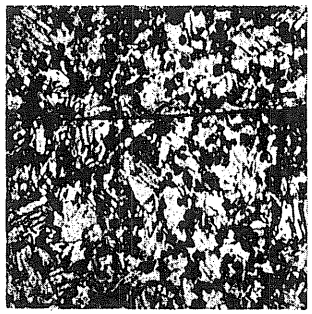

a) Spheroidized Lamellar inclusion (214.4x)

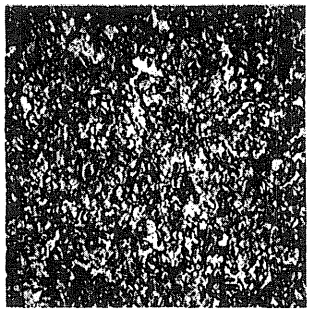

b) Refined (214.4x)

c) Coarsened (214.4x)

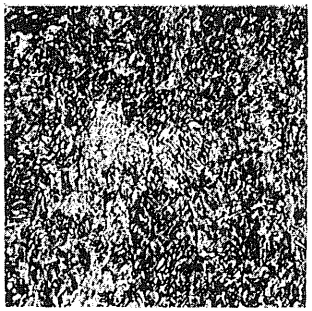

d) Weld Metal (214.4x)

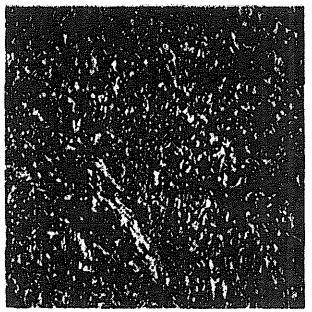

e) Weld Metal Small inclusion (214.4x)

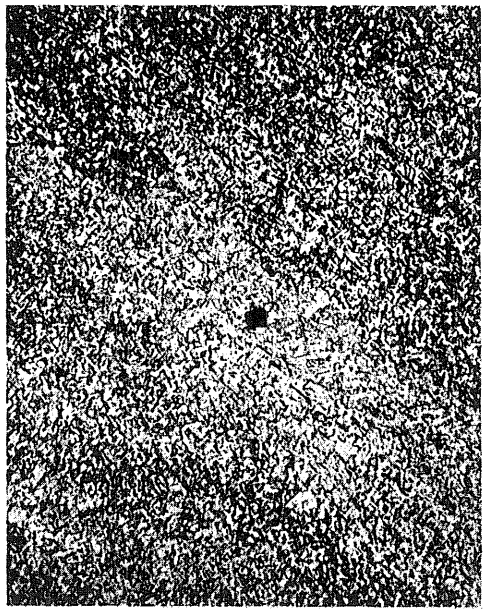

f) Weld Metal - Porosity (214.4x)

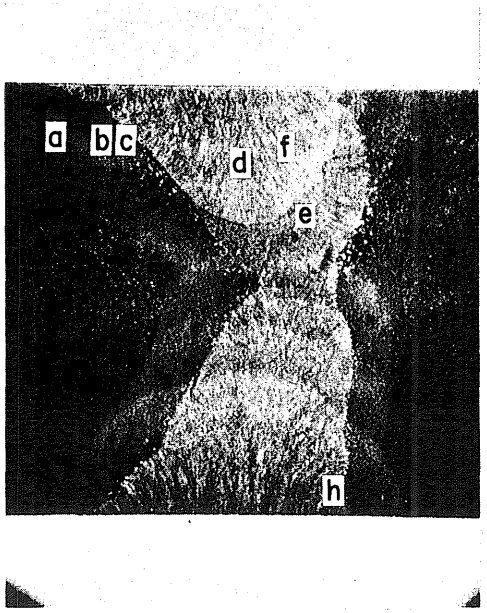


g) Photomacrograph (3.2x)

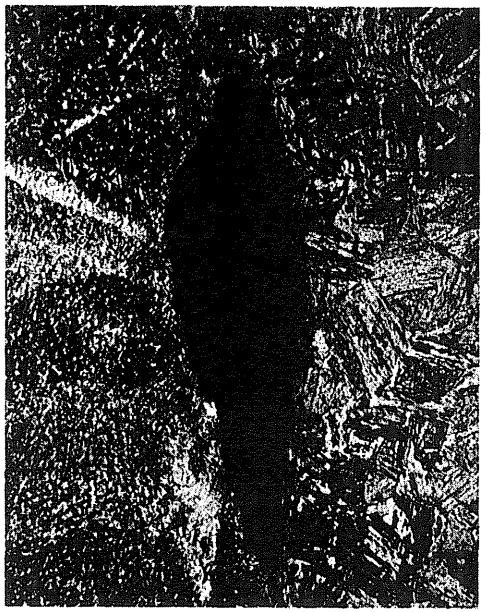

h) Weld Metal - Coarsened slag (214.4x)

Fig. A1.23 Photomacrograph and Photomicrographs of Specimen C1B. (2% Nital)

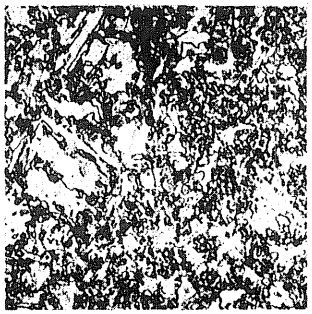

a) Spheroidized
(214.4x)

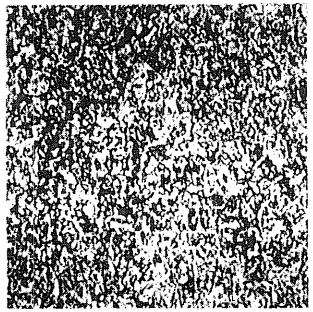

b) Refined
(214.4x)

c) Coarsened
(214.4x)

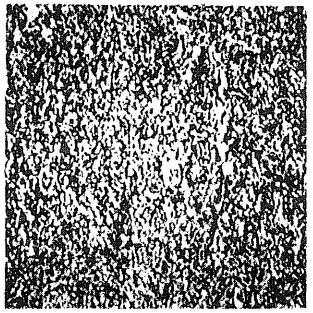

d) Weld Metal
(214.4x)

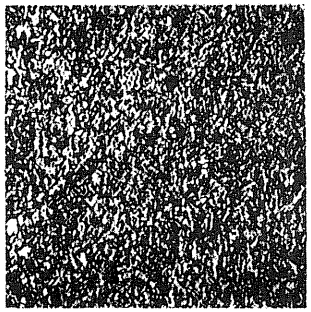

e) Weld Metal
Porosity
(214.4x)

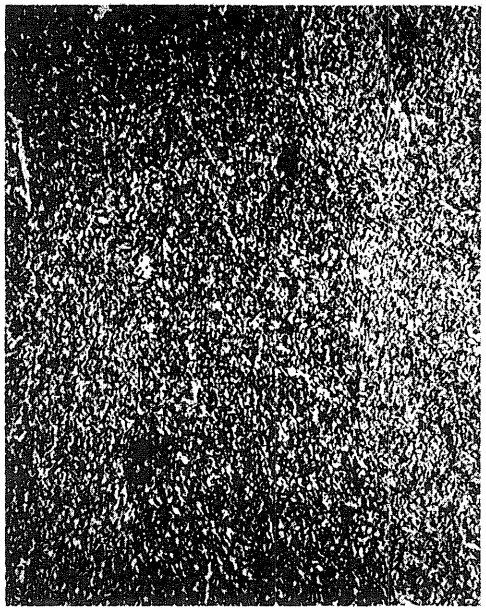

f) Weld Metal - Small inclusions
(214.4x)

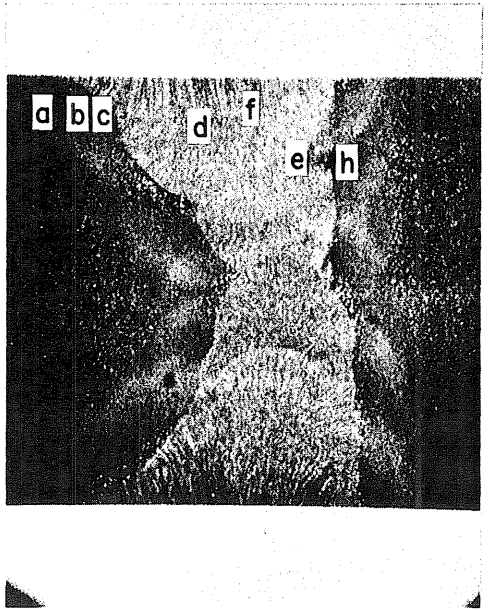


g) Photomacrograph
(3.2x)

h) Weld Metal - Coarsened slag
(53.6x)

Fig. A1.24 Photomacrograph and Photomicrographs of Specimen C1C. (2% Nital)

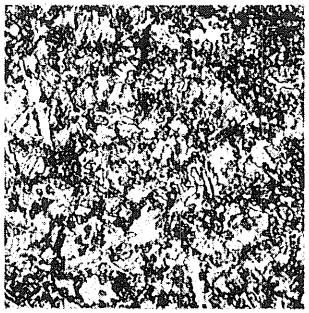

a) Spheroidized
(214.4x)

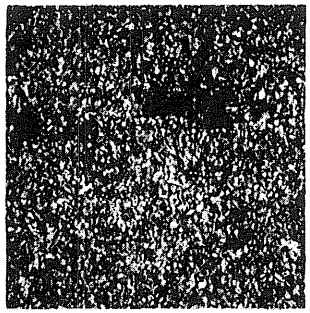

b) Refined
Lamellar inclusion
(214.4x)

c) Coarsened
(214.4x)

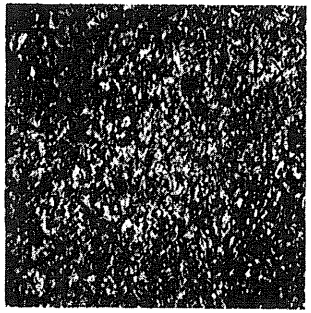

d) Weld Metal
Small inclusions
(214.4x)

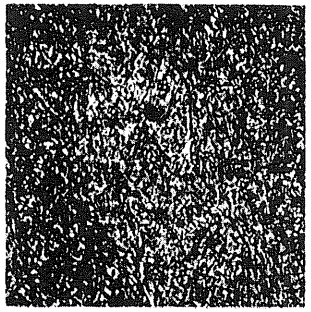

e) Weld Metal
Porosity
(214.4x)

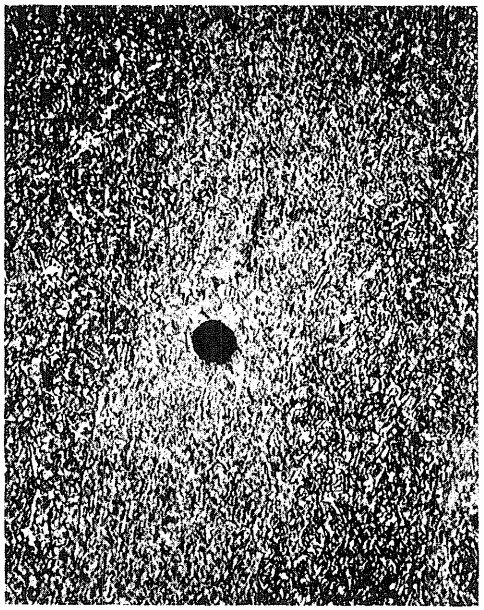

f) Weld Metal - Slag
(214.4x)

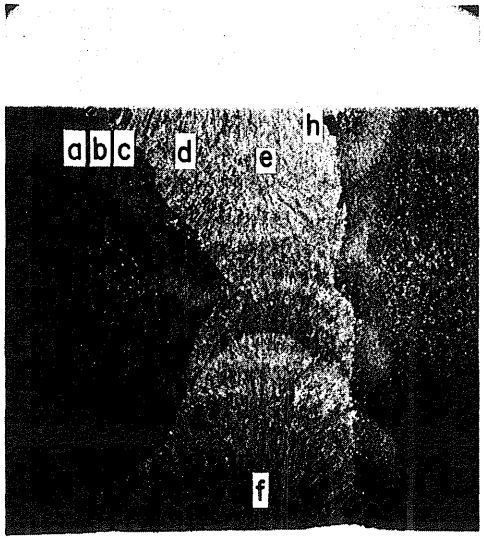


g) Photomacrograph
(3.2x)

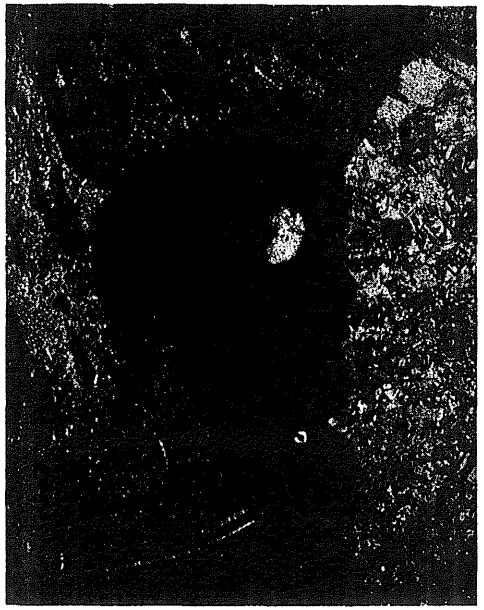

h) Weld Metal - Coarsened slag
(53.6x)

Fig. A1.25 Photomacrograph and Photomicrographs of Specimen C2A. (2% Nital)

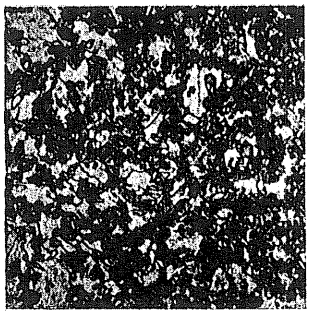

a) Spheroidized
(214.4x)

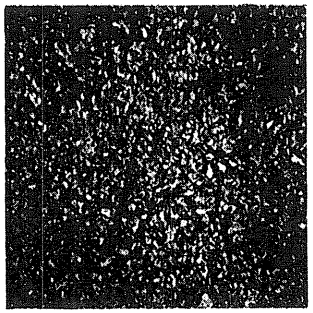

b) Refined
(214.4x)

c) Coarsened
Lamellar inclusions
(214.4x)

d) Weld Metal
Porosity
(214.4x)

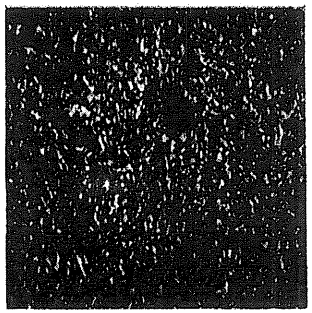

e) Weld Metal
Slag
(214.4x)

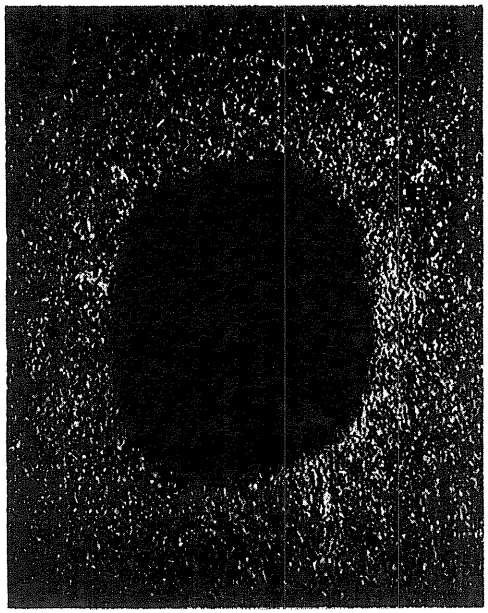

f) Retemepred - Porosity
(107.2x)

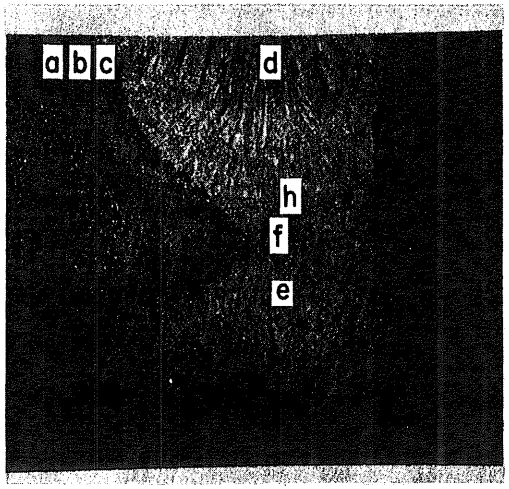


g) Photomacrograph
(3.2x)

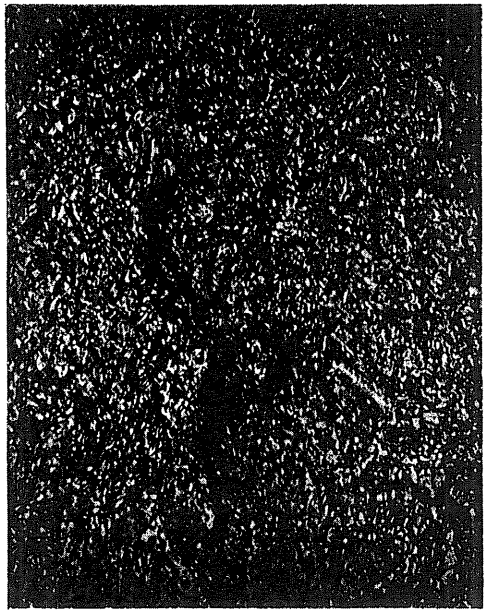

h) Weld Metal - Hot crack
(107.2x)

Fig. A1.26 Photomacrograph and Photomicrographs of Specimen C2B. (2% Nital)

a) Spheroidized
(214.4x)

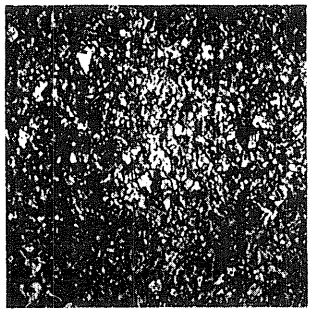

b) Refined
(214.4x)

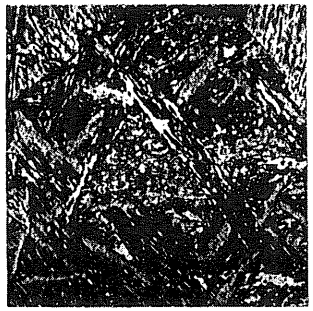

c) Coarsened
(214.4x)

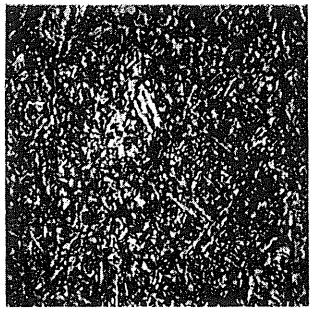

d) Weld Metal
(214.4x)

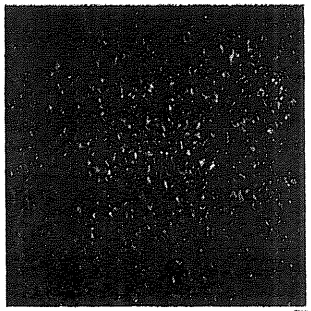

e) Weld Metal
Porosity
(214.4x)

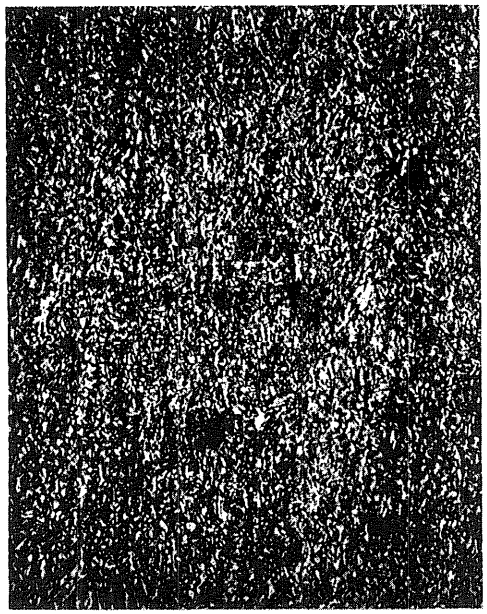

f) Weld Metal - Small inclusions
(214.4x)

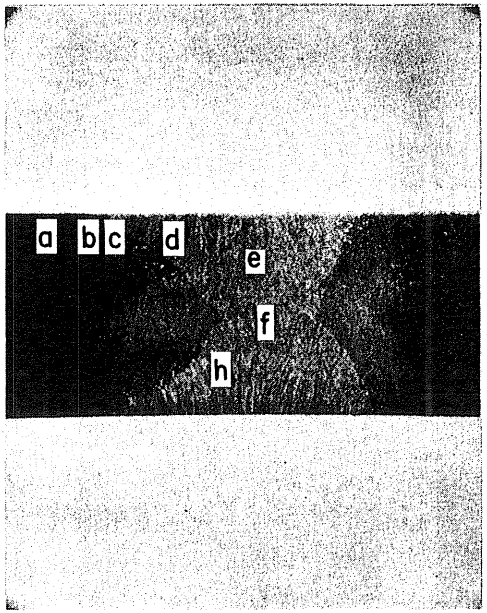


g) Photomacrograph
(3.2x)

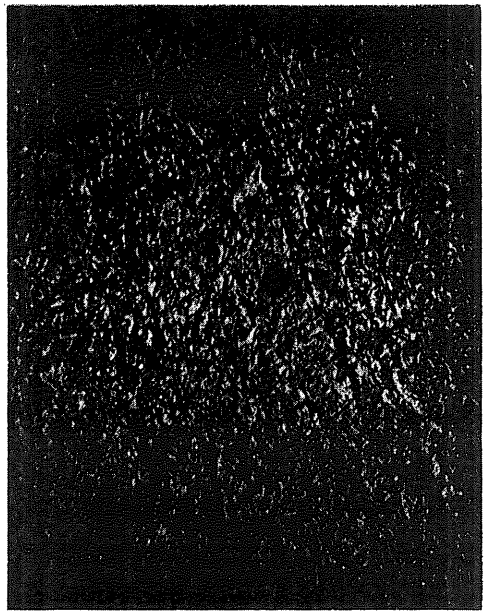

h) Weld Metal - Porosity
(214.4x)

Fig. A1.27 Photomacrograph and Photomicrographs of Specimen C3A. (2% Nital)

a) Spheroidized
(214.4x)

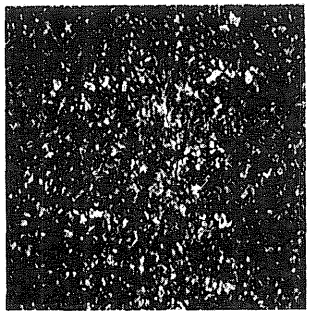

b) Refined
(214.4x)

c) Coarsened
(214.4x)

d) Weld Metal
(214.4x)

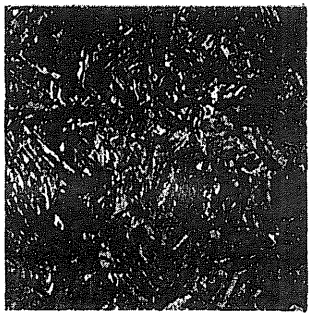

e) Coarsened
Lamellar inclusion
(214.4x)

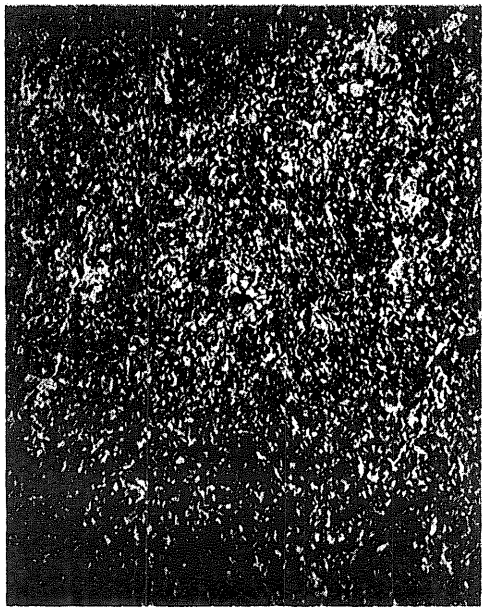

f) Weld Metal - Small inclusion
(214.4x)

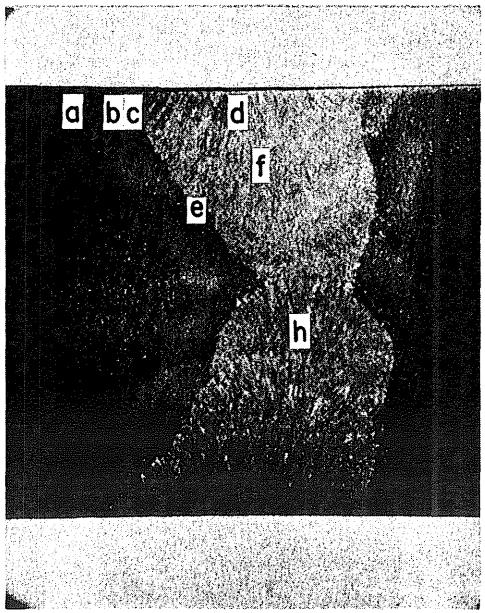


g) Photomacrograph
(3.2x)

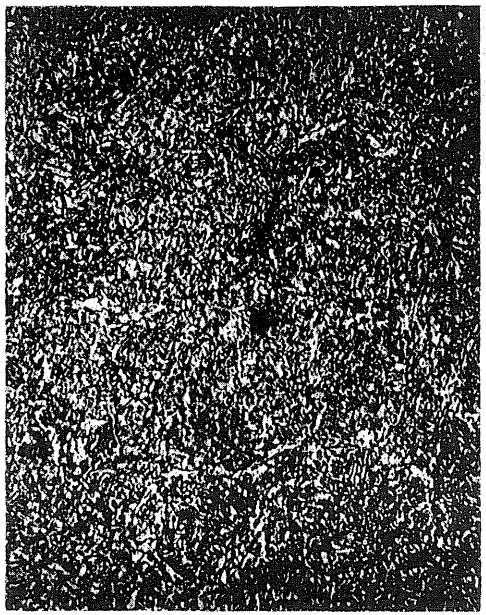

h) Weld Metal - Porosity
(214.4x)

Fig. A1.28 Photomacrograph and Photomicrographs of Specimen C3B. (2% Nital)

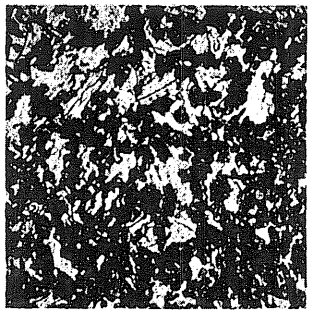

a) Spheroidized
(214.4x)

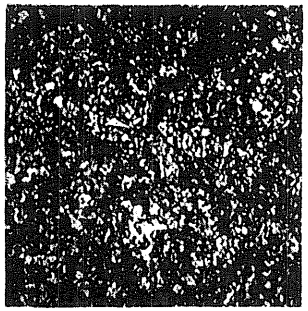

b) Refined
(214.4x)

c) Coarsened
(214.4x)

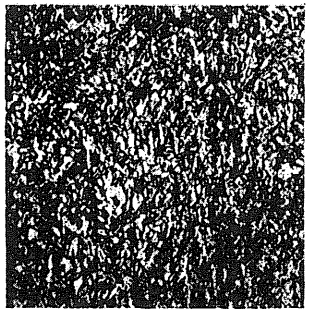

d) Weld Metal
Small inclusion
(214.4x)

e) Weld Metal
Porosity
(214.4x)

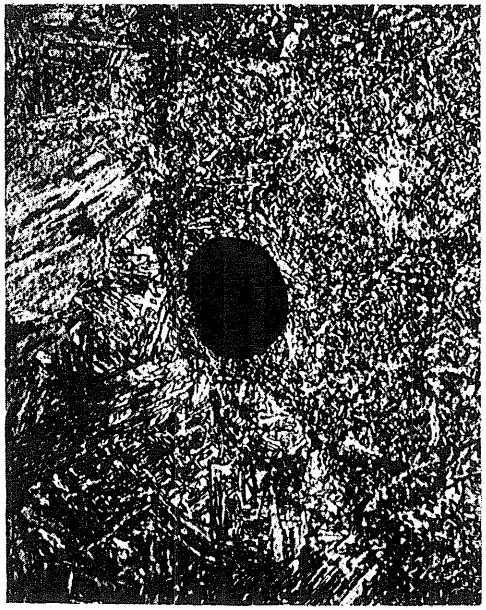

f) Weld Metal - Slag
(214.4x)

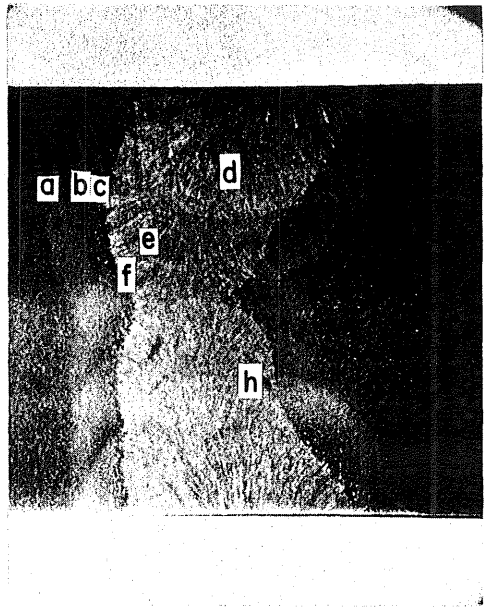


g) Photomacrograph
(3.2x)

h) Weld Metal - Slag
(107.2x)

Fig. A1.29 Photomacrograph and Photomicrographs of Specimen C3C. (2% Nital)

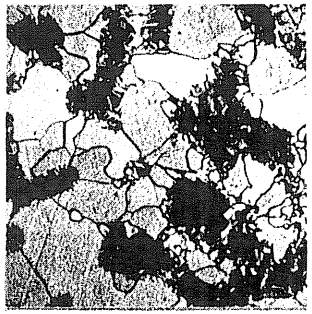

a) Spheroidized
(214.4x)

b) Refined
(214.4x)

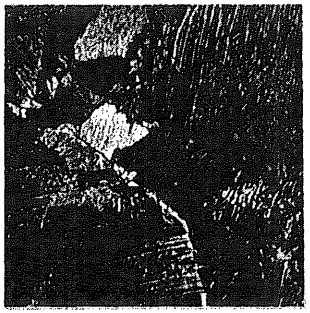

c) Coarsened
(214.4x)

d) Weld Metal
Microcrack
(214.4x)

e) Retempered
Mirocrack
(214.4x)

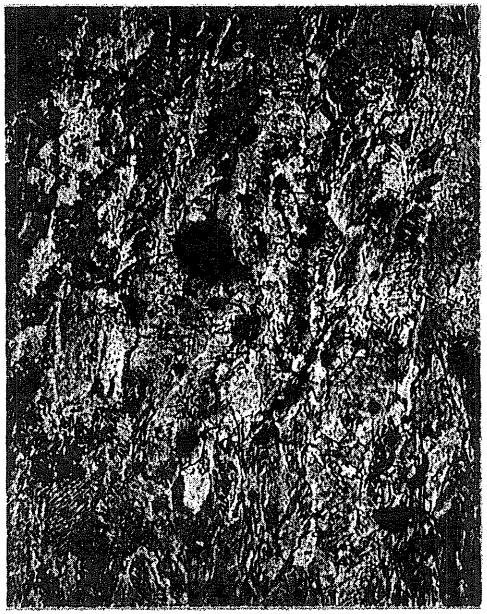

f) Weld Metal - Microcracks
(107.2x)

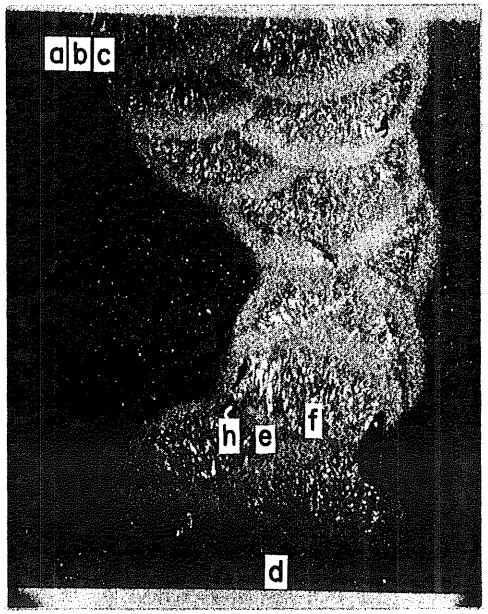


g) Photomcarograph
(3.2x)

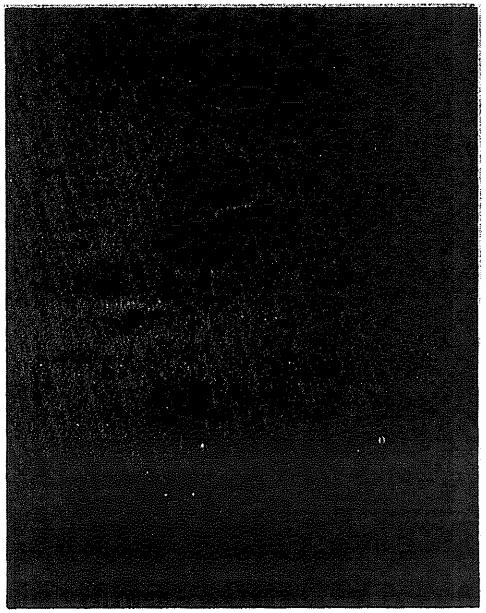

h) Crack tip - Unetched
(214.4x)

Fig. A1.30 Photomacrograph and Photomicrographs of Specimen D1A. (2% Nital)

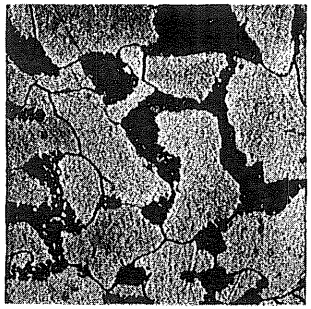

a) Spheroidized
(214.4x)

b) Refined
(214.4x)

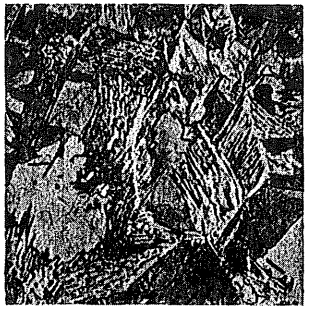

c) Coarsened
(214.4x)

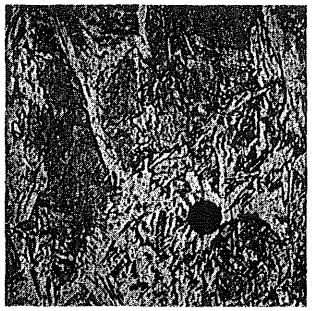

d) Weld Metal
Porosity
(214.4x)

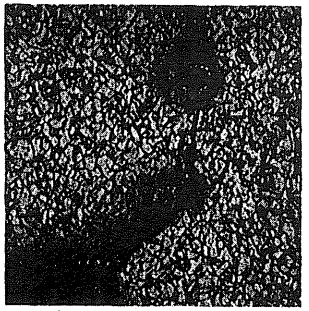

e) Retempered
Microcrack
(214.4x)

f) Weld Metal - Microcrack
(214.4x)

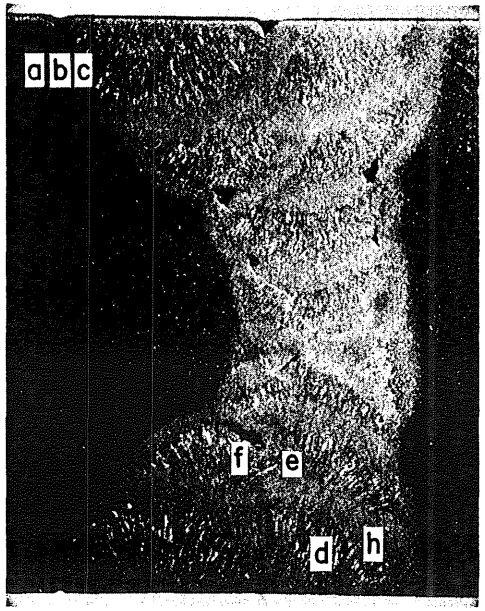


g) Photomacrograph
(3.2x)

h) Weld Metal - Slag
(107.2x)

Fig. A1.31 Photomacrograph and Photomicrographs of Specimen D1B. (2% Nital)

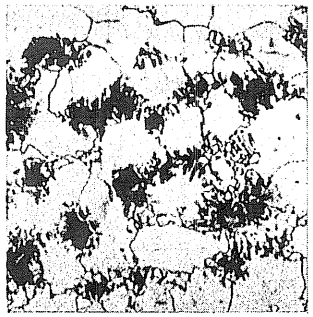

a) Spheroidized
(214.4x)

b) Refined
(214.4x)

c) Coarsened
(214.4x)

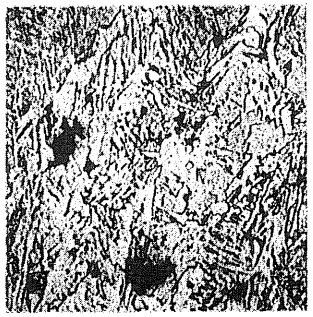

d) Weld Metal
Small inclusions
(214.4x)

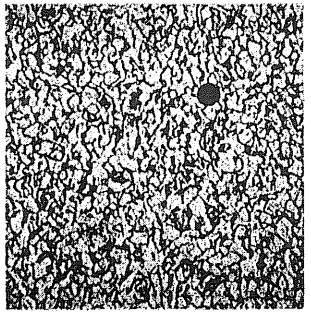

e) Retempered
Porosity
(214.4x)

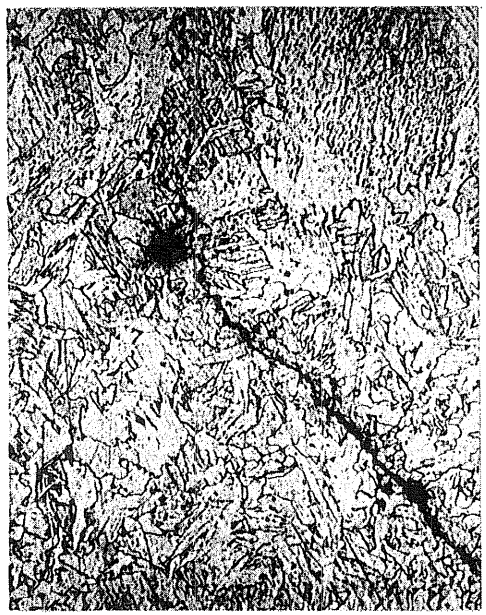

f) Crack Tip
(214.4x)

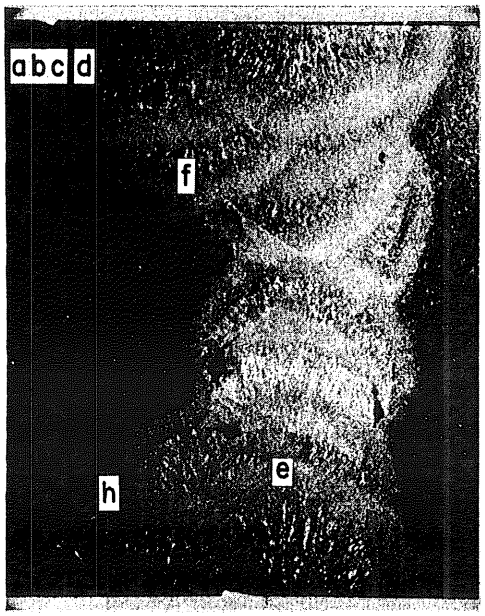


g) Photomacrograph
(3.2x)

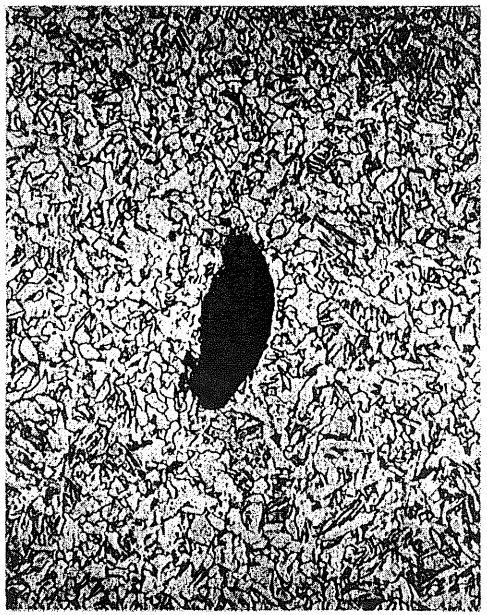

h) Retempered slag
(214.4x)

Fig. A1.32 Photomacrograph and Photomicrographs of Specimen D1C. (2% Nital)

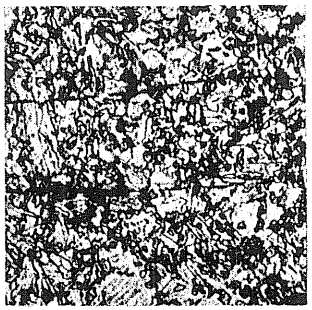

a) Spheroidized Lamellar inclusions (214.4x)

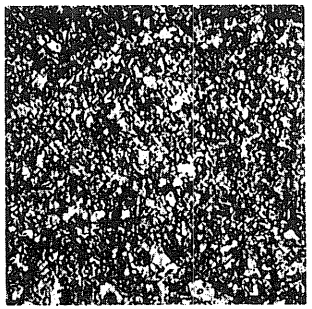

b) Refined (214.4x)

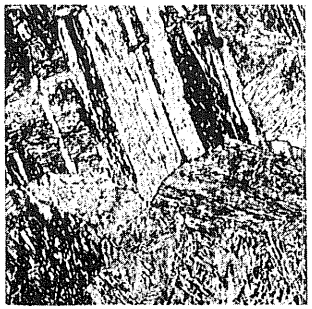

c) Coarsened (214.4x)

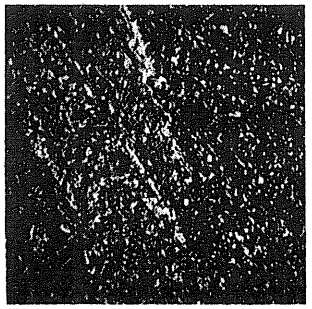

d) Weld Metal Porosity (214.4x)

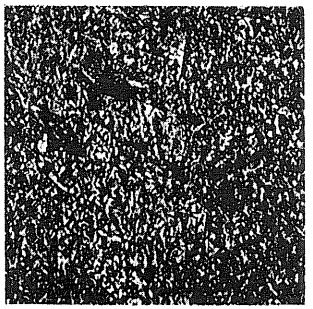

e) Weld Metal Small inclusions (214.4x)

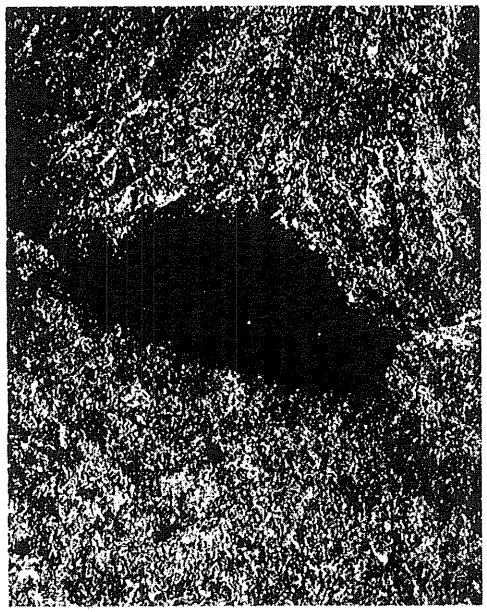

f) Weld Metal - Slag (53.6x)

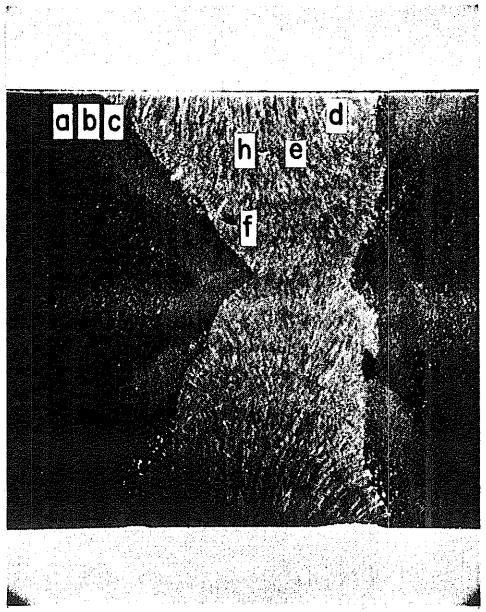


g) Photomacrograph (3.2x)

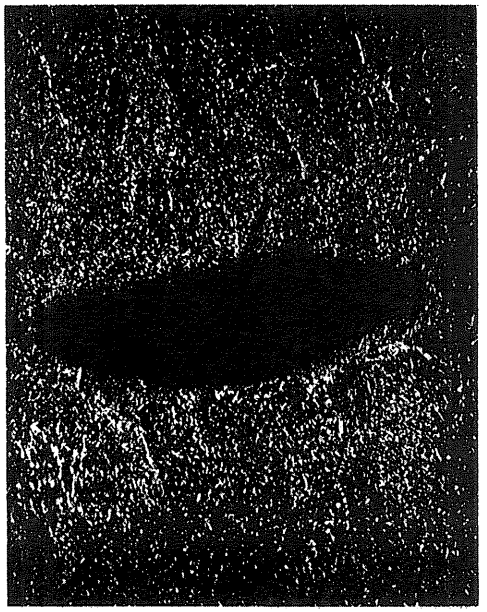

h) Weld Metal - LOF (107.2x)

Fig. A1.33 Photomacrograph and Photomicrographs of Specimen D2A. (2% Nital)

a) Spheroidized Lamellar inclusion (214.4x)

b) Refined Lamellar inclusion (214.4x)

c) Coarsened Lamellar inclusions (214.4x)

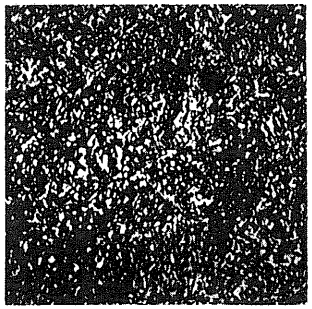

d) Weld Metal Porosity (214.4x)

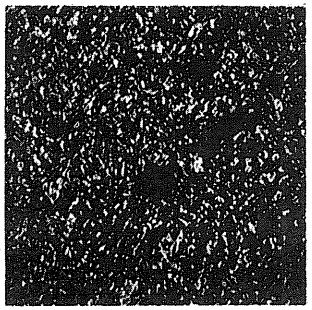

e) Weld Metal Small inclusions (214.4x)

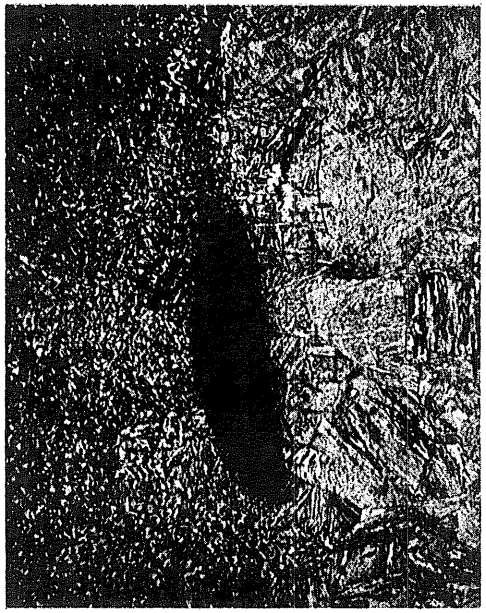

f) Weld Metal - Coarsened slag (214.4x)

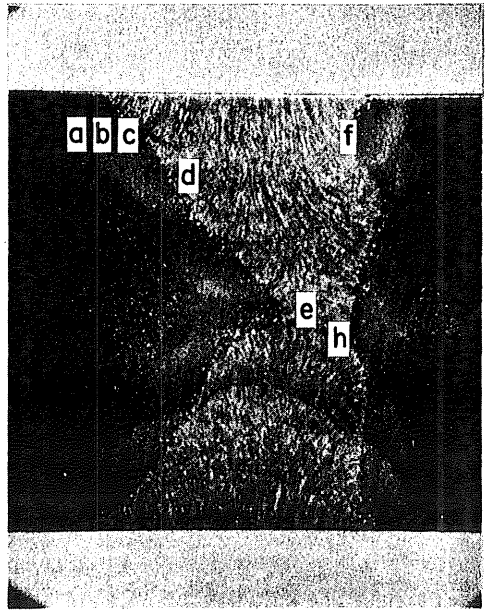


g) Photomacrograph (3.2x)

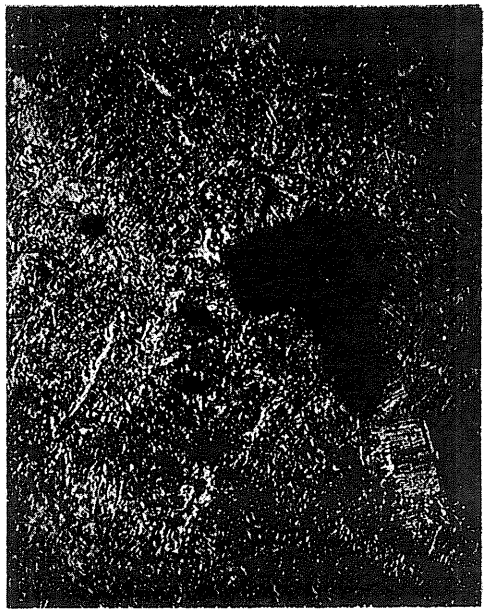

h) Weld Metal - Coarsened slag (107.2x)

Fig. A1.34 Photomacrograph and Photomicrographs of Specimen D2B. (2% Nital)

a) Spheroidized
(214.4x)

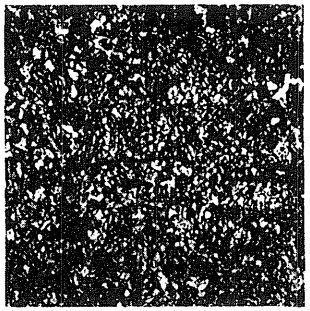

b) Refined
Lamellar inclusion
(214.4x)

c) Coarsened
(214.4x)

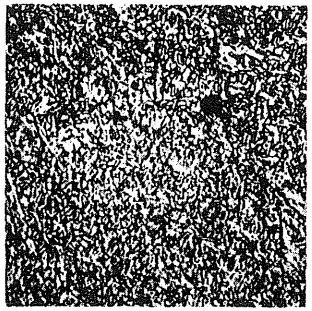

d) Weld Metal
Porosity
(214.4x)

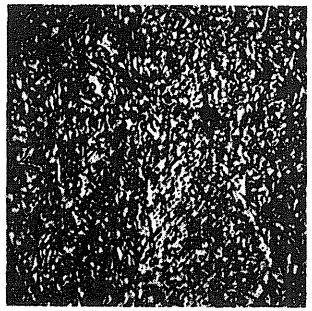

e) Weld Metal
Small inclusion
(214.4x)

f) Enlargement of photo h - Hot crack
(214.4x)

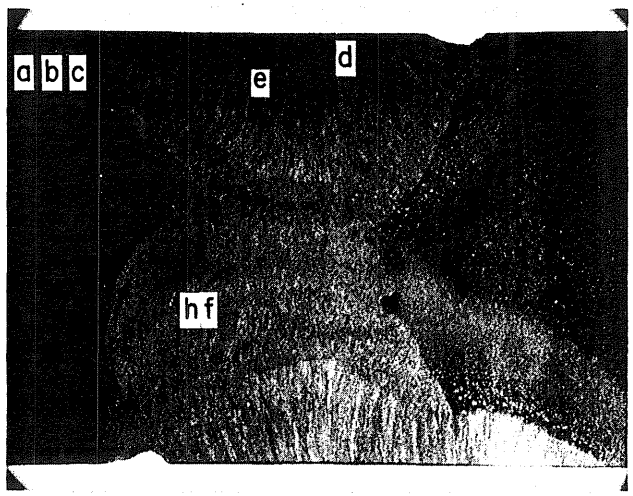


g) Photomacrograph
(3.2x)

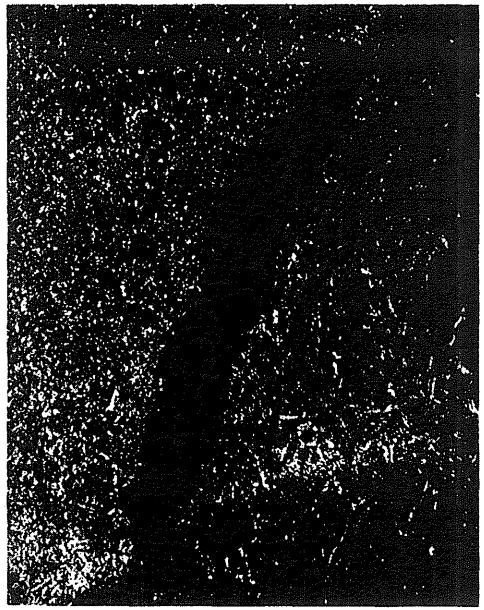

h) Weld Metal - Hot crack
(53.6x)

Fig. A1.35 Photomacrograph and Photomicrographs of Specimen D2C. (2% Nital)

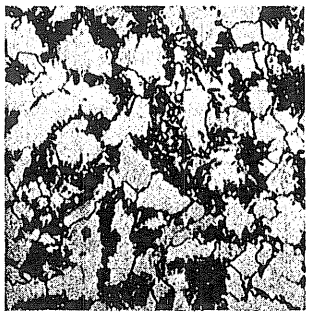

a) Spheroidized (214.4x)

b) Refined inclusion (214.4x)

c) Coarsened (214.4x)

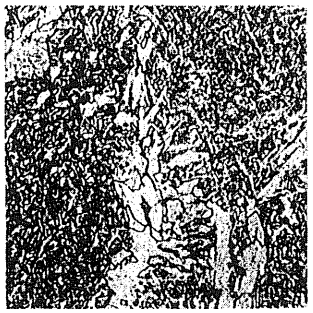

d) Weld Metal (214.4x)

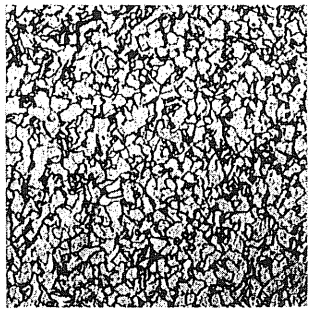

e) Retempered (214.4x)

f) Weld Metal - Porosity (214.4x)

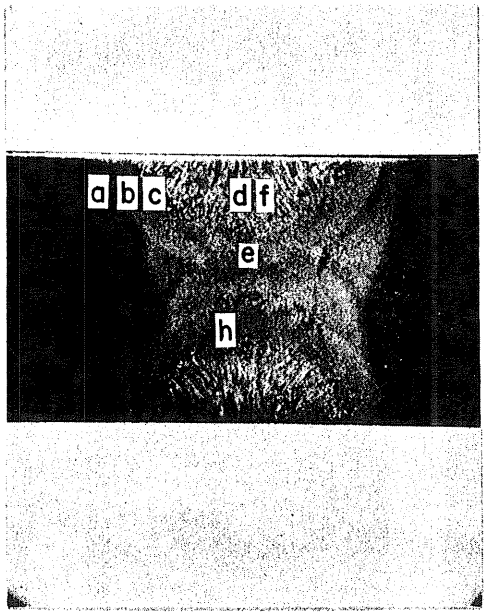


g) Photomacrograph (3.2x)

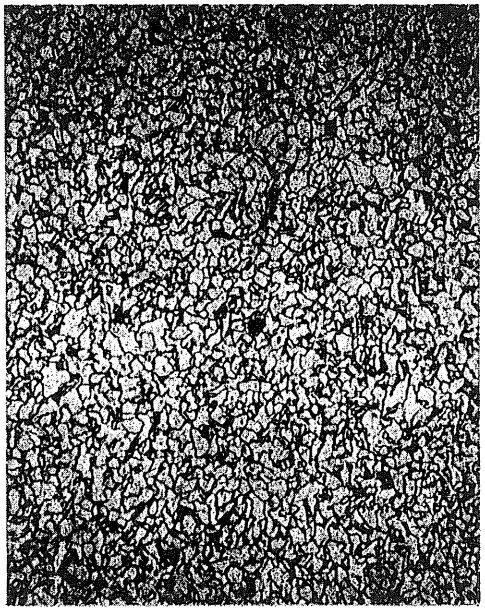

h) Retempered - Small inclusion (214.4x)

Fig. A1.36 Photomacrograph and Photomicrographs of Specimen D3A. (2% Nital)

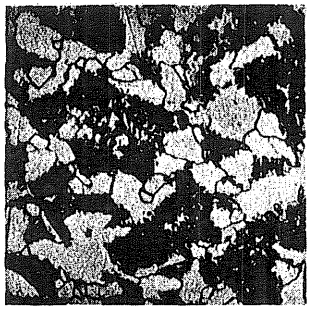

a) Spheroidized
(214.4x)

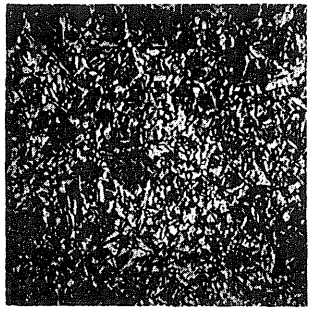

b) Refined
(214.4x)

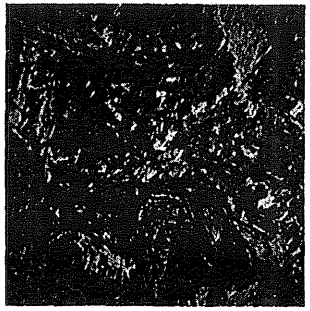

c) Coarsened
(214.4x)

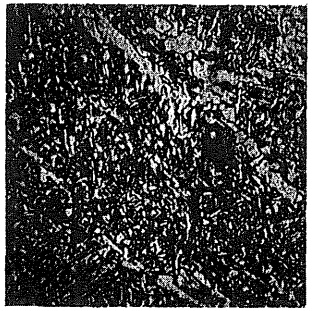

d) Weld Metal
Small inclusion
(214.4x)

e) Retempered
Small inclusion
(214.4x)

f) Weld Metal - Crack tip
(214.4x)

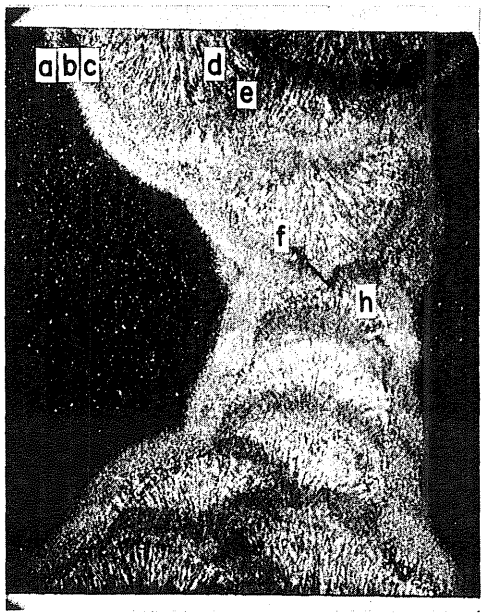


g) Photomacrograph
(3.2x)

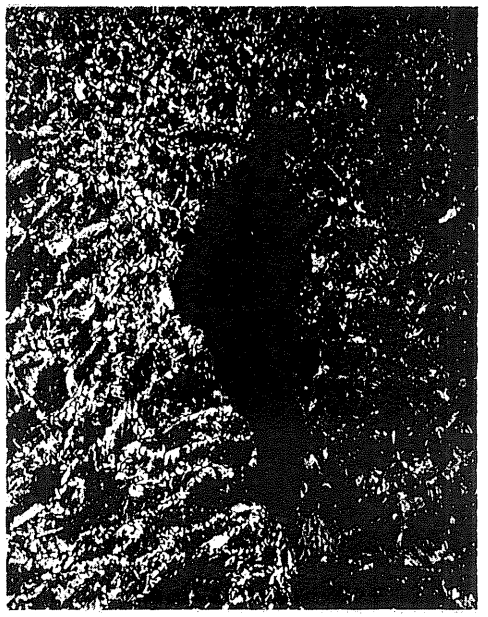

h) Weld Metal - Coarsened LOF
(107.2x)

Fig. A1.37 Photomacrograph and Photomicrographs of Specimen D3B. (2% Nital)

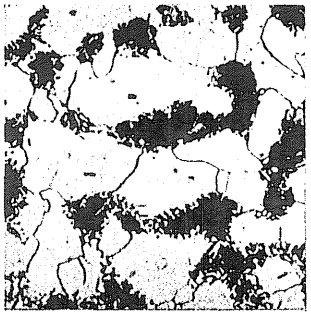

a) Spheroidized
(214.4x)

b) Refined
(214.4x)

c) Coarsened
(214.4x)

d) Weld Metal
Small inclusions
(214.4x)

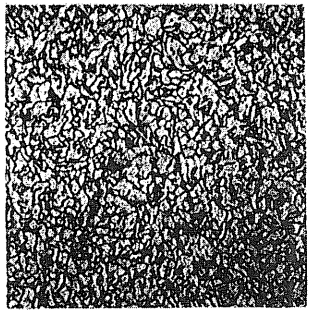

e) Retempered
(214.4x)

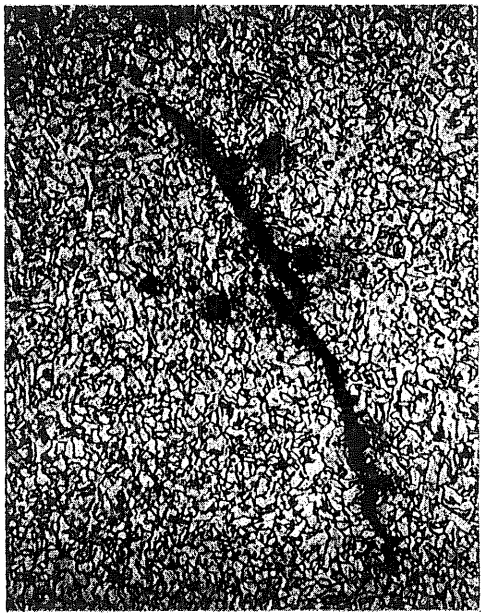

f) Retempered - Microcrack
(214.4x)

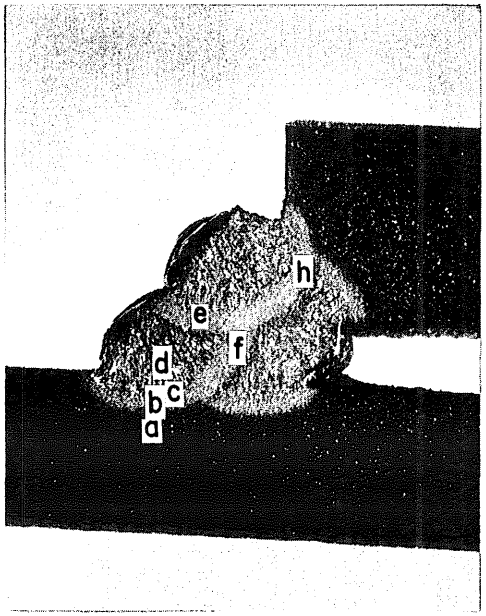


g) Photomacrograph
(3.2x)

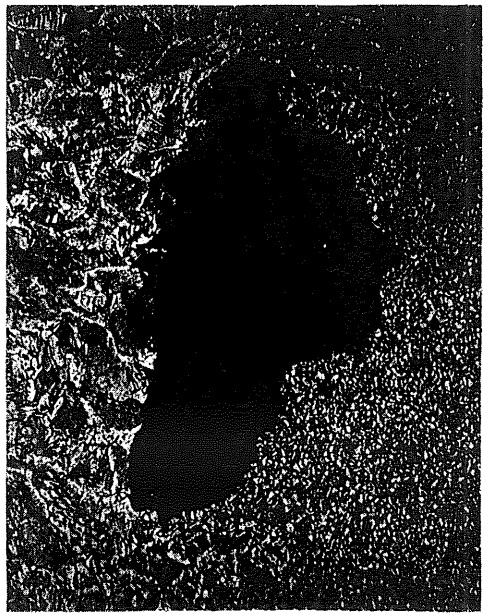

h) Weld Metal - Retempered slag
(107.2x)

Fig. A1.38 Photomacrograph and Photomicrographs of Specimen E1A. (2% NItal)

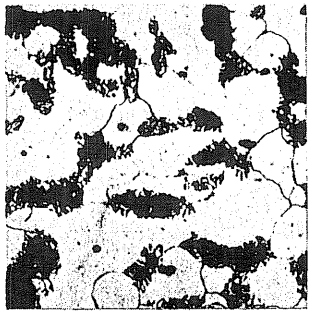

a) Spheroidized
(214.4x)

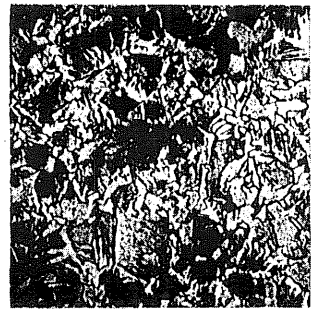

b) Refined
(214.4x)

c) Coarsened
(214.4x)

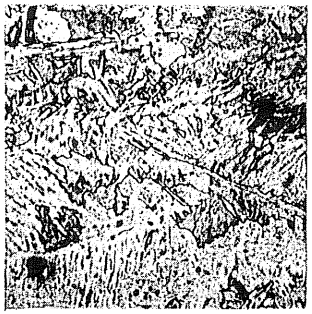

d) Weld Metal
Small inclusions
(214.4x)

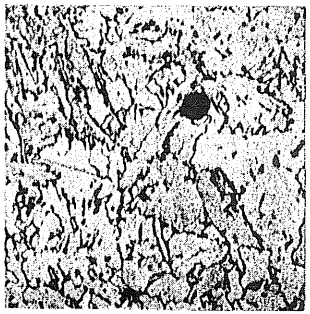

e) Retempered
Porosity
(214.4x)

f) Weld Metal - Microcrack
(214.4x)

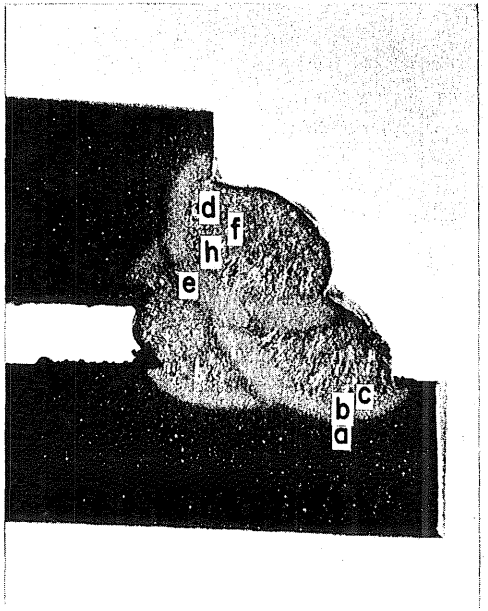


g) Photomacrograph
(3.2x)

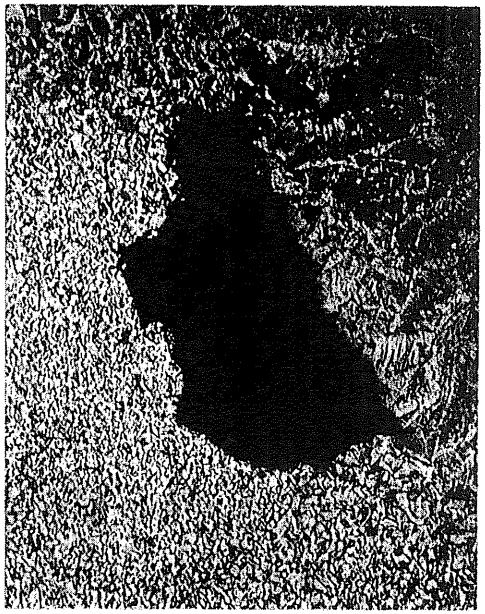

h) Weld Metal - Retempered slag
(107.2x)

Fig. A1.39 Photomacrograph and Photomicrographs of Specimen F1A. (2% Nital)

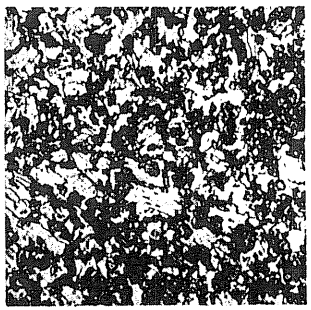

a) Spheroidized
(214.4x)

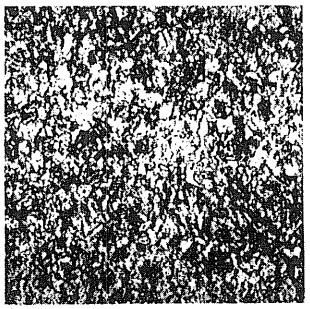

b) Refined
(214.4x)

c) Coarsened
(214.4x)

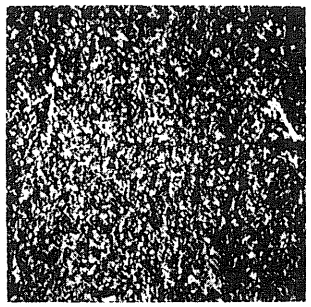

d) Weld Metal
(214.4x)

e) Weld Metal
Small inclusions
(214.4x)

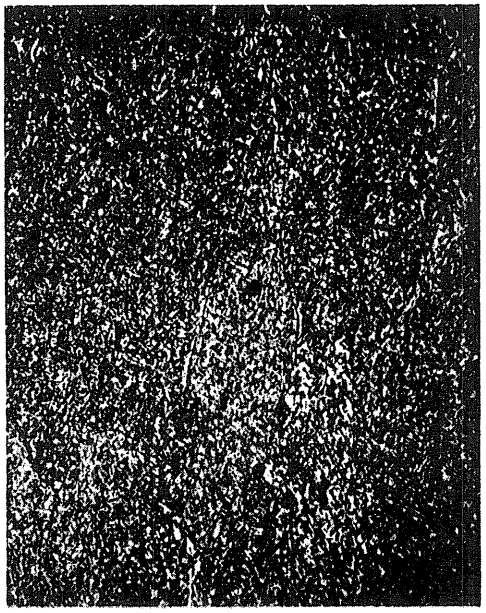

f) Weld Metal - Porosity
(214.4x)

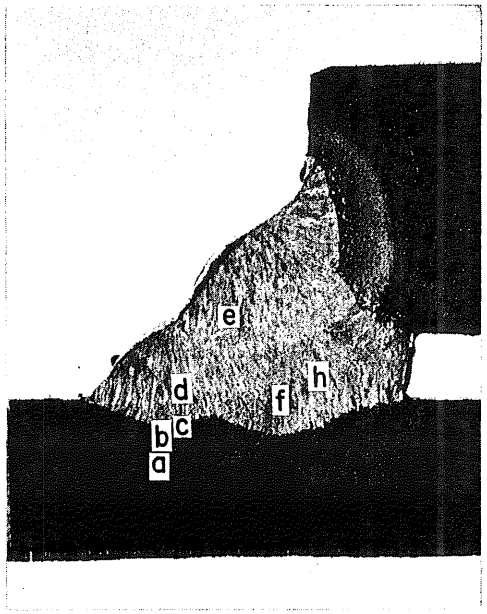


g) Photomacrograph
(3.2x)

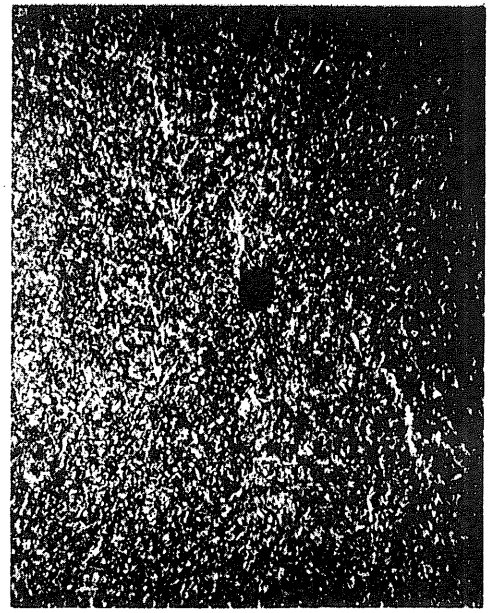

h) Weld Metal - Porosity
(214.4x)

Fig. A1.40 Photomacrograph and Photomicrographs of Specimen E2A. (2% Nital)

a) Spheroidized Lamellar inclusions (214.4x)

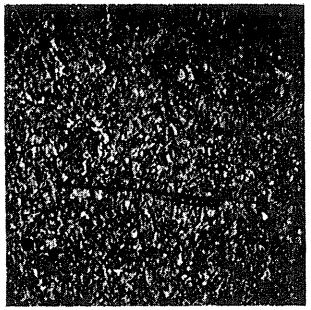

b) Refined Lamellar inclusion (214.4x)

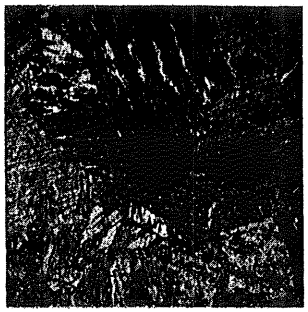

c) Coarsened Lamellar inclusion (214.4x)

d) Weld Metal Small inclusion (214.4x)

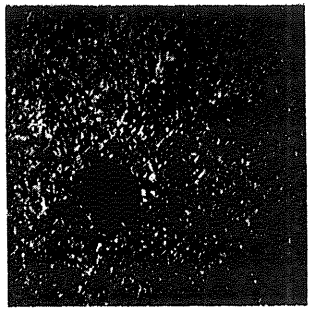

e) Weld Metal Porosity (214.4x)

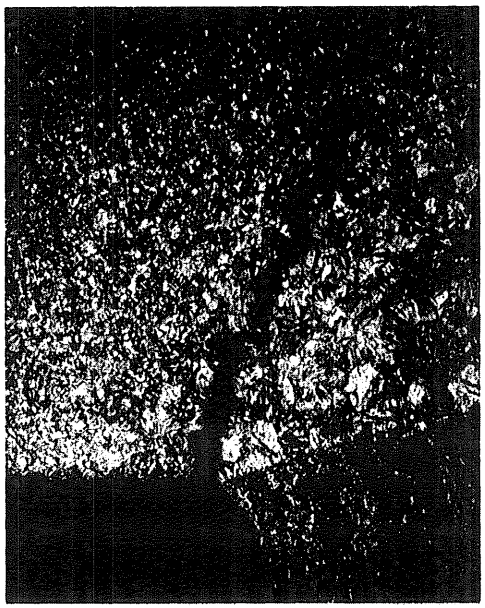

f) Coarsened - HAZ Crack (53.6x)

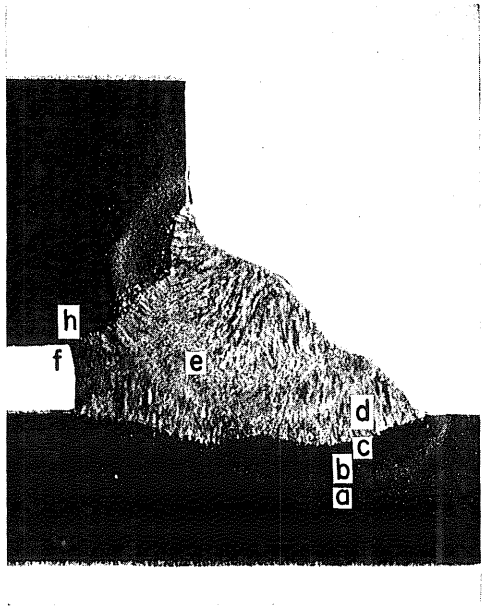


g) Photomacrograph (3.2x)

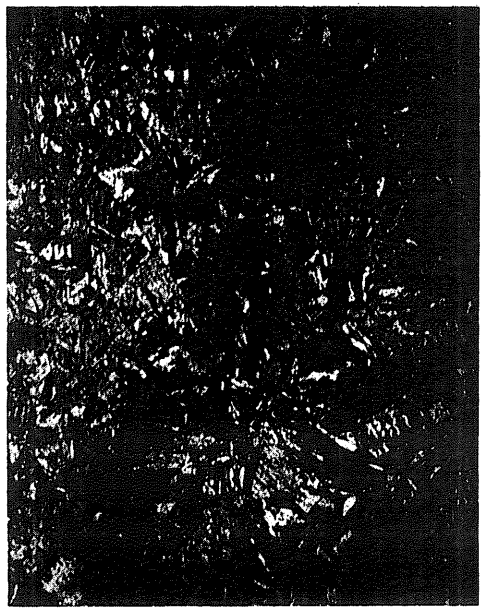

h) Tip of crack in photo f (214.4x)

Fig. A1.41 Photomacrograph and Photomicrographs of Specimen F2A. (2% Nital)

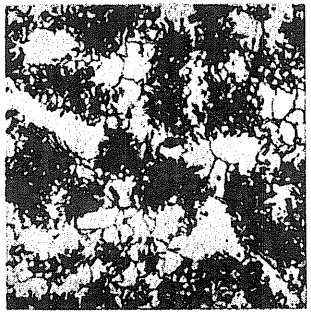

a) Spheroidized
(214.4x)

b) Refined
(214.4x)

c) Coarsened
(214.4x)

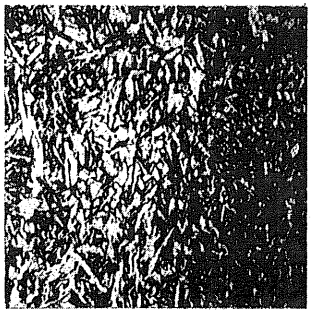

d) Weld Metal
(214.4x)

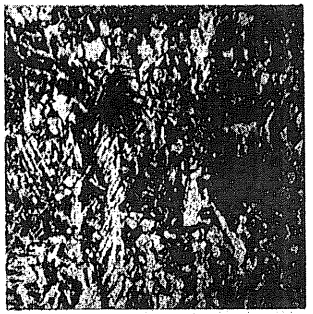

e) Weld Metal
Small inclusions
(214.4x)

f) Weld Metal - Slag
(214.4x)

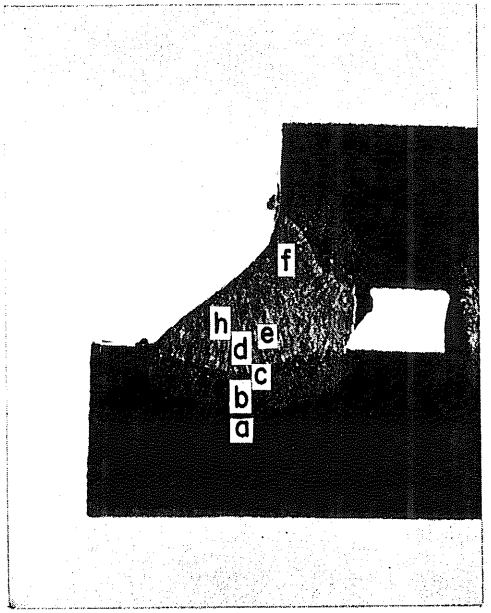


g) Photomacrograph
(3.2x)

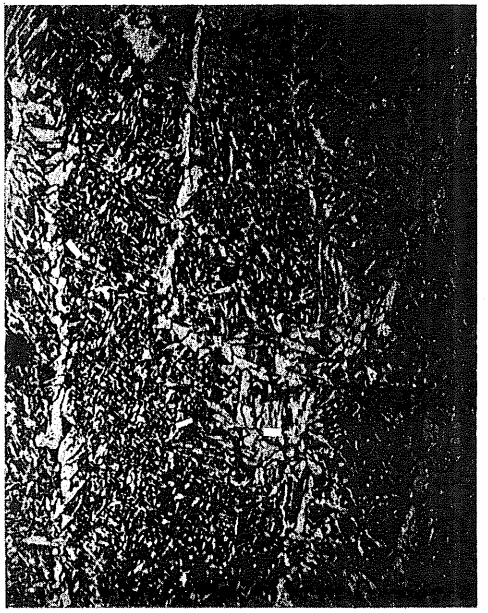

h) Weld Metal - Porosity
(214.4x)

Fig. A1.42 Photomacrograph and Photomicrographs of Specimen E3A. (2% Nital)

a) Spheroidized (214.4x)



b) Refined (214.4x)



c) Coarsened (214.4x)



d) Weld Metal (214.4x)



e) Coarsened Small inclusions (214.4x)



f) Weld Metal - Small inclusion (214.4x)




g) Photomacrograph (3.2x)



h) Weld Metal - Porosity (214.4x)

Fig. A1.43 Photomacrograph and Photomicrographs of Specimen F3A. (2% Nital)

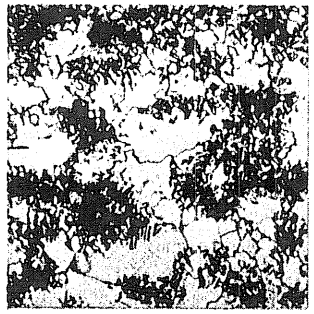

a) Spheroidized
(214.4x)

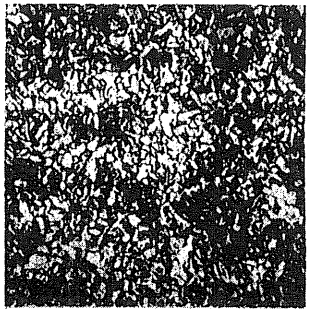

b) Refined
(214.4x)

c) Coarsened
(214.4x)

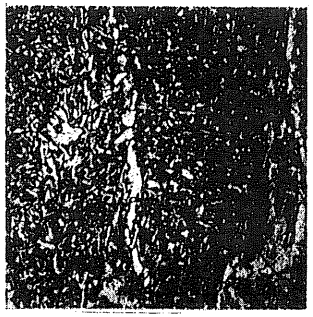

d) Weld Metal
(214.4x)

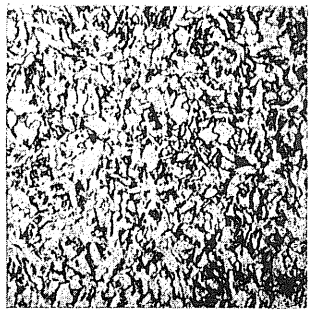

e) Retempered
(214.4x)

f) Weld Metal - Porosity
(214.4x)

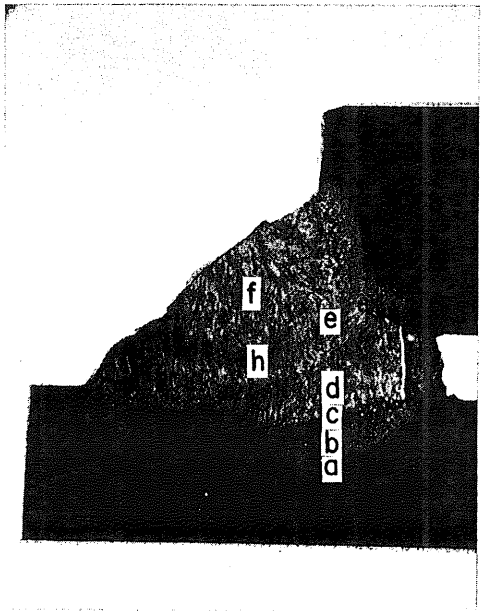


g) Photomacrograph
(3.2x)

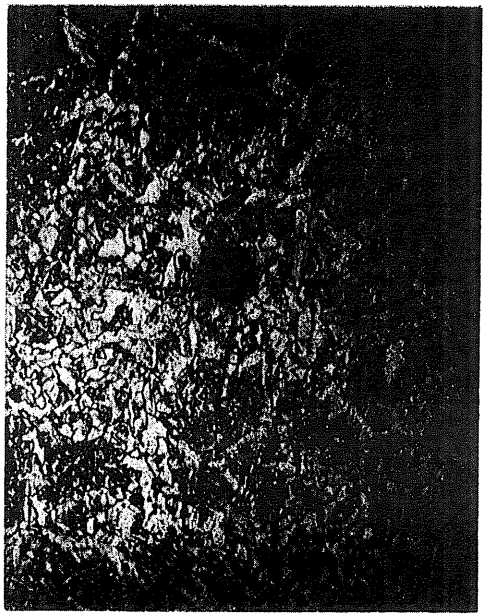

h) Retempered slag
(214.4x)

Fig. A1.44 Photomacrograph and Photomicrographs of Specimen E3B. (2% Nital)

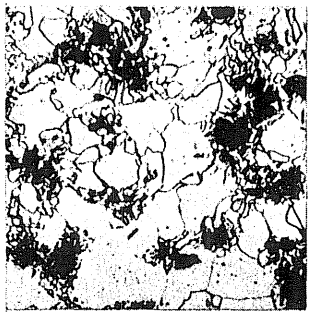

a) Spheroidized
(214.4x)

b) Refined
(214.4x)

c) Coarsened
(214.4x)

d) Weld Metal
(214.4x)

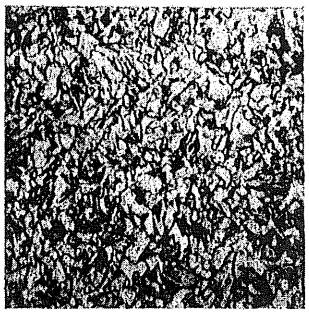

e) Retempered
(214.4x)

f) Weld Metal - Porosity
(214.4x)

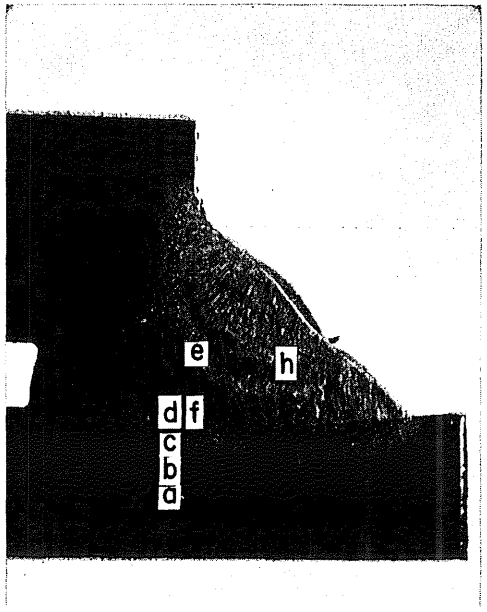


g) Photomacrograph
(3.2x)

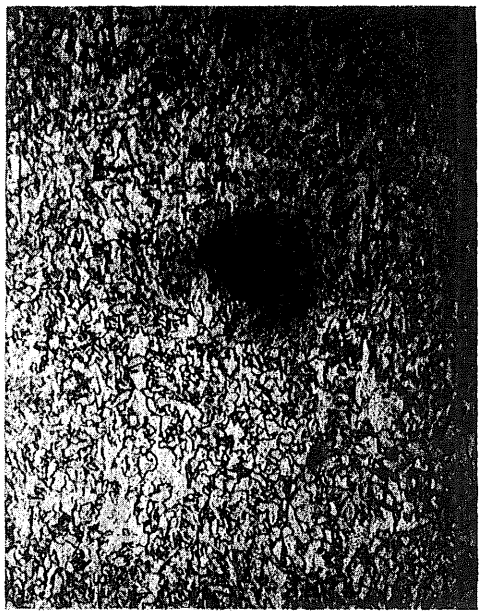

h) Retempered slag
(214.4x)

Fig. A1.45 Photomacrograph and Photomicrographs of Specimen F3B. (2% Nital)

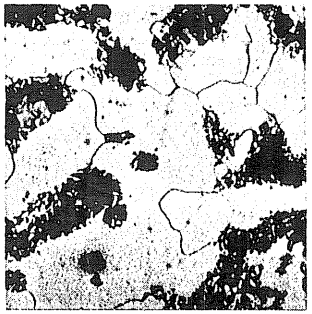

a) Spheroidized
(214.4x)

b) Refined
(214.4x)

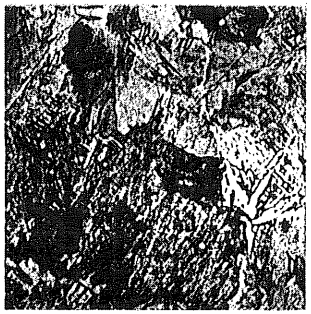

c) Coarsened
(214.4x)

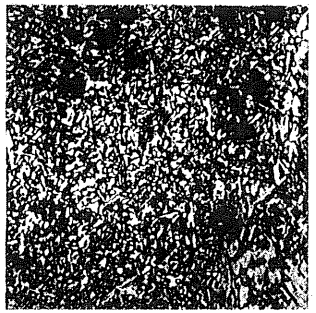

d) Weld Metal
Small inclusions
(214.4x)

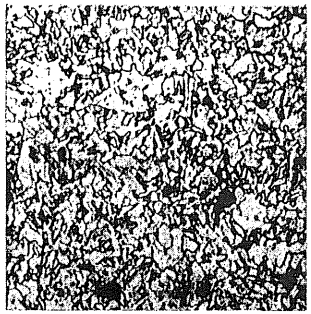

e) Retempered
Small inclusions
(214.4x)

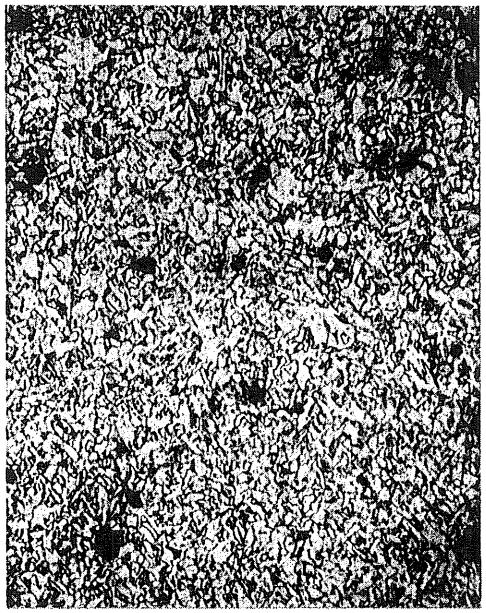

f) Retempered - Small inclusions
(214.4x)

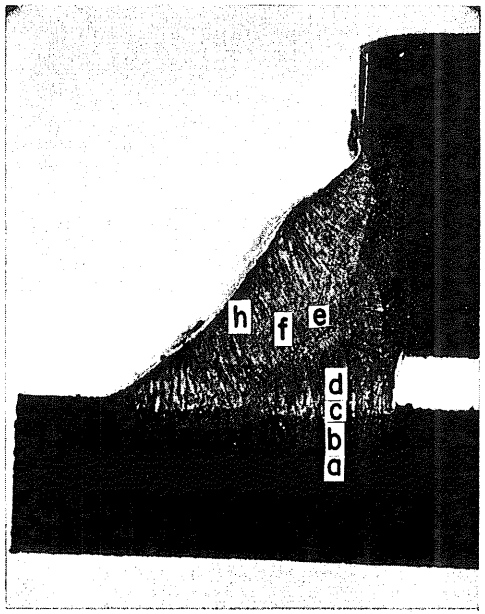


g) Photomacrograph
(3.2x)

h) Weld metal - Slag
Small inclusions
(214.4x)

Fig. A1.46 Photomacrograph and Photomicrographs of Specimen E4A. (2% Nital)

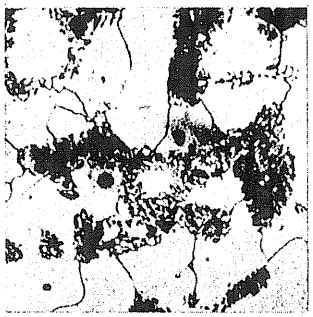

a) Spheroidized
(214.4x)

b) Refined
(214.4x)

c) Coarsened
(214.4x)

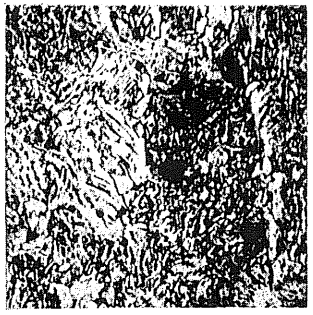

d) Weld Metal
Small inclusions
(214.4x)

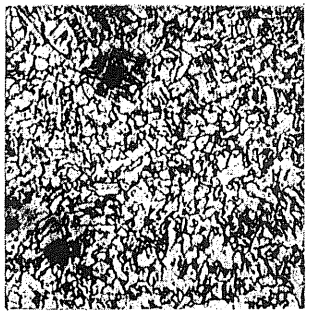

e) Retempered
Small inclusions
(214.4x)

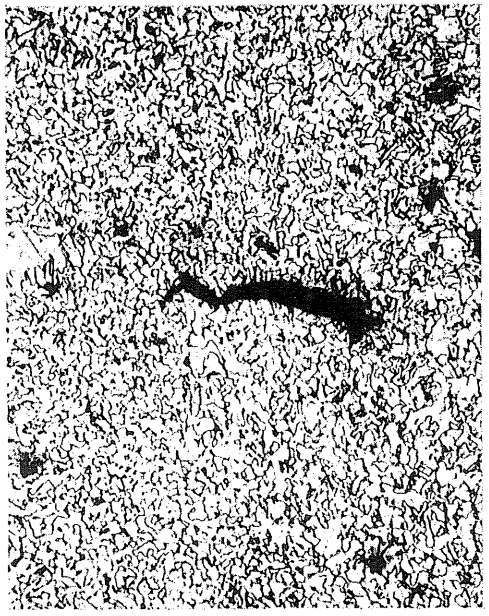

f) Retempered - Hot crack
(214.4x)

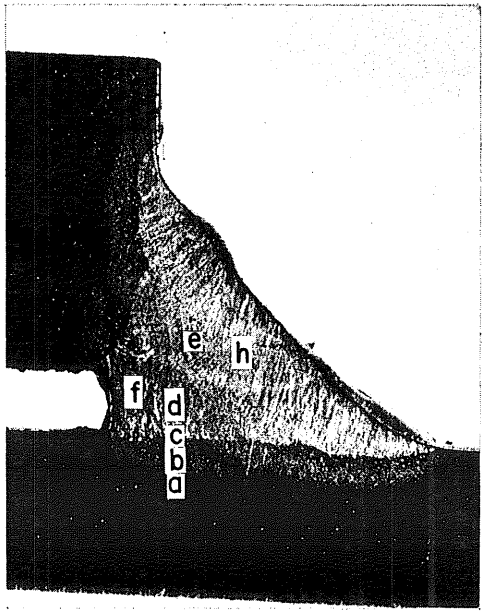


g) Photomacrograph
(3.2x)

h) Weld Metal - Slag
Small inclusions
(214.4x)

Fig. A1.47 Photomacrograph and Photomicrographs of Specimen F4A. (2% Nital)

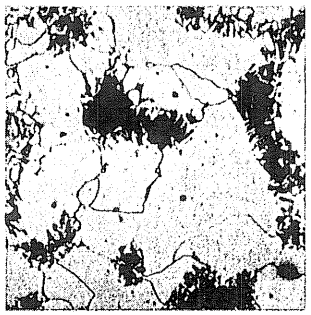

a) Spheroidized
(214.4x)

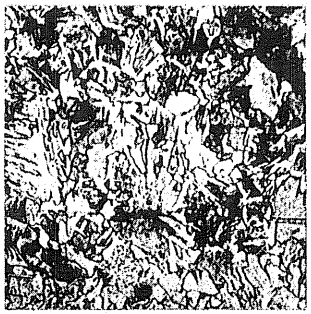

b) Refined
(214.4x)

c) Coarsened
(214.4x)

d) Weld Metal - Slag
Small inclusions
(214.4x)

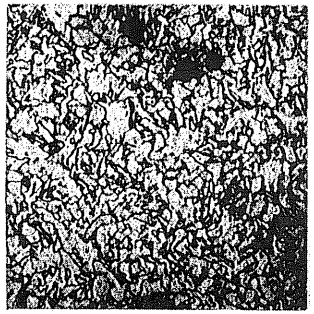

e) Retempered
Small inclusions
(214.4x)

f) Weld Metal - Hot crack
(53.6x)

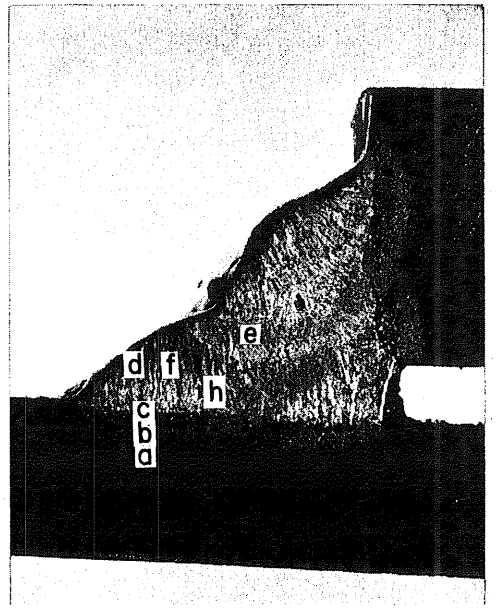


g) Photomacrograph
(3.2x)

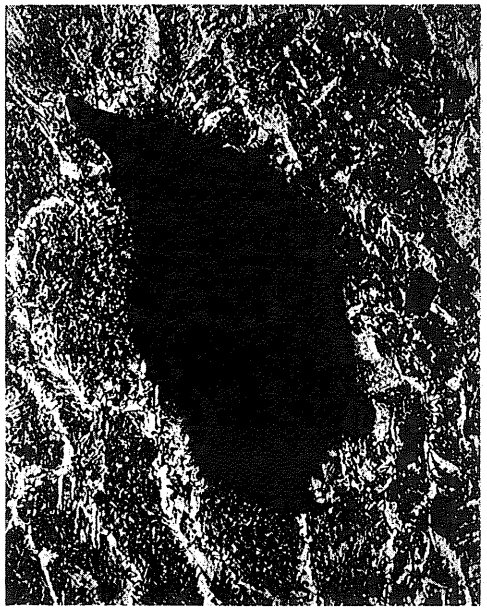

h) Weld Metal - LOF
(107.2x)

Fig. A1.48 Photomacrograph and Photomicrographs of Specimen E4B. (2% Nital)

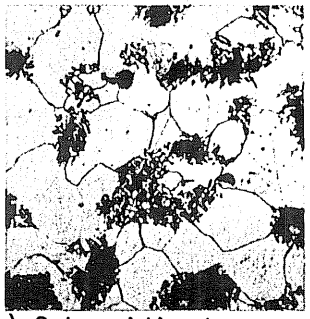

a) Spheroidized
(214.4x)

b) Refined
(214.4x)

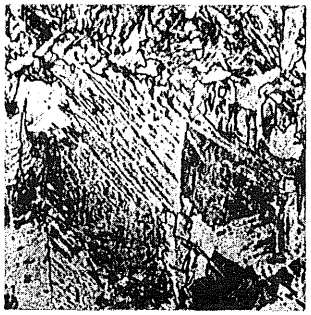

c) Coarsened
(214.4x)

d) Weld Metal
Porosity
(214.4x)

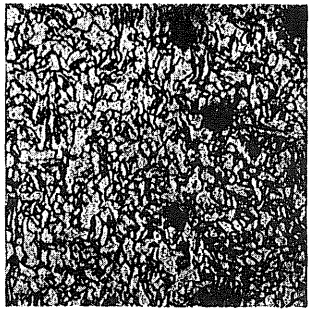

e) Retempered
Small inclusions
(214.4x)

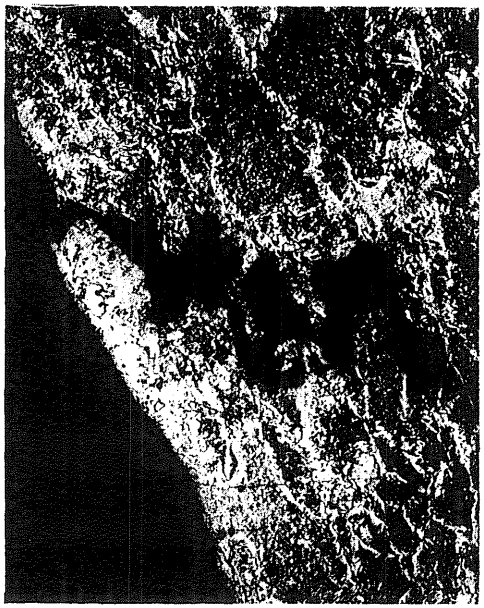

f) Weld Metal - Hot crack
(53.6x)

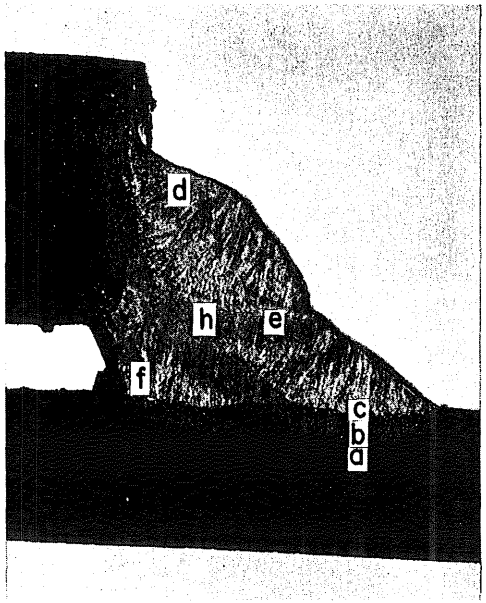


g) Photomacrograph
(3.2x)

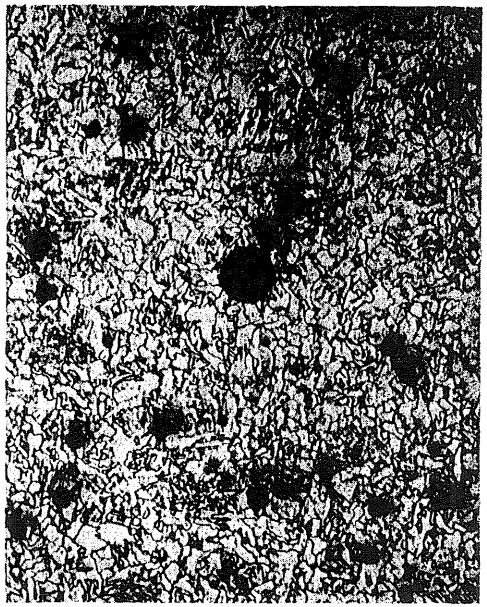

h) Retempered slag
Small inclusions
(214.4x)

Fig. A1.49 Photomacrograph and Photomicrographs of Specimen F4B. (2% Nital)

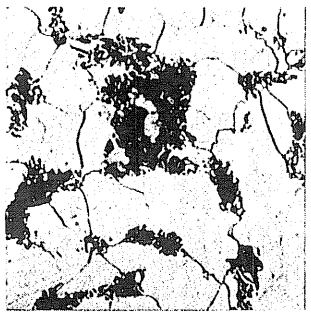

a) Spheroidized
(214.4x)

b) Refined
(214.4x)

c) Coarsened
(214.4x)

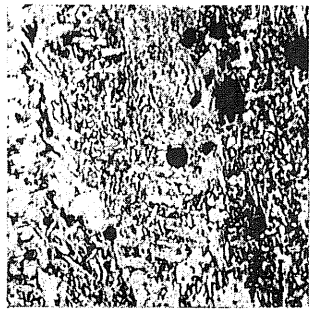

d) Weld Metal - Slag
Small inclusions
(214.4x)

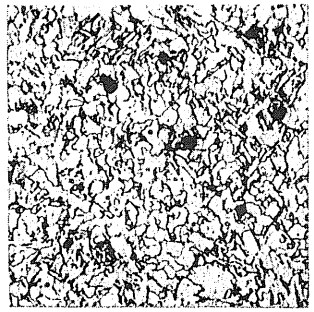

e) Retempered
Small inclusions

f) Weld Metal - Hot crack
(107.2x)

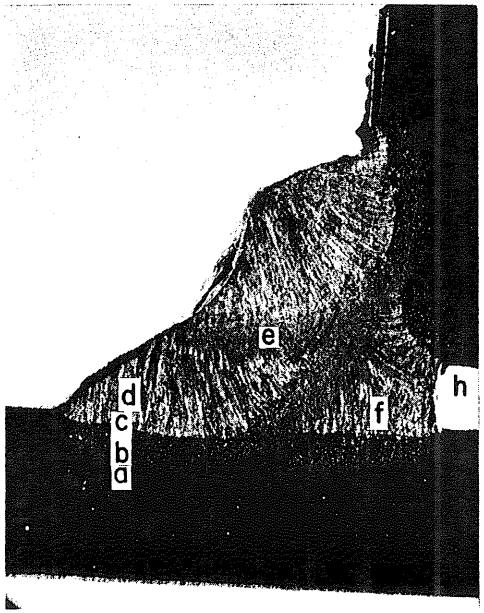


g) Photomacrograph
(3.2x)

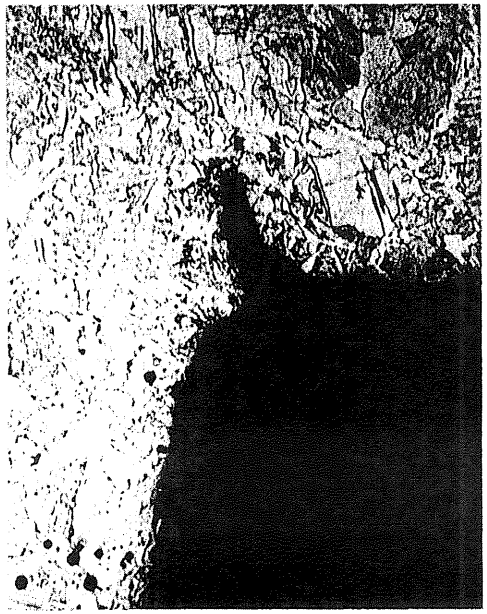

h) Weld Metal - Coarsened
Hot crack
(214.4x)

Fig. A1.50 Photomacrograph and Photomicrographs of Specimen E4C. (2% Nital)

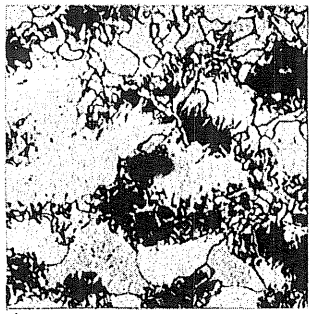

a) Spheroidized
(214.4x)

b) Refined
(214.4x)

c) Coarsened
(214.4x)

d) Weld Metal
Small inclusions
(214.4x)

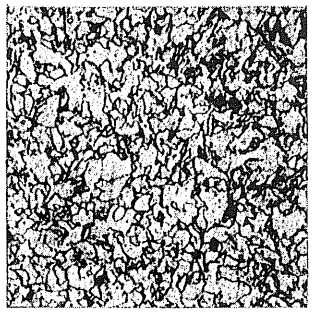

e) Retempered
(214.4x)

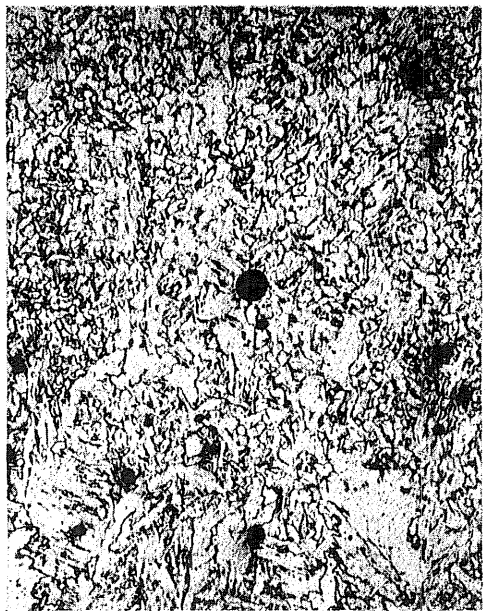

f) Retempered slag
Small inclusions
(214.4x)

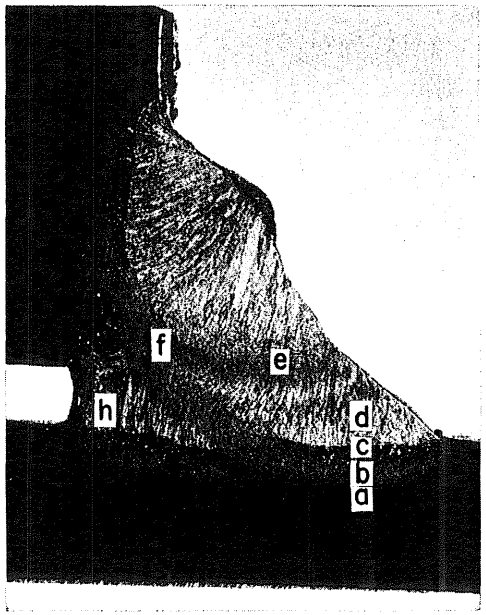


g) Photomacrograph
(3.2x)

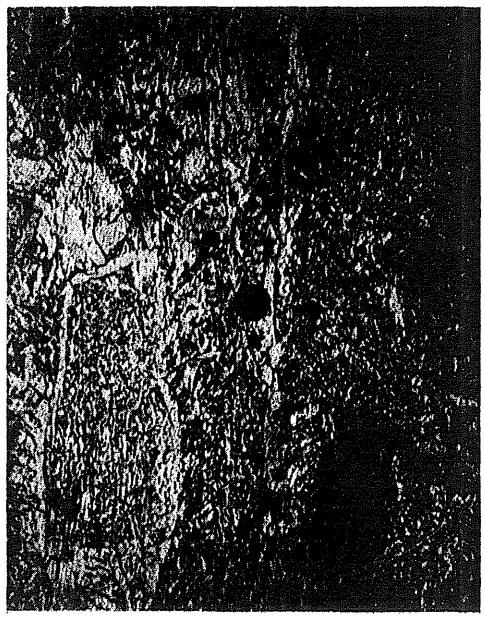

h) Weld Metal - Slag
Small inclusions
(214.4x)

Fig. A1.51 Photomacrograph and Photomicrographs of Specimen F4C. (2% Nital)